On the World Ocean Circulation: Volume II

The Pacific and Indian Oceans / A Global Update

by

William J. Schmitz, Jr.

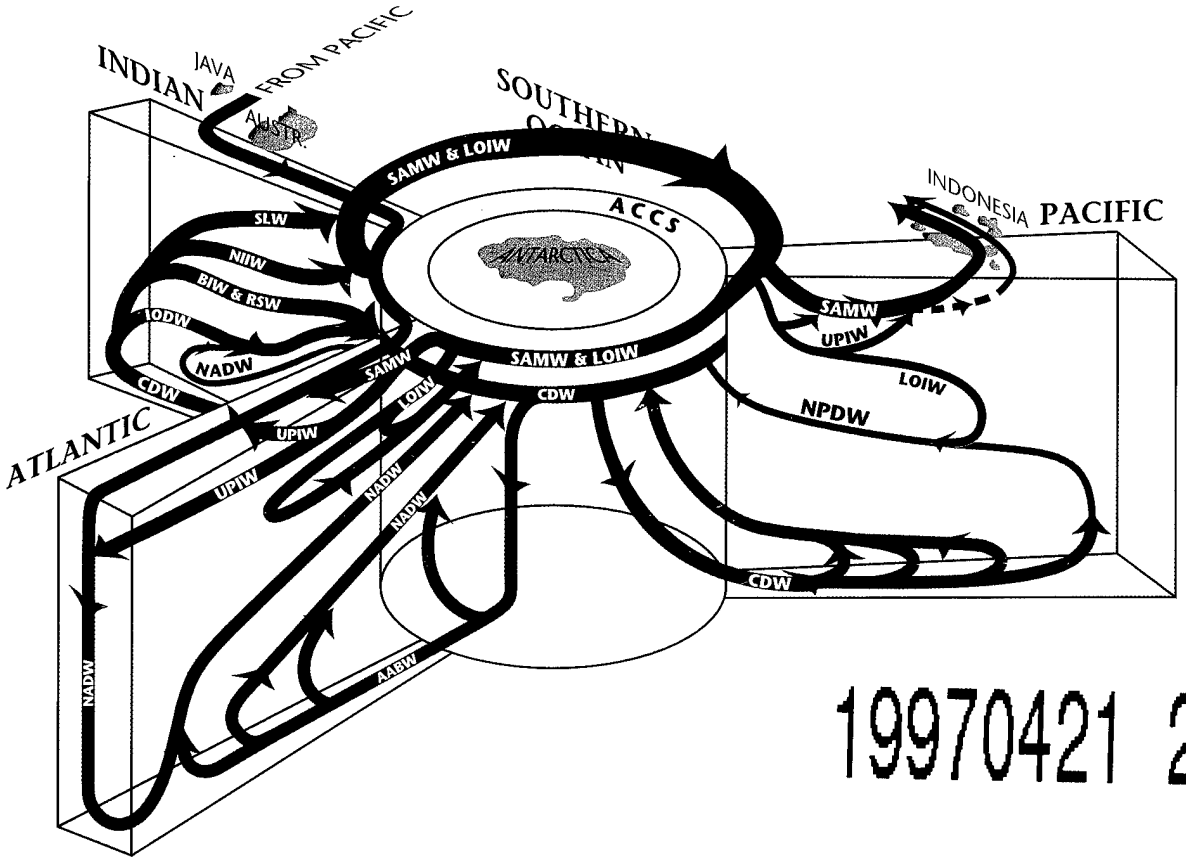

December 1996

Woods Hole Oceanographic Institution

Technical Report

WHOI-96-08

Funding was provided by the Office of Naval Research, Grant Nos. N00014-89-J-1039 and N00014-95-1-0356, and the Clark Foundation.

DISCLAIMER NOTICE

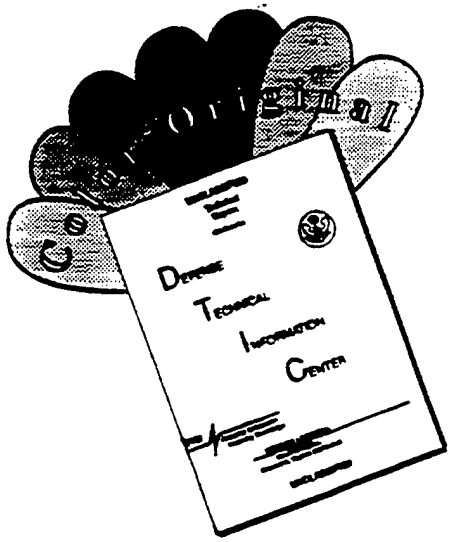

THIS DOCUMENT IS BEST QUALITY AVAILABLE. THE COPY FURNISHED TO DTIC CONTAINED A SIGNIFICANT NUMBER OF COLOR PAGES WHICH DO NOT REPRODUCE LEGIBLY ON BLACK AND WHITE MICROFICHE.

WHOI-96-08

On the World Ocean Circulation: Volume II

The Pacific and Indian Oceans / A Global Update

by

William J. Schmitz, Jr.

Woods Hole Oceanographic Institution
Woods Hole, Massachusetts 02543

December 1996

Technical Report

Funding was provided by the Office of Naval Research, Grant Nos. N00014-89-J-1039 and N00014-95-1-0356, and the Clark Foundation.

Approved for Distribution:

Philip L. Richardson, Chair
Department of Physical Oceanography

Front Cover Figure Caption: A three-dimensional interbasin flow schematic with "typical" meridional–vertical sections for the indicated oceans, and their horizontal connections in the Southern Ocean and the Indonesian Passages. The surface layer circulations are in purple, intermediate and SAMW are in red, deep in green, and near bottom in blue. Also shown as Figure II-8 (page 22).

SLW	Surface Layer Water
SAMW	Subantarctic Mode Water
RSW	Red Sea Water
AABW	Antarctic Bottom Water
NPDW	North Pacific Deep Water
ACCS	Antarctic Circumpolar Current System
CDW	Circumpolar Deep Water
NADW	North Atlantic Deep Water
UPIW	Upper Intermediate Water, $26.8 \leq \sigma_\theta \leq 27.2$
LOIW	Lower Intermediate Water, $27.2 \leq \sigma_\theta \leq 27.5$
IODW	Indian Ocean Deep Water
BIW	Banda Intermediate Water
NIIW	Northwest Indian Intermediate Water

Contents

Abstract

This is the second and final volume of a report that describes some of my investigations over the last 35 years or so into low-frequency ocean current structures, a topic which I will call the World Ocean Circulation (WOC). The material presented constitutes my final report to the Office of Naval Research, and their support over the years is deeply appreciated. I was also fortunate to have been partially supported by the National Science Foundation during my career and, for some of the preparation of this report, by the Clark Foundation. Volume I was focused on the North Atlantic Ocean, after a global scale summary. This volume (II) will consider first the Pacific and Indian Oceans, concentrating on interbasin circulations, meridional cells, and mesoscale eddy fields. Then, there is an exceptionally brief discussion of the Southern Ocean(s) for background only, followed by a global summary. Lately, I have worked intensely on intergyre and interbasin exchanges, including an intercomparison of some of the properties of the eddy field in the World's Oceans (Schmitz, W. J., Jr., *Rev. Geophys., 33,* 151–173, 1995; *J. Geophys. Res., 101*, 16,259–16,271, 1996). Volume II contains not only an update of the global picture, but also new representations of the transport structure of various components of the meridional overturning cells for each ocean. In summary, several similarities as well as dissimilarities between different oceans relative to both their general circulation and their mesoscale eddy field are shown to be associated with interbasin exchanges.

This report is meant to be an informal, occasionally anecdotal, state-of-the-art summary account of the World Ocean Circulation. Seemingly simple questions about how ocean currents behave, such as where various brands of sea water are coming from and going to, have been exciting research topics for many years. This report is not remotely about "all" of the WOC, it is simply a set of comments about what I have looked into during the preparation of this document. I do believe that the results in this report, although presented in a personal way, are consistent with community wisdom. The document is intended to be readable by non-specialists who have a basic scientific/technical background, especially in other oceanographic areas or meteorology or the geophysical disciplines, not only by specialists in physical oceanography.

Previous Work in This Series

Schmitz, William J., Jr., 1996. On the World Ocean Circulation: Volume I, Some Global Features/North Atlantic Circulation. Woods Hole Oceanographic Institution Technical Report WHOI-96-03, 150 pp.

1. Introduction

This is the second and last volume of a "final report" that summarizes, often in a speculative manner, some of the research areas that I have found interesting about the low-frequency ocean circulation, primarily with support from the Office of Naval Research. I was also fortunate to have been partially supported by the National Science Foundation on a variety of earlier projects and, during the preparation of this report, by the Clark Foundation. A one-page summary of my activities and accomplishments over the years is contained in Appendix A. Many of my publications are contained in the references. Citations for the medals I have been fortunate enough to receive from the Navy are in Appendix B. A couple of summary cartoons have been included in Appendix C. I am grateful to Nick Downes for permission to use his cartoons at a reasonable price, which I personally covered.

My description of the World Ocean Circulation (WOC) is focused on large-scale ocean currents, with emphasis on meridional cells and interbasin flows, and on mesoscale eddies. I concentrate on interbasin exchanges because they play a major role in determining the differences between ocean basins, both in the nature of their general circulation and in patterns and amplitudes of mesoscale variability (Schmitz, 1995, 1996; hereafter S95, S96). Meridional cells are a zero order representation of the thermohaline flows primarily associated with interbasin exchanges, keeping in mind that wind-influenced upward diapycnal transformations are also involved. The terms "general circulation," "mean flow," and "large-scale" or "average" currents will typically be used for quasi-stationary flow patterns with dimensions of a few hundreds of kilometers and larger, typically ocean-basin and/or interbasin scale in at least one horizontal dimension. Mesoscale eddies have horizontal scales of $\sim$ 100 km, time scales from several days to, say, a few years or so, and are the strongest where the general circulation (the primary mesoscale eddy energy source) is most intense. However, the term "mesoscale" can often refer to one spatial dimension only, perhaps without regard to time scale, or the above-noted time-scale range only, independent of space scale. As examples, in the general ocean circulation there are typically currents with a width that is mesoscale, but whose downstream dimension is ocean-basin or even interbasin scale; and mesoscale variability can be defined by some band in a frequency spectrum.

1. Introduction

This effort is an informal, occasionally anecdotal, state-of-the-art account of the WOC. Seemingly simple questions about how ocean currents behave, such as where various brands of sea water are coming from and going to, are at the heart of physical oceanography and have been exciting and challenging research topics for many years. The approach taken is primarily to synthesize diverse data-based results, obviously because I am an observationalist. I believe that the results in this report, although presented in a personal way, are consistent with community wisdom. The report is intended to be readable by non-specialists who have a basic scientific/technical background, especially in other oceanographic areas or in meteorology or the geophysical disciplines, not just for specialists in physical oceanography. Anyone wishing to get spun up on the observational basis for the WOC could use this report and associated references as a starting point. Mesoscale fluctuations were studied intensely in the 1970s and 1980s, and I believe that we now have a zero-order description and initial understanding of the global eddy field (please see S96). Our description of the global interbasin circulation is advancing rapidly (Fieux *et al.* 1994, 1996a, b; Garzoli and Gordon, 1996; Mantyla and Reid, 1995; Macdonald, 1993; McCartney and Baringer, 1993; Rintoul, 1991; Robbins and Toole, 1996; Schmitz and Richardson, 1991; S95; Talley, 1995; Wijffels, 1993; Wijffels *et al.*, 1996; this report). Key publications in the 1980s were by Gordon (1986), Mantyla and Reid (1983), and Rintoul (1988).

The first volume of this report was focused on the North Atlantic Ocean, where I have done most of the research in my career. Volume I also contained some summary material on global interbasin exchanges, a partial update of S95. This volume (II) of my report deals first of all with the general circulation and mesoscale eddy fields in the Pacific and Indian Oceans (Sections 2 and 3 respectively), with concentration on meridional cells, interbasin exchanges, and mesoscale eddy statistics, and includes a few remarks on model–data intercomparisons. A nice recent review of the general circulation of the Pacific Ocean (Talley, 1995) is now available, as well as a good summary of western boundary current regimes in general (Hogg and Johns, 1995). The work by Fieux *et al.* (1994) is a magnificent source of ideas and information concerning the area between Sumatra, Java and Australia (please also see in this regard Fieux *et al.*, 1996a, b; Hautala *et al.*, 1996; and Rochford, 1961, 1963, 1966), a location that is important not only to the Indonesian Throughflow (IT) but also to the upward limb of the large-scale thermohaline flows in the Indian Ocean (in this regard the latest

word is contained in a critically important article by Robbins and Toole, 1996, hereafter RT96) and globally (Gordon, 1986). Godfrey's (1996) review of the IT scenario is particularly timely and useful.

I've done only a bit of personal research on the Pacific (essentially the North Pacific) or Indian Oceans (the Agulhas Current System, hereafter ACS), so these oceans won't be covered in the same way as the North Atlantic in Volume I (please also see for the North Atlantic, Reid, 1994, plus Schmitz and McCartney, 1993). In writing my recent review article on thermohaline interbasin circulations (S95), I became intrigued with the ways the various oceans interact, even to the extent of interbasin flows influencing their eddy fields (S96). The original plan, as articulated in Volume I of this report, was for three volumes with the last one on the Southern Oceans, the global picture and special topics. However, Volumes II and III have been combined, so Sections 2 and 3 have an expanded, globally-linked content, and the Southern Oceans will be discussed (briefly) here in Section 4, with a world ocean view emphasizing interbasin flows contained in Section 5, and a few Conclusions etc. in Section 6. I like to describe the circulation by various plots and tables of transports (volume fluxes, in 10^6 m^3 s^{-1} ≡ 1 Sverdrup) in layers bounded by density surfaces (Table 1). Appendix D

Table II-1: Typical potential density ranges for various layers

Water Mass Layer Name	Abbreviation	σ Range (kg m^{-3})
Surface Layer Water	SLW	$\sigma_\theta < 26.5$
Upper Layer Water	ULW	$\sigma_\theta < 26.8$
Subantarctic Mode Water	SAMW	$26.5 \le \sigma_\theta \le 27.2$
Upper SAMW	USAMW	$26.5 \le \sigma_\theta \le 26.8$
Lower SAMW	LSAMW	$26.8 \le \sigma_\theta \le 27.2$
Upper Intermediate Water	UPIW	$26.8 \le \sigma_\theta \le 27.2$
Lower Intermediate Water	LOIW	$27.2 \le \sigma_\theta \le 27.5(6)$
Antarctic Intermediate Water	AAIW	$27.2 \le \sigma_\theta \le 27.5$
Total Intermediate Water	IW	$26.8 \le \sigma_\theta \le 27.5(6)$
Deep Water		$27.5(6) \le \sigma_\theta \le 27.8$
Bottom Water		$\sigma_\theta > 27.8$

contains a list of most of the abbreviations used in this report volume. In this report I will typically discuss transport layers defined by density parameter (σ_α) intervals or ranges or classes, whether identified with property extrema or not. The subscript will identify the reference horizon, with units that are understood to be kilograms per cubic meter (kg m^{-3}) and mentioned only occasionally. α will be denoted as 0 or θ (potential temperature) for layers near the sea surface down to LOIW, and for situations where outcropping is involved. α will often be in kilometers or decibars; normally 1.5, 2 ... to 4 or 4.5 for deeper classes. σ_t denotes the density difference from 1 mg cm^{-3} or 1 kg m^{-3} at in-situ temperature t.

A fair amount of time in Section 2 is spent on the western South Pacific where there is a flow via the South Equatorial Current (SEC) into low-latitude current systems, thence the North Pacific, and eventually into the IT (*e.g.*, Godfrey, 1996; Lukas *et al.*, 1991). It seems to me that there are both similarities and differences between the cross-equatorial flows and their sources in the Pacific and Atlantic Oceans that have not been previously high-lighted to the best of my knowledge. The South Pacific and South Atlantic both appear to have a net northward cross-equatorial transfer of ~ 10 Sv of Upper Layer Water (ULW; with potential density $\sigma_\theta \leq 26.8$ kg m^{-3}, units hereafter understood), along with a net intermediate water (IW) transfer northward of a few (2–5) Sverdrups, as well as "supplying" or recirculating much of the Equatorial Undercurrent (EUC) in their respective oceans. Recirculations and transformations in the equatorial current systems may act to change upper Subantarctic Mode Water (USAMW, $26.5 \leq \sigma_\theta \leq 26.8$ mg cm^{-3}) into surface layer water (SLW, from the sea surface down to $\sigma_\theta = 26.5$), ULW = SLW + USAMW.

In this report I take IW to span the σ_θ range 26.8 to 27.5, as do RT96, and also take Subantarctic Mode Water (SAMW) to include $26.5 \leq \sigma_\theta \leq 27.2$. I use layers much like RT96, with their SAMW layer being called USAMW in this report, and their combined surface and SAMW layers referred to as an upper layer (from the sea surface down to $\sigma_\theta = 26.8$), as noted above. Upper IW (UPIW) or Lower SAMW (LSAMW) span $\sigma_\theta = 26.8 \rightarrow 27.2$, and Lower IW (LOIW) or Antarctic Intermediate Water (AAIW) spans $\sigma_\theta = 27.2 \rightarrow 27.5$, IW = UPIW (LSAMW) + LOIW (AAIW); AAIW or LOIW typically contains a salinity minimum. Occasionally I will combine ULW and IW into a layer encompassing the upper ocean (UPOCN, or UPOCNW, upper ocean water), the entire flow above deep and bottom water.

Although the structure of the net cross-equatorial flows may be similar to some extent in the Pacific and Atlantic Oceans, the "original" sources and "final" destinations are different. In the Pacific Ocean the net upper layer cross-equatorial flow is primarily to supply the IT, whereas in the Atlantic a net northward upper ocean cross-equatorial exchange is a major component of the replacement flow for the formation of North Atlantic Deep Water (NADW). In both cases the net IW cross-equatorial flow is a few Sverdrups, say, perhaps slightly more in the Atlantic, where ~ 5 Sv UPIW exits the northern Straits of Florida (please see Volume I of this report). On the other hand, seemingly a lot of IW, including LOIW, crosses the equator and recirculates as such in the Atlantic, keeping in mind that Rintoul (1988, 1991; hereafter R8891) found no net flow of LOIW (AAIW) in the Atlantic Ocean (S95). What is the global scale picture of IW (and SAMW; please see McCartney, 1977, 1982; and McCartney and Baringer, 1993) circulation, including sites and mechanisms for diapycnal modification upward as well as water mass formation?

Although much of our thinking on cross-equatorial flows in the UPOCN has been focused on the low-latitude and generally western boundary current regimes where the exchange geographically takes place, there are interesting, now almost historical comments on the circumpolar origin of the source waters of both the Benguela and Peru Currents by Wooster and Reid (1963, their p. 254) that have led me to view these features as key ingredients in the global picture of interbasin exchange. The Peru and Benguela Currents, in addition to returning equatorward some part of the subtropical gyre, also involve direct flow from the Antarctic Circumpolar Current System (ACCS) from its Subantarctic Frontal Zone (SFZ). The circumpolar components of the Benguela and Peru Currents are IW and SAMW. These eastern boundary current systems also typically include upwelling regimes in which water of circumpolar characteristics may be diapycnally modified upward along its path into an SEC, and eventually ends up, after considerable modification, feeding low-latitude and cross-equatorial flows in the west. These are the key issues that make these boundary current regimes a focal point in the global interbasin exchange picture. In the case of the UPIW (S95) approaching the Benguela Current System (BCS) from Drake Passage, there is an apparent need for both isopycnal and diapycnal transformation south of 32°S prior to entering the BCS (R8891, S95), so upward diapycnal conversion in the BCS itself may be less crucial than in the Peru Current System (PCS). The ACCS is a (partial) source

for NADW replacement via the BCS and the primary (only ultimate?) source for the IT via the PCS. There are even more intriguing possibilities for the southernmost eastern South Pacific, relative to the upward diapycnal modification of upper Circumpolar Deep Water (CDW) to LOIW and LOIW to UPIW. In this regard, the area off Chile in the latitude range 40–50°S, say, may be much more important than previously realized/appreciated (discussed further in the following).

Wooster and Reid (1963, their p. 254) also note the absence of a corresponding eastern boundary current in the South Indian Ocean, but, nevertheless, about 20 Sv of CIW (IW of circumpolar origin) enters the Indian Ocean east of the Agulhas Current, flowing northward across 32°S, along with approximately the same volume flux of USAMW (RT96). According to RT96 the incoming volume flux of CIW is returned southward across 32°S in the Agulhas Current, being joined there by an additional 7 Sv of "other" intermediate water that is a component of the upward limb of the meridional cell in the Indian Ocean. Where and how is this transformation occurring? Where and how is the "needed" upward conversion (diapycnal) of IW and SAMW taking place in the South Atlantic and South Pacific Oceans, prior to approaching the equator in the west? Questions about specifically unique intermediate water transformations, more or less ignored in 2-layer views of a conveyor belt, are critical to the global interbasin circulation picture.

My guess is that there is a net 10 Sv transfer of IW and SAMW into the eastern South Pacific from the ACCS that is transformed upward in the Peru Current (understood to include the area off Chile where a variety of critical upward diapycnal conversions might occur) and eventually joins the equatorial current systems to "resupply" the IT. As either a complementary or an alternative possibility, the needed water mass conversion(s) may occur along upward spirals around the subtropical gyre. The 10 Sv net transfer could be the residual of a gyre-scale recirculation that includes water mass transformation, and reaches the Peru Current as USAMW, or LSAMW as appropriate. This kind of process might be what McCartney and Baringer (1993) had in mind when they noted that the lighter varieties of SAMW on the Scorpio 43°S section did not reach the Scorpio 28°S section. Alternatively, their observation might also imply that some of the ($\sigma_\theta \sim 26.8 \rightarrow 26.9$) lighter varieties of SAMW (but still called LSAMW here) might have been diapycnally converted to USAMW between 43° and 28°S. To complete the loop, the IT crosses the Indian Ocean in the SEC and enters the Agulhas

Current (and into the Agulhas Front, AF). Some of this flow is modified to SAMW on its journey to the vicinity of the Drake Passage after entering the SFZ in the Crozet Basin where these fronts merge. Park *et al.* (1993) have made a good case for a strong interaction between the current structures at the Agulhas Front, the Subtropical Convergence and the SFZ in the Crozet Basin.

Is the IT simply part of a relatively large-scale recirculation of SAMW and SLW with a "weak interaction" involving NADW replacement, or is there a strong coupling, and if so, what and where? In S95, I opted for a weak interaction of a few Sverdrups because of a possible "dominant" contribution of the meridional cell in the Indian Ocean to diapycnal upward modification from CDW to UPIW, and because I knew of no evidence for sufficient upwelling from CDW through the thermocline in the interior of the Pacific Ocean. With the revision of the structure of the meridional cell in the Indian Ocean by RT96, as well as other ideas and data as discussed above and below, I now see the possibility of, or even need for, a stronger coupling between the IT and NADW replacement. This update not only involves the IT and NADW replacement via exchange around the tip of Africa, but also connects various "other" water mass transformation processes that involve the IT and the contribution to NADW replacement that enters the Atlantic through Drake Passage. I also introduce a new type of coupling between the upper deep waters formed in the Pacific and Indian Oceans with the formation of LOIW.

There is a focus in Volume II on the exchange between the ACCS and the Pacific (Section 2) and Indian Oceans (Section 3). As noted above, I presume that the ACCS is the "source" of the IW and SAMW that enter the eastern South Pacific and, after much modification throughout a long and complex path, are the source of the IT. One presumption is that some LOIW is transformed upward to LSAMW (UPIW) off Chile, with some UPIW (or LSAMW) diapycnally modified to USAMW in the Peru Current, perhaps by ~ 28°S. Upper SAMW is then modified to SLW in the equatorial current system before entering the Indonesian Passages from the Mindanao Current (Wyrtki, 1961; Lukas *et al.*, 1991, 1996; Godfrey, 1996). A recent set of numerical experiments (Shriver and Hurlburt, 1996) actually yields this type of result explicitly, that is, that the ACCS is the southern "source" of the IT, requiring complex pathways and diapycnal transformations in the eastern South Pacific, as well as in the equatorial and North Pacific to arrive at the Indonesian Passages in the "right" density range (please

also see Cox, 1975; Godfrey, 1989, 1996; Godfrey and Golding, 1981; Godfrey *et al.*, 1993; Lukas *et al.*, 1991; Wijffels, 1993; Wijffels *et al.*, 1996).

The mechanism for intermediate water formation in the numerical experiment by Shriver and Hurlburt (1996) does not appear to include SAMW formation, but rather wind-forced upwelling in the ACCS, perhaps to some extent as described by Toggweiler and Samuels (1993a); also see Toggweiler (1994). According to Wijffels (1993) and Wijffels *et al.* (1996), significant (5 Sv, say) transformation of the Circumpolar Deep Water flowing into the Pacific to thermocline level water by uniform upwelling in the ocean interior is not likely, so a direct conversion of CDW (or NADW) probably does not supply the IT as originally hypothesized by Gordon (1986); please also see Toggweiler and Samuels (1993b) and Toole *et al.* (1994a). However, the area off Chile may also be a location where lighter varieties of CDW may be converted to LOIW (but not salinity minimum LOIW). It would be very intriguing if lighter varieties of CDW or upper CDW (UCDW) being converted to LOIW were in fact deep/bottom meridional cell components like North Pacific Deep Water (NPDW) and Indian Ocean Deep Water (IODW). This would couple the deep/bottom cells in the Pacific and Indian Oceans to both the IT and NADW replacement in a new way.

Insofar as I can tell, there is only one place in the entire global ocean where CDW has been quantitatively hypothesized on an observational basis to be diapycnally converted upward to UPIW (LSAMW), USAMW, or SLW, and this is in the Indian Ocean (RT96), for a total of 6 Sv. Since a total of 14 Sv is needed to replace the NADW that ultimately joins the PFZ, we need to find sources for another 8 Sv. To get to UPIW we need to go through LOIW. The convection mechanism to SAMW (upper and lower) and eventually to salinity minimum AAIW, as developed by McCartney (1977, 1982) and used extensively here and elsewhere, is normally used to convert water down, not up, but perhaps the other possibility exists. One published possibility, as articulated by RT96, is to form 3 Sv of LOIW from CDW in the Indian Ocean meridional cell. In addition, I have heard the "classical" or "traditional" scheme for AAIW formation articulated in a couple of ways. One version, as described by McCartney (1977), involves cross-polar-frontal mixing of low salinity Antarctic Surface Water (AASW) and Subantarctic Surface Water. This scheme is not what we need unless upwelling of CDW to AASW is involved. The second scheme does this, and I think Shriver and Hurburt

(1996) may also, that is, deep water is diapycnally modified upward by and subducted into the SFZ by wind-induced means.

So one might hypothesize that about 5 Sv is transformed upward from CDW to AAIW by the second variation of the classic scheme to supply the global interbasin circulation. This should not be taken to imply that most LOIW (especially AAIW) is formed by this mechanism, only the 5 Sv or so needed by the global interbasin circulation. Another possibility would be diapycnal upward modification by convection off Chile of UCDW to (comparatively high salinity) non-salinity-minimum LOIW, which does exist at a recent section (Toole *et al.*, 1994b) across 32°S (see below). But how does this LOIW get converted into UPIW (LSAMW)? I suggest, again, upwelling in the Peru Current; perhaps there is an upward modification there of quite a bit of water below "typical" LSAMW. In the mid-latitude reaches (perhaps by 28°S as mentioned previously) of the Peru Current it is also suggested that LSAMW is upwelled to USAMW. On the other hand this latter conversion could occur in a spiral within the subtropical gyre. It should be emphasized that in no case am I ruling out the recirculation of any of these layers in the subtropical gyre of the South Pacific, just looking for where the net conversions presumably required by global mass balance for the IT and other interbasin flows might occur. A most interesting part of all this is if USAMW is thenceforth upwelled to SLW in the equatorial current systems in the Pacific and exits through the IT via the Mindanao Current, and thence around the tip of Africa, either advectively or as cut-off Agulhas Eddies. Such a scheme would be a strong interaction between the IT and NADW replacement.

The ACCS is the source of CDW flowing northward into the Pacific and Indian Oceans, returning to the ACCS after both recirculation and diapycnal modification to less dense products (Mantyla and Reid, 1983, 1995; RT96; S95; Toole and Warren, 1993). Circumpolar Deep Water is resupplied by NADW joining the ACCS south of the Atlantic Ocean, primarily in the east (Siedler *et al.*, 1996), with some modified NADW proceeding directly into the Indian Ocean (RT96, Mantyla and Reid, 1995). I think that it is important to realize that the deep/bottom thermohaline cells in all the oceans could strongly influence how upper layer replacement for NADW can develop. Deep water has to go through IW (both LOIW and UPIW) to even get into the thermocline, much less to be converted to SLW, so that a two-layer picture (upper, lower) of the global thermohaline circulation is misleading in some sense. It takes three layers for

upper ocean replacement of both deep and bottom water formation, and at least four layers to distinguish between IW and ULW in that part of the ocean above deep and bottom water (UPOCNW). To depict recirculations of modified CDW could require another layer, and if NPDW and/or IODW are converted to LOIW directly, it might take a total of 6 layers to describe the global exchange of water mass properties adequately.

The flow around the tip of Africa from the Indian Ocean into the South Atlantic was reviewed by S95, with of course several publications as essential background (*i.e.*, Clement and Gordon, 1995; Clowes, 1950; Duncombe Rae *et al.*, 1992, 1996; Garzoli and Gordon, 1996; Gordon, 1986; Gordon *et al.*, 1992), and my ideas have evolved or changed some in the writing of this report, as discussed throughout. A flow of approximately 10 Sv of IW (actually UPIW, S95) through Drake Passage and into the Benguela Current System was found in an inverse model calculation by R8891, with 5 (about) Sv of this UPIW (LSAMW) converted to ULW by 32°S, and also the remaining 5 Sv UPIW undergoing layer average Temperature (T) and Salinity (S) changes from (T,S) = (4.18, 34.14) to (6.73, 34.49) between Drake Passage and the BCS at 32°S. A recent investigation by Saunders and King (1995) of the volume fluxes across a section spanning the South Atlantic yielded as a preferred estimate the "typical" 13–15 Sv of upper ocean replacement flow for NADW, as has now been found at many locations (please see Volume I of this report, and a recent independent verification of this estimate by Johns *et al.*, 1997). The preferred estimates by Saunders and King (1995), composed of 11 Sv for a surface layer and 4 Sv of IW flowing north at mid-latitudes, are within a couple of Sverdrups of the R8891 results at 32°S, and even the estimates for NADW replacement in the Florida Current by Schmitz and Richardson (1991).

The net transport from the South Atlantic into the BCS along a line from about 3°E, 30°S to 12°E, 38°S was recently observed to be 6–9 Sv in the upper 1000 m by Garzoli and Gordon (1996), who in addition found 2–4 Sv advected from the ACS into the BCS in the upper 1000 m along a line normal to that previously mentioned and the African coast. Cut-off Agulhas eddies or rings might contribute a net of 2–4 Sv of transport to the South (and eventually North) Atlantic (Duncombe Rae, 1991; Duncombe Rae *et al.*, 1996). So the total transport (advective plus eddy-based) into the South Atlantic Ocean from the South Indian Ocean could be 4–8 Sv. For this and other reasons discussed in the following, I now take the contributions to NADW replacement from Drake Passage and the ACS to be about equal (7 ± 1 Sv or so). Another important

role of Agulhas Rings might lie in their influence on the temperature and salinity of the South Atlantic subtropical gyre, and eventually the UPIW in the Falkland/Malvinas Current at the Brazil–Malvinas confluence (Garzoli and Garraffo, 1989; Gordon, 1989).

It was demonstrated from an examination of the R8891 results by S95 that the type of IW that both exited Drake Passage eastward and did not continue past the southern tip of Africa was essentially confined to the σ_θ range 26.8 → 27.2. This is above the salinity minimum typically used to define AAIW, depending on location. I originally (S95) focused on UPIW because it is water in and above this σ_θ class that also exits the Straits of Florida at its northern end (please see Volume I of this report) and contributes directly to the replacement flow for NADW formation (Schmitz and Richardson, 1991; Schmitz and McCartney, 1993). The σ_θ range of 26.8 → 27.2 (UPIW) is in the lower segment of the density parameter range of SAMW ($26.5 \leq \sigma_\theta \leq 27.2$) in the SFZ (McCartney, 1977, 1982). Lower intermediate water (LOIW) is pretty much AAIW regardless of location although there may be places (*i.e.*, the easternmost South Pacific) where the AAIW salinity minimum (normally located in the σ_θ range 27.2 → 27.5) creeps up to $\sigma_\theta \sim 27.15$ or so.

A major concern with the R8891 results, and one motivation for looking for a "large" flow around the tip of Africa into the South Atlantic, is to account for the *T/S* (Temperature/Salinity) properties of the water flowing northward (essentially in the BCS) in the eastern South Atlantic at ~ 30°S. This water tends to be significantly warmer and saltier (in both the isopycnal and the diapycnal sense) than any component of the flow out of Drake Passage, and the explanation for this is still, in my opinion, an open question (R8891 discussed an "atmospheric interaction"). Given the higher salinities in the Agulhas Current, it is tempting to rule out Drake Passage as a primary source and hypothesize a major "leakage" around the tip of Africa from the Indian to the Atlantic Ocean. My guess right now, based on "new" data along 25°W (nominal, R.V. *Melville* Cruise Hydros 3/4; Tsuchiya *et al.*, 1994) and on the proximity of the relevant current structures along the South American coast, is that the UPIW ($27.2 \leq \sigma_\theta \leq 26.8$) flowing out of Drake Passage as part of the Malvinas or Falkland Current System and eventually into the BCS first interacts (mixes) strongly with the subtropical flows in the western South Atlantic, becoming warmer and saltier before leaving the SFZ for the BCS. Schmitz (1995) previously pointed out that the average salinity of the UPIW on the Greenwich Meridian section (Whitworth and Nowlin,

1987), 15 to 20° west of the tip of Africa and a section also used by R8891, was substantially larger than found for UPIW at Drake Passage. Using new data (Tsuchiya *et al.*, 1994) I demonstrate in Section 5 that the salinity of UPIW is approaching the needed isopycnal transfer level for flow into the BCS as early as 25°W. This observation does not of course explain the diapycnal transformation(s) of UPIW between Drake Passage and 32°S found by R8891. On the other hand, the mechanisms may be similar, that is, mixing of the UPIW flow in the SFZ as part of the confluence of the Malvinas Current with the subtropical gyre circulation. In this regard there exist several articles on cut-off Brazil Current Rings and the interaction of the Malvinas/Falkland Current System with these rings and with the Brazil Current; please see Garzoli and Garraffo (1989), Gordon (1989), and Peterson (1992). These issues are discussed further in Sections 4 and 5 of this report.

I have developed a strong interest (starting with S95) in the exchange of water between the South Indian Ocean and the ACCS (Toole and Warren, 1993; Mantyla and Reid, 1995; S95; RT96), in the context of global interbasin exchange. The possible linkage (S95) between the incoming transport of near bottom CDW that is diapycnally modified upward north of 32°S and exits southward across 32°S in the ACS and participates in the replacement flow for NADW needs more attention. The idea that some of the 7 Sv of CDW that is diapycnally converted to IW in the Indian Ocean (RT96; basically a new mechanism for intermediate water formation, see also in this regard Toole and Warren, 1993) eventually exits through Drake Passage (as UPIW initially) and into the BCS is fascinating (S95). Circumpolar Deep Water is taken here to be strongly modified NADW, having transited the World's Oceans as a component of various deep/bottom thermohaline cells and completed many circuits in the ACCS. Circumpolar Deep Water enters the Indian Ocean from the ACCS along with some "newer" NADW directly from the South Atlantic (RT96), and the IW component of its return flow from the Indian Ocean southward above upper deep water across 32°S is roughly equipartitioned between UPIW and LOIW (RT96). My hypothesis is that some of the intermediate water that replaces CDW is transported in the ACS and the South Indian Ocean Current (Stramma, 1992), along either the Agulhas Front or Subtropical Convergence (STC), and thence into the SFZ where all these fronts merge near the Crozet Basin (Belkin and Gordon, 1996; Park *et al.*, 1991, 1993). According to S95, this IW flows eastward in the SFZ south of Australia, across the South Pacific and through

Drake Passage and into the BCS as partial replacement for O(10) Sv of NADW (S95). An update of this flow scheme is discussed throughout the report. My present thinking is that a total 7 Sv contribution to NADW replacement from Drake Passage consists of 4 Sv UPIW as a product of the diapycnal upper arm of the meridional cell in the Indian Ocean via the ACS and SFZ. The other 3 Sv of UPIW exiting through Drake Passage into the BCS takes the same path from the Indian Ocean but is modified from SLW to LSAMW (UPIW) en route by well-documented means (McCartney, 1977, 1982). The origin of this SLW is either or both of the IT and the meridional cell in the Indian Ocean.

The new estimate of the strength of the meridional cell in the Indian Ocean by RT96 yields a net 2 Sv of lower deep water ("NADW") along with lower (1 Sv) plus upper (10 Sv) bottom water, the lowest three layers out of the total of 8 layers used by RT96, a total of 13 Sv flowing northward across 32°S into the Indian Ocean from the ACCS. This 13 Sv is returned south (RT96) across 32°S, primarily in the ACS, as 4 Sv upper deep water, 3 Sv LOIW, 4 Sv UPIW, and 2 Sv in a surface layer ($\sigma_\theta \leq 26.45$). The RT96 estimate of a 13 Sv meridional cell (actually 9 Sv net transfer from total deep and bottom water to intermediate water and above) is about half of a previous estimate by Toole and Warren (1993) and close to the guess by S95, the latter based on a global mass balance. The suggestion by S95 that some of the upper ocean replacement flow for the formation of NADW is initially derived from CDW and NADW upwelled to intermediate water in the Indian Ocean is a totally new hypothesis for the global thermohaline interbasin circulation. In Sections 3 and 5 below, I present some new speculations on how the diapycnal upper limb from CDW to intermediate water might work in the Indian Ocean, using "old" results by Rochford (1961, 1963, 1964, 1966), with some modification in interpretation. Much of the IW associated with the meridional cell that is diapycnally raised in the North Indian Ocean and influenced by the overflow from the Red Sea is presumably transferred across the equator in the eastern Indian Ocean in a boundary-like current off Sumatra. This UPIW, and possible LOIW types affected by the meridional cell, including mixing with AAIW, were observed, in my opinion, by Rochford to occur in the easternmost part of the Indian Ocean between, say, 5°N and 25°S, the "same" region into which the IT (when it flows westward) enters the Indian Ocean and joins the SEC there (please also see Fieux *et al.*, 1994).

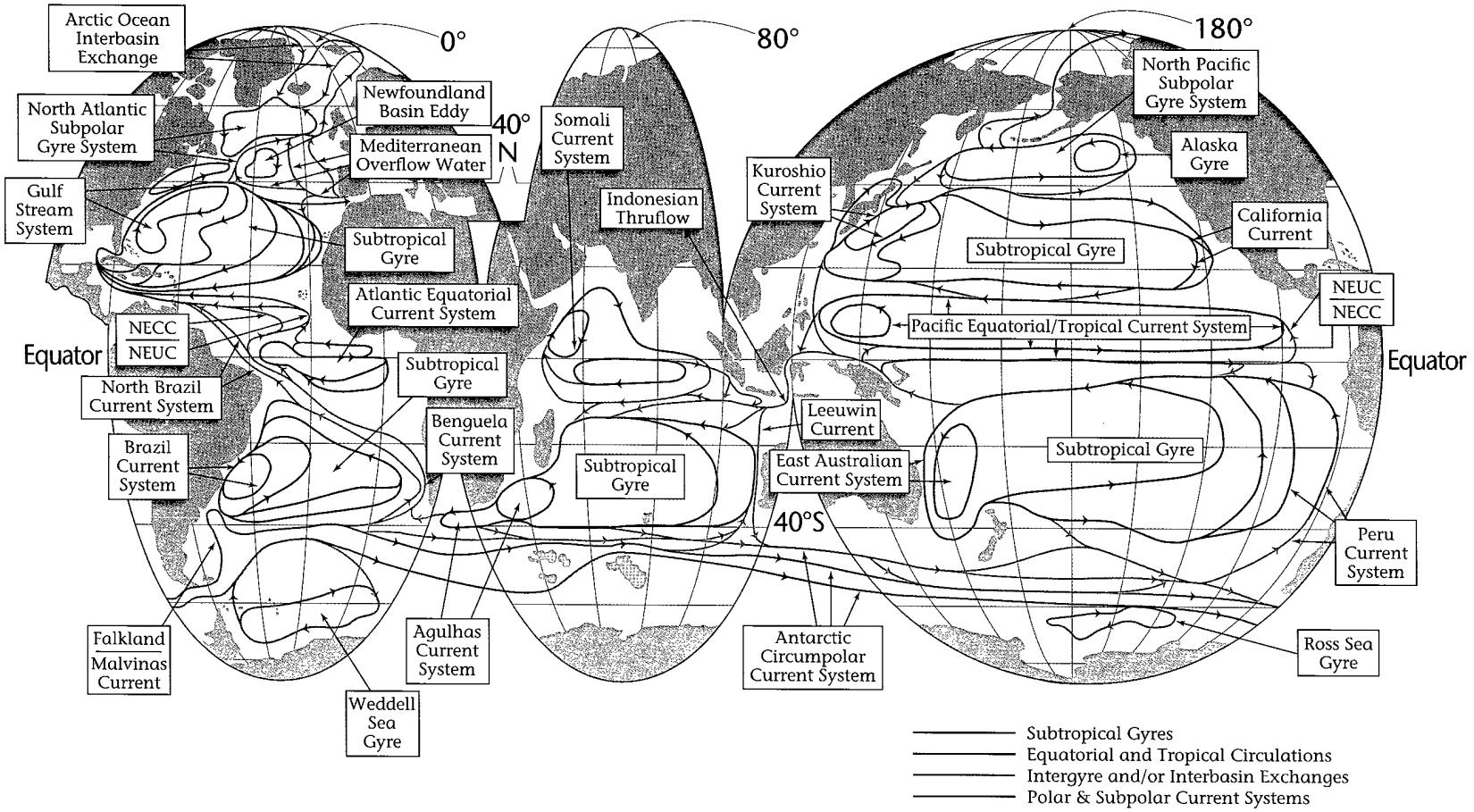

Figure II-1: A global map schematically identifying the location and nomenclature for many major upper ocean current systems and the connections between these flow patterns. Subtropical gyre circulations are in red, polar and subpolar flows in blue, equatorial current systems are in purple, and intergyre or interbasin exchanges are in green. Please refer to text for definitions, discussion, details.

A schematic global summary map (Figure II-1) of many but obviously not all major flow patterns in the upper ocean (taken to span the depth interval from the sea surface down to, say, several hundred meters depth; or water above $\sigma_\theta = 27.2$, which includes UPIW, or $\sigma_\theta = 27.5$ if LOIW is also included) was also used as a starting point in Volume I of this report (this figure is non-trivially updated here). The color coding scheme is such that red lines denote subtropical circulations (15°–40°N, say), blue lines denote subpolar and polar circulations (latitudes higher than 40°N, say), and purple lines denote equatorial current systems. The unique feature of Figure II-1 is the green lines suggesting intergyre and interbasin exchanges. Since my priority is on the flows represented by these green lines, there may be areas where other elements of the large-scale circulation are not presented, especially in the tropics.

A lot of nomenclature is included in Figure II-1, but instead of dwelling on this topic all at once, it is handled piecemeal. The only abbreviations used in Figure II-1 are NECC (North Equatorial Countercurrent) and NEUC (North Equatorial Undercurrent). An attempt was made in Figure II-1 to reproduce as faithfully as possible the general horizontal dimensions of various currents. Flows near the equator have a lot of vertical diversification even in the upper ocean, so what is represented in Figure II-1 tends to include the undercurrent-related systems but not the surface currents. A sectional schematic of the various low-latitude upper-layer currents in the Pacific is introduced in Section 2c below, and a variety of maps of surface currents are introduced throughout this report, including the next few figures. Current patterns for the North and Equatorial Indian Ocean in Figure II-1 are "special averages," or subjective summary climatology. What has been done is simply to include in Figure II-1 both a version of the Somali Current System and a highly idealized equatorial circulation, so features for both monsoonal regimes are to some extent included.

Surface current maps based on the yearly average of ship drift data for the Pacific and Indian Oceans are shown in Figures II-2 and II-3. These maps are superimposed on sea surface temperature (SST) contours. In Figure II-2, it is difficult to make out the East Australian Current (EAC) or the poleward arm (here called the South Pacific Current, following Stramma *et al.*, 1995b) of the subtropical gyre in the South Pacific. However, the SEC in the approximate latitude range 0–20°S is very well defined in Figure II-2. It is also not possible to pick out a southern recirculation for the Kuroshio or a subpolar gyre in the North Pacific. The other segments (Kuroshio, Oyashio, North

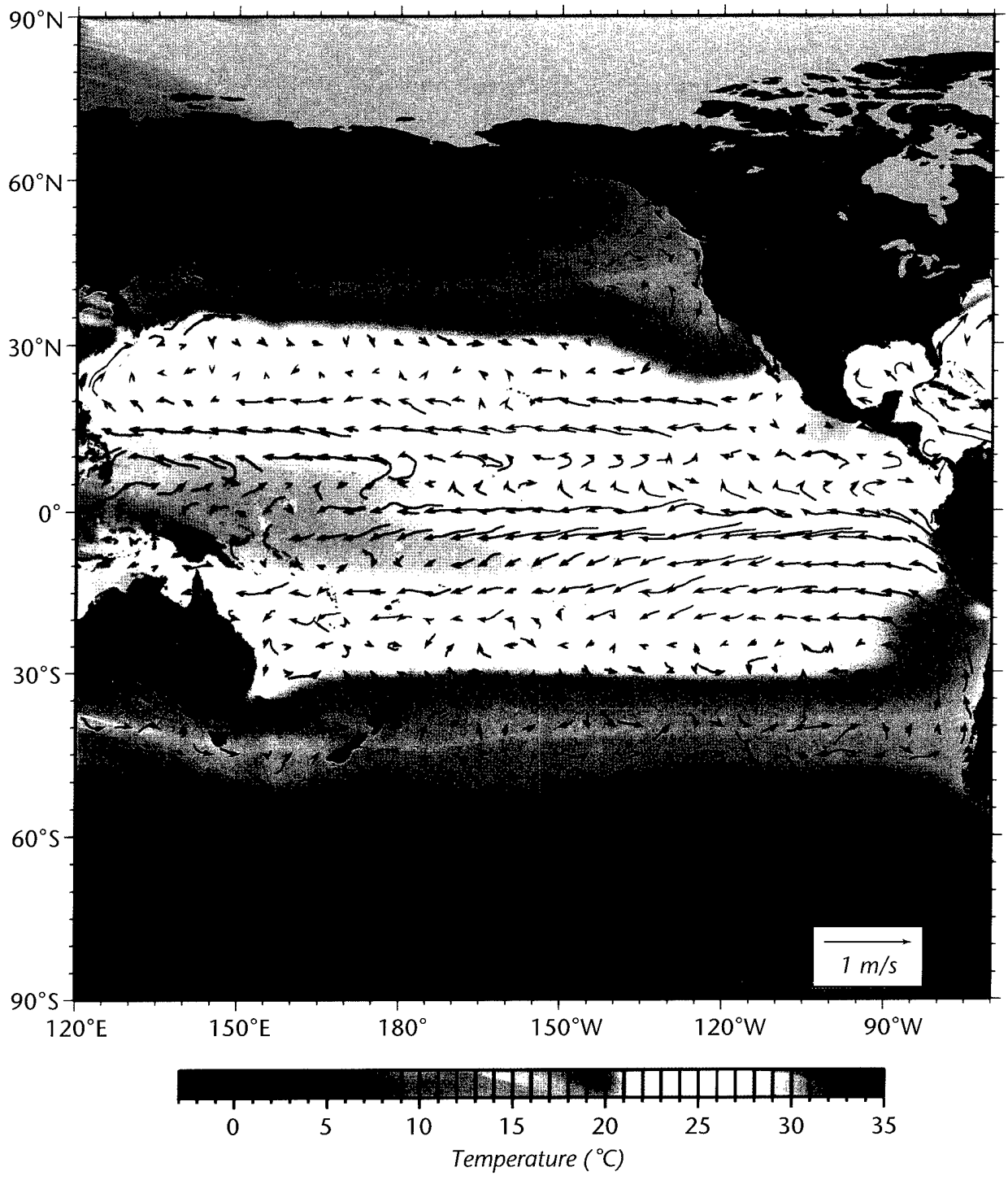

Figure II-2: Yearly-averaged surface current vectors for the Pacific Ocean based on ship drift observations, superimposed on SST contours.

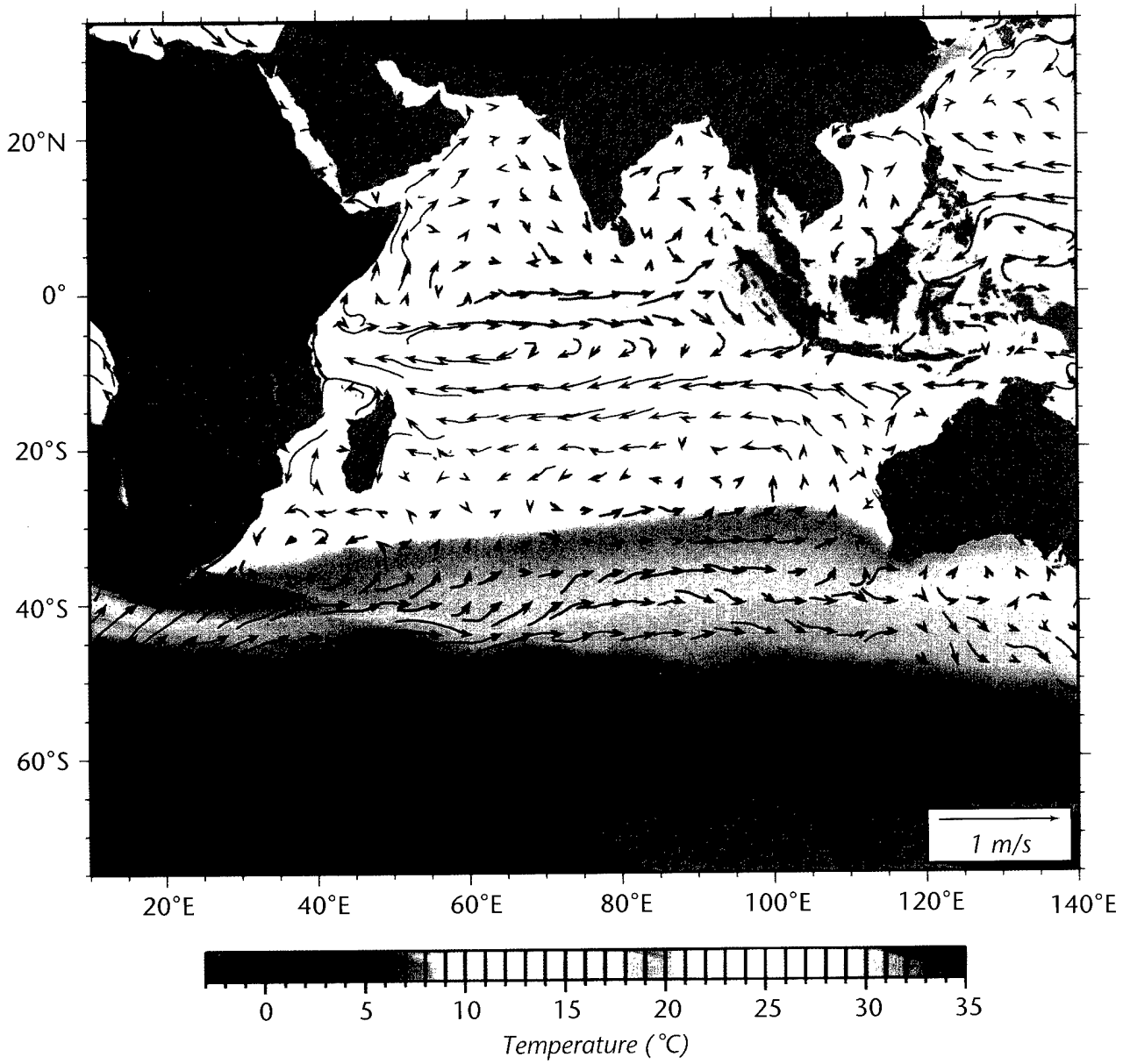

Figure II-3: Yearly-averaged surface current vectors for the Indian Ocean based on ship drift observations, superimposed on SST contours.

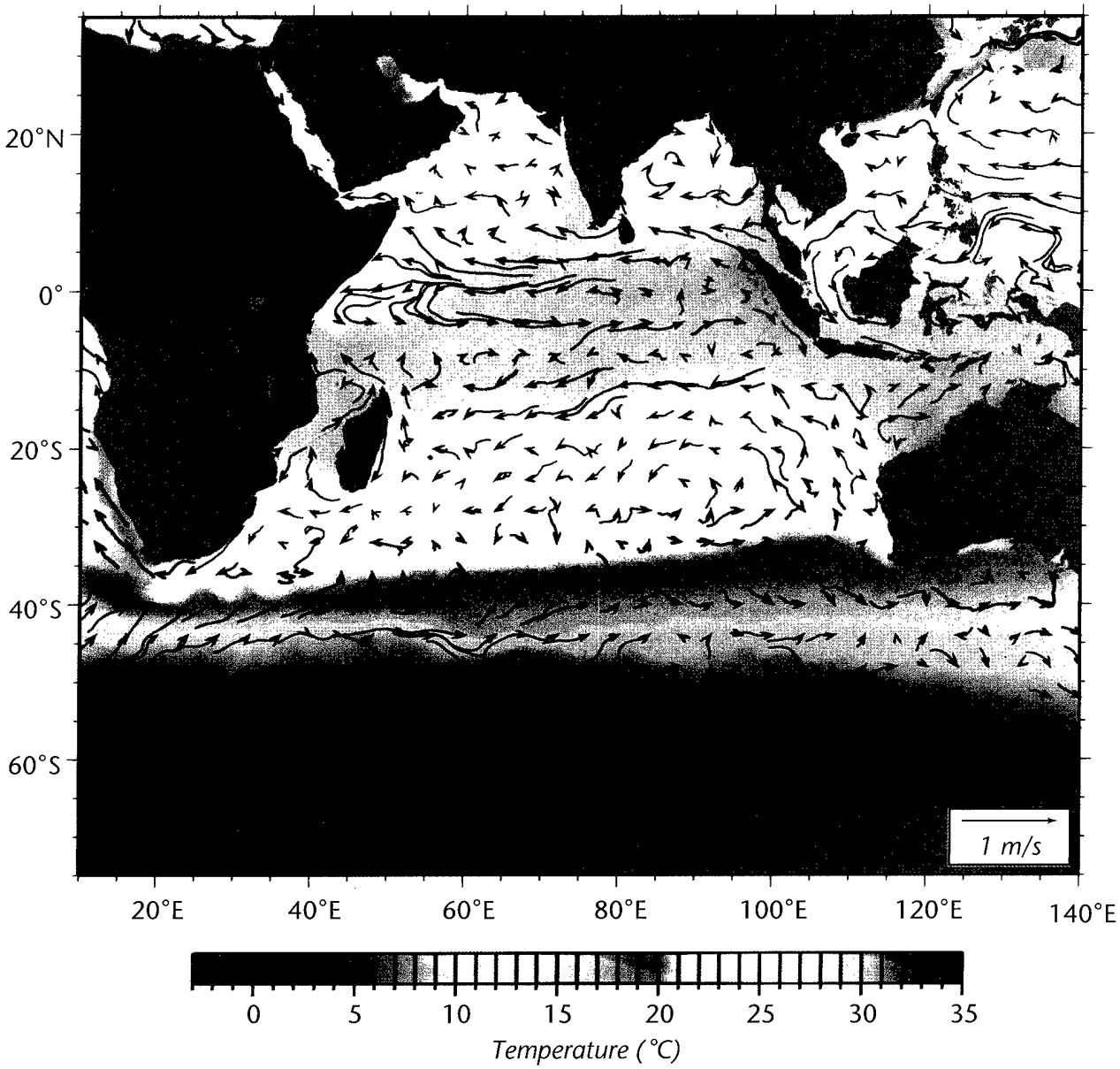

Figure II-4: Seasonally-averaged surface current vectors for the Indian Ocean based on ship drift observations, superimposed on SST contours: January through March.

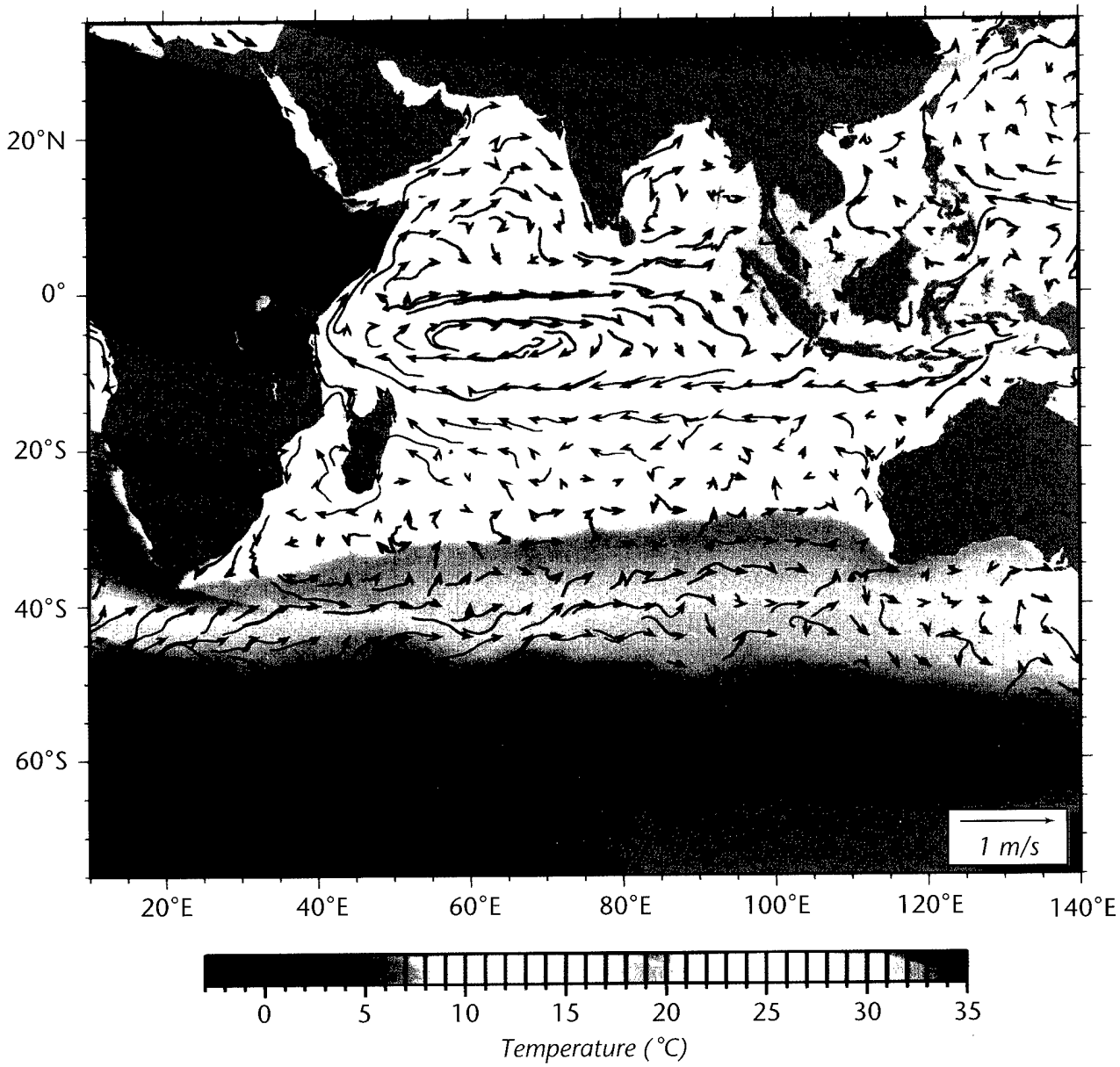

Figure II-5: Seasonally-averaged surface current vectors for the Indian Ocean based on ship drift observations, superimposed on SST contours: April through June.

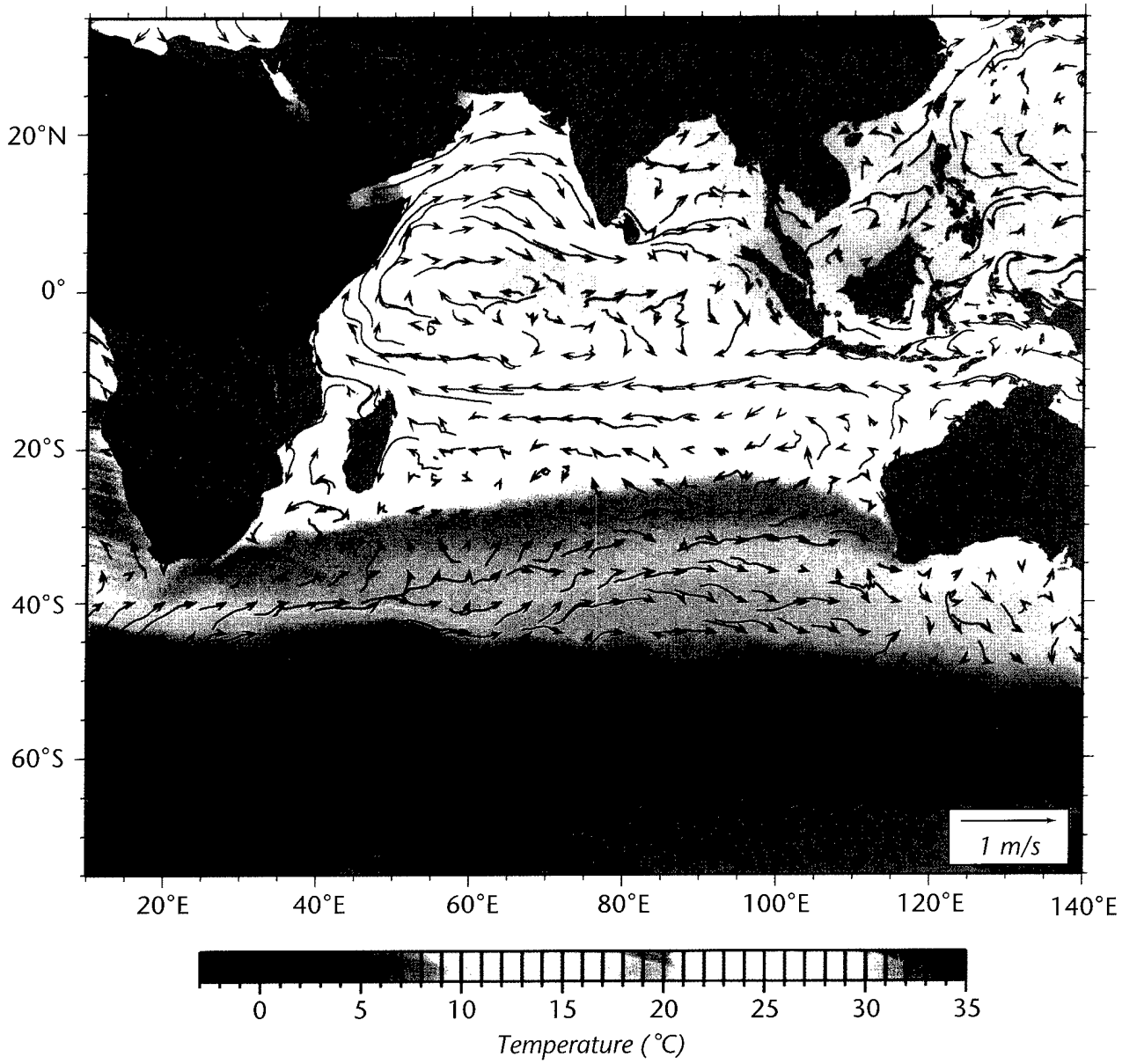

Figure II-6: Seasonally-averaged surface current vectors for the Indian Ocean based on ship drift observations, superimposed on SST contours: July through September.

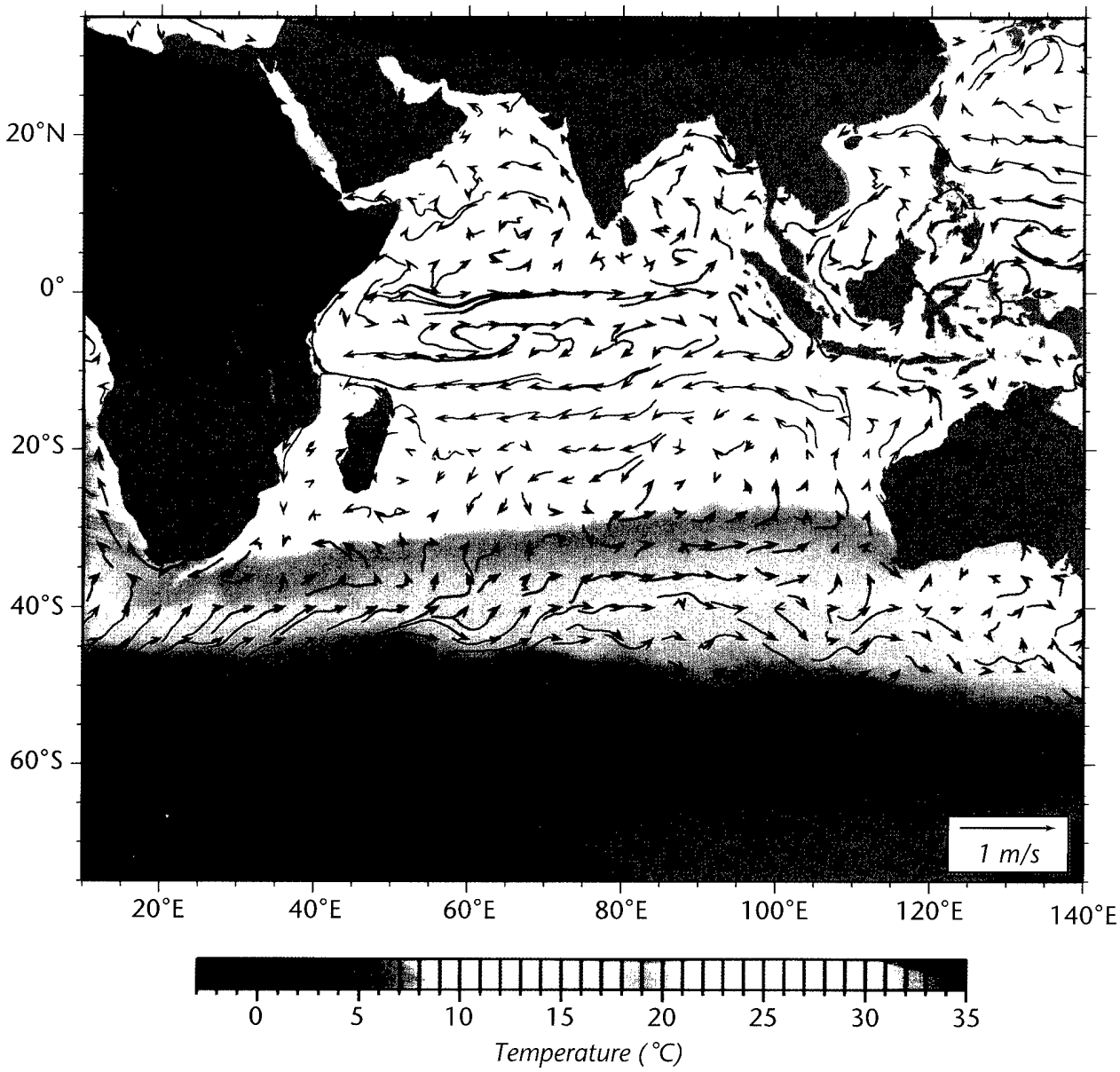

Figure II-7: Seasonally-averaged surface current vectors for the Indian Ocean based on ship drift observations, superimposed on SST contours: October through December.

Pacific Drift, etc.) of the subtropical gyre in the North Pacific are reasonably well defined. Note the westward flowing surface current at the equator, not represented in Figure II-1. In Figure II-3, the Agulhas Current is not well represented. Seasonal maps for the Indian Ocean in the same format as Figures II-2 and II-3 are shown in Figures II-4 through II-7, because of their special significance for the large-scale, seasonally varying circulation of the northern and equatorial segments of the Indian Ocean. The Southwest Monsoon is more or less represented by Figures 5 and 6 and the Northeast

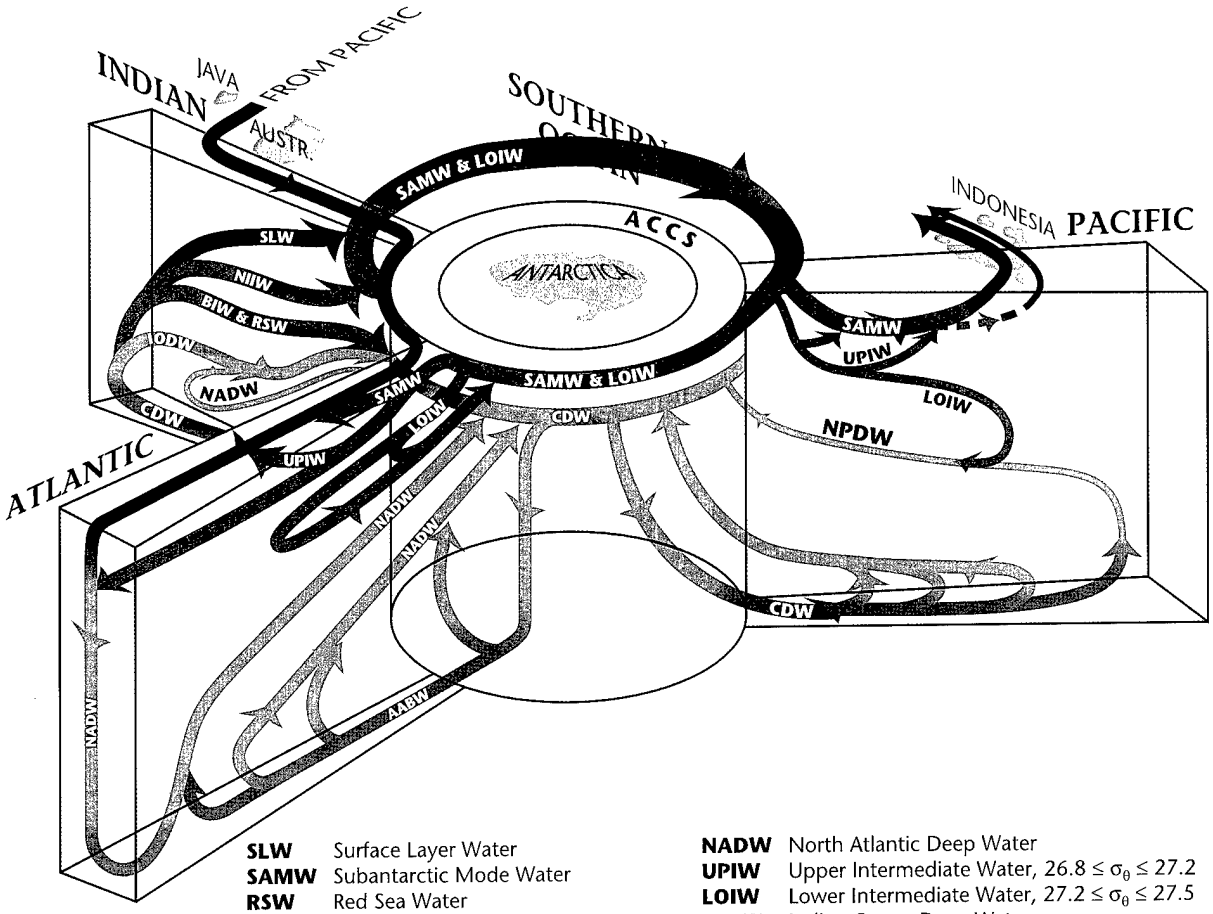

SLW	Surface Layer Water	**NADW**	North Atlantic Deep Water
SAMW	Subantarctic Mode Water	**UPIW**	Upper Intermediate Water, $26.8 \leq \sigma_\theta \leq 27.2$
RSW	Red Sea Water	**LOIW**	Lower Intermediate Water, $27.2 \leq \sigma_\theta \leq 27.5$
AABW	Antarctic Bottom Water	**IODW**	Indian Ocean Deep Water
NPDW	North Pacific Deep Water	**BIW**	Banda Intermediate Water
ACCS	Antarctic Circumpolar Current System	**NIIW**	Northwest Indian Intermediate Water
CDW	Circumpolar Deep Water		

Figure II-8: A three-dimensional interbasin flow schematic with "typical" meridional–vertical sections for the indicated oceans, and their horizontal connections in the Southern Ocean and the Indonesian Passages. The surface layer circulations are in purple, intermediate and SAMW are in red, deep in green, and near bottom in blue.

Monsoon mostly by Figure 4 and to some extent 7. Figures II-2–7 are based on graphs that were kindly made available by Arthur Mariano (personal communication, 1996).

A three-dimensional, global thermohaline flow schematic from Volume I of my report (Figure I-91 there) is included here (somewhat updated) as Figure II-8. This figure contains a qualitative summary meridional section for each ocean basin, plus key horizontal connections in the Southern Ocean and Indonesian Passages. The format for this diagram is based on a figure layout I first saw in a report by Gordon (1991), although the flow patterns shown constitute a substantial modification of the original figure. But I would like to emphasize that I feel that Arnold Gordon's contributions to the topics under consideration are both crucial and stimulating. Figure II-8 is also the front cover picture for this volume of my report. Many of the water mass names and abbreviations used in this report are in Figure II-8. This figure is intended to be complementary to Figure II-1 in order to orient the reader to the material I will be presenting later concerning meridional cells and interbasin circulations (the first large-scale meridional cell transport sections that I know of will be presented below for the Pacific and Indian Oceans, in analogy to Figure I-12 for the Atlantic Ocean in Volume I of this report).

A schematic (Figure II-9) of the uppermost layer current pattern (0–100 m depth range, say) in the low-latitude western Pacific (according to Lukas *et al.*, 1991) indi-

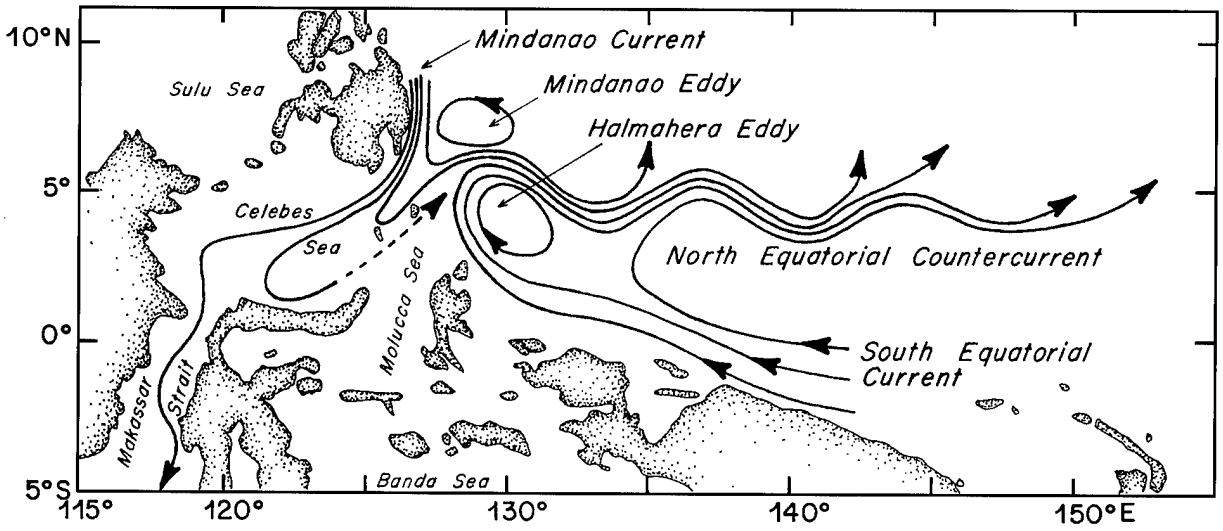

Figure II-9: A schematic of the near-surface (0–100 m) flow pattern in the low-latitude western Pacific Ocean, adapted from Lukas *et al.* (1991).

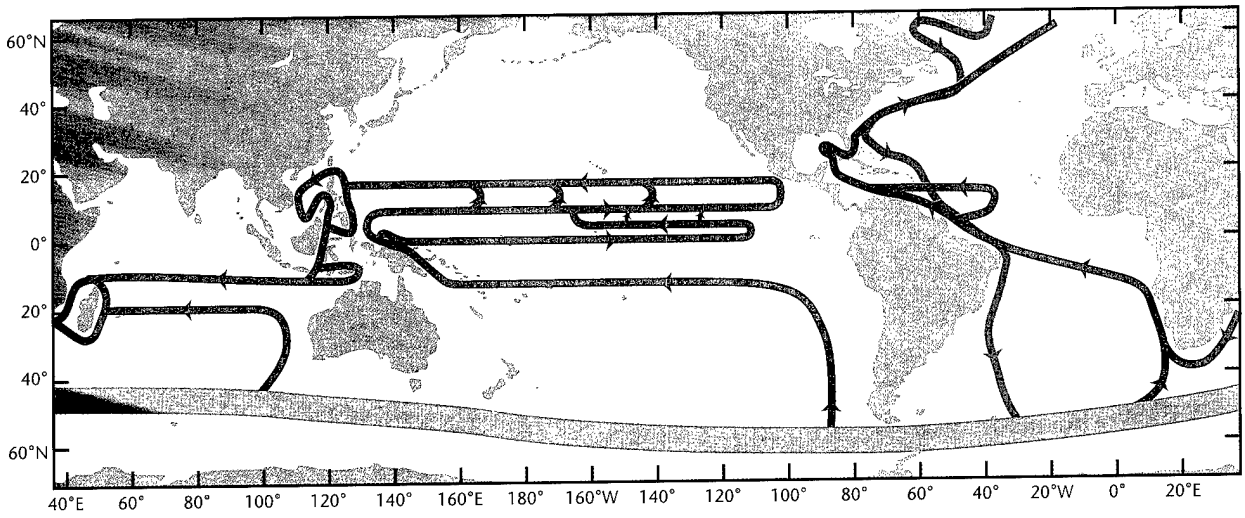

Figure II-10: An adaptation of the equivalent two-layer schematic of the upper (red) and lower (blue) layer interbasin-scale circulations as modeled by Shriver and Hurlburt (1996, their figure 7). The lower blue layer in this figure is model layer 6, and the upper layer the sum over model layers 1–5. The green line at the bottom of the figure denotes a region of wind-driven upwelling in the ACCS.

cates that the IT is supplied from the Mindanao Current. The interbasin-scale flows associated with the IT have been discussed by, for example, Godfrey (1996), Hirst and Godfrey (1993), Gordon (1986, 1995), S95, Shriver and Hurlburt (1996), and Wijffels (1993). A "new" possibility in this vein has recently been developed as an outcome of a set of numerical experiments by Shriver and Hurlburt (1996). Their results in terms of IT-related pathways are summarized in Figure II-10. Perhaps the least well-determined component pathway of the interbasin-scale circulation pattern involving IT is the path segment in the North Pacific prior to the supply by the Mindanao Current (Gordon, 1995; Wijffels, 1993; Wijffels *et al.*, 1996). In order to link the transports associated with the large-scale meridional cells in the Pacific and Indian Oceans with the Atlantic cell and the exchanges with IT and the ACCS, we need first to develop diagrams for these cells individually, as I have done in Volume I for the Atlantic Ocean (Figure I-12 there, reproduced in this volume as Figure II-11). In the first two sections of Volume II we construct figures like II-11 for the Pacific and Indian Oceans (please see Sections 2f and 3e, respectively). Generally speaking, throughout the World's Oceans, the formation of abyssal water masses and occasionally their transports are better documented than the associated replacement flows, that is, the upward diapycnal limbs of the various meridional cells.

Let us consider, first, meridional property sections through the "middle" of the Pacific and Indian Oceans. Figures II-12, 13 and 14 are adapted from Reid's (1965, his figures 2, 3 and 4, respectively) ground-breaking monograph on intermediate water. These are sections of temperature, salinity and oxygen, respectively, along 160°W approximately, from Antarctica to Alaska. In Figures II-12, 13 and 14 the dashed lines are two density parameter surfaces, from the vicinity of the S_{min} associated with North Pacific Intermediate Water (NPIW, $\sigma_t \sim 26.8$) and from the S_{min} associated with AAIW ($\sigma_t \sim 27.3$). Major features of these sections for present purposes are the nearly vertical isothermal (Figure II-12) and isohaline structure in the upper 1000 m or so of the SFZ (50–60°S), and the associated northward penetration (Figure II-13) of low salinity IW (which includes LSAMW) into the South Pacific; in Figure II-14 this is water of comparatively high oxygen content. But this low salinity and high oxygen IW recently

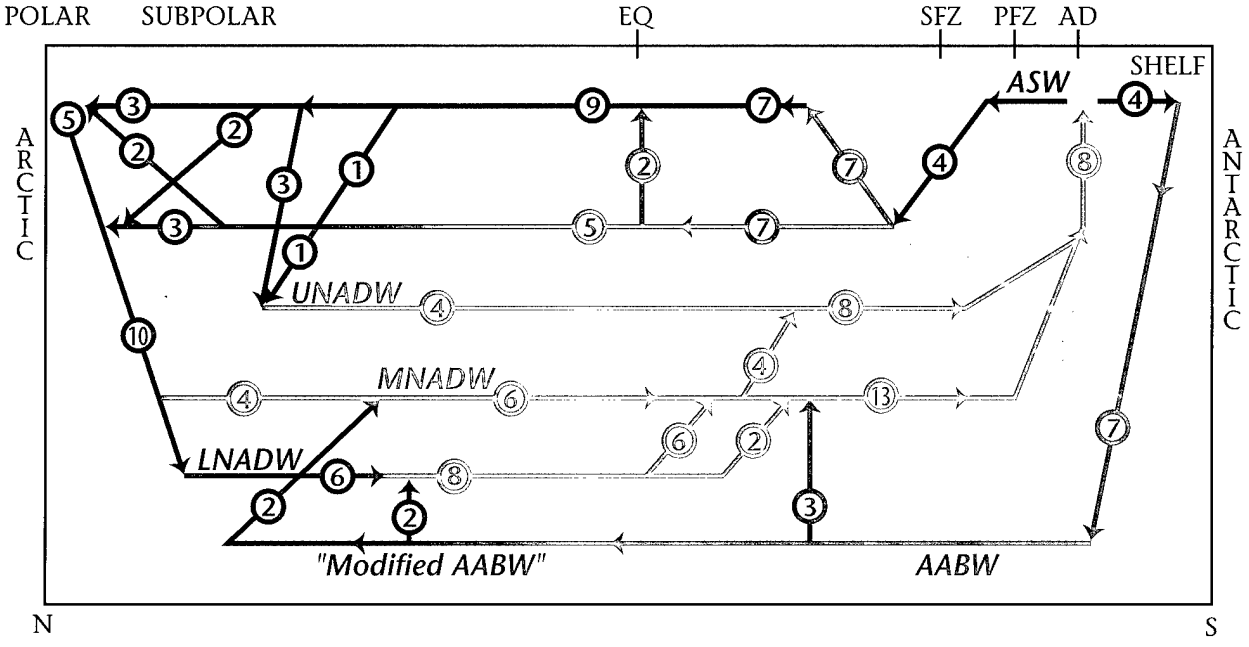

Figure II-11: A six-vertical-element meridional section for the thermohaline flow in the Atlantic Ocean, with a "simplified global linkage (CDW)." Purple denotes an upper layer, red indicates intermediate water, green deep, and dark blue bottom. Circumpolar Deep Water (CDW) is set off in light blue lines. There are three branches for NADW: Upper, Middle, and Lower North Atlantic Deep Water (UNADW, MNADW, LNADW, respectively). Various geographical and oceanographic features are inserted around the border of the figure. EQ denotes the equator, SFZ is Subpolar Frontal Zone, PFZ is Polar Frontal Zone, AD is Antarctic Divergence, AABW is Antarctic Bottom Water, ASW is Antarctic Surface Water. Transports in Sverdrups in circles.

formed by convection in the SFZ tends to be restricted to the southern segment of the subtropical gyre, although a couple of Sverdrups do appear to approach the western boundary and flow through Vitiaz Strait. So how do we supply the IT? Clearly some diapycnal upward conversion to USAMW (and eventually SLW) is required. In this report I have opted for the Peru Current as a likely location for this interaction, but another possibility would involve a recirculating spiral in the subtropical gyre. In Figure II-14 there is also high oxygen near bottom water penetration north with indications of a deep replacement flow just above at intermediate oxygen values. The discus-

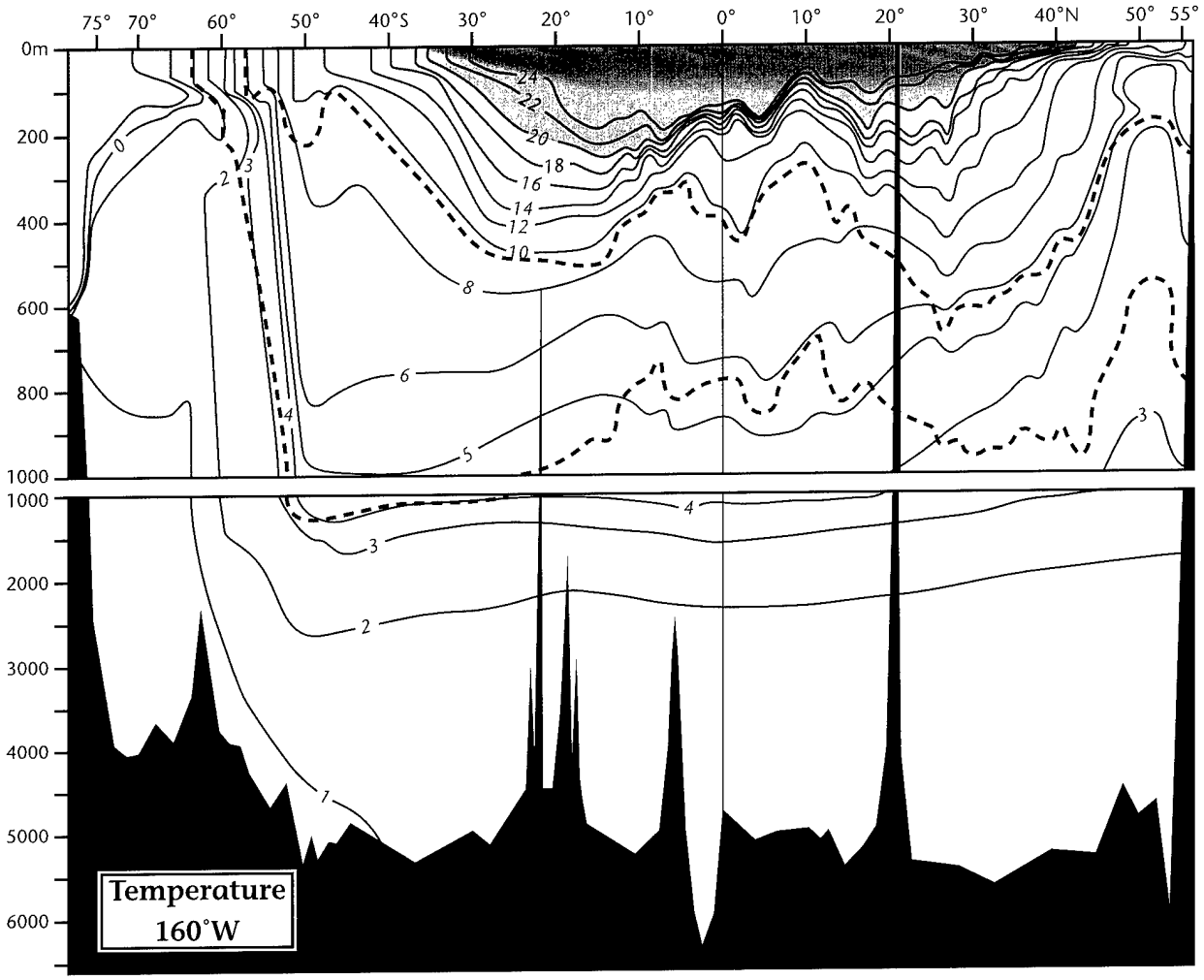

Figure II-12: Temperature (°C) along approximately 160°W, from Antarctica to Alaska, adapted from Reid (1965, his figure 2). The dashed lines are the depths of the surfaces with σ_t approximately equal to 26.8 and 27.3.

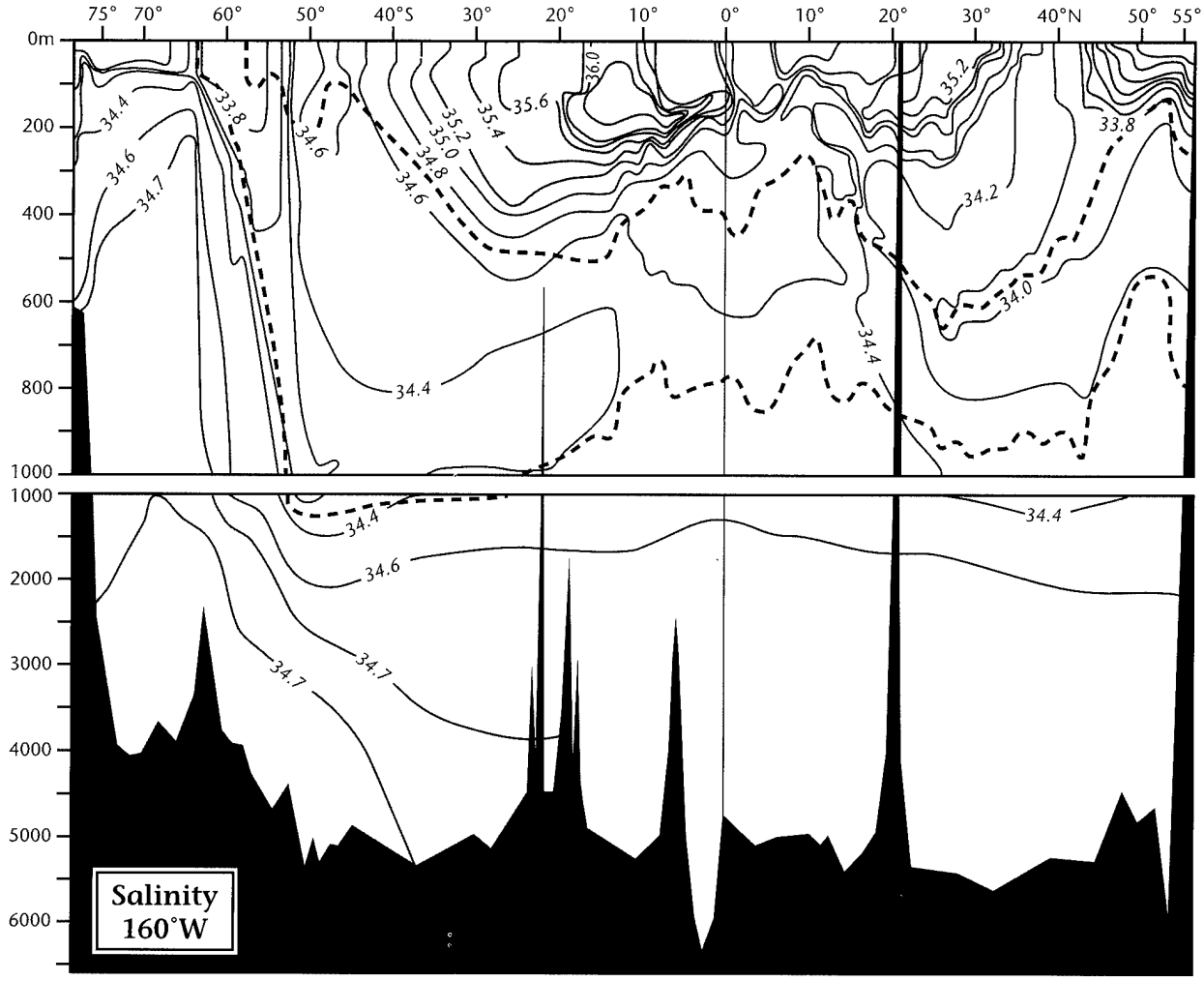

Figure II-13: Salinity (psu) along approximately 160°W, from Antarctica to Alaska, adapted from Reid (1965, his figure 3). The dashed lines are the depths of σ_t surfaces as in Figure II-12.

sion of the bottom/deep cell in the Pacific Ocean is best done with silica distributions; please see Section 2 below. There is perhaps a hint in Figures II-13 and II-14 that some NPIW penetrates toward and moves upward into the low-latitude regimes supplying the IT.

Meridional sections down the interior of the Indian Ocean, taken from the Indian Ocean Atlas (Wyrtki, 1971), are shown in Figures II-15, 16 and 17. These sections were to some extent selected for different reasons than the choices for the Pacific. For the Indian Ocean there are recent publications (Toole and Warren, 1993; Mantyla and Reid, 1995; RT96) that are comparatively clear about the pathways for how the CDW

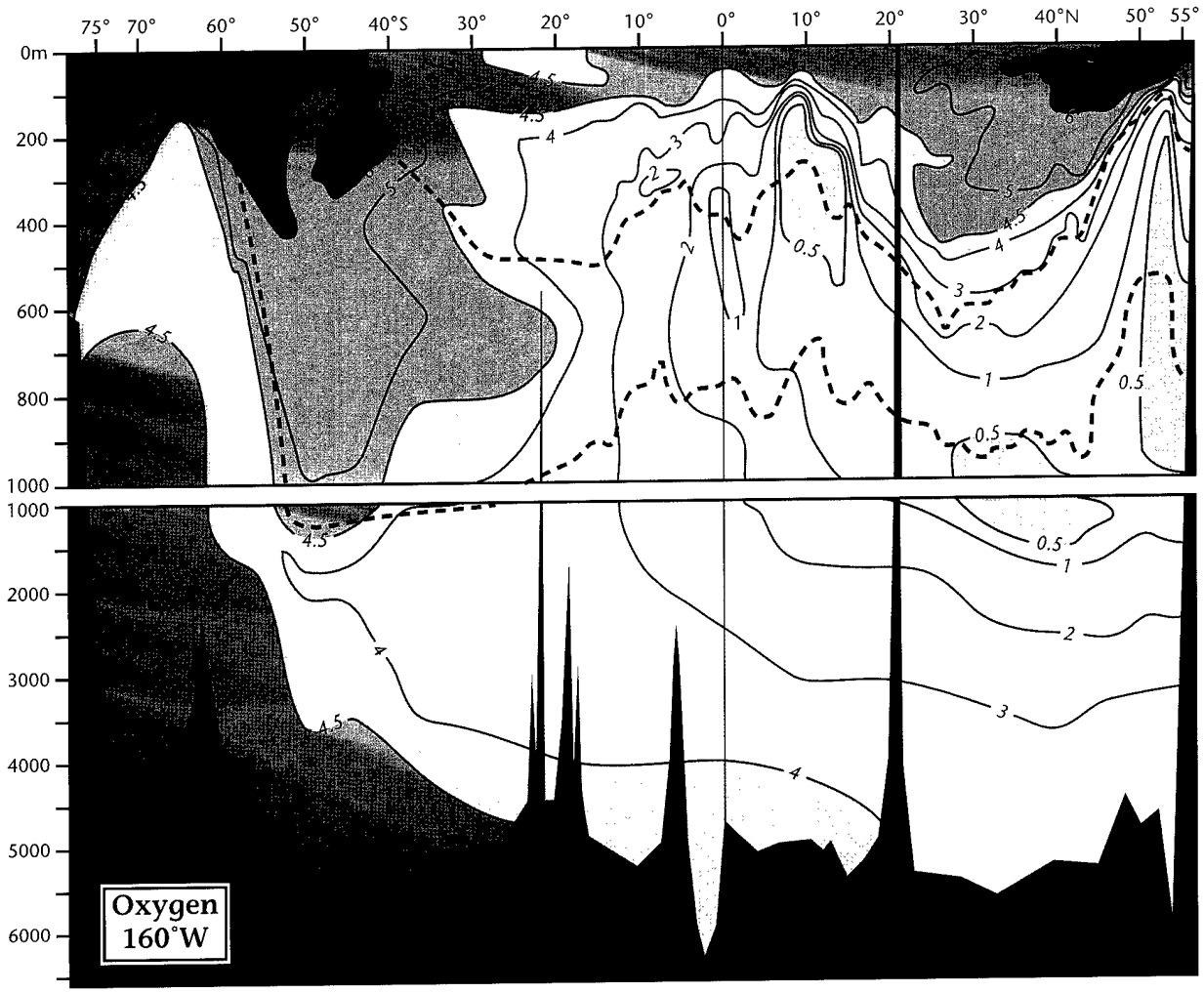

Figure II-14: Oxygen (ml L^{-1}) along approximately 160°W, from Antarctica to Alaska, adapted from Reid (1965, his figure 4). The dashed lines are the depths of σ_t surfaces as in Figure II-12.

and NADW enter and transit the Indian Ocean from the south (please also see the Indian Ocean Atlas, Wyrtki, 1971, pp. 471–474). These pathways also have, at 32°S, a well-defined transport amplitude, including recirculations (RT96, Section 3 below). The location and transport amplitudes of the upper ocean return flows in the ACS at 32°S are well documented by RT96, but identification of how and where these deep flows are converted to upper layer flows and the distribution and path of these flows is much less well developed observationally. The sections in II-15, 16 and 17 were chosen to introduce a discussion of the (diapycnal) upward limb of the meridional cell north of 32°S in the Indian Ocean, that is, the replacement flow for CDW and "NADW," to a

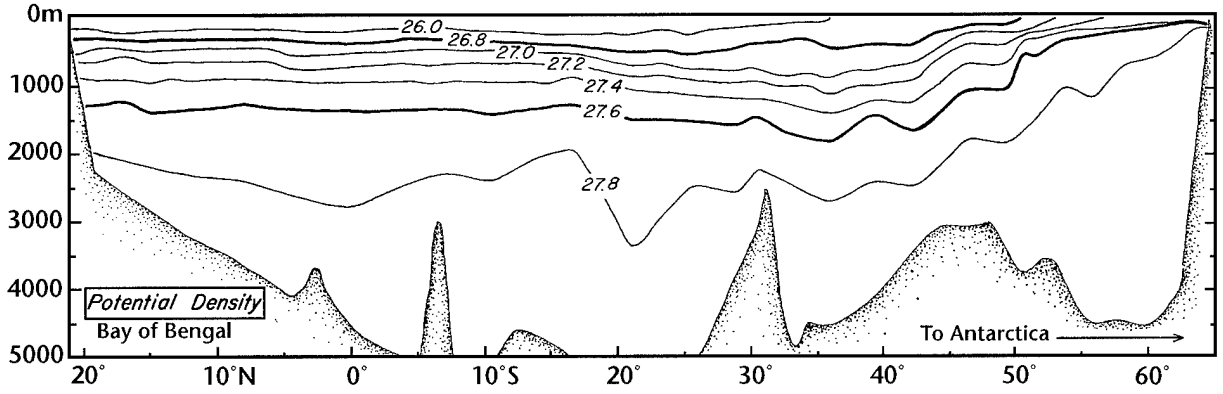

Figure II-15: A potential density section from the Bay of Bengal to Antarctica, adapted from p. 410 in the Indian Ocean Atlas (Wyrtki, 1971).

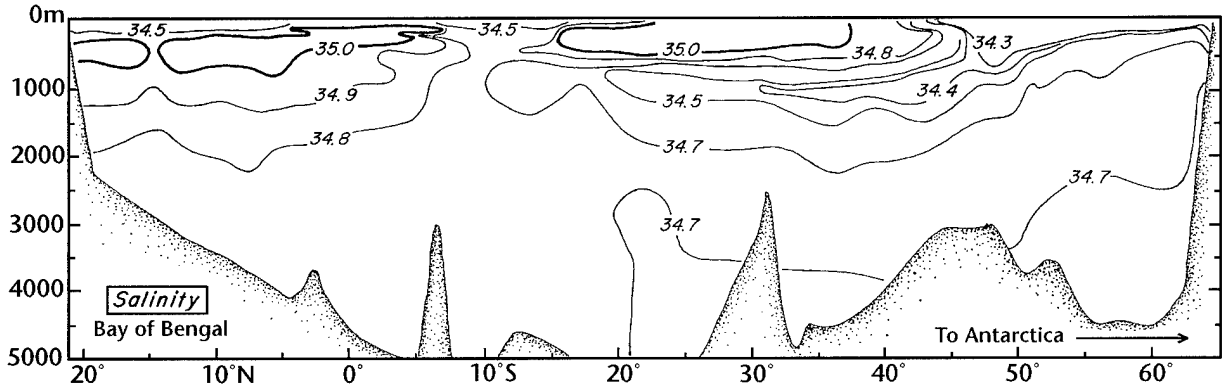

Figure II-16: A salinity section from the Bay of Bengal to Antarctica, adapted from p. 412 in the Indian Ocean Atlas (Wyrtki, 1971).

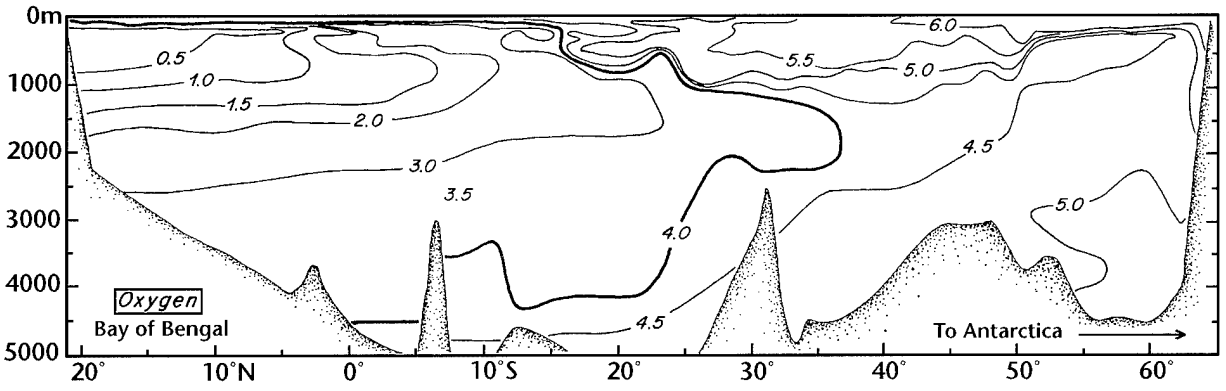

Figure II-17: An oxygen section from the Bay of Bengal to Antarctica, adapted from p. 413 in the Indian Ocean Atlas (Wyrtki, 1971).

large extent by IW (please see Section 3d for a detailed discussion of IW in the Indian Ocean).

The salinity section in Figure II-16 is characterized by S = 34.7–34.8 over the bottom 2000–3000 m of the entire section, that is, below $\sigma_\theta \doteq 27.8$. In the northern Indian Ocean salinity values increase moving up into the IW density parameter range ($26.8 \leq \sigma_\theta \leq 27.5$, located in the depth range 400 to 1100 m), say, north of the equator. South of about 15–20°S one sees the typical strong tongue of low salinity intermediate water of circumpolar origin. Moving up in the North Indian Ocean across 34.7 to 34.8 and 34.9 salinity values, oxygen values (Figure II-17) become lower and contours penetrate south in the IW density parameter range. This was called Northwest Indian Intermediate Water by Rochford (1961, 1963).

The upper density range of Northwest Indian Intermediate Water (NIIW) has, in my opinion, recently been observed by Fieux *et al.* (1994) to flow from the North to South Indian Oceans in a boundary current along the coasts of Sumatra and Java and probably to join the SEC under the IT south of Java and west of the longitude of Bali. If this water is taken to be part of the component of the SEC that is driven west by the wind field, then an additional reason for a "large" SEC in the Indian Ocean, other than the IT only (Godfrey and Golding, 1981), exists. I am using the abbreviation NIIW for Northwest Indian Intermediate Water as opposed to NIW (North Indian Water) as proposed by Fieux *et al.* (1994) because I want to retain Intermediate in the title. Please also note in Figure II-16 the blob associated with the 34.7 salinity contour in the 10–15°S range, at around 1000 m depth, for σ_θ 27.2 → 27.6 or so and potential temperatures approximately 4–6°C. This was called Banda Intermediate Water (hereafter BIW) by Rochford (1961, 1963, 1966), with BIW's more pristine characteristics in Rochford's main area of operations about 20° of longitude east of the section in Figure II-16 being slightly fresher and cooler than noted above in this paragraph.

Banda and Northwest Indian Intermediate Water could represent the result of diapycnal transformations from deep water to IW by the meridional cell in the Indian Ocean, to some extent in contrast to a small increase in the T, S properties of intermediate water of circumpolar origin associated with "more routine" vertical and horizontal mixing. The southward penetration of the 4.0 oxygen contour near 2000 m depth from the northern Indian Ocean to 25–35°S in Figure II-17 represents (to me) the

return of upper deep water (RT96; discussed in Section 3 below), or what will also here be called Indian Ocean Deep Water (IODW), toward the ACCS. The suggestions that I'm making about BIW and NIIW representing a diapycnal transformation for the lower part of the Indian Ocean meridional cell are new but not substantiated (see Section 3d below). The transport of Banda Intermediate Water may be too low to be a major player in the upward limb of the meridional cell, and may be associated with exchange with the Banda Sea. Please note that Banda Sea Water and BIW may or may not be the same water masses (discussed below). According to Fieux *et al.* (1994), Wyrtki (1961) took Banda Sea Water to be formed by mixing of North Pacific Subtropical Water, Pacific Intermediate Water, and some water from the shallow and low salinity Java Sea.

A global eddy kinetic energy (K_E) map at the sea surface (also from Volume I, Figure I-13 there) is reproduced here as Figure II-18 to orient the reader to the material I will be presenting on the mesoscale eddy field. K_E, $(\bar{u}, \bar{v})$ (u', v'), and $\overline{u'v'}$ are defined as usual; see, for example, Volume I of this report or S96. The North Pacific, South Indian and North Atlantic Oceans have roughly (Figure II-18) the same general amplitudes and pattern of geographical variation in K_E. In Figure II-18, the area occupied by the K_E = 1000 and 600 cm^2 s^{-2} contours in the western boundary current regions of the South Pacific (East Australian Current) and South Atlantic (Brazil Current) is significantly smaller than in the other, more energetic, ocean basins. According to S96, this is dependent on the strength of the mean flows (the main source of mesoscale eddies via an instability process) which are less intense in the South Pacific and South Atlantic as a result of upper ocean cross-equatorial transports of 10–15 Sv in each ocean.

The distributions of K_E as a function of depth $[K_E(z)]$ in the most energetic segments of the Western Boundary Currents in the more energetic oceans are shown to be similar in Figure II-19 (adapted from S96), except that the Kuroshio $K_E(z)$ distribution in Figure II-19 is shifted by a barotropic factor of 100 m^2 s^{-2}. In the Agulhas Retroflection area, K_E values are largest in the "sock" or Agulhas Retroflection where rings pinch off (S96). Different amplitudes and patterns of K_E in various ocean basins may be related to differences in interbasin exchanges. A more detailed examination shows that the zonal scales are somewhat shorter and near-surface energy intensities are smaller in the North Pacific relative to the North Atlantic (Figures II-20, 21 and 22), at all depths sampled. In Figure II-20, there are two estimates for the zonally averaged distri-

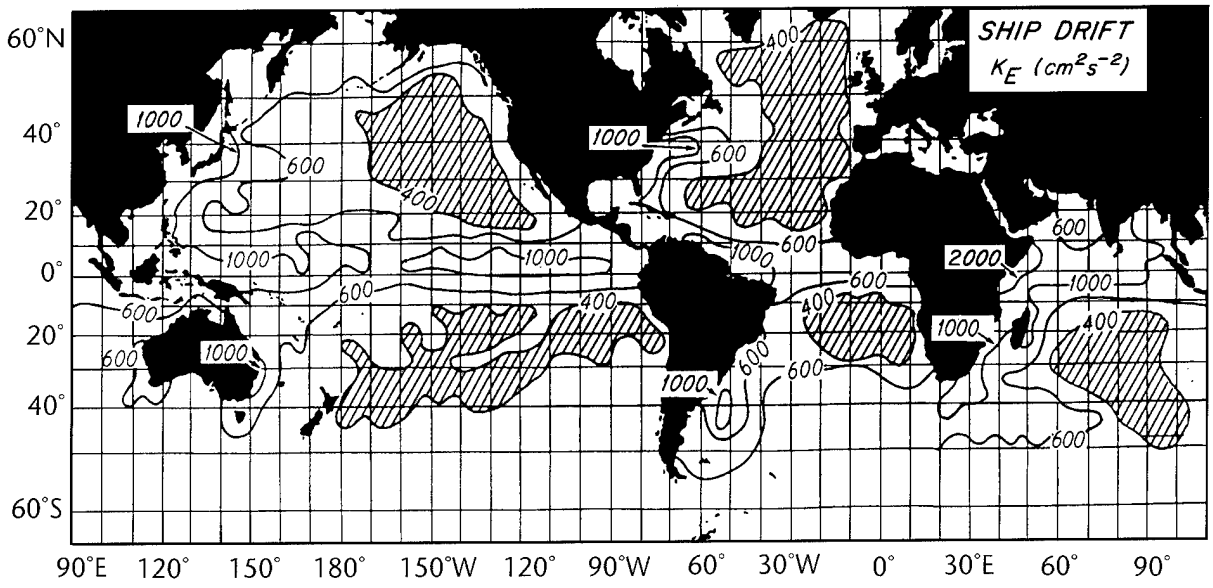

Figure II-18: The global distribution of eddy kinetic energy (K_E) at the sea surface, taken from a combination of Wyrtki *et al.* (1976), Schmitz *et al.* (1983), and Schmitz (1996).

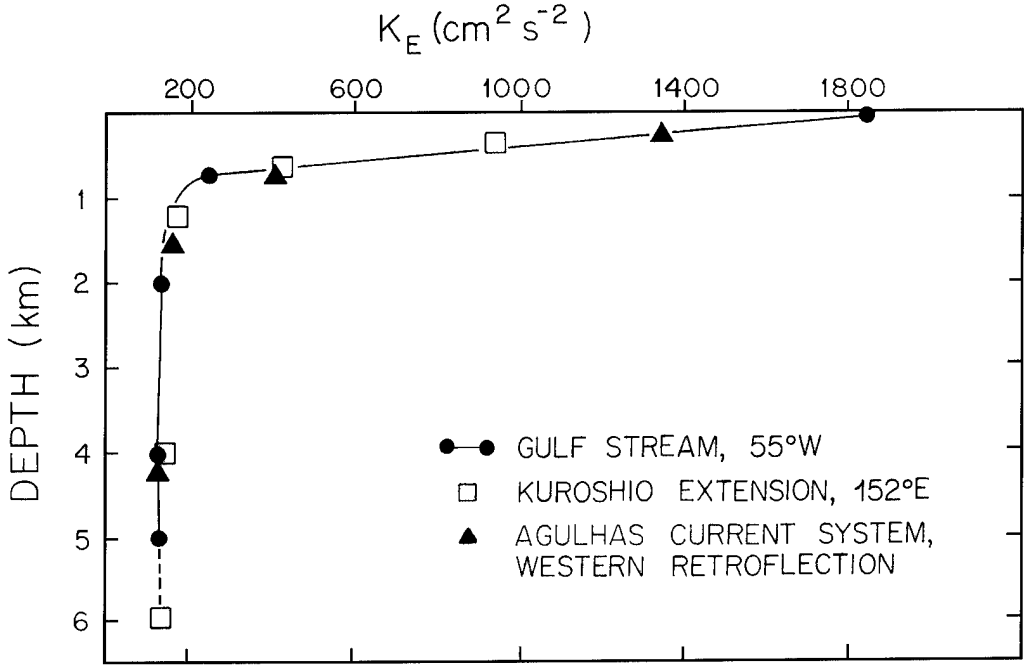

Figure II-19: A comparison of the vertical structure of eddy kinetic energy [$K_E(z)$] at comparatively energetic locations in the three indicated western boundary current systems. A depth-independent 100 cm^2 s^{-1} has been added to the K_E distribution for the Kuroshio Extension at 152°E.

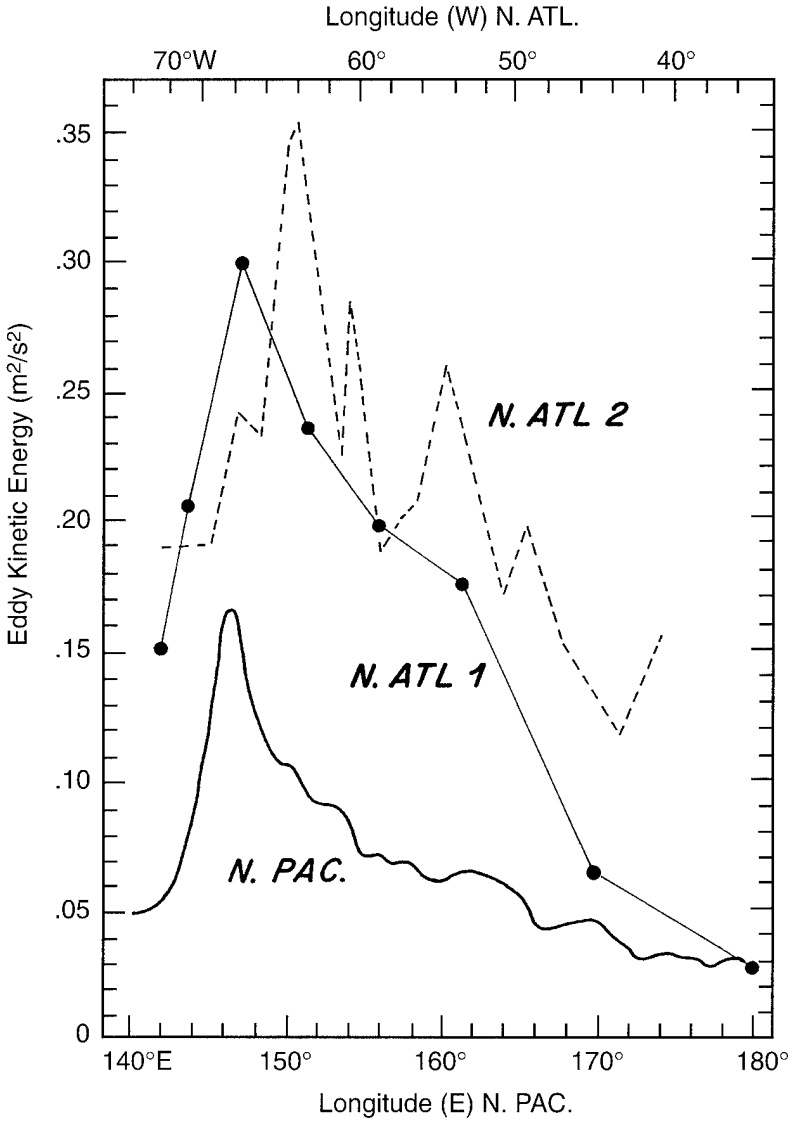

Figure II-20: K_E as a function of longitude at the sea surface for both the Gulf Stream System (solid and dashed lines labeled N. ATL 1 and N. ATL 2, respectively) and the Kuroshio Current System (heavy solid line, labeled N. PAC). The N. PAC results (Qiu *et al.*, 1991, their figure 7) are based on altimetric data, as is N. ATL 2 (S. Singh, K. Kelly, and B. Qiu, personal communication, 1996). N. ATL 1 is based on surface drifter data (Schmitz and Holland, 1986, their figure 22).

bution of K_E along the Gulf Stream, N. ATL 1 and N. ATL 2, the latter based on satellite data and the former on surface drifters. The two estimates are fairly close considering, and there is a ~ 15% bias high of the satellite-based estimates. But both N. ATL estimates are about a factor of 2 higher than for the N. PAC, and penetrate farther east. And there is clearly not a globally canonical barotropic scale factor as is the case for a particular choice of mooring sites and instrument depths in Figure II-19. However, the cross-stream distributions of K_E (and $\overline{u'v'}$) for the Kuroshio and Gulf Stream are similar in shape (Figure II-23). Dickson (1983, 1989) may be consulted for various statistical summaries pertaining to the global eddy field.

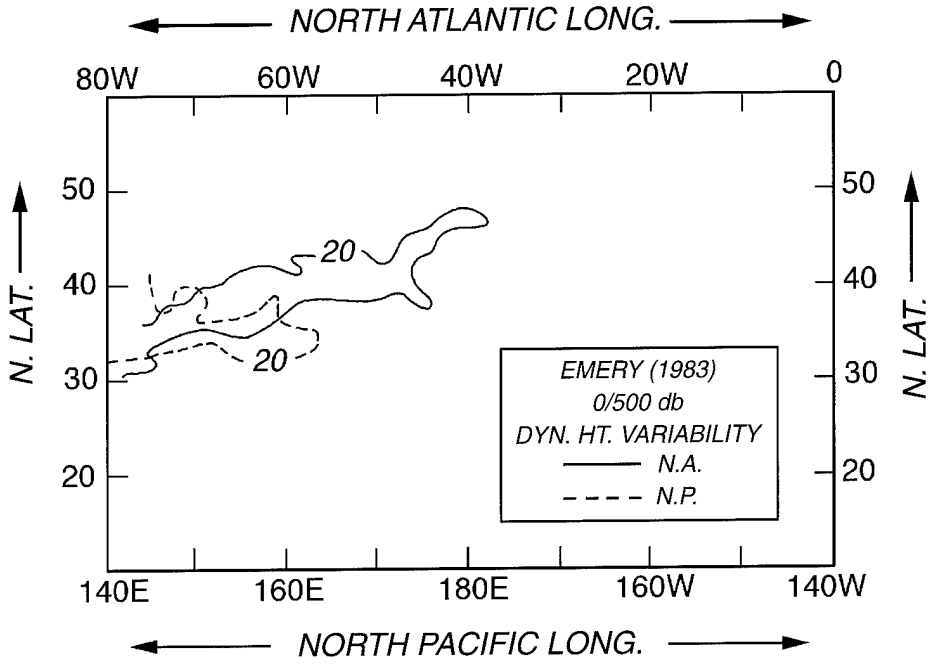

Figure II-21: A comparison of the rms variability (in dynamic centimeters) for contours of dynamic height ΔD (0/500 db) in the Kuroshio Extension (North Pacific) and in the Gulf Stream (North Atlantic), adapted from Emery (1983).

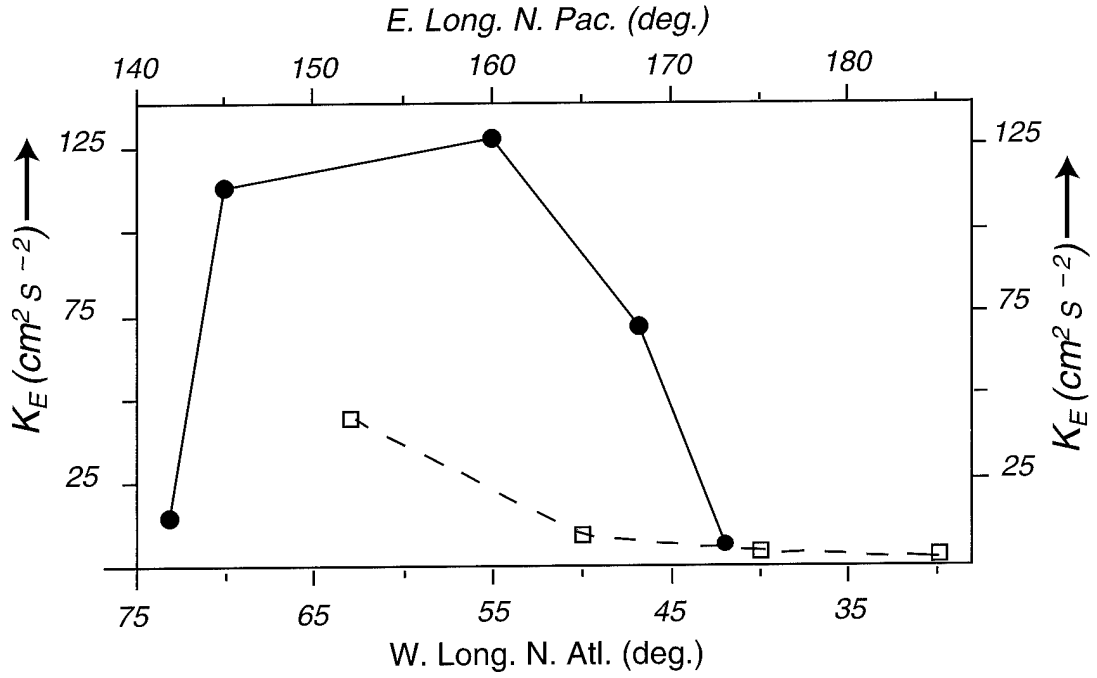

Figure II-22: K_E as a function of longitude at 4000 m depth for the Kuroshio Extension (dashed line) and for the Gulf Stream (solid line), adapted from Schmitz and Holland (1986).

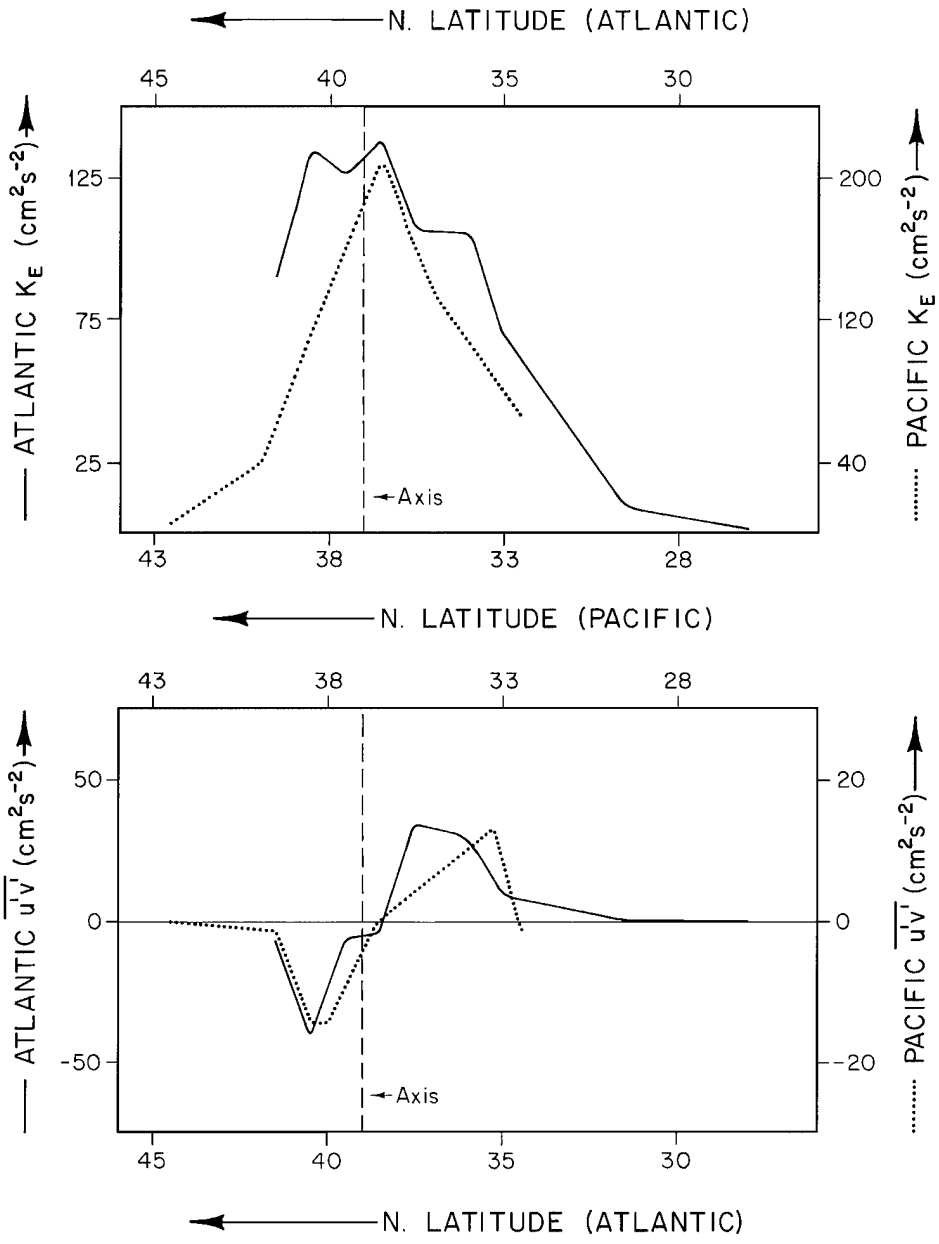

Figure II-23: The cross-stream distributions of K_E and $\overline{u'v'}$ for the Gulf Stream (Atlantic) and the Kuroshio Extension (Pacific), adapted from Schmitz (1982). In this figure, the current axes have been lined up approximately. The Atlantic values are from 4000 m depth at 55°W. The Pacific values were taken from Nishida and White (1982), who used zonally averaged XBT data scaled to vertical shears (speed differences) between 100 and 1000 m depth, west of the Shatsky Rise (~ 165°E).

2. The Pacific Ocean

A sketch of some general features of the interbasin circulation in the World's Oceans was shown in the Introduction as Figure II-8, and the regional structure of upper-layer currents, including those in the Pacific, in Figure II-1. Explicitly data-based, large-scale circulation features of the Pacific Ocean are indicated by a map

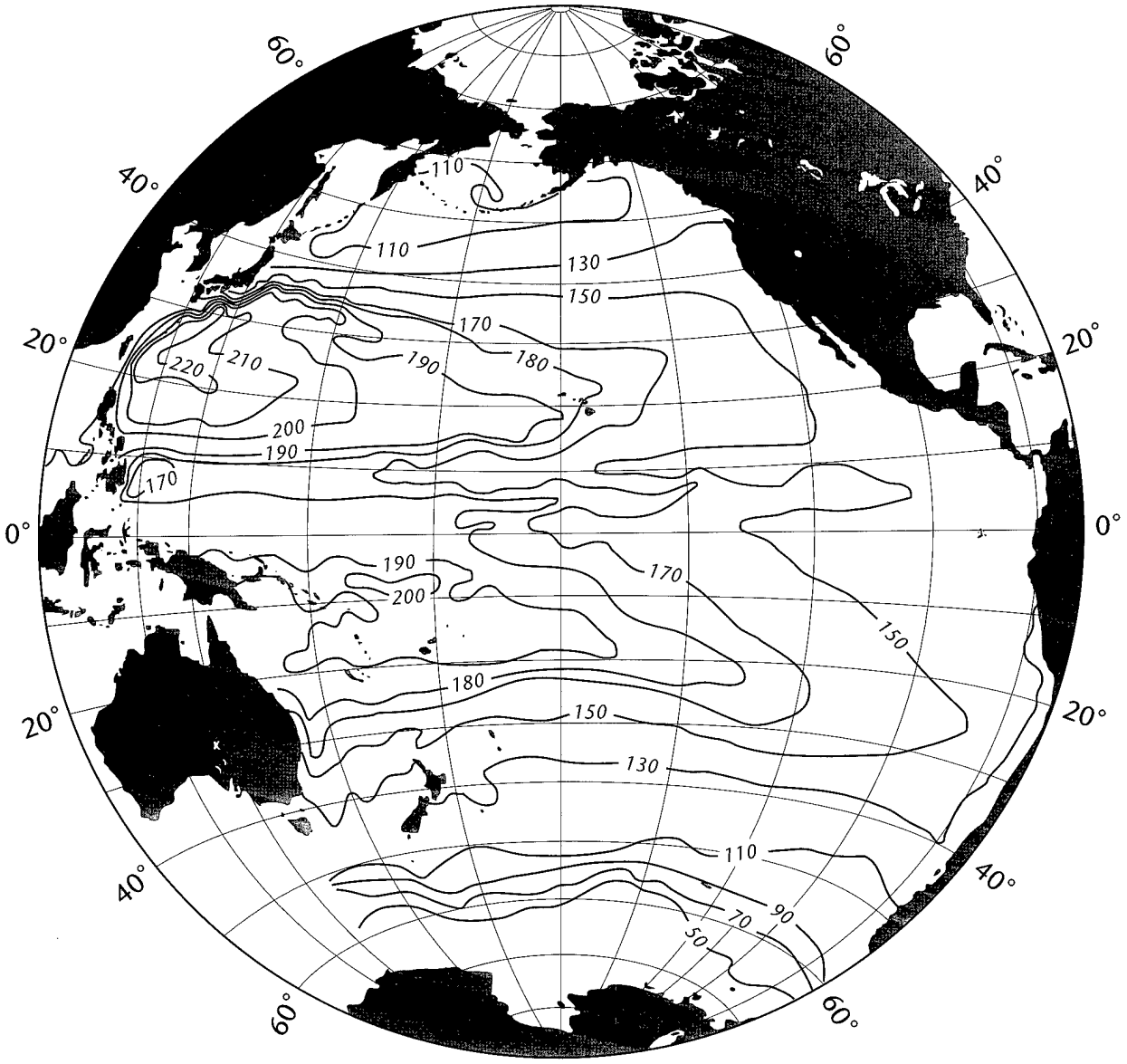

Figure II-24: Selected dynamic height (0/1000 m) contours (in dynamic centimeters) for the Pacific Ocean, adapted from Wyrtki (1974).

(Figure II-24) of the mean dynamic height contours (in dynamic centimeters) for the sea surface relative to 1000 db, adapted from Wyrtki (1974). Nomenclature for the upper-layer currents in the Pacific Ocean to go along to some extent with Figure II-24 is contained in Figure II-25 (the latter adapted from Tabata, 1975). The suite of subtropical western boundary currents in the upper layer North Pacific was referred to as

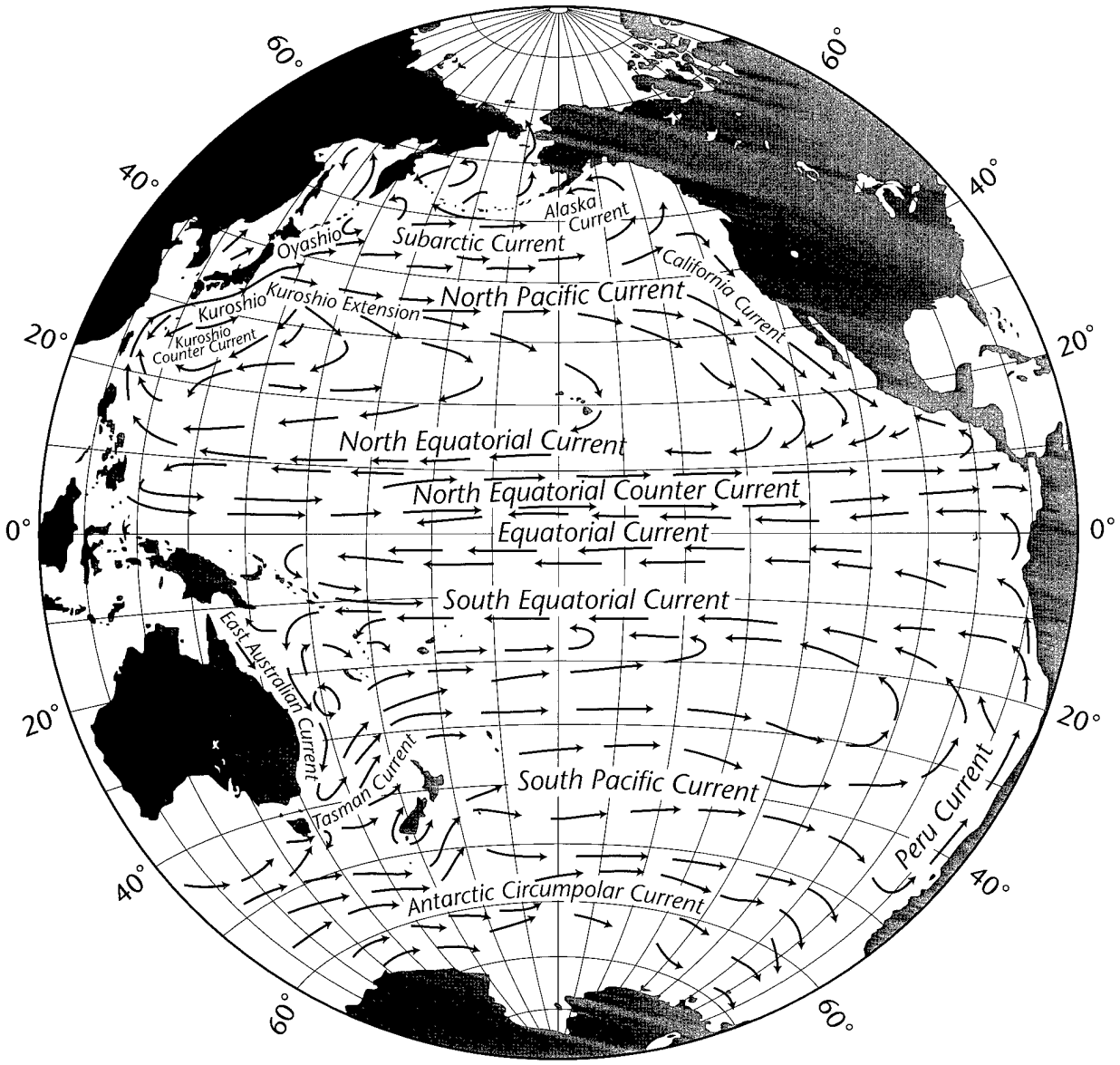

Figure II-25: Nomenclature for selected currents in the Pacific Ocean, adapted from Tabata (1975).

the Kuroshio Current System (KCS) in Figure II-1, and for the South Pacific (in Figure II-1) there is the East Australian Current System (EACS). According to Figure II-25, the KCS is composed of the Kuroshio, Kuroshio Extension and Kuroshio Counter-Current, and the EACS is composed of the East Australian Current (EAC), a recirculation (barely visible in II-25, but see below), and an eastward flow toward the north of New Zealand called the Tasman Current. Here, the Kuroshio Counter-Current will be referred to as the Kuroshio Recirculation, in at least partial analogy to the Gulf Stream

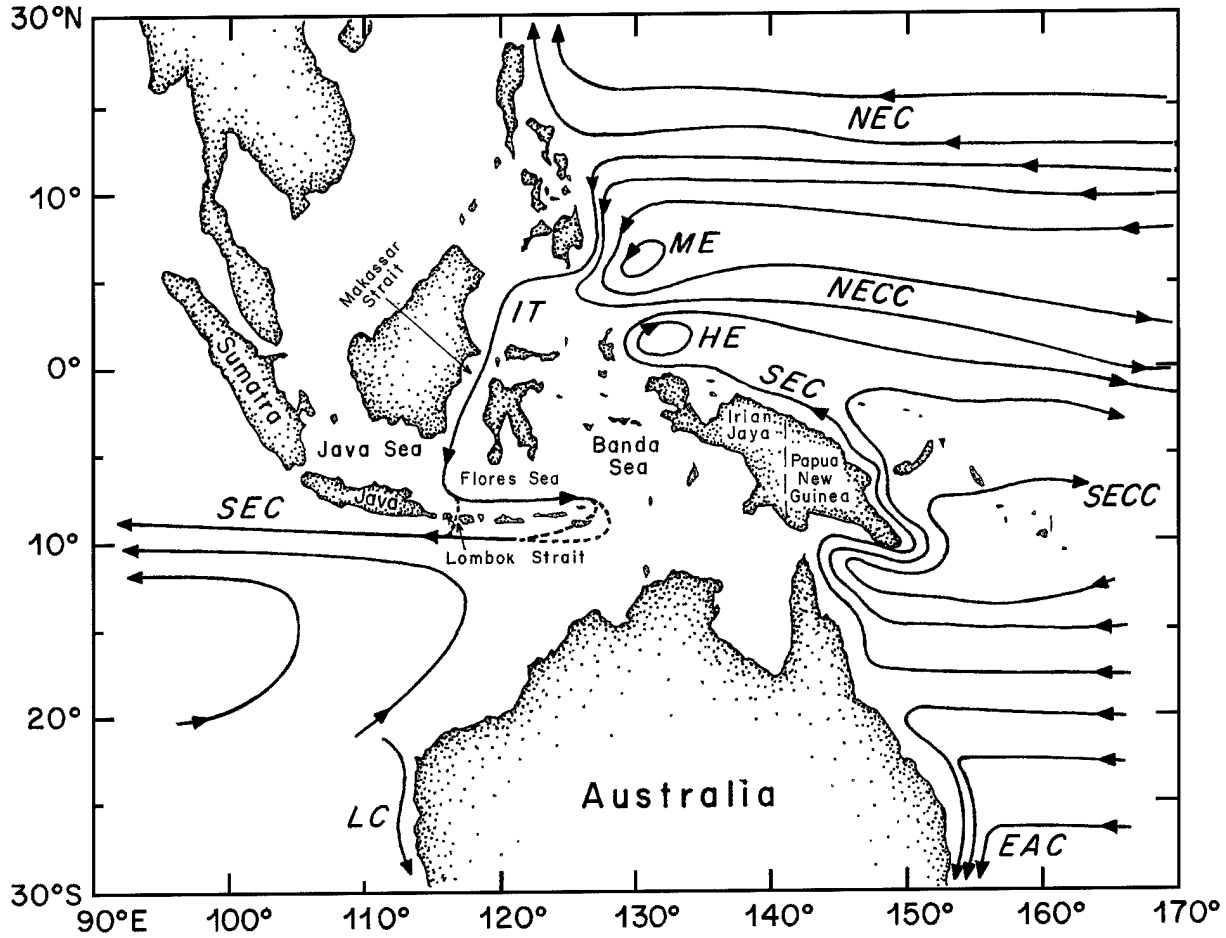

Figure II-26: A schematic of the current patterns near the Indonesian Passages, adapted from Godfrey (1996). NEC, North Equatorial Current; NECC, North Equatorial Countercurrent; HE, Halmahera Eddy; ME, Mindanao Eddy; IT, Indonesian Throughflow; SEC, South Equatorial Current; SECC, South Equatorial Countercurrent; EAC, East Australian Current; and LC, Leeuwin Current.

(please see Volume I of this report). Please note that a list of abbreviations may be found in Appendix D.

A recirculation for the EAC is well documented (Boland and Hamon, 1970; Boland and Church, 1981; Hamon, 1965, 1970; Ridgway and Godfrey, 1994). The article by Ridgway and Godfrey (1994) contains a good definition of the transport of the EAC and its recirculation (their figure 11), and an article by Godfrey and Golding (1981) includes a clear statement of why the EACS is comparatively weak. That is, part of the upper layer, presumably wind-driven, flow in the South Pacific subtropical gyre goes north of Australia and New Guinea (along with some intermediate water I think, and, insofar as I know, the upper layer flow in question has to originate as IW in the ACCS) into various low-latitude current systems and thence the North Pacific, and eventually supplies the IT. The upper layer circulation pattern in the low-latitude western Pacific according to Godfrey (1996) is shown here as Figure II-26. Figures II-26 and II-9, a somewhat analogous figure from Lukas *et al.* (1991), are very consistent, virtually identical, where they overlap. But where does this water originate? If it goes through the IT into the Indian Ocean, then it must approach the South Pacific from south of Australia, possibly by then mostly as SAMW (or IW). So where is SAMW (or intermediate water) transformed into water that becomes "part" of the Sverdrup flow in the South Pacific? A flow of circumpolar water into the eastern South Pacific was identified by Wooster and Reid (1963), and a follow-on (via the SEC) circulation of intermediate water from the South to North Pacific in the west was suggested early on by Reid (1965); see in addition Reid and Mantyla (1978). According to Tsuchiya (1991), intermediate water from the western South Pacific also feeds the Equatorial Current System (but then what?).

The distribution of intermediate water in the Pacific Ocean (Taft, 1963; Reid, 1965; Reid and Mantyla, 1978; McCartney, 1977, 1982; Talley, 1993, 1995) is dominated property-wise by AAIW, NPIW, and LSAMW. Vertical sections of temperature, salinity and oxygen along approximately 160°W from Antarctica to Alaska, taken in modified form from Reid (1965), were shown in Section 1 above as Figures II-12, 13, and 14, respectively. In these figures dashed lines denote the depths of σ surfaces in regions of both UPIW and LOIW, the former, approximately σ_t = 26.8, also coinciding with the core of NPIW, and the latter approximately σ_t = 27.3, representing AAIW. In this report, for interbasin exchange purposes, I tend to think of an upper and a lower

intermediate water where UPIW is defined by $26.8 \leq \sigma_t$ or $\sigma_\theta \leq 27.2$. Lower intermediate water is something like $27.2 \leq \sigma_t$ or $\sigma_\theta \leq 27.5$ and usually, but not always, contains the $S_{\min}$ typically used to define AAIW (in the easternmost South Pacific, the $S_{\min}$ is closer to $\sigma_\theta = 27.15$, *e.g.*, McCartney and Baringer, 1993). In the vicinity of the ACCS, I take SAMW (the nearly isothermal region in the upper 1000 m of Figure II-12

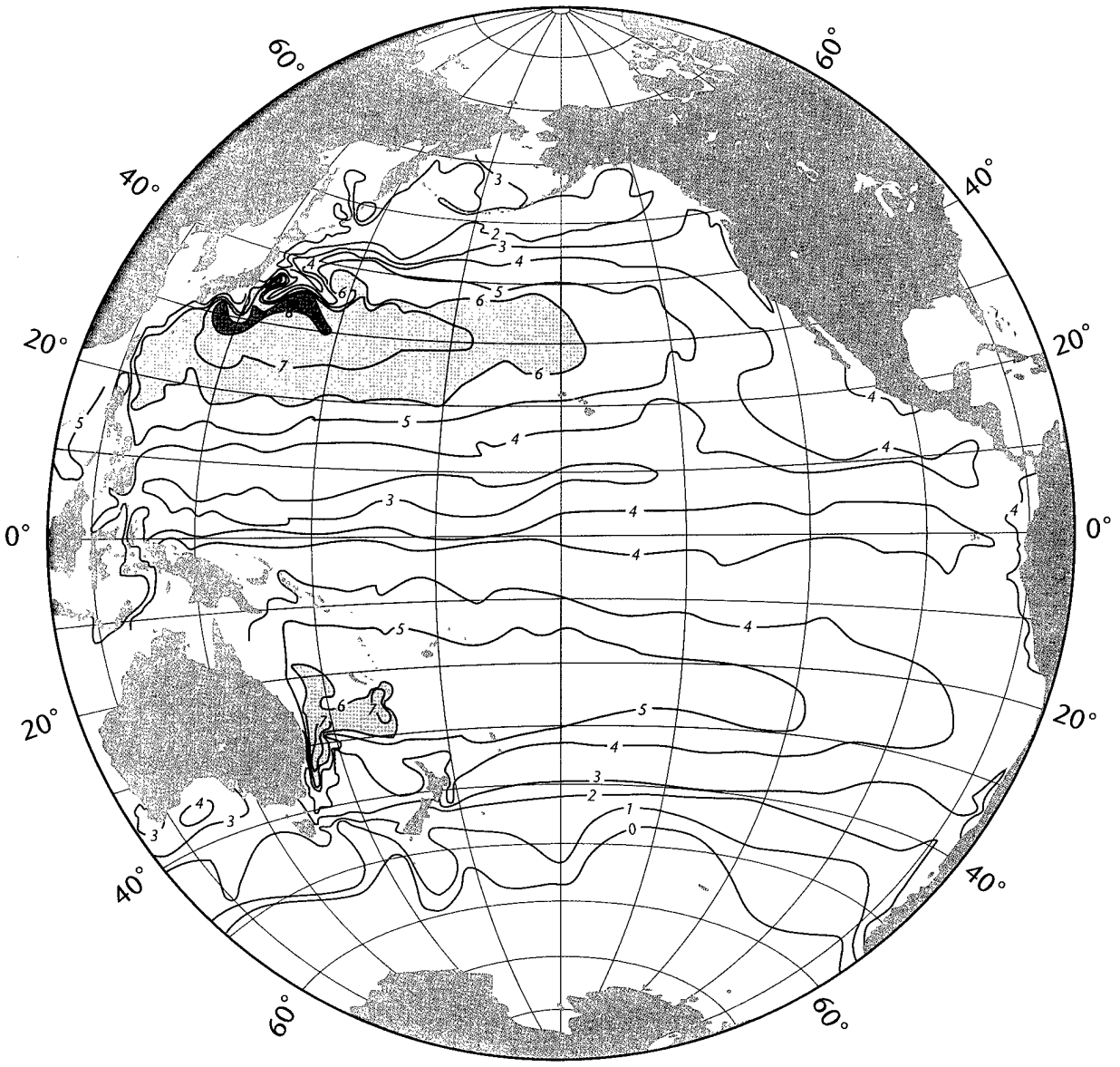

Figure II-27: Depth contours (in hectometers) for the σ_t horizon 26.8 (approximately), adapted from Reid (1965, his figure 17).

between 50 and 60°S) to include UPIW, and, in the northern North Pacific the least dense end of UPIW contains the NPIW core. The vertical–meridional penetration of AAIW and NPIW and SAMW (UPIW) is very clear on the 160°W salinity section (Figure II-13).

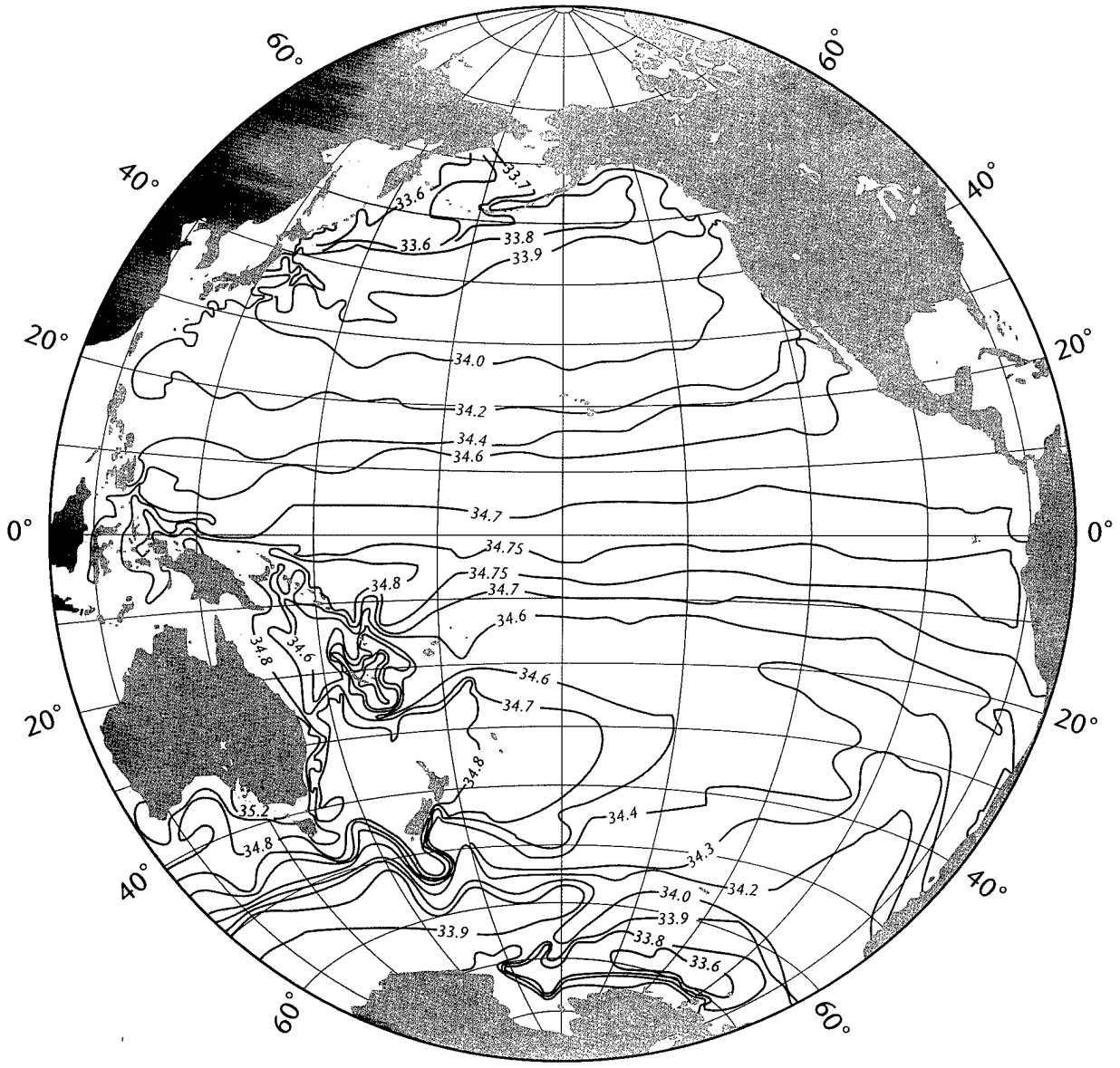

Figure II-28: Salinity contours (psu) on the σ_t horizon 26.8 (approximately), adapted from Reid (1965, his figure 19).

The penetration of UPIW (SAMW) from the ACCS, not only north in the eastern South Pacific, but also along roughly 20°S and then toward Papua New Guinea (in the 400–600 m depth range, say; reference Figure II-27) and thereafter into the North Pacific is clear in Figures II-28 (salinity map for $\sigma_t \doteq 26.8$) and II-29 (corresponding O_2

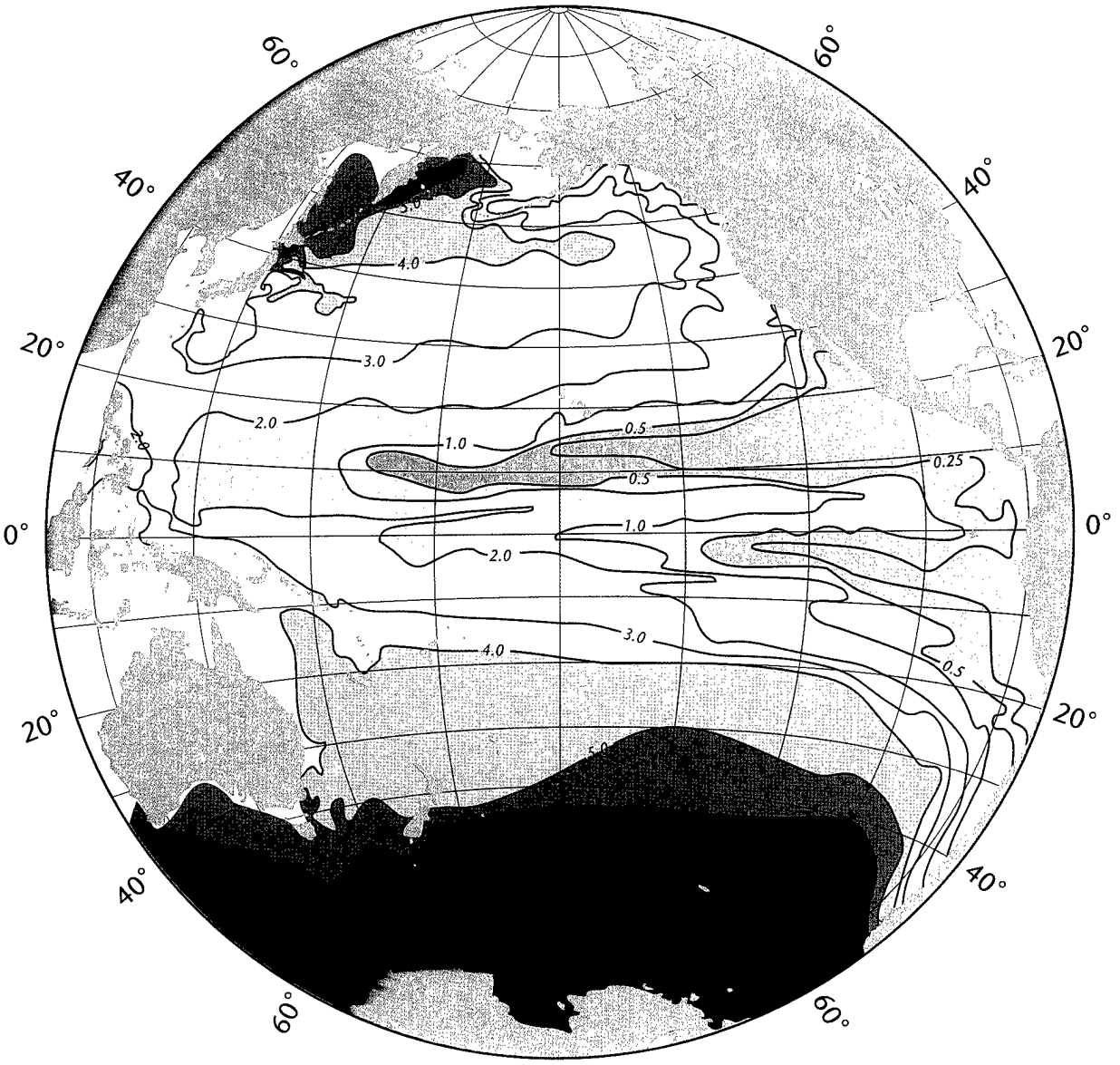

Figure II-29: Oxygen contours (ml L^{-1}) on the σ_t horizon 26.8 (approximately), adapted from Reid (1965, his figure 20).

map). That is, not only are there indications (Figures II-9 and II-26) of an upper layer flow from the wind-driven circulation of the South Pacific, *i.e.*, from the SEC, into the North Pacific (Godfrey and Golding, 1981), but there are also indications of a somewhat similarly located flow of intermediate water (Reid, 1965; Reid and Mantyla, 1978; Tsuchiya, 1991), discussed further in Section 2d. The upper layer ($\sigma_\theta > 26.8$) flow from the South Pacific and into the current patterns and IT as indicated in Figures II-9 and II-26 probably originated in the ACCS as SAMW, or even perhaps some AAIW (LOIW). The highest oxygens in the northwest Pacific in Figure II-29 are indicative of the source area of NPIW. This water presumably circulates with the subpolar and subtropical gyres in the North Pacific (Reid, 1965). North Pacific Intermediate Water ($\sigma_\theta = 26.7 \rightarrow 26.9$, say) has been described by Reid (1965), Talley (1993, 1995), and Qiu (1995), and is characterized by a salinity minimum located at $\sigma_\theta = 26.8$, roughly coincident with the density horizon described by Figures II-27–29. Intermediate Water (see Section 2d) also propagates northward (Reid, 1965; Wooster and Reid, 1963) from the ACCS into the South Pacific, mostly in its eastern segments and then flows in the SEC, to some extent along with the subtropical gyre. Intermediate water from the South Pacific penetrates into the North Pacific as well (Reid, 1965; Reid and Mantyla, 1978). According to Wijffels (1993, her figure 3.12), AAIW also circulates anticyclonically in the Coral Sea. There may also be a slight northward penetration into the western South Pacific (Burling, 1961; Reid, 1965) near New Zealand from the ACCS (see also for example, figures 8 and 9 by Reid, 1986).

A meridional section of silica along 170°W is contained in Figure II-30, adapted from Reid (1986, his figure 15). This section is separated from that contained in Figures II-12, 13 and 14 by only 10° in longitude, but it is shown here because silica is the key indicator of the Pacific deep and bottom water circulation. In this report, the usage of the nomenclature "silica" is adopted for all such measurements, to be consistent with Talley and Joyce (1992) and Talley (1995). The silica distribution in Figure II-30 suggests a northward abyssal flow from the ACCS of CDW (low silica), and a southward flow of NPDW (North Pacific Deep Water) at 2000–3500 m depth, say, where there is a silica maximum. There is also an indication of this flow pattern in the O_2 section along 160°W in Figure II-14. But does the tongue of "high" silica in Figure II-30 or of "low" O_2 in Figure II-14 imply a contiguous circulation south all the way from the northern North Pacific to 40°S?, or is there a "set of recirculations" in between? (see below, and

Section 2e). The meridional and zonal sections available yield a fairly reasonable picture of the general features of the CDW/NPDW meridional cell components (Section 2f) in the Pacific Ocean, including recirculations of CDW. But the horizontal flow patterns of this cell are more difficult to sort out (Section 2e below). The 160°W (Figures 12, 13 and 14) and 170°W (Figure II-30) meridional sections cut through the section recently completed by Roemmich *et al.* (1996) along a quasi-zonal path (15–20°S) across the abyssal gap (150°W–170°E) that must contain the Pacific bottom/deep cell.

There are questions in my mind about the relative roles played by the "recirculation" of comparatively low silica water versus a replacement flow of "high silica NPDW," in terms of the return of mass to the ACCS. For example, in Figure II-30 the value of the silica maximum (120 mol m^{-3}) of the return flow to the ACCS near 40–45°S is not significantly different from the source silica value of ~ 100–120 in CDW at 45–60°S, and a long way removed from the silica maximum values of ~ 170 that occur in the actual North Pacific according to Figure II-30. Also the highest value of silica (Figure II-30) at the silica maximum is only 140 in the low-latitude South Pacific. So the "continuity" of the silica maximum down the entire Pacific Ocean in Figure II-30

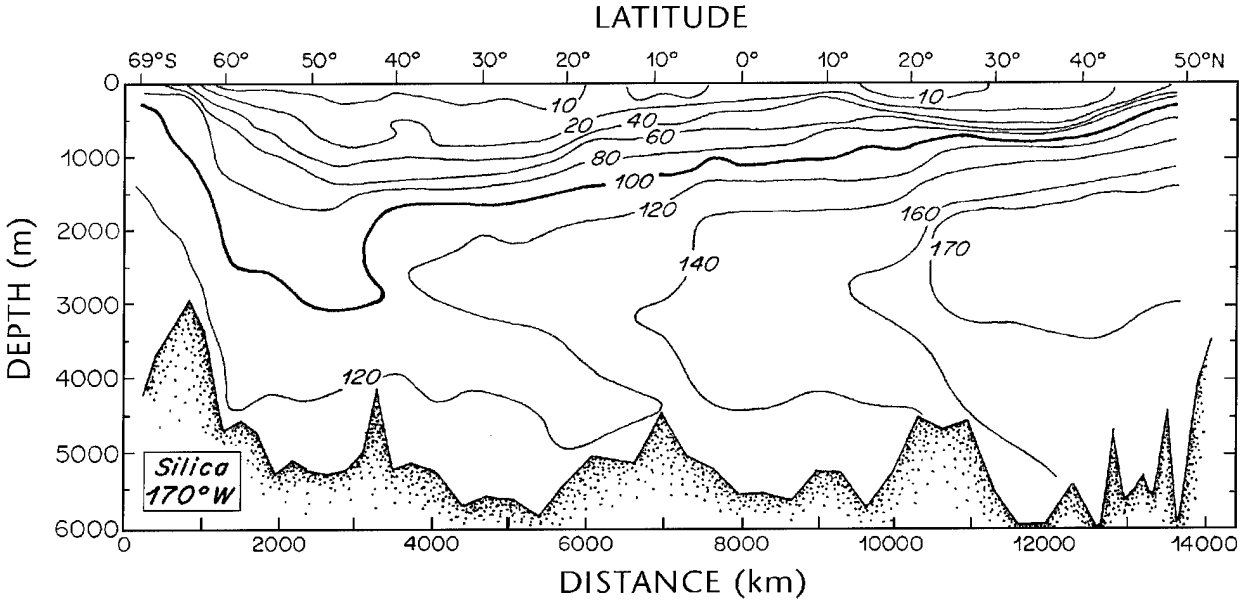

Figure II-30: A meridional section of silica (mol m^{-3}) along 170°W. Adapted from Reid (1986; his figure 15); depths in meters.

might not be an unambiguous indicator of a flow of NPDW from the northern North Pacific to the ACCS. There may instead exist a few (2–4) quasi-horizontal gyres of deep water, interacting with modified CDW below (and even AAIW above), and therefore containing "moderate" silica concentrations, to return much of the necessary mass (volume) flux to the ACCS through intergyre exchanges. These points are discussed further in Sections 2e and 2f.

A zonal section across 24°N was made in the spring of 1985 (Roemmich *et al.*, 1991) and the data contours presented as color plates in the *Deep-Sea Research* volume honoring Joe Reid (Supplement No. 1 to Vol. *38*). Potential temperature and silica sections are shown here in idealized form in Figures II-31 and II-32. In these sections one can clearly see CDW in the west (the near bottom 140 silica contour, and the ~ 4000-m 150 contour) and NPDW east of 170°E, along with possible indications of some recirculation of CDW (*i.e.* the silica 150 contour in the eastern part of the section centered on 150°W near the bottom). Transport estimates for this data set across 24°N by Bryden *et al.* (1991) are presented in Section 2f.

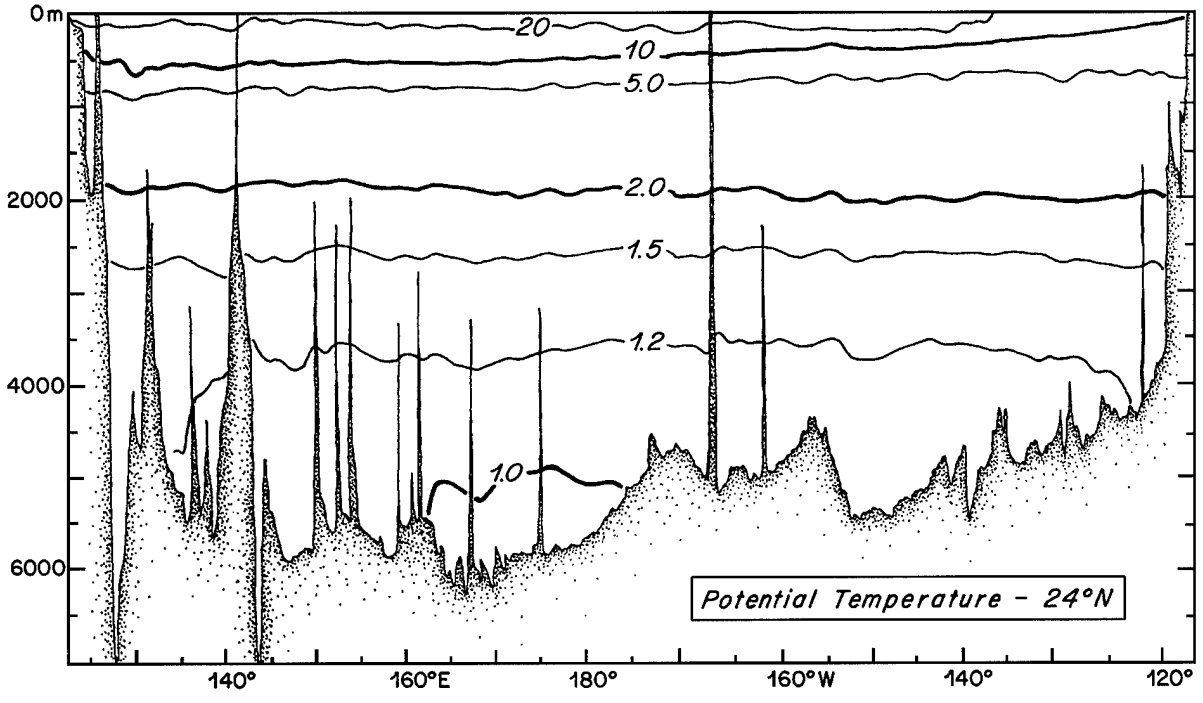

Figure II-31: A potential temperature (°C) summary section at 24°N in the Pacific Ocean, adapted from Roemmich *et al.* (1991).

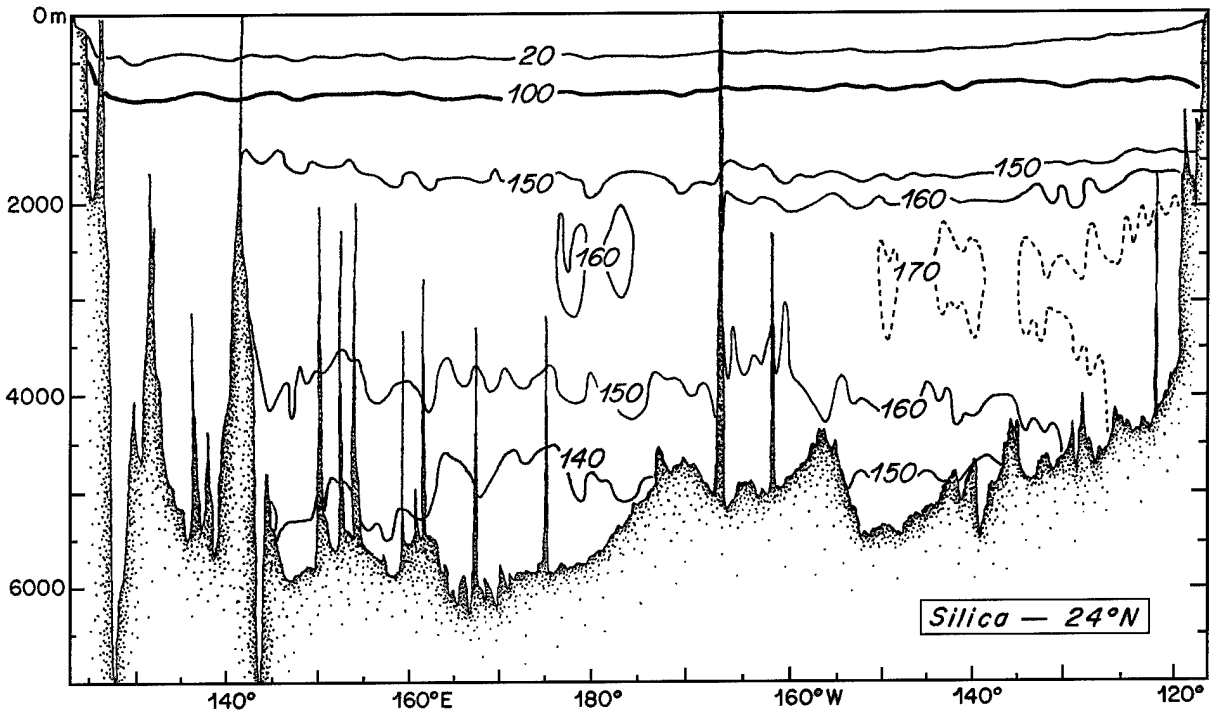

Figure II-32: A summary section for silica at 24°N in the Pacific Ocean, adapted from Roemmich *et al.* (1991).

A 10°N section has been written up by Johnson (1990), Johnson and Toole (1993), Wijffels (1993), and Wijffels *et al.* (1996). Potential temperature and silica transects are included here as Figures II-33 and II-34. At 10°N, incoming CDW is the cold water near the bottom between roughly 170°E and 170° W, recirculating CDW is identified by the sloping 1 and 1.1° isotherms and low silica near the bottom between 160°W and 140°W, and NPDW by the sloping 1.1, 1.2, 1.4 and 1.6°C isotherms between 100 and 125°W. Although CDW shows up in the θ sections at both 10° and 24°N (more clearly at 10°N), it is the silica distributions across both 10°N and 24°N (Figures II-32 and 34) that are clear (but see comments below on horizonal patterns) with respect to the incoming, northward-flowing (and recirculating) CDW (comparatively low silica) and outgoing, southward-flowing NPDW (high silica). At 10°N, it looks like both the 150 and 140 silica contours that are associated with the incoming (northward flowing) CDW between 170°E and 170°W are recirculating east of 170°W. Furthermore, there are downward sloping isotherms (Figure II-33) between 105 and 130°W along 10°N near the bottom on the East Pacific Rise associated with the 150–160 silica range

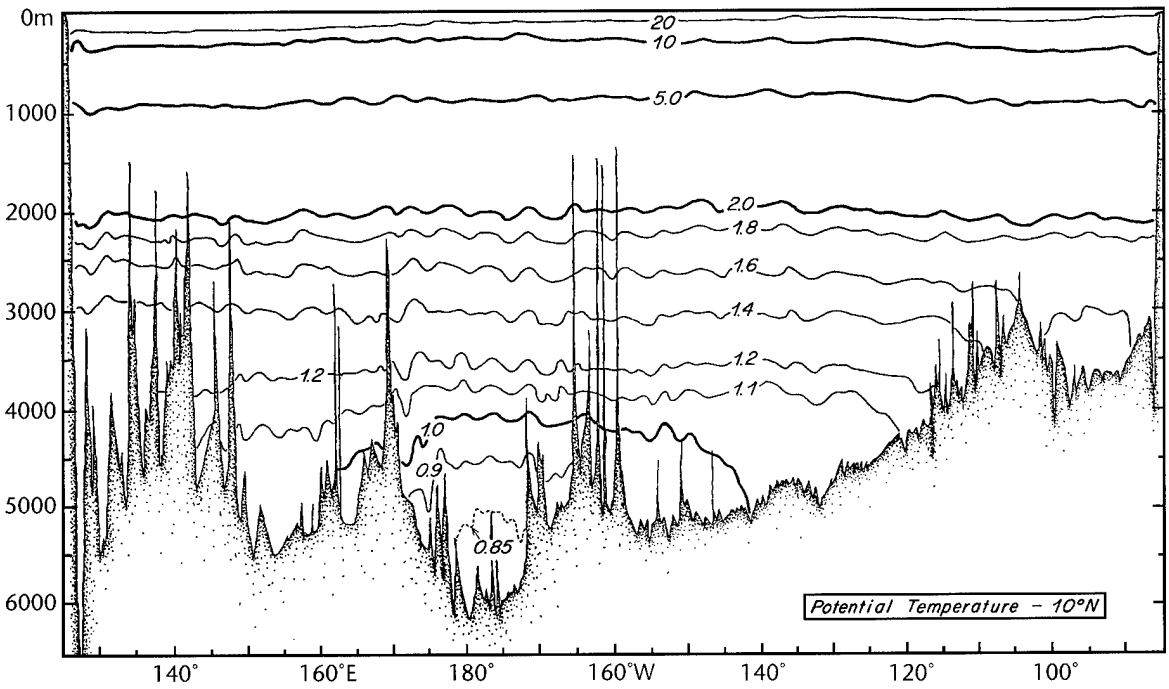

Figure II-33: A potential temperature (°C) summary section at 10°N in the Pacific Ocean, adapted from Wijffels *et al.* (1996).

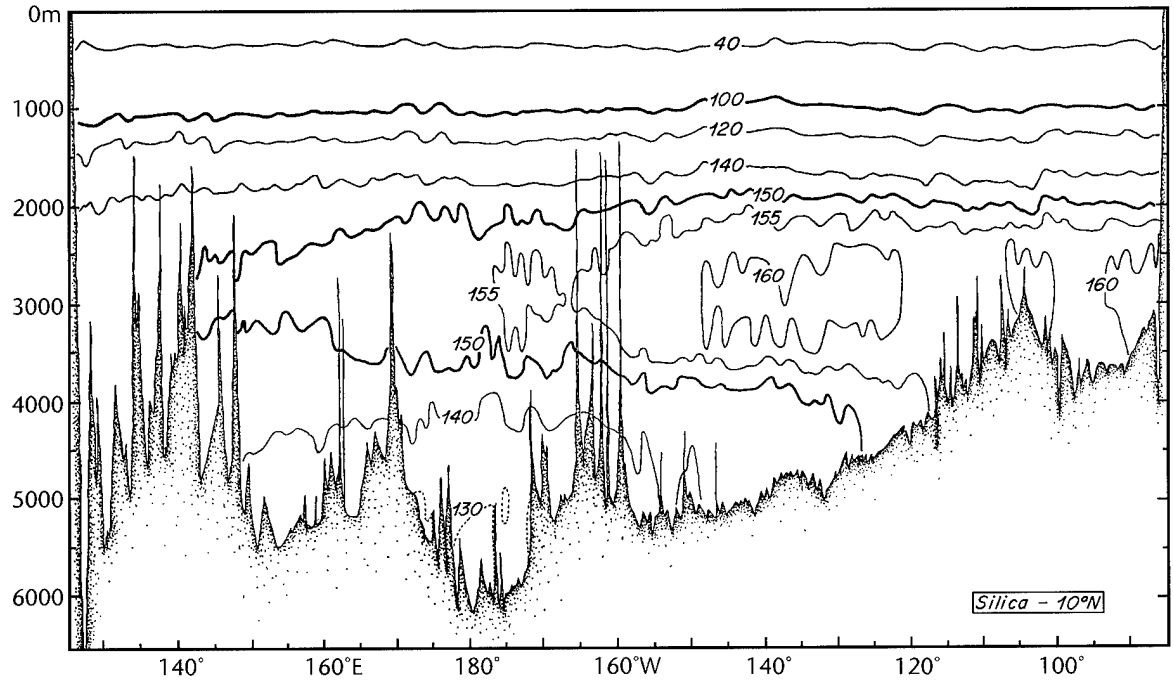

Figure II-34: A summary section for silica at 10°N in the Pacific Ocean, adapted from Wijffels *et al.* (1996).

(Figure II-34). This observation has been used by Wijffels (1993) to resolve a dilemma connected with balancing CDW and NPDW. Johnson and Toole (1993, their figure 11) have suggested a low-latitude recirculation gyre for Lower Circumpolar Water. Their figure has been discussed further by Hogg and Johns (1995). Partial results of an inverse calculation (Wijffels *et al.*, 1996; see their table 3) in terms of transport across 10°N in broad water-mass classes are also discussed in Section 2f.

Recent quasi-zonal, near bottom sections of θ and silica between 150 and 180°W across the Samoan Passage region are shown in Figures II-35 and II-36 (adapted from Roemmich *et al.*, 1996). Circumpolar Deep Water flowing northward across this section is very clear, and the transport estimates by Roemmich *et al.* (1996) are the best yet, rather definitive at approximately 10 Sv (about 6 of which are in the "conventional" Samoan Passage regime). Toole *et al.* (1994b) have recently completed a zonal section across (nominal) 32°S. Potential temperature and silica sections are shown in

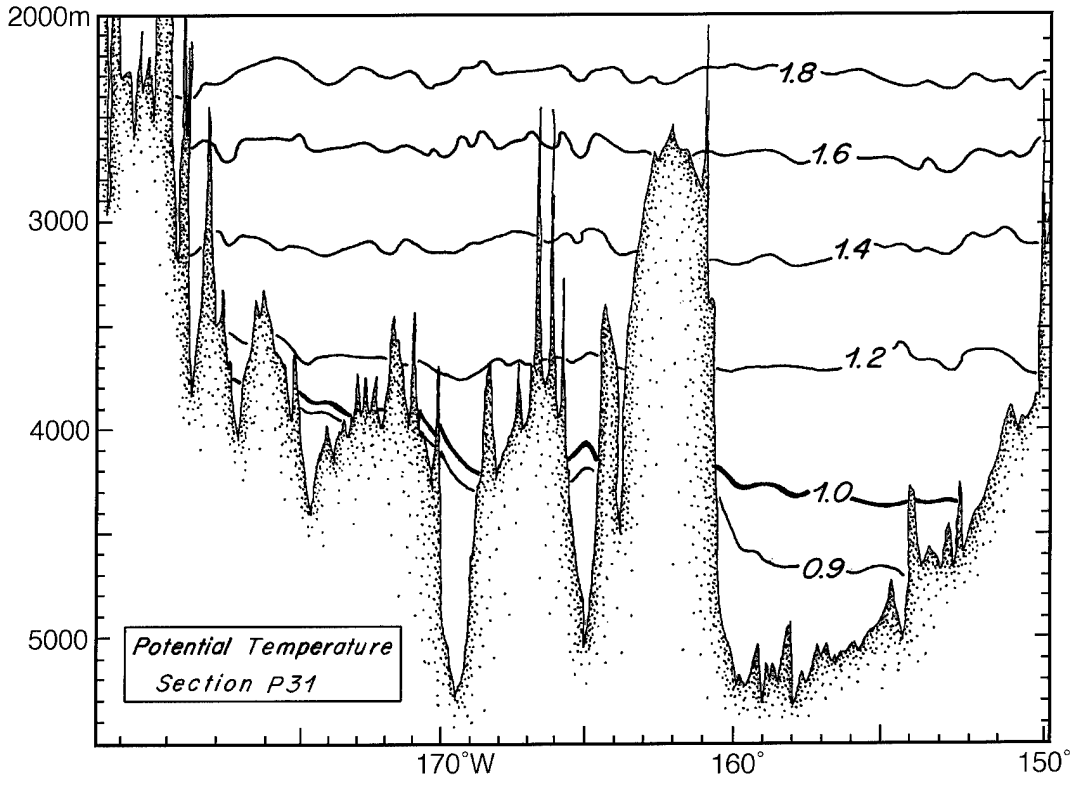

Figure II-35: A simplified sketch of potential temperature (°C) along a section across the Samoan Passage region in the indicated longitude range, adapted from Roemmich *et al.* (1996).

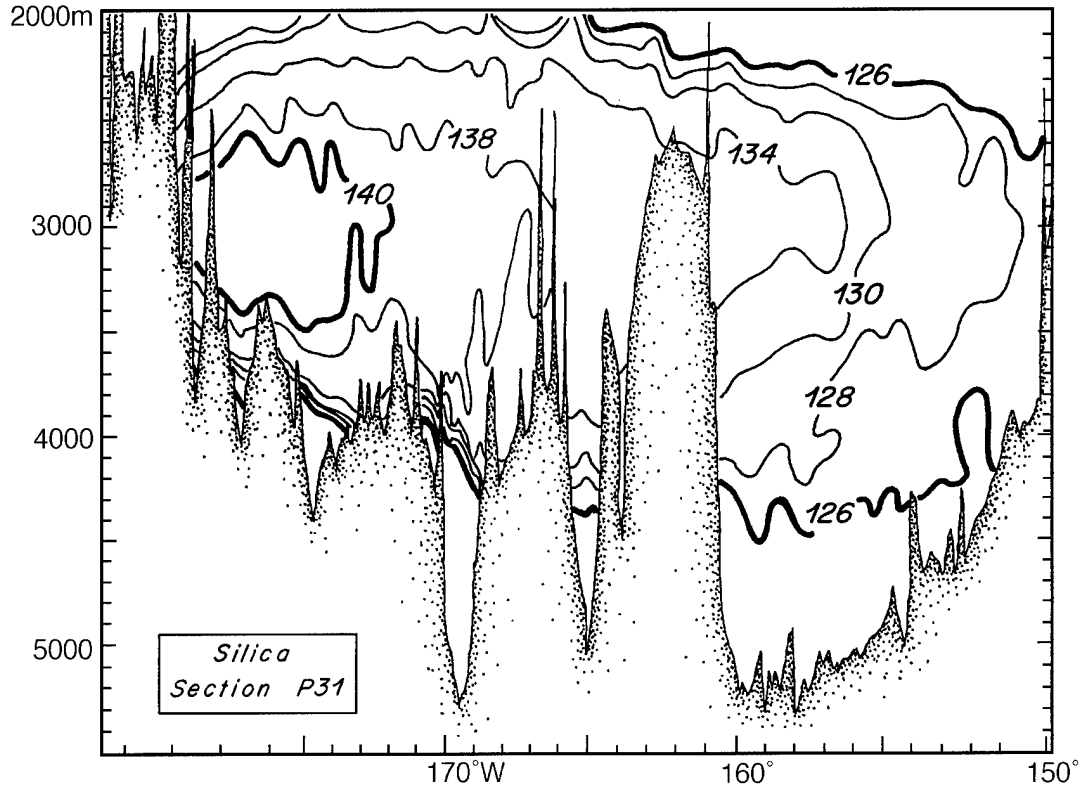

Figure II-36: A simplified sketch of silica (μmol L^{-1}) in conjunction with Figure II-35.

summary form in Figures II-37 and II-38. Their transport estimates across 32°S are also discussed in Section 2f. Figures II-37 and II-38, across 32°S, are not dramatically different in the basic structure of deep and near bottom water masses from sections across 43°S made about 25 years earlier (please see Reid, 1986, pp. 16 and 17, his figures 17 and 20). Silica sections across 47°N (Figure II-39) and down 152°W were presented by Talley and Joyce (1992). Along 47°N (Figure II-39) silica values are all greater than 160 below ~ 1000 m depth, and the 170 contour (centered at about 2000 m depth) stretches zonally almost all the way across the Pacific. A meridional transect down 135°W has recently been presented and discussed by Tsuchiya and Talley (1996). Tongues of silica ~ 160, but centered at ~ 3000 m depth, penetrate down 135°W to about 15°N, and the 170 silica contour penetrates to ~ 30°N, as was the case at 152°W, centered at about 2500 m.

Lynn and Reid (1968), Reid and Lynn (1971), and Mantyla and Reid (1983, 1995) first identified and then elaborated on the influence of NADW in the Pacific Ocean (as

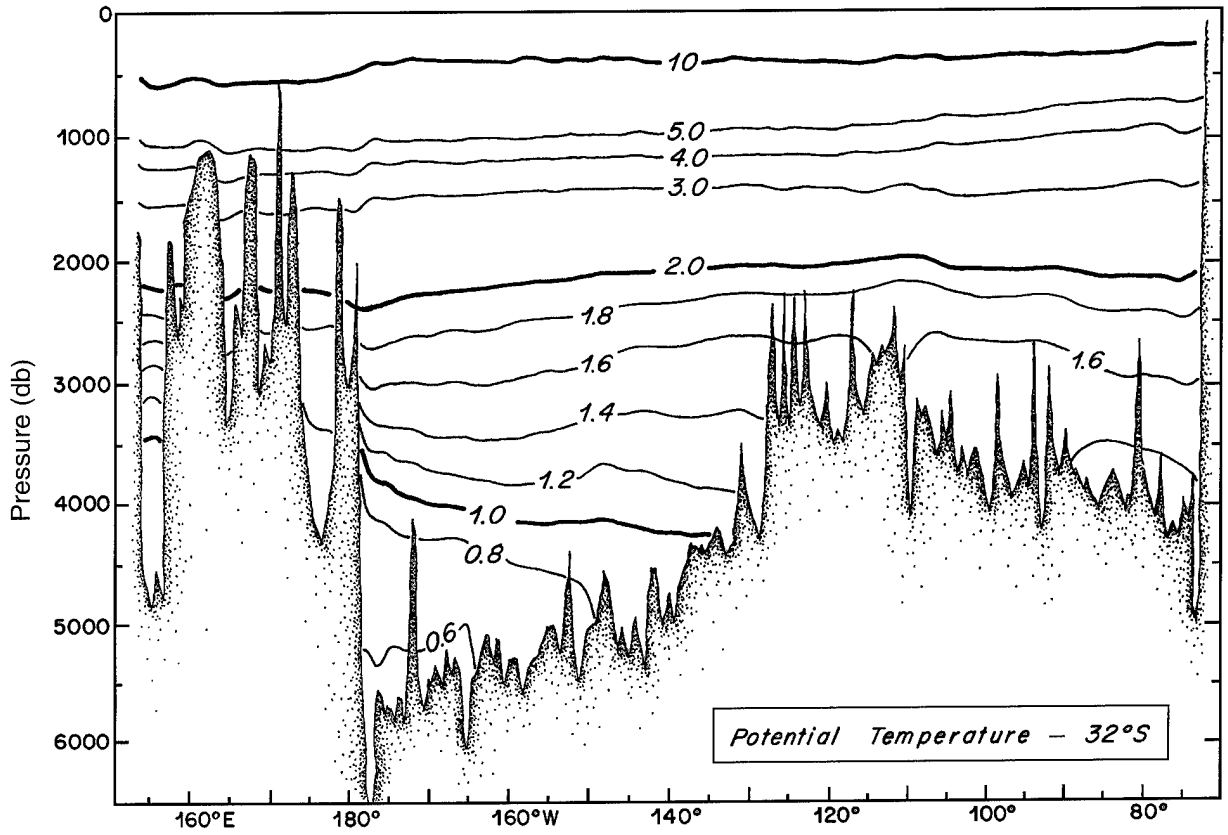

Figure II-37: A potential temperature (°C) summary section across 32°S, adapted from Toole *et al.* (1994b).

well as the Indian and Circumpolar Oceans) and how this works through the distribution of CDW. Perhaps the bottom ↔ deep meridional cell (Section 2f) in the Pacific Ocean is most simply described, in very general terms of course, by examining a combination of "zonal" potential temperature and silica sections (Figures II-31 through II-39). In all of these, low θ, low silica bottom water (CDW) is seen in the "western" segment of both the South and North Pacific. Comparatively high silica water is seen above the temperature range of CDW moving southward in all of the Pacific "zonal" sections noted above. Actually, most of what has been inferred from these sections was also suggested by Mantyla (1975), and, in addition, his map of abyssal potential temperature also implies recirculations of CDW, various features of NPDW, and a horizontal flow picture somewhat like that inferred (Talley and Joyce, 1992; Talley, 1995) from modern silica maps.

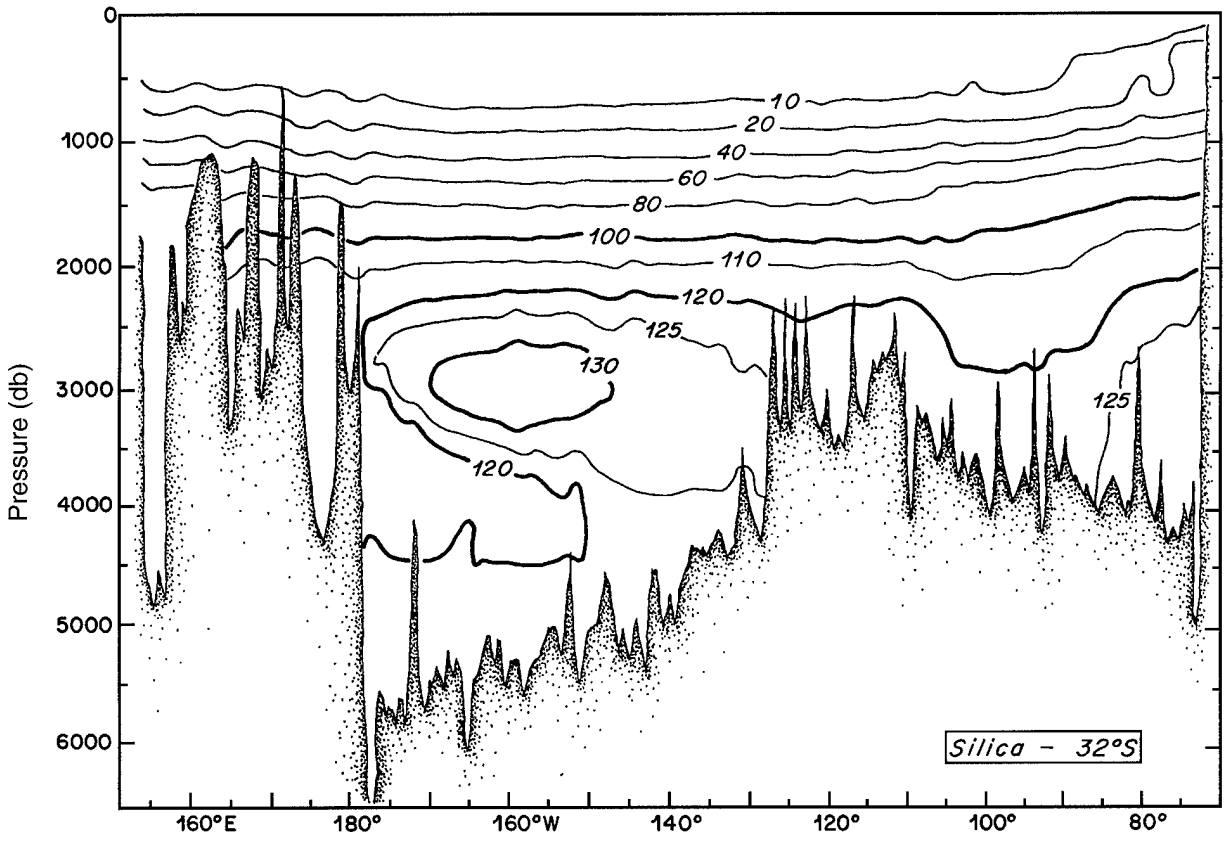

Figure II-38: A simplified section summarizing the silica distribution across 32°S, adapted from Toole *et al.* (1994b).

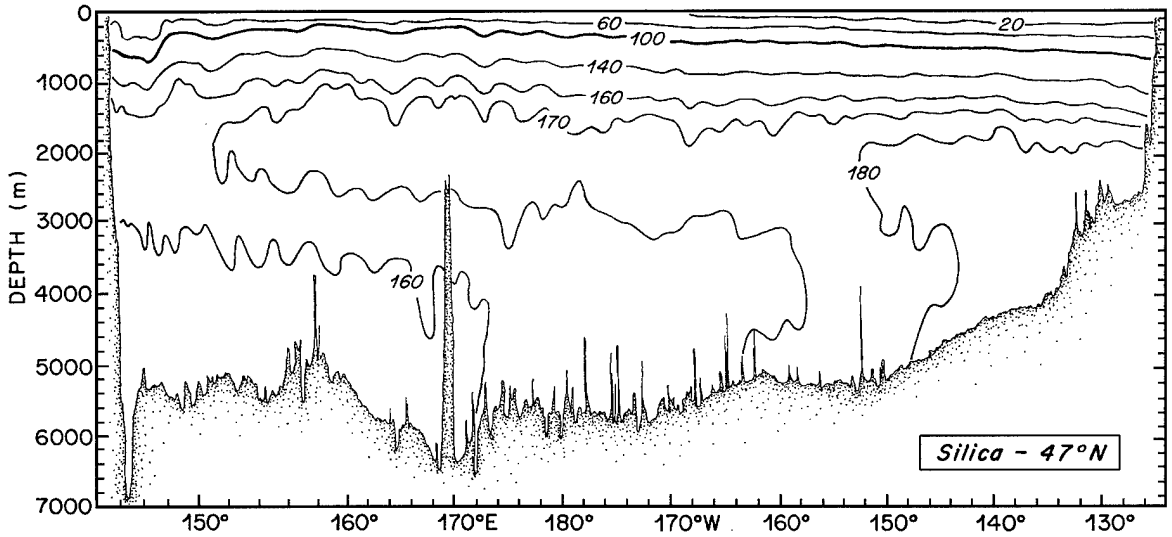

Figure II-39: A highly schematicized vertical section of silica (μmol L^{-1}) along 47°N in the Pacific Ocean, adapted from Talley and Joyce (1992).

2a. The Upper Level Subtropical and Subpolar Gyres in the North Pacific

An early schematic summarizing the transport patterns of the upper layer circulation in the North Pacific is shown in Figure II-40 (adapted from Sverdrup *et al.*, 1942, their figure 205). There is a well-defined subtropical gyre with a strong (~ 65 Sv) western boundary current (Kuroshio) including a recirculation regime (~ 30 Sv), the North Pacific Drift, a California Current, a NEC, the low-latitude NECC, the Mindanao Current (~ 10 Sv), and indications of a cross-equatorial flow from the South Pacific (~ 10 Sv). All in all, this circulation scheme resembles to a large extent the modern picture of the upper layer flow patterns, although a clear-cut subpolar gyre (flow lines are dashed and transports not assigned in this region) and strong Oyashio or Subarctic Frontal System are lacking in Figure II-40. Note the presence of an eastern sub-gyre (still controversial).

The Sverdrup transport of the mid-latitude North Pacific is shown in Figure II-41 (please see also Table II-2), adapted from Hautala *et al.* (1994). In Table II-2, the various estimates of Sverdrup transport (36–40 Sv) along 24°N are very close (± 5%) and ballpark-consistent with Figure II-40, but various estimates of the maximum Sverdrup transport (40–60 Sv) in the subtropical gyre vary by ± 20%. The North Pacific was recently examined relative to the classical Sverdrup balance question in detail along 24°N by Hautala *et al.* (1994). Basic results are shown in Figure II-42 and Table II-3.

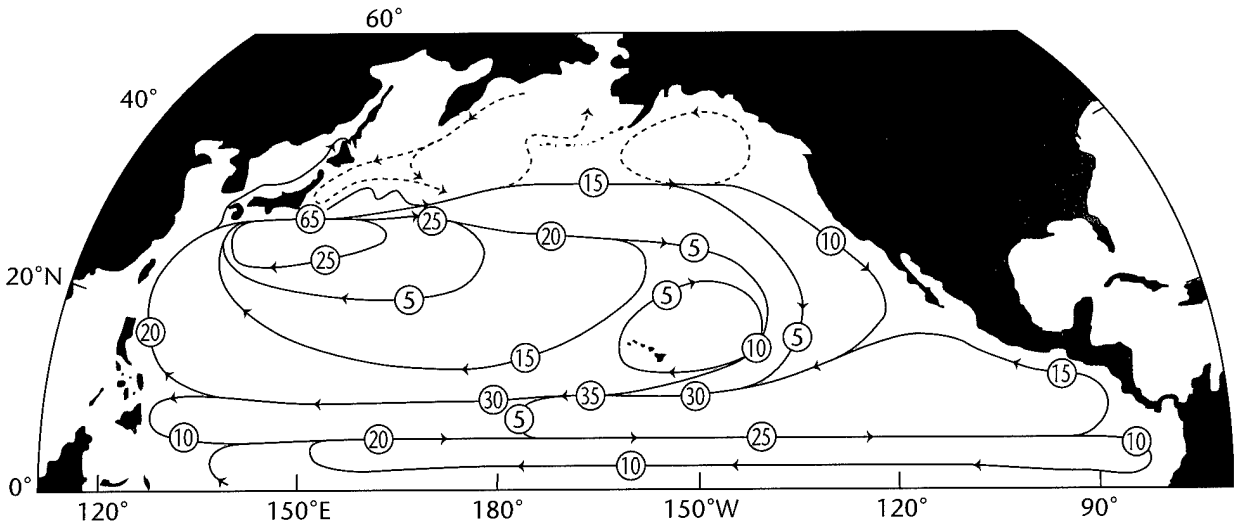

Figure II-40: Transport (in Sverdrups) chart for the upper 1500 m of the North Pacific Ocean, adapted with modification from Sverdrup *et al.* (1942).

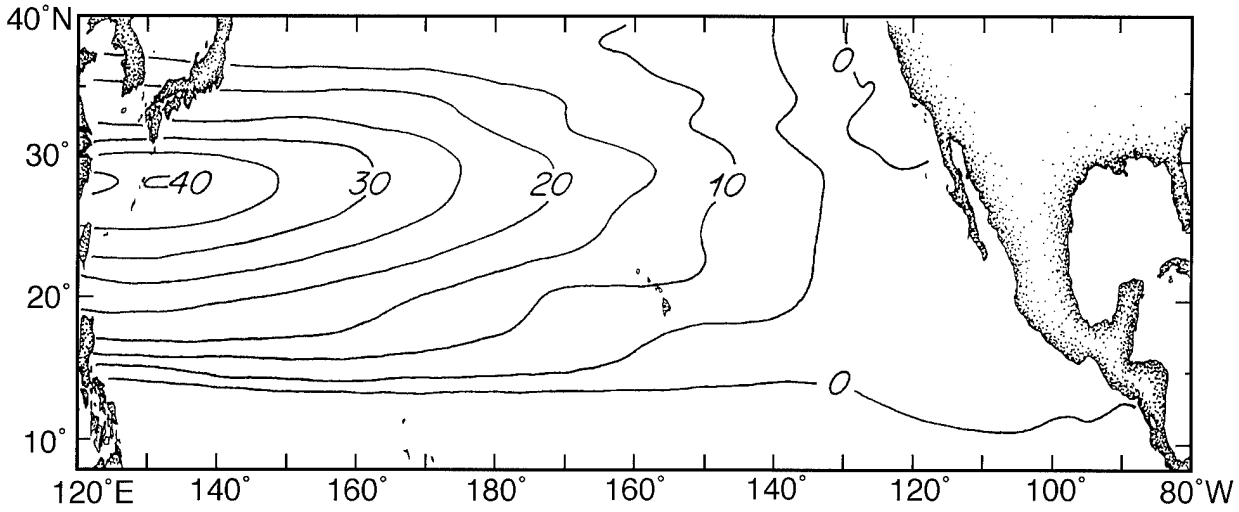

Figure II-41: Sverdrup transport streamlines (Sv) for the mid- and low-latitude North Pacific, adapted from Hautala *et al.* (1994, their figure 1).

The difference between the observed geostrophic transport and the estimate of geostrophic transport based on Sverdrup balance depends on the assumed vertical penetration of the wind-driven gyre (*i.e.*, should NPIW be included in the observed geostrophic transport to be compared with the wind-driven geostrophic component of Sverdrup transport?), on reference level (or levels), and on longitude, the latter as a

Table II-2: Comparison of Sverdrup Transports in the North Pacific Subtropical Gyre as calculated in various studies

Study	Sverdrup Transport	
	Total*	24°N
B. Qiu (personal communication, 1993)	60+	~ 38
Trenberth *et al.* (1990)	50–60	~ 40
Godfrey (1989)	50–60	~ 40
Hautala *et al.* (1994)	42	36

*Maximum southward Sverdrup Transport (in Sverdrups) in the subtropical gyre as a whole. Adapted from Hautala *et al.* (1994).

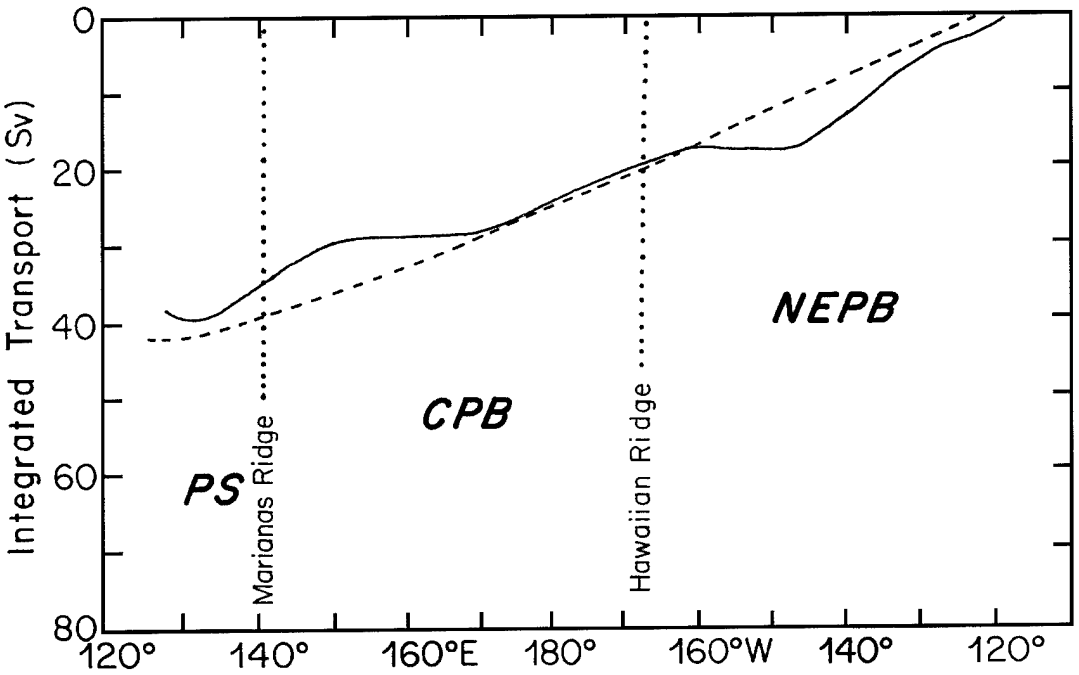

Figure II-42: Integrated and smoothed geostrophic transport (solid line) referenced (Hautala *et al.*, 1994; their figure 2) along the 24°N hydrographic section described by Roemmich *et al.* (1991). Dashed line is the wind-driven geostrophic transport calculated (Hautala *et al.*, 1994) from Sverdrup balance. PS denotes Philippine Sea, CPB denotes the Central Pacific Basin, NEPB denotes Northeast Pacific Basin.

result of the large-amplitude eddy variability approaching the western boundary (strongly filtered from the observed geostrophic transport curve in Figure II-42 in an attempt to suppress this potential confusion). The geostrophic estimates in Figure II-42 agree to within ± 5 Sv or so, with a couple of possibly systematic regional divergences at this order (5 Sv). However, according to Table II-3 the integrated geostrophic transport in the PS (from the non-smoothed data) is 10–15 Sv to the north relative to the estimate from the Sverdrup relation. If the PS is taken to be part of the western boundary regime, and its geostrophic transport (11.6 Sv.) added to the values of the transport (Table II-4) of the Kuroshio in (near) the East China sea, then there is a transport balance across 24°N to within 1.5 to 7 Sv. Qiu and Joyce (1992) find that interannual variations in the transport of both the Kuroshio and the North Equatorial Currents (7°–25°N) are closely correlated to variations in Sverdrup transport. A general description of the North Pacific circulation and hydrography along 24°N has been presented by Roemmich *et al.* (1991); see also Bryden *et al.* (1991).

Table II-3: Upper Layer Transports across 24°N in the Pacific

	California Coast to 170°W (NEPB)	170°W to 142°E (CPB)	California Coast to 142°E	142°E to 127°E (PS)
Ekman	4.1	2.8	6.9	0.5
Wind-driven geostrophic	–20.5	–19.1	–39.6	–3.5
Sverdrup	–16.4	–16.3	–32.7	–3.0
Geostrophic	–19.3	–25.7	–45.0	+11.6

Geostrophic transport is referenced to 2000 dbar and integrated down to 26.5 σ_θ in the Northeast Pacific Basin (NEPB) and to 27.0 σ_θ in the Central Pacific Basin (CPB) and Philippine Sea (PS), adapted from Hautala *et al.* (1994), their table 2.

Table II-4: Estimates of Kuroshio Transport in the East China Sea

Estimate	Method	Reference
26.3 ± 3.3	inverse	Bingham and Talley (1991)
28.3	geostrophic (referenced to ADCP)	Bryden *et al.* (1991)
30.3	geostrophic (referenced to ADCP)	Chen *et al.* (1992)
32.0	inverse	Roemmich and McCallister (1989)

The developmental stages of the Kuroshio (Ichikawa and Beardsley, 1993; Nitani, 1972; Liu *et al.*, 1986) are outlined schematically in Figure II-43. Various transport estimates for the Kuroshio in the vicinity of the South China Sea are shown in Table II-4, adapted from Ichikawa and Beardsley (1993). Results from a recent survey of the early reaches of the KCS in the East Taiwan Channel (Johns *et al.*, 1995) are shown in Table II-5 and Figure II-44. Taft (1972, 1978) has summarized what was known at that time concerning the structure of the Kuroshio south of Japan. Taft *et al.* (1973) examined the relationship of the current path and bottom velocity south of Japan. Water-mass properties in the Philippine Sea have been described by Liu *et al.* (1986). Qiu and Joyce (1992) have used historical hydrographic data along 137°E (sections of θ, S, and

σ_θ shown in Figure II-45) to calculate transports (and their time variability) for a variety of currents (Table II-6).

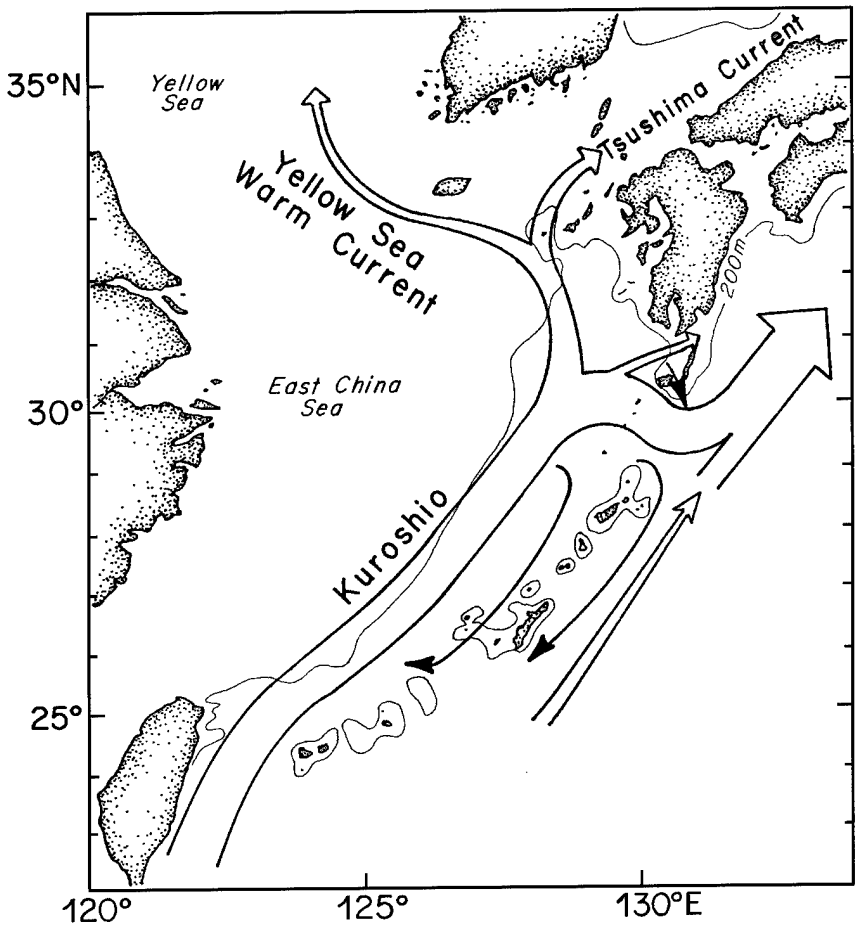

Figure II-43: A schematic representation of the currents in the vicinity of the East China Sea, adapted from Nitani (1972, his figure 10) and Ichikawa and Beardsley (1993, their figure 1).

Distributions of MKE (Mean Kinetic Energy) and EKE (Eddy Kinetic Energy, same as K_E) along the axis of the Kuroshio Extension from Qiu *et al.* (1991) are contained in Figure II-46; please also see Figure II-18. The mean and fluctuating flows in the vicinity of the KCS have been studied using moored current meter observations by Schmitz *et al.* (1982, 1987) plus Schmitz (1984a, b, 1987, 1988), and in combination with hydrographic data by Niiler *et al.* (1985) and Joyce and Schmitz (1988). The time-dependent results from these moored instrument observations are mostly discussed in this report in Section 2g on the North Pacific eddy field, with some of the deep mean flows observed with moored instruments briefly presented in Section 2e. The time scales of the eddy field in the Kuroshio are very similar to those observed in the Gulf Stream (Figure II-47, adapted from Schmitz and Holland, 1986; see also Schmitz and Luyten, 1991). The spectral distribution of K_E in the deep interior of the western North Pacific (Imawaki and Takano, 1982; Schmitz *et al.*, 1982, 1987) is similar to that observed in a corresponding area (~ 28°N, 70°W) in the North Atlantic (Schmitz, 1989).

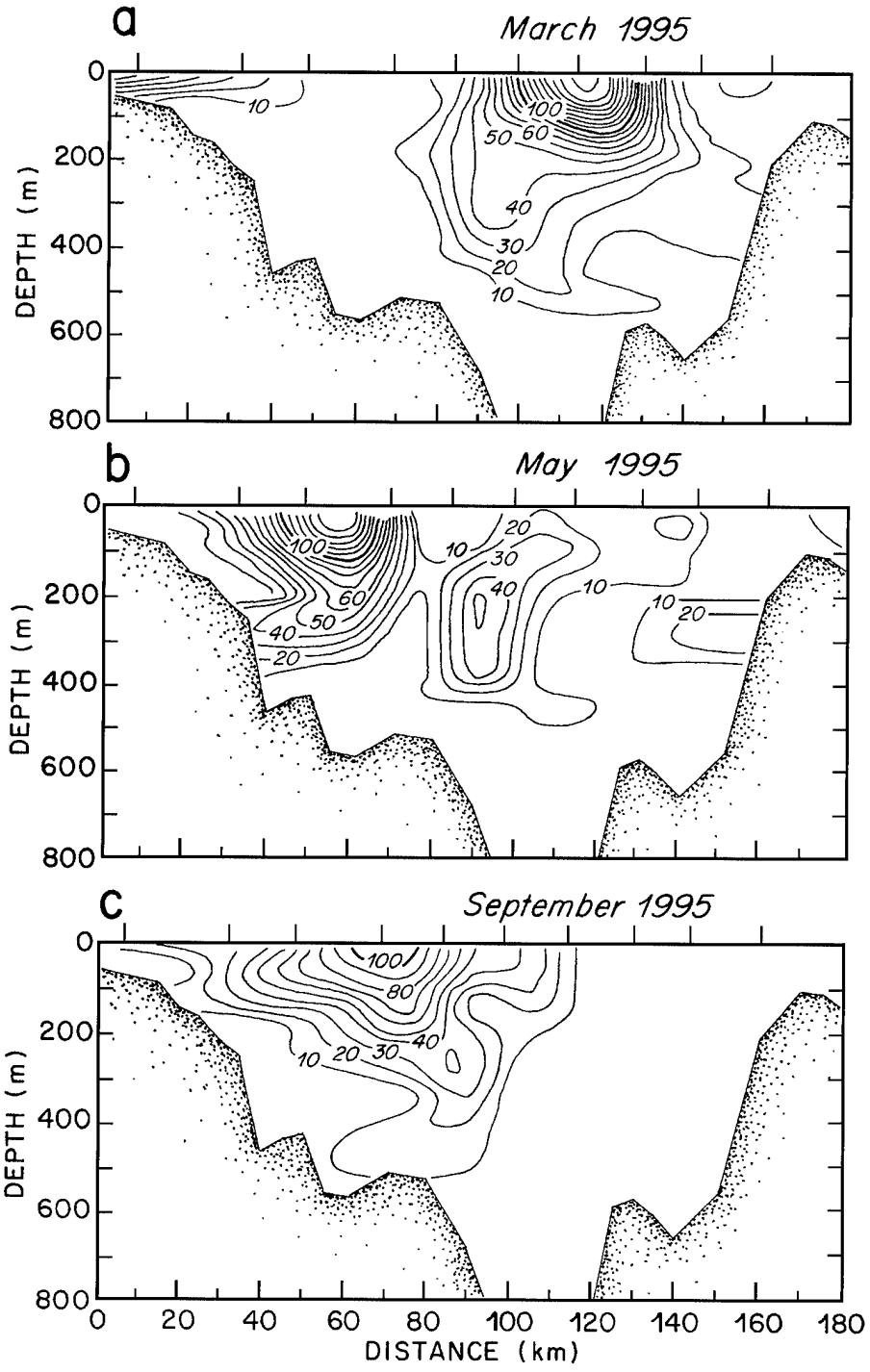

Figure II-44: Speed contours (cm s^{-1}) normal to sections across the East Taiwan Channel: (a) March 1995, (b) May 1995, and (c) September 1995.

Table II-5: The geostrophic volume transport through the East Taiwan Channel calculated from hydrographic data with zero velocity at the bottom. The mean volume transport is 12.5 ± 2.5 Sv.

Section Number	Cruise	Date	Geostrophic Volume Transport (Sv) 0/Bottom
1	257	10/18/90	14.9
2	294	09/07/91	9.8
3	334	10/29/92	12.5
4	354	05/26/93	8.5
5	370	10/22/93	10.8
6	387	05/26/93	8.5
7	401	09/17/94	14.2
8	407	12/19/94	11.3
9	412	03/16/95	15.0
10	418	05/15/95	12.1

Table II-6: Transport Estimates (Sv) for various currents along 137°W

	Kuroshio	KCC	NEC	NECC
Total mean	52.4	–18.1	–62.3	51.5
Winter mean	49.7	–16.2	–58.5	48.9
Summer mean	55.7	–20.5	–67.2	54.9
Straight-path years	52.5	–23.4	—	—
Meander-path years	52.2	–10.9	—	—
ENSO years	52.5	–17.0	–70.8	68.6
Non-ENSO years	52.3	–18.8	–57.0	42.3

KCC = Kuroshio Counter Current
NEC = North Equatorial Current
NECC = North Equatorial Countercurrent

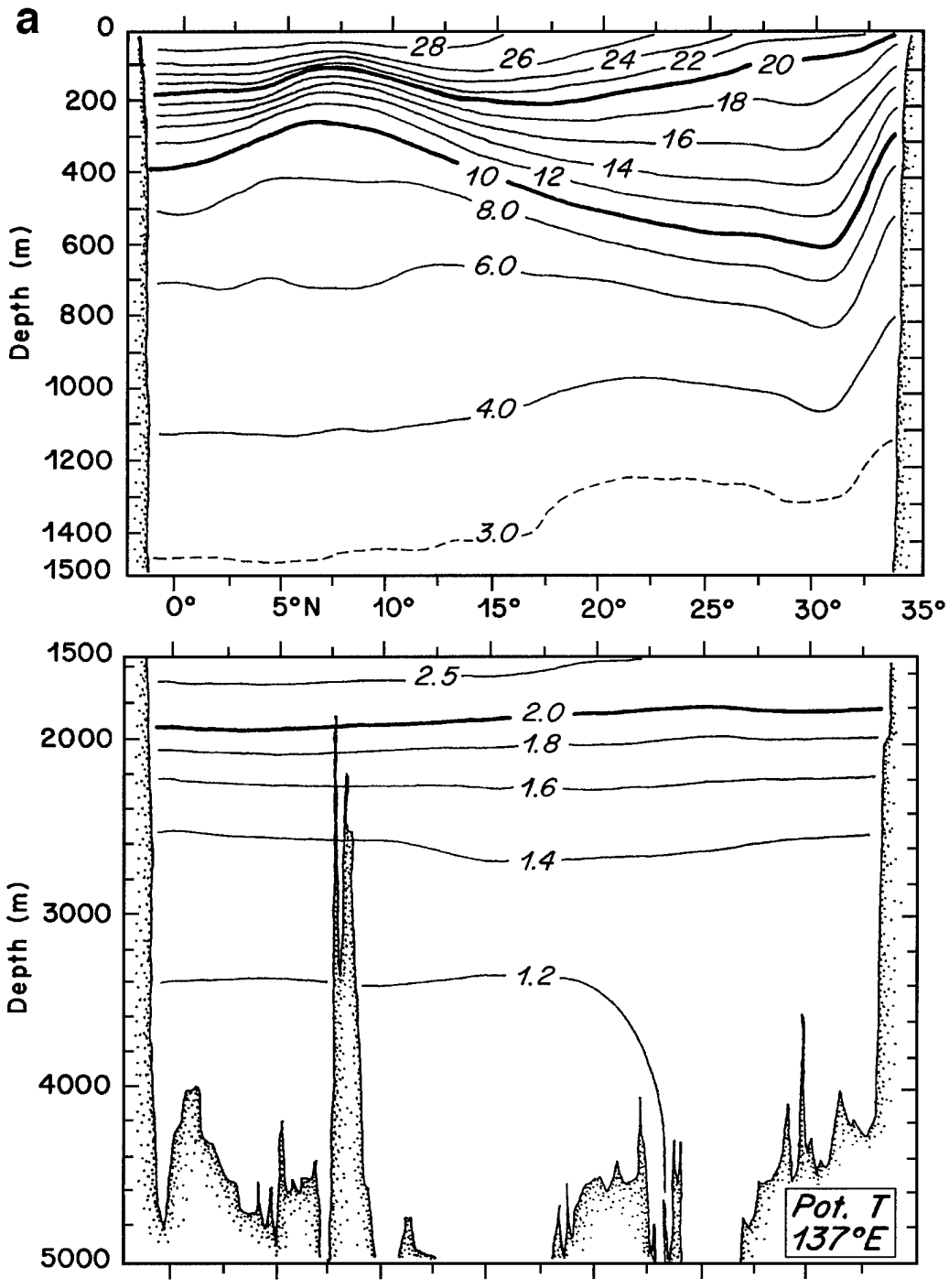

Figure II-45: θ (a), S (b), and σ_θ (c) sections along 137°E, averaged over the period 1967–1988, a total of 39 cruises, adapted from Qiu and Joyce (1992).

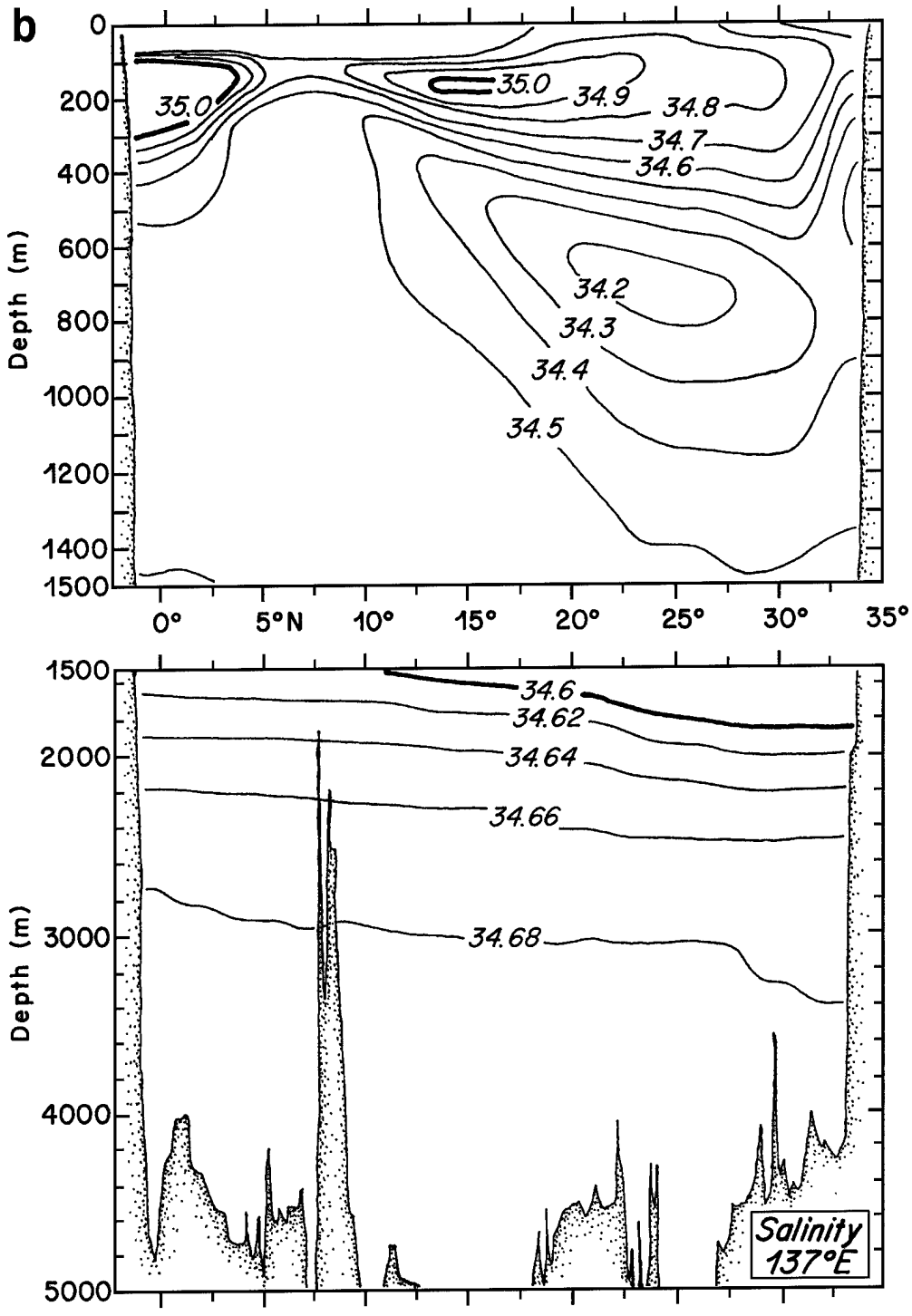
b
Depth (m)
0
200
400
600
800
1000
1200
1400
1500
35.0
35.0
34.9
34.8
34.7
34.6
34.2
34.3
34.4
34.5
0°
5°N
10°
15°
20°
25°
30°
35°
1500
2000
3000
4000
5000
34.6
34.62
34.64
34.66
34.68
Salinity
137°E

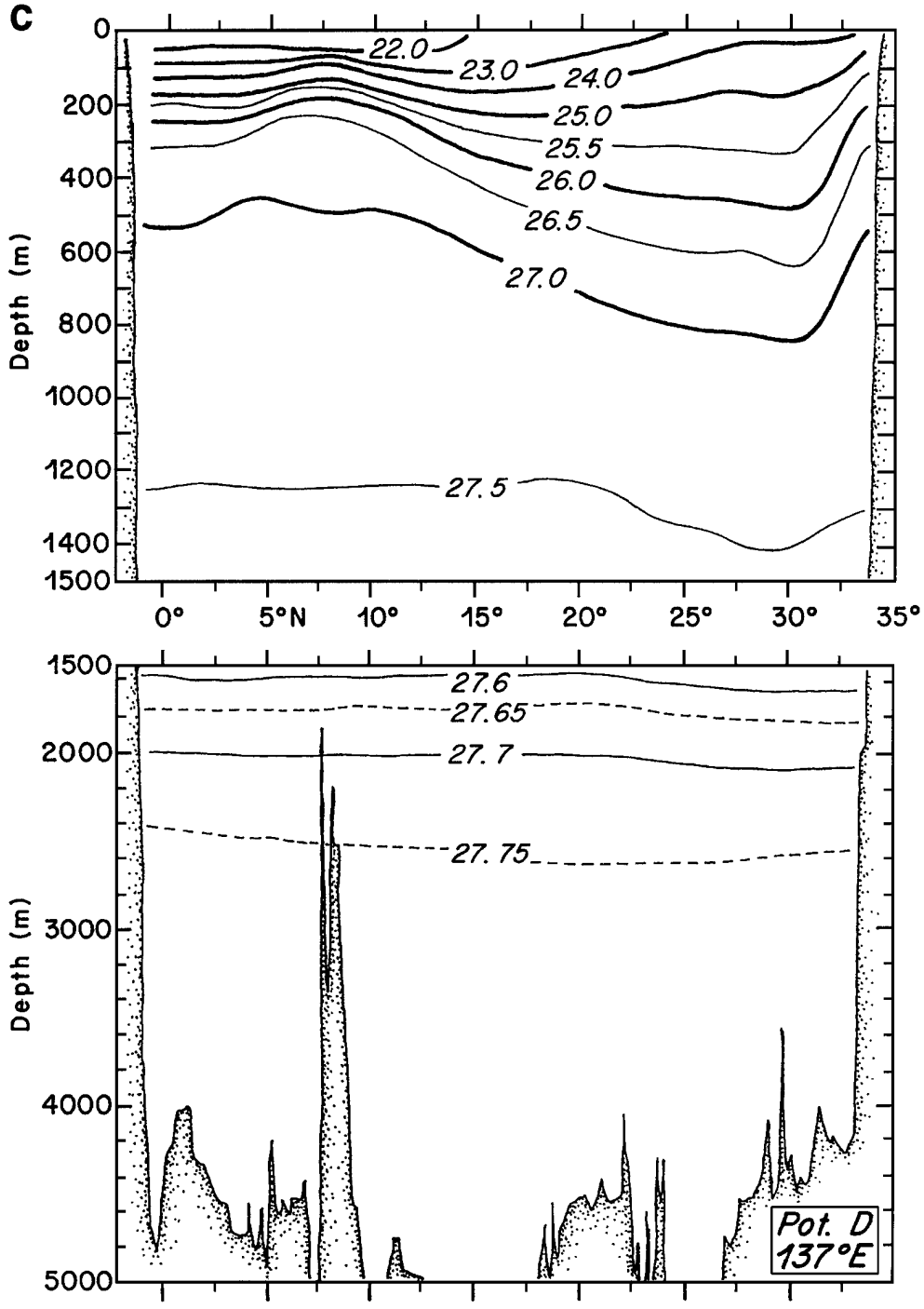
C
Depth (m)
0
200
400
600
800
1000
1200
1400
1500
22.0
23.0
24.0
25.0
25.5
26.0
26.5
27.0
27.5
0°
5°N
10°
15°
20°
25°
30°
35°
1500
2000
3000
4000
5000
27.6
27.65
27.7
27.75
Pot. D
137°E

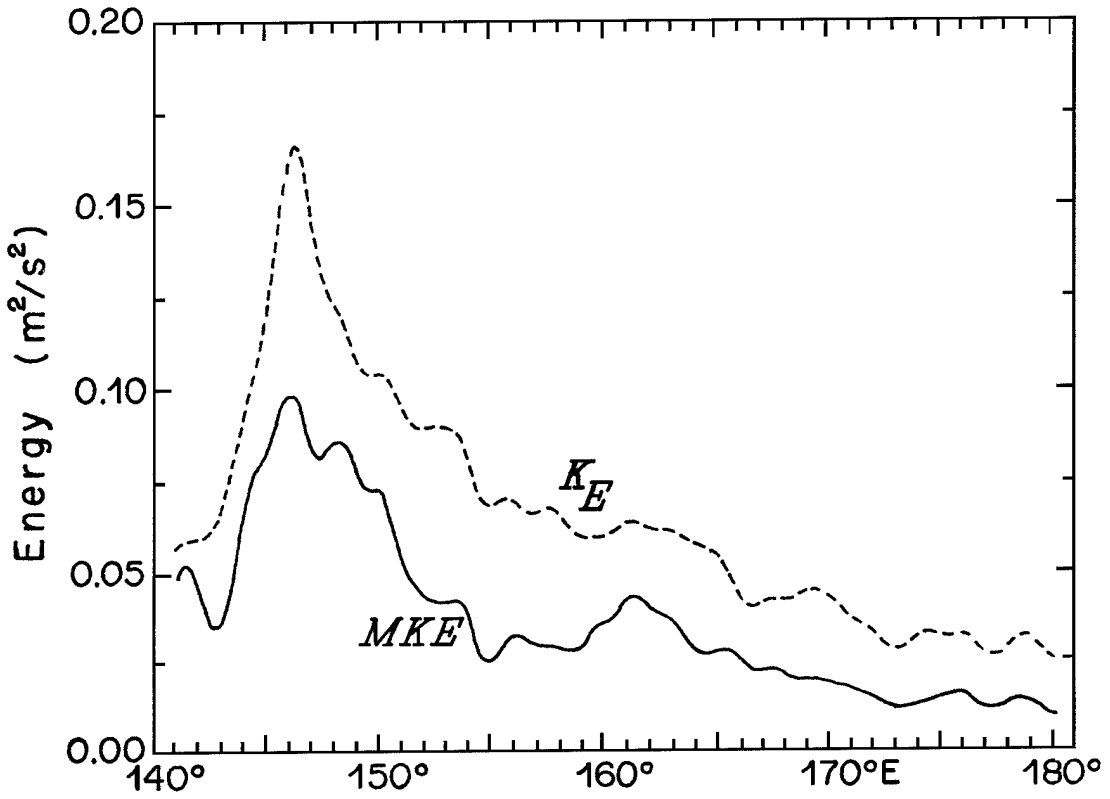

Figure II-46: Mean (MKE) and eddy kinetic energy (K_E) along the Kuroshio Extension, averaged between 33° and 37°N, taken from Qiu *et al.* (1991).

Joyce and Schmitz (1988) have estimated the transport of the Kuroshio Extension and associated currents at three longitudes using a combination of current meter and hydrographic data. At 165°E, the hydrographic data are comparatively complete in the latitude range 30–42°N where there were six moorings with very stable mean flows, seemingly on a horizontal scale resolved by the mooring distribution. The transport of the Kuroshio was found to be 57 ± 2 Sv, and for the Oyashio or subarctic frontal region ~ 22 Sv, both of course eastward. Elsewhere along 165°E the flow was weakly (order few centimeters per second) westward but with large transport, ~ 85 Sv for a southern recirculation and ~ 55 Sv for a northern recirculation. In my opinion these are mostly eddy-driven recirculations as found at 152°E (Schmitz *et al.*, 1982) and in the Gulf Stream System (Schmitz *et al.*, 1983; Schmitz and Holland, 1986). The hydrography of the Kuroshio Extension was described early on by Kawai (1972). The shallow salinity minimum in the North Pacific has been described by Reid (1973), Talley (1985), and

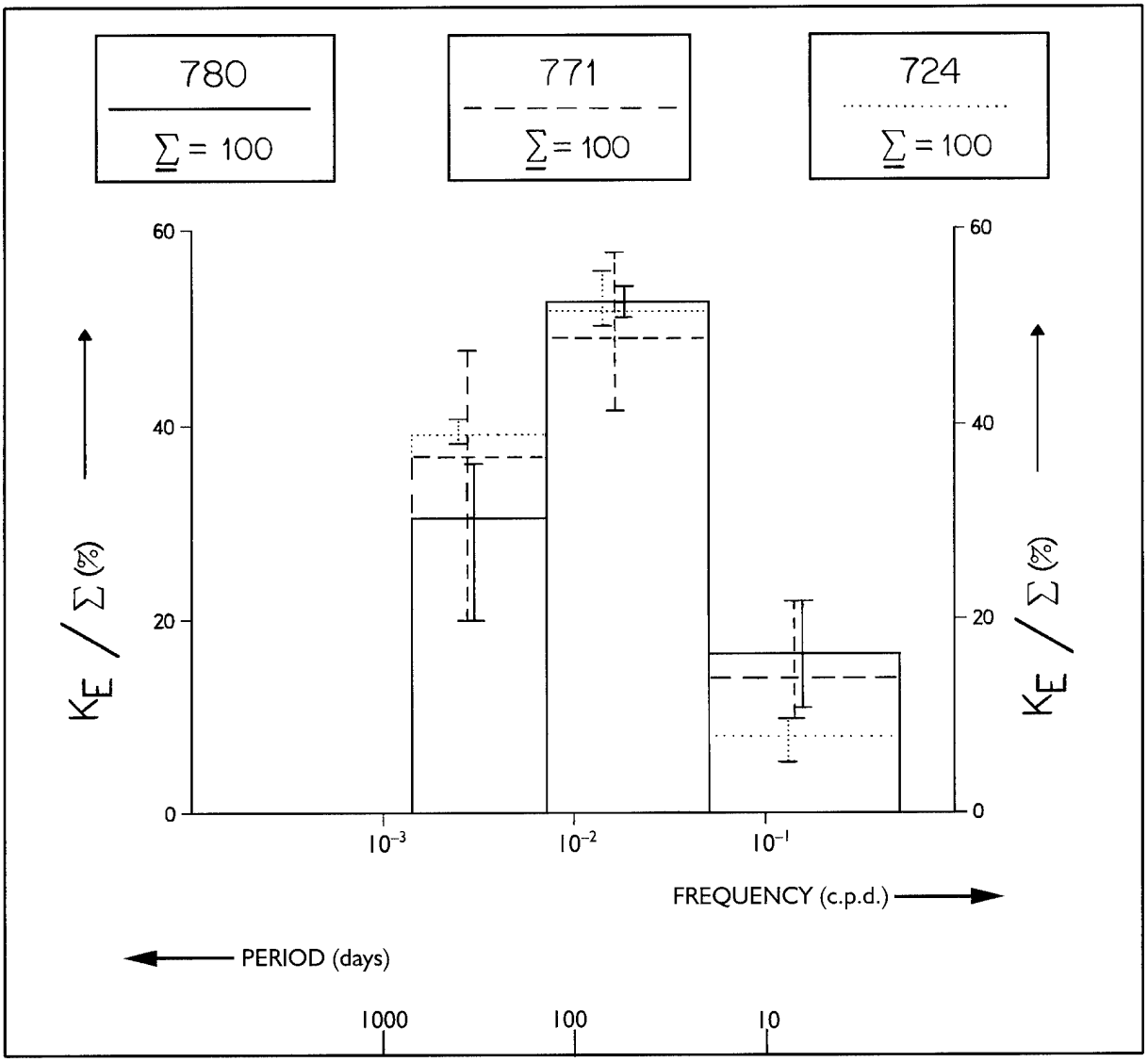

Figure II-47: Vertically averaged and nomalized frequency distributions of eddy kinetic energy. Moorings 771 and 780 are from different longitudes in the vicinity of the Gulf Stream, and 724 is from the Kuroshio along 152°E. Adapted from Schmitz and Holland (1986).

Tsuchiya (1982). Talley (1985) and Yuan and Talley (1992) also discuss how the shallow salinity minima of the North Pacific can be related to the subduction of surface waters. The seasonal and interannual variability in various areas of the North Pacific has received a lot of attention (*i.e.*, Qiu and Joyce, 1992; Qiu and Lukas, 1996; Wyrtki, 1974).

2b. The Upper Level Subtropical Gyre in the South Pacific

The subtropical gyre in the South Pacific is well defined in Tabata's (1975) schematic of the currents in the Pacific Ocean (Figure II-25). The poleward branch of the South Pacific subtropical gyre is not well defined in the mean on the surface current map based on ship drift data (Figure II-2). The salinity contours on σ_θ = 26.44 (Figure II-48) qualitatively define the configuration of the upper level subtropical gyre, along with a strong circumpolar influx of fresh water in the easternmost South Pacific; this inflow and associated salinity contours $\leq$ 34.4 originate south of the dashed line in Figure II-48 along which σ_θ = 26.44 outcrops. There is also a strong indication in Figure II-48 of northwestward flow in the SEC of the circumpolar water having entered the South Pacific but now enhanced in salinity from 34.2 $\rightarrow$ 34.4 progressively to about 35.0 toward the straits just north of New Guinea, along with recirculation near the equator (possibly feeding the EUC). An ~ 15 Sv mean transport has recently been measured directly in Vitiaz Strait (Murray *et al.*, 1995; see also Lindstrom *et al.*, 1990), as discussed in more detail in Section 2c. The SEC splits approaching the coast of

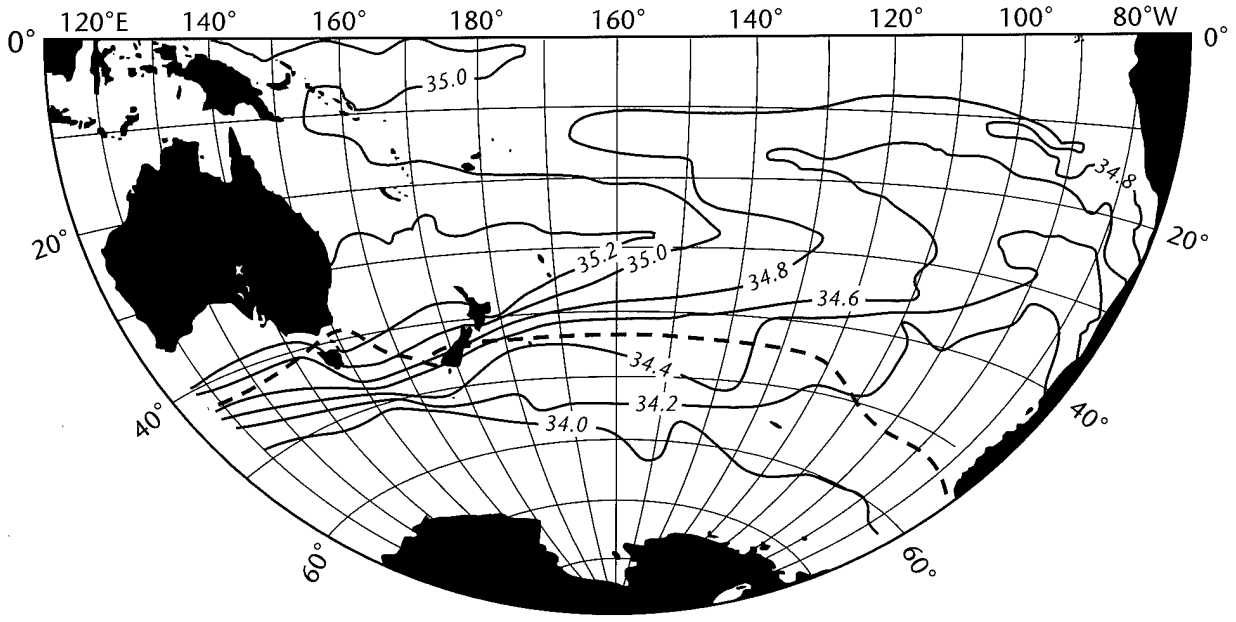

Figure II-48: Salinity on the isopycnal surface σ_θ = 26.44, depths near 400 m along 20°S, adapted from Reid (1986, his figure 6). The dashed line at "high" latitudes is the location at which σ_θ = 26.44 outcrops, and S contours south (poleward) of this line are for the sea surface.

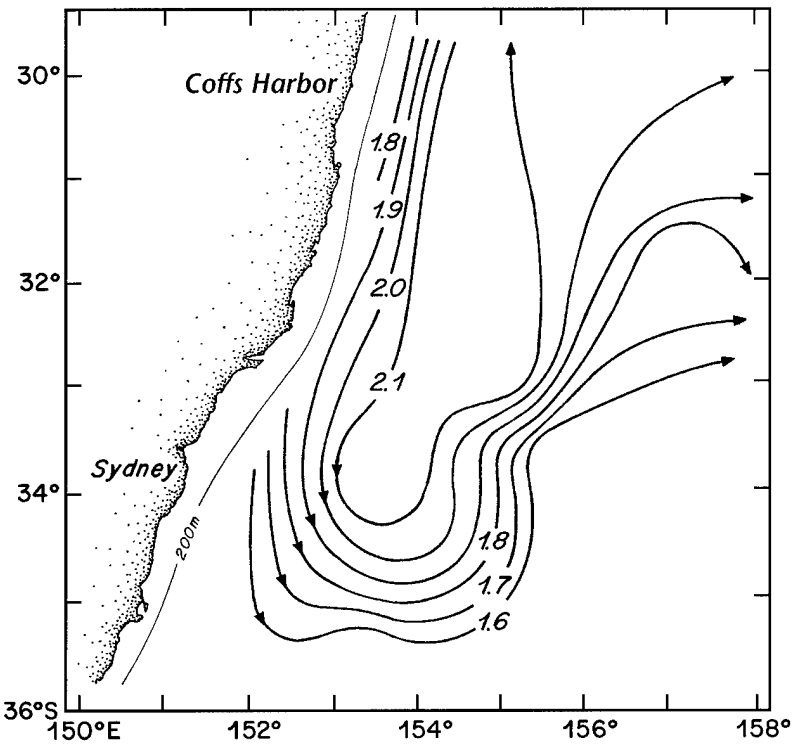

Figure II-49: Surface dynamic topography (dynamic meters) relative to 1300 db for a cruise to the EACS region in 1964, adapted from Hamon (1965, 1970).

Australia into a branch feeding the EAC (Godfrey and Golding, 1981) and a branch directed toward the northern hemisphere that presumably mostly goes through Vitiaz Strait (see Figures II-9 and II-26). I take this flow to be at least part of the re-supply of, or replacement flow for, the IT, thence from the Indian Ocean to the ACCS to the Pacific.

The cross-equatorial exchange of intermediate water in the Pacific Ocean (Reid, 1965; Reid and Mantyla, 1978; Tsuchiya, 1991) proceeds along a roughly similar path (Figures II-27, 28, 29; see also Section 2d) to that of the thermocline layer in Figure II-48. One point that I would like to concentrate on in this report is the potential similarity between the source elements of the interhemispheric flow in the Pacific and Atlantic Oceans. That is, there are both upper layer and intermediate flow components (at least some of which is of circumpolar origin) leaving the subtropical South Atlantic and South Pacific Oceans in the west, entering tropical latitudes from the south and at least to some extent the northern hemisphere.

Wyrtki (1960) reviewed the surface circulation in the Coral and Tasman Seas and in a later article (Wyrtki, 1962) identified the major water masses in the western subtropical South Pacific. A classic review article on the EAC was written by Hamon (1970); see also Hamon (1965). Figure II-49 is a plot of the surface dynamic topography relative to 1300 db for a particular cruise in 1964 (adapted from Hamon, 1965, 1970), which is a very clear-cut example of the recirculation and retroflection associ-

ated with the EAC. Figure II-50 is a plot of the vertical structure of meridional speeds in the EAC, for two particular station pairs, from a cruise in 1967 (see Hamon, 1970). The geostrophic speeds estimated from hydrographic data at the corners of a 50 km or so square were fit to Sofar float observations at 1300 m. Note that for one case there is significant deep southward flow, but not in the other. Other important articles on the EACS are those of Boland and Hamon (1970), Boland and Church (1981), Godfrey and Golding (1981), and Ridgway and Godfrey (1994).

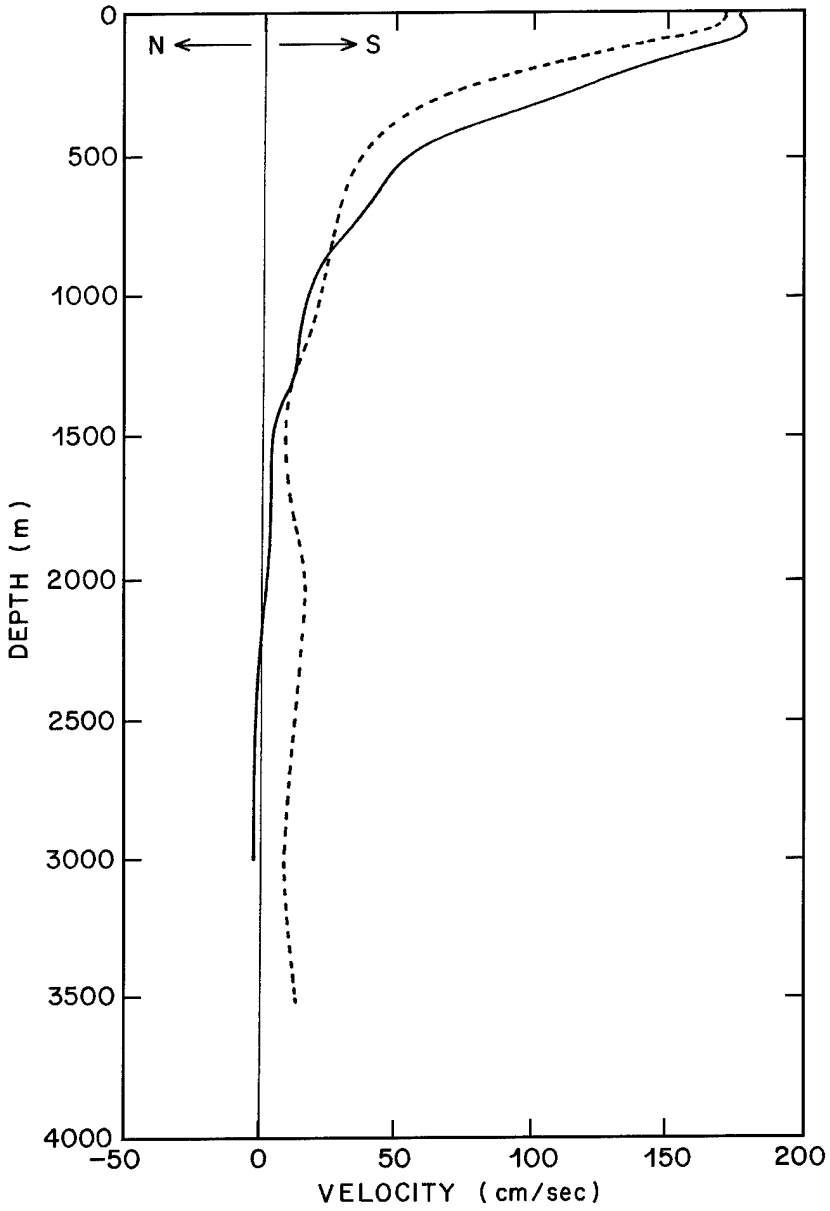

Figure II-50: Curves of north–south geostrophic speeds for two station pairs in the EAC as a function of depth.

A recent estimate of the transport of the EAC and its recirculation (Ridgway and Godfrey, 1994) along 28°S is shown in Figure II-51. This estimate is for the upper 2000 m or so depth range. Basically, the EAC transport in Figure 51 is ~ 27.5 Sv and its recirculation is about 15 Sv, leaving a net of 12.5 Sv for the EACS to feed toward New Zealand and thence into the poleward limb of the South Pacific Subtropical Gyre (called the South Pacific Current by Stramma *et al.*, 1995b;

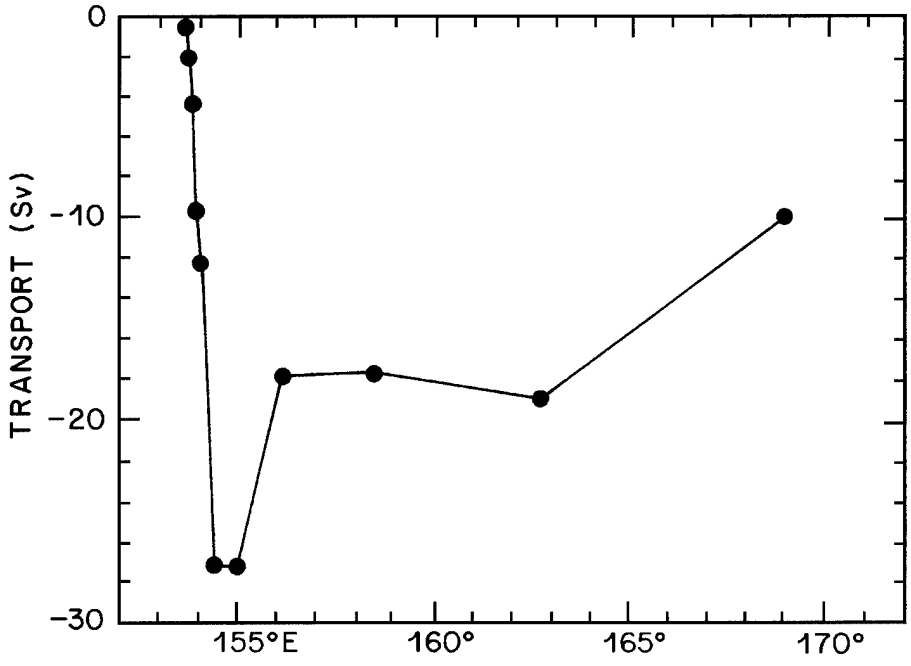

Figure II-51: An estimate of the cumulative southward transport of the EACS along 28°S, adapted from Ridgway and Godfrey (1994).

please note that there may be a multiple-branch structure to this poleward-located, eastward-flowing return flow for the EAC). Cox (1975) pointed out that the expected EAC transport could be reduced relative to the wind-driven transport in the interior of the South Pacific (east of, say, the longitude of New Zealand) by the transport through the IT. Cox (1975) found 18 Sv for the transport of the IT in one of his numerical experiments along with 22 Sv for the EACS and its recirculation. Godfrey and Golding (1981) reviewed this topic and estimated that the net transport of the EAC is ~ 15 Sv, out of their estimate of 29 Sv for the interior transport across 28°S in the Pacific, the latter estimate comparing favorably with the estimate of 26 Sv by Meyers (1980), leaving ~ 14 Sv as their estimate of the IT transport, which they suggested may be a bit high.

The South Pacific Current or the high latitude branch of the subtropical gyre has recently been described in some detail by Stramma *et al.* (1995b). Only a 5 Sv transport (the total transport of the poleward limb of the South Pacific Subtropical gyre ought to be at least ~ 15 Sv) was estimated by Stramma *et al.* (1995b), possibly implying multiple branches [perhaps somewhat like Cox (1975) found] out of the EACS–New Zealand Region, and as possibly suggested by Figure II-48. The Peru Current has been described by Wooster (1970) and Wyrtki (1963); see also Toggweiler *et al.* (1991) and Wooster and Reid (1963). One of the really neat ideas of Wooster and Reid (1963, p.

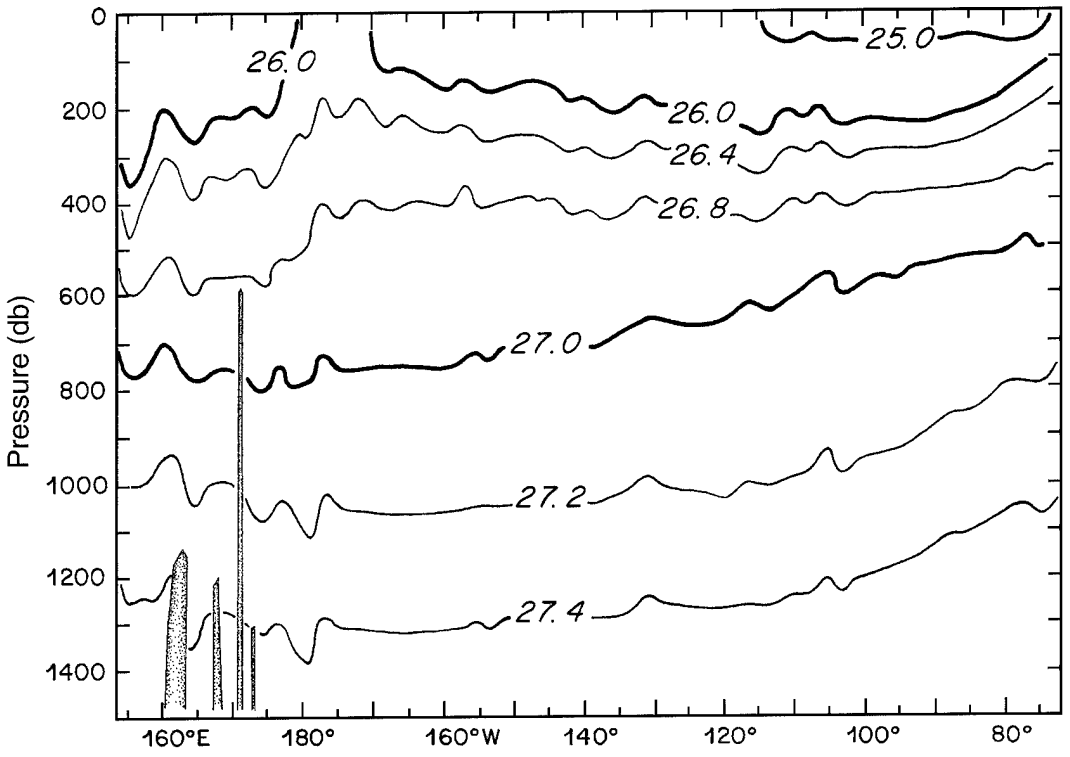

Figure II-52: Contours of σ_θ for the upper 1500 db of a section across 32°S, adapted with smoothing and simplification from Toole *et al.* (1994b).

254) is their recognition of the similarities (even including transports, Wooster and Reid, 1963, their table I) of the Benguela and Peru Currents, an observation that I link to interbasin flow(s). The South Equatorial Current (SEC) in the South Pacific, along with the Peru Current, is well defined (Figure II-2) in this ship-drift-data-based surface current map, although some parts of the subtropical gyre are not. The circulation in the South Pacific along 32°S, a section nearly centered across the subropical gyre, has been discussed recently by Toole *et al.* (1994b). Upper level (0–1500 m) sections (smoothed) of σ_θ, S and O_2 across 32°S from Toole *et al.* (1994b) are shown in Figures II-52–54. In these figures, a huge area of very fresh and high oxygen UPIW ($26.8 \leq \sigma_\theta \leq 27.2$, SAMW farther south) spanning about the 500–1000 m depth interval dominates the section in terms of recent ACCS vintage. I can't help but see this as the (eventual) source of the IT. Wooster and Reid (1963, p. 263) also present upper-layer profiles across 33°S that are comparable to that region of the eastern end of the Toole *et al.* (1994b) 32°S section.

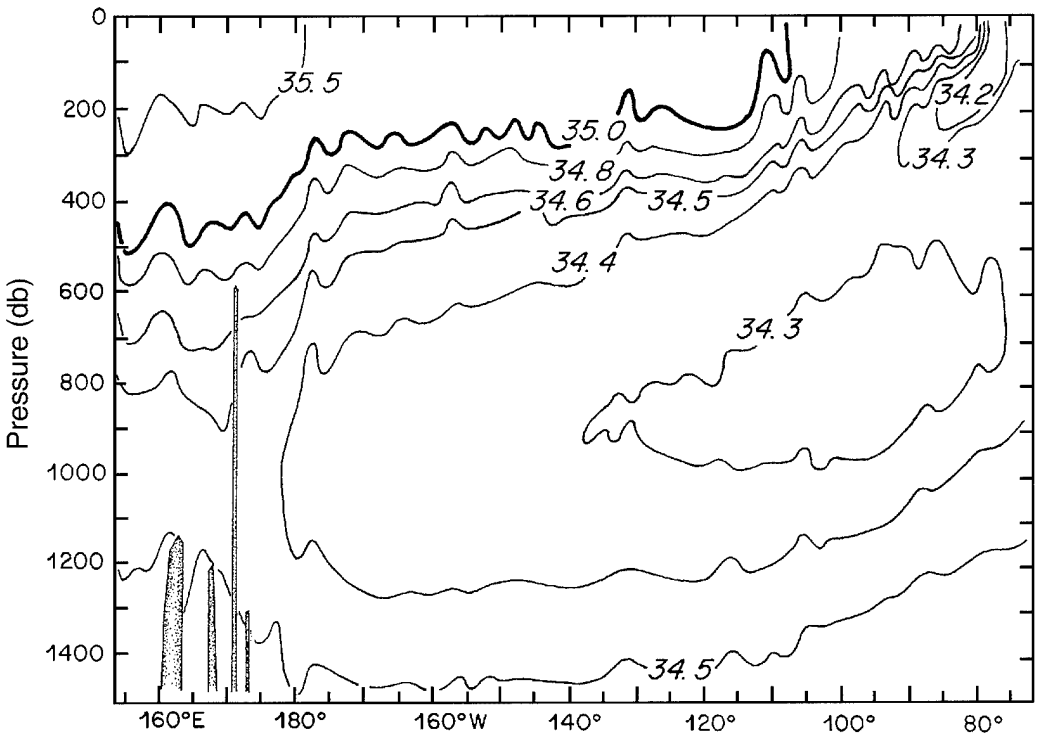

Figure II-53: Contours of S for the upper 1500 db of a section across 32°S, adapted with smoothing and simplification from Toole *et al.* (1994b).

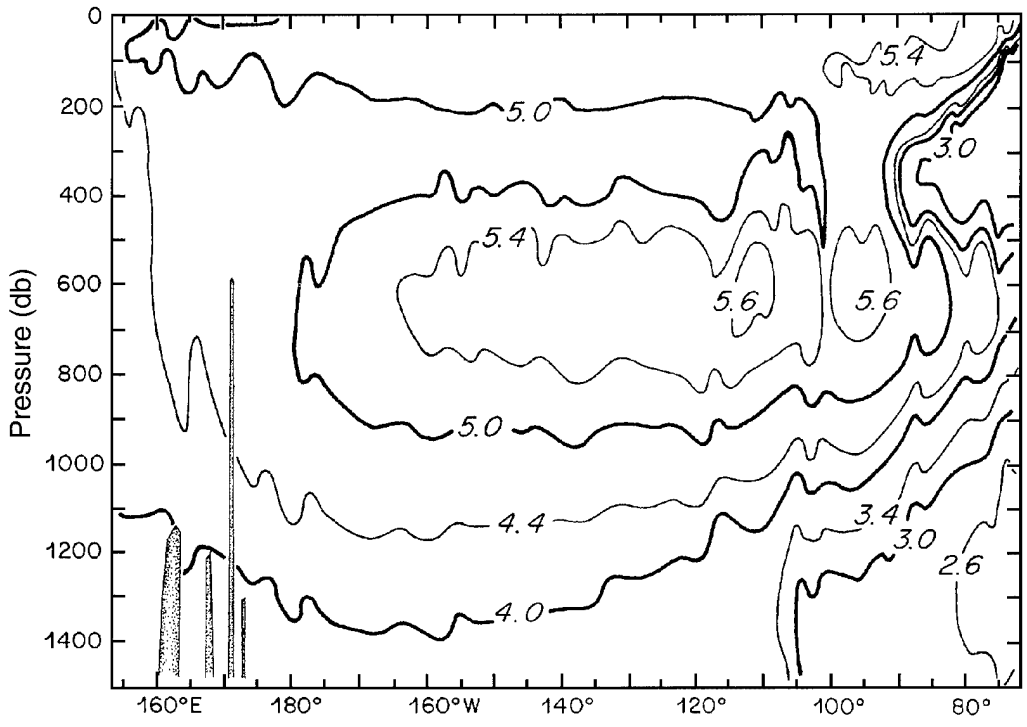

Figure II-54: Contours of O_2 for the upper 1500 db of a section across 32°S, adapted with smoothing and simplification from Toole *et al.* (1994b).

2c. The Low-Latitude Upper Layer Circulation

There has been a lot of very nice work in the low-latitude western Pacific in the last decade (*e.g.*, Butt and Lindstrom, 1994; Lindstrom *et al.*, 1987, 1990; Fine *et al.*, 1994; Tsuchiya, 1991; Tsuchiya *et al.*, 1989; Wijffels, 1993; Wijffels *et al.*, 1996). These efforts have also included detailed examination of the Mindanao Current (Lukas *et al.*, 1991, 1996; Toole *et al.*, 1988, 1990; Wijffels *et al.*, 1995). Although interesting in its own right, the oceanography of the western tropical Pacific is also important due to its participation in the El Niño–Southern Oscillation (ENSO) process (*e.g.*, Philander, 1990) and in the Indonesian Throughflow (*e.g.*, Godfrey, 1996). A summary map of the upper level currents in the low-latitude western Pacific Ocean by Godfrey (1996) was included earlier in this volume as Figure II-26; see also Figure II-9, adapted from Lukas *et al.* (1991) and Fine *et al.* (1994). There has also been a considerable amount of recent work in the vicinity of 10°N (Johnson, 1990; Johnson and Toole, 1993; Wijffels, 1993; Wijffels *et al.*, 1996), results important both for determining

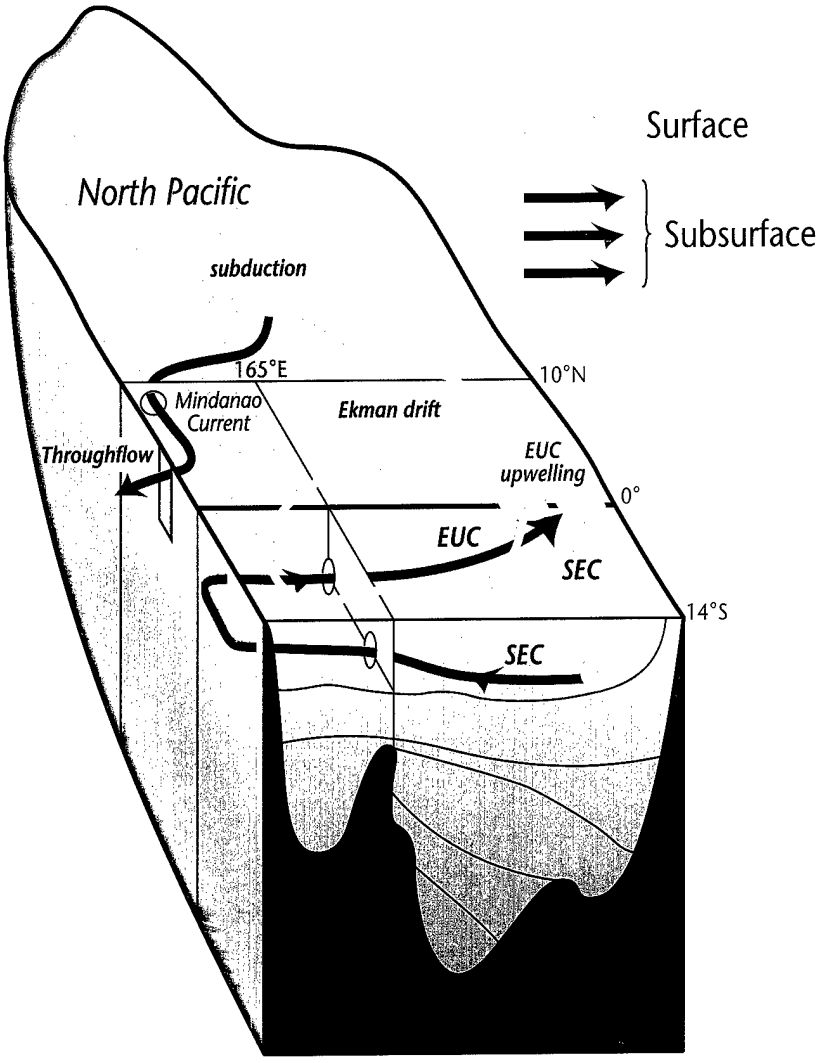

Figure II-55: A schematic version of the upper ocean cross-equatorial flow in the Pacific Ocean, adapted from Wijffels (1993, her figure 6.1).

the structure of the large-scale meridional cell and also for illuminating the nature of low-latitude current systems. A schematic version by Wijffels (1993) of how the flow from the tropical South Pacific to the equatorial and North Pacific might make it to the IT is shown in Figure II-55. Where comparable, the model estimates of the IT path (Figure II-10) by Shriver and Hurlburt (1996) are compatible in general terms with Wijffels's (1993) ideas in Figure II-55, the notable exception being the subduction north of the Mindanao Current (MC) by Wijffels (1993), perhaps an excursion needed to get "full blown" North Pacific characteristics into the IT.

Fine *et al.* (1994) and Butt and Lindstrom (1994) have identified the western low-latitude Pacific as a water mass and low-latitude boundary current crossroads for thermocline and intermediate waters. The upper ocean exchange between the South and North and Equatorial Pacific in the low-latitude western Pacific, as suggested in Figures II-9 and II-48 as well as Figures II-10, 26 and 55, has recently been measured directly in Vitiaz Strait (Figures II-56, 57 and 58). Mean transports through this strait are about 16 Sv (Murray *et al.*, 1995). Tsuchiya *et al.* (1989) and Tsuchiya (1991) demonstrate that the flow through Vitiaz Strait is a major source of the EUC as well as the pathway of Intermediate Water of circumpolar origin from the South to North Pacific. Previous measurements combining current meter and hydrographic data led to estimates (Lindstrom *et al.*, 1990) of 8–14 Sv through Vitiaz Strait and perhaps half that amount through St. Georges Channel. In Figures II-57 and

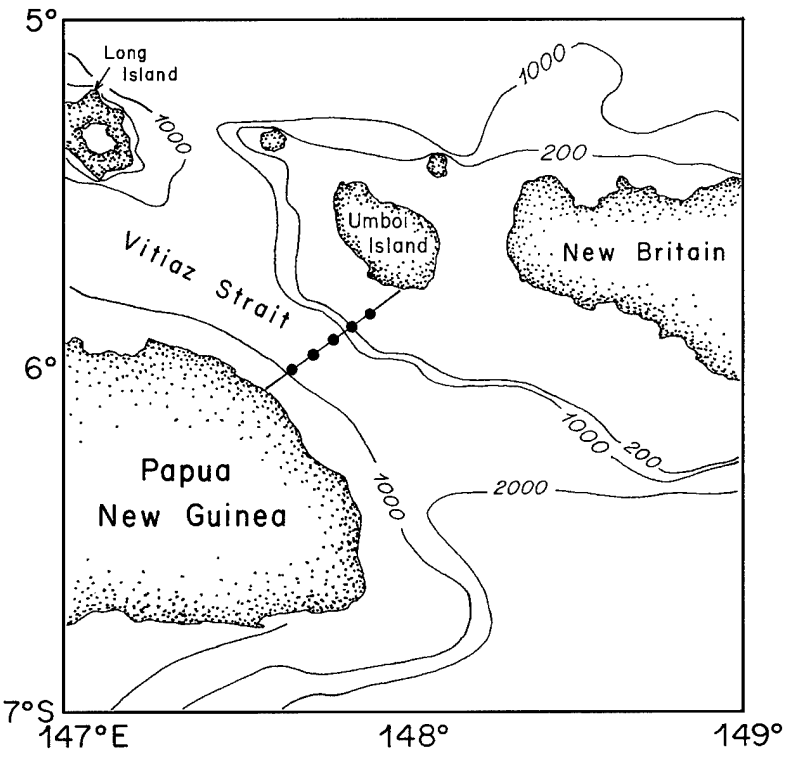

Figure II-56: Location of Vitiaz Strait moorings (dots) and section line, taken from Murray *et al.* (1995).

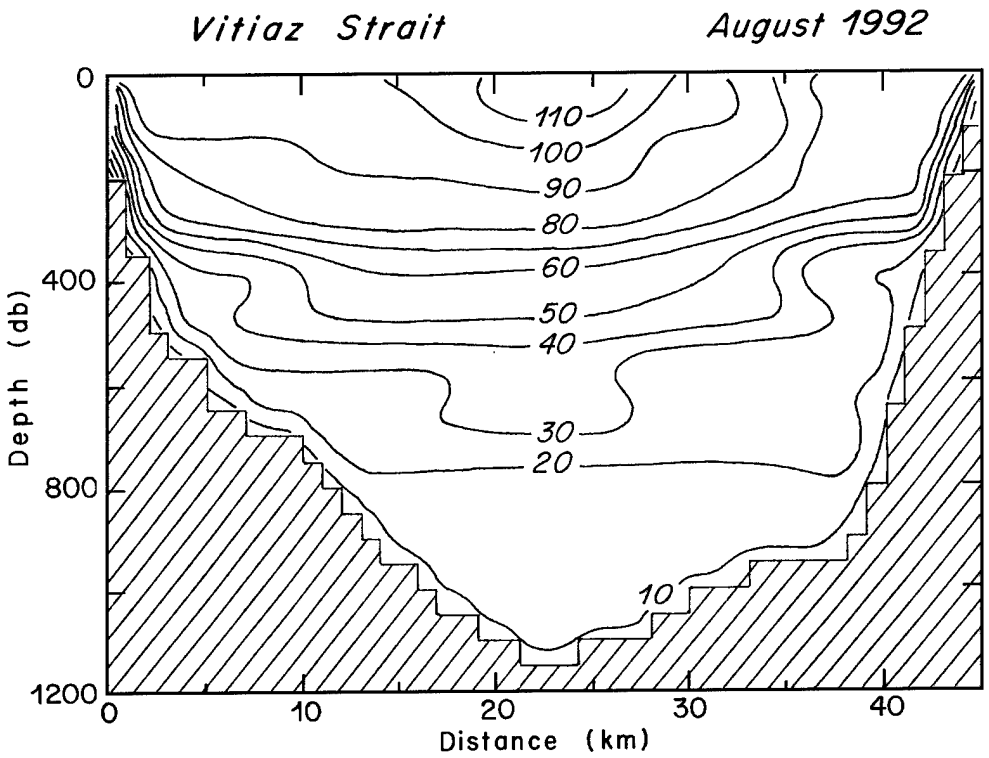

Figure II-57: Monthly averaged along-channel speeds (cm s^{-1}) in Vitiaz Strait, August 1992, taken from Murray *et al.* (1995).

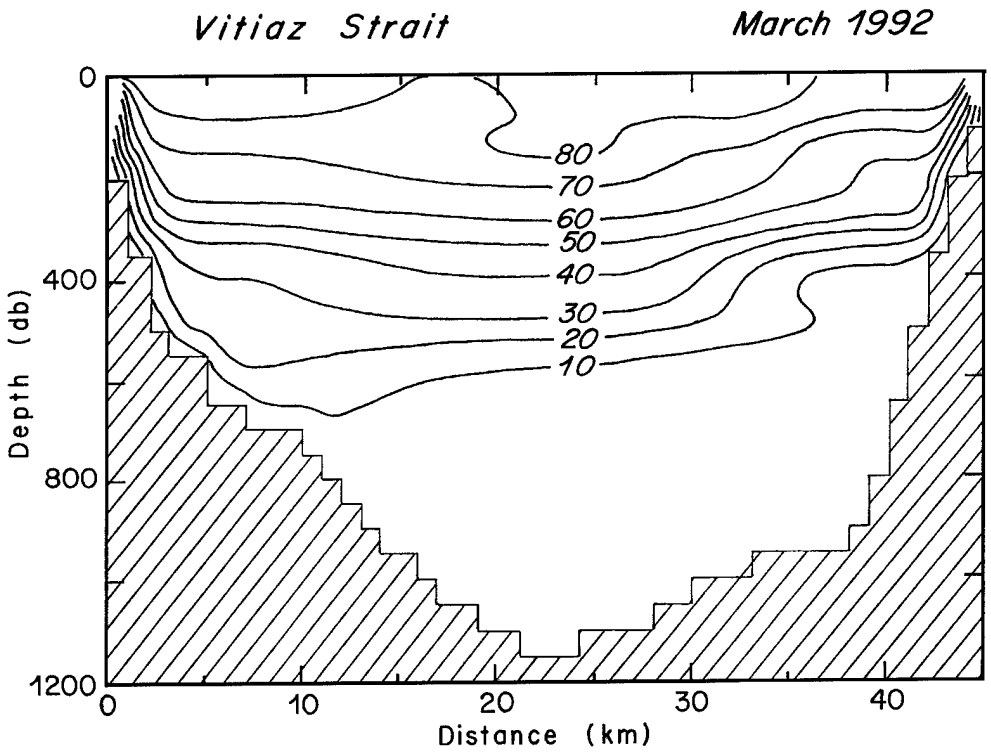

Figure II-58: Monthly averaged along-channel speeds (cm s^{-1}) in Vitiaz Strait, March 1992, taken from Murray *et al.* (1995).

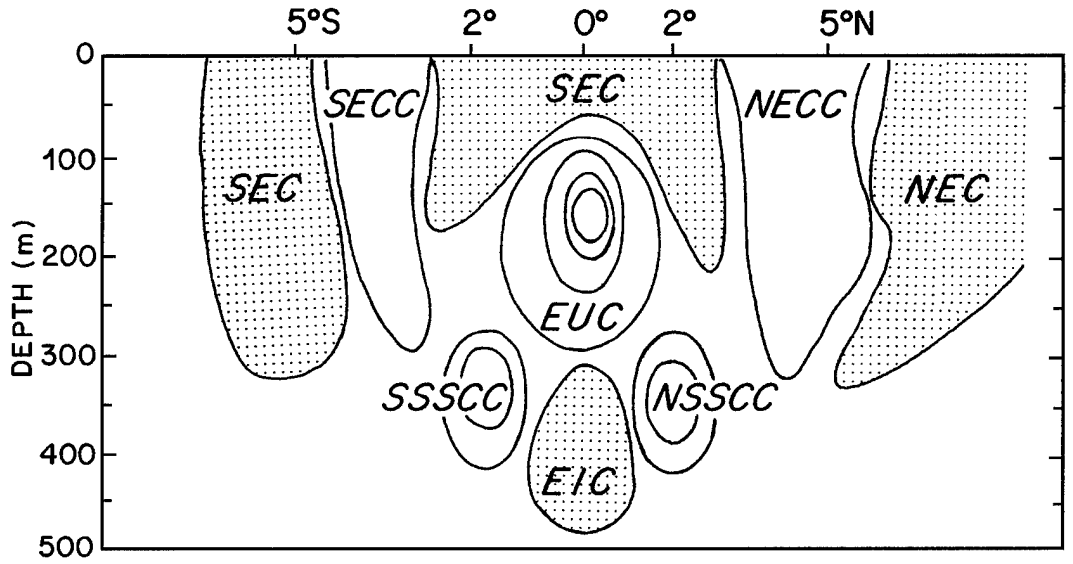

Figure II-59: A schematic of the low-latitude, upper-ocean flows near the equator. Stippled areas indicate westward flow, otherwise eastward. SEC = South Equatorial Current, NEC = North Equatorial Current, SECC = South Equatorial Countercurrent, NECC = North Equatorial Countercurrent, EUC = Equatorial Undercurrent, EIC = Equatorial Intermediate Current, SSSCC and NSSCC = Southern and Northern Subsurface Countercurrents.

II-58, the currents (and associated transports) below 400–500 m depth are in the σ_θ range (based on data presented for nearby sections by Tsuchiya *et al.*, 1989) of IW as defined here ($26.8 \leq \sigma_\theta \leq 27.5$ kg m^{-3}). Very crude estimates of the transport below $\sigma_\theta = 26.8$ from Figures II-57 and 58 suggest an IW transport of perhaps 1–3 Sv (consistent with the 2–4 Sv found by Tsuchiya, 1991) out of the average of 16 flowing through Vitiaz Strait. This implies (to me) the necessity of considerable upstream conversion of IW to upper layer water or another major conduit for IW into the low-latitude current systems in the western Pacific in order to supply the IT.

A sectional schematic of the major upper-ocean, low-latitude current systems near the equator is shown in Figure II-59, adapted from Wijffels (1993). An early review of the oceanography of the equatorial Pacific Ocean, primarily in the east, was completed by Wyrtki (1966). Figure II-60 is his summary of the surface flow in October in the eastern Pacific, with specific current names appended. Other important early summary articles are by Cane and Sarachik (1983), Knauss (1963, 1966), Philander (1990), and Tsuchiya (1961, 1970, 1975, 1981); please see also Tsuchiya *et al.* (1989). Although the upper level equatorial circulation in the Pacific has received tremendous attention,

deeper measurements are scarce. But along with shallow equatorial jets (Firing, 1988), one also observes deep equatorial jets (Eriksen, 1982; Firing, 1987).

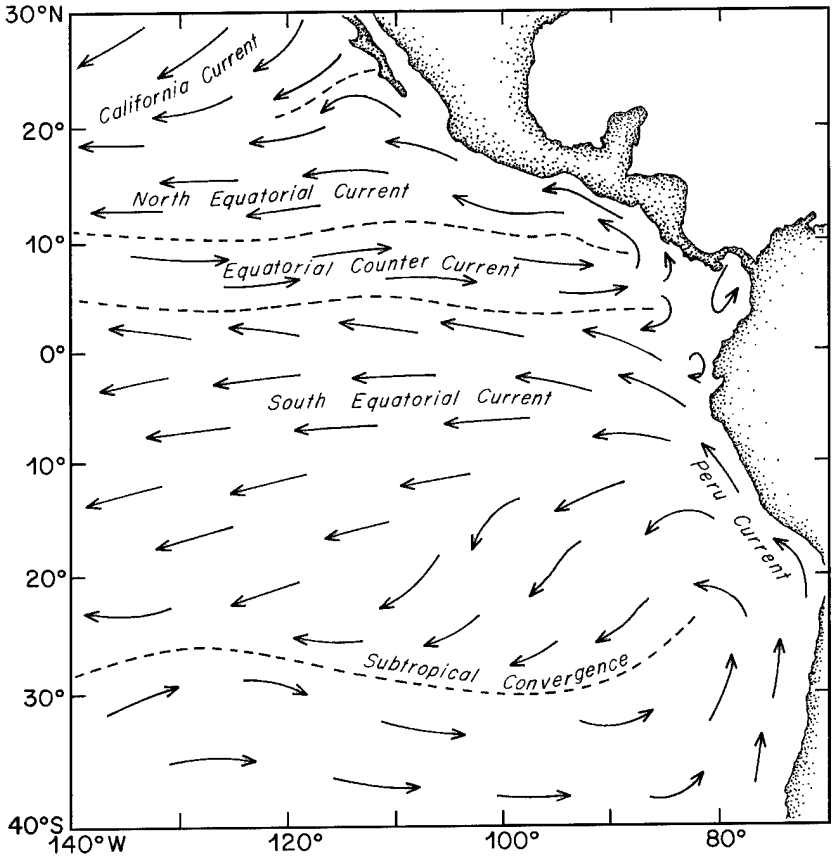

Figure II-60: Surface circulation in the eastern low latitude Pacific in October and names of the major current systems.

A new summary of the low latitude circulation of the North Pacific along 10°N has been published by Wijffels (1993) and Wijffels *et al.* (1996). According to these sources, the upper 500 m of the North Pacific along 10°N can be divided into three regions: a layer of weak temperature and salinity gradients extending from the surface to roughly 100 m depth, a sharp thermocline where temperature changes from 28°C to around 12°C over a vertical interval of order 100 m, and a region of lower stratification below. Along 10°N, the NPSTW (North Pacific Subtropical Water) salinity maximum occupies the upper thermocline between 20 and 25°C, and is found between the Philippines coast and about 150°W. A salinity minimum occupies the lower part of the thermocline, below the NPSTW salinity maximum. Found at progressively lower densities going eastward, the salinity minimum terminates in the surface layer at 140°W, just east of where the NPSTW outcrops. More recently, Tsuchiya (1981) proposed that the Southern Subsurface Counter Current (SSSCC) advects South Pacific Subtropical Water (SPSTW) to the eastern Pacific and maintains the 13°C thermostad: a layer of low stratification that lies below the EUC in the eastern Pacific.

2d. Intermediate Water

The two dominant intermediate water masses in the Pacific Ocean in terms of salinity minima are AAIW and NPIW (Reid, 1965). The section along 160°W (Figures II-12 through II-14), in combination with maps at two key density horizons presented by Reid (1965), form the basis for a general description of the circulation of both AAIW

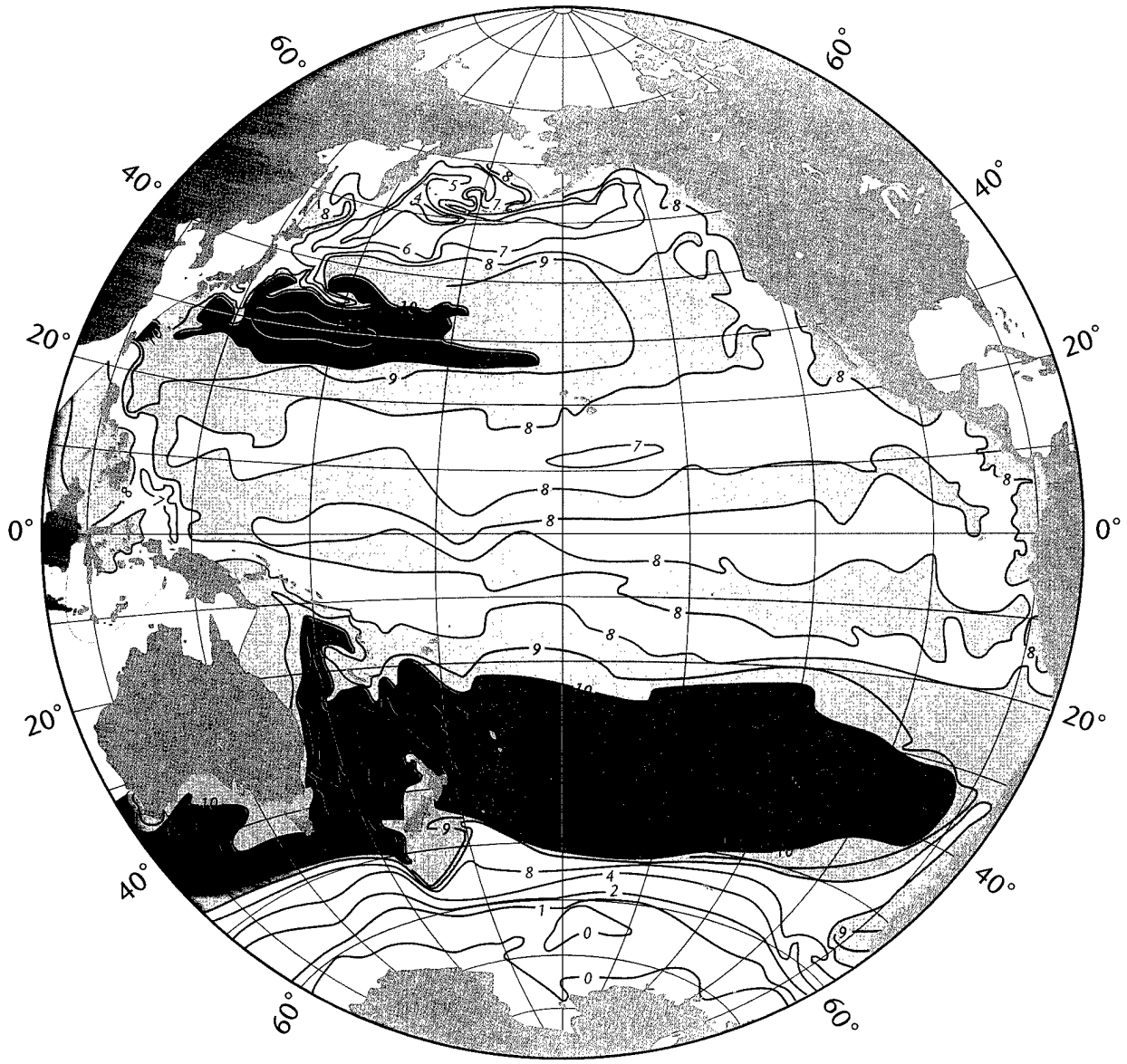

Figure II-61: Depth contours (in hectometers) on the σ_t horizon 27.3 (approximately), adapted from Reid (1965, his figure 22).

(Figures II-27 through II-29) and NPIW in the Pacific Ocean (Figures II-61 through II-63). Similar maps for all the Southern Hemisphere Oceans at four density horizons were constructed by Taft (1963). Maps of salinity and oxygen on density surfaces (Reid, 1965; Taft, 1963) indicate that IW (spanning the σ_θ range from ≐ 26.8 to 27.5) moves north from the ACCS in the eastern Pacific and thence west in the SEC at about

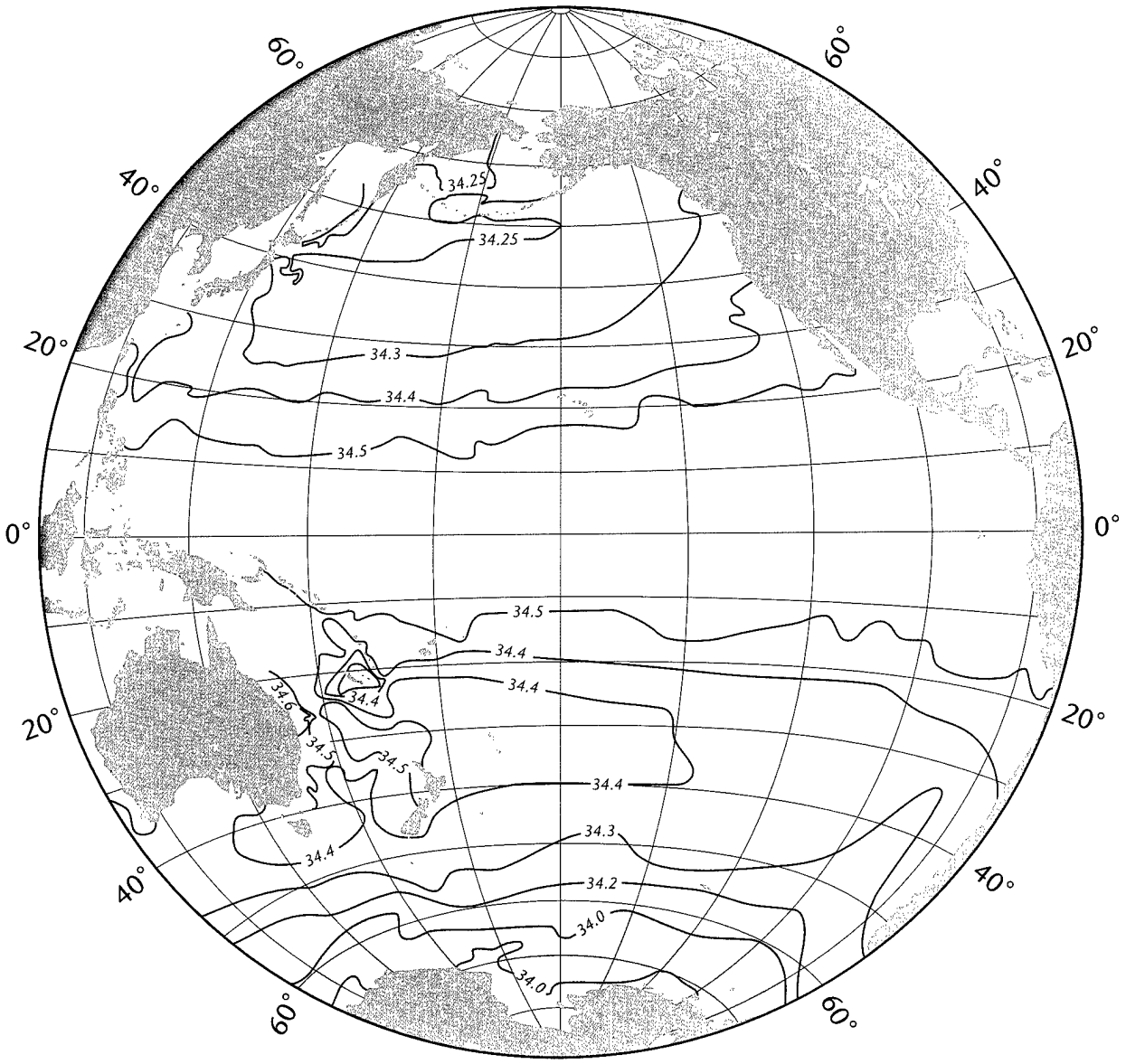

Figure II-62: Salinity contours (psu) on the σ_t horizon 27.3 (approximately), adapted from Reid (1965, his figure 24).

20°S (to some extent with the subtropical gyre). Intermediate water in the South Pacific is predominantly lower Subantarctic Mode Water (McCartney, 1977, 1982; McCartney and Baringer, 1993). Some IW approaching the equator in the west gets caught up in equatorial and tropical circulation schemes, part of which also makes its way across the equator in the western equatorial Pacific then northward along the

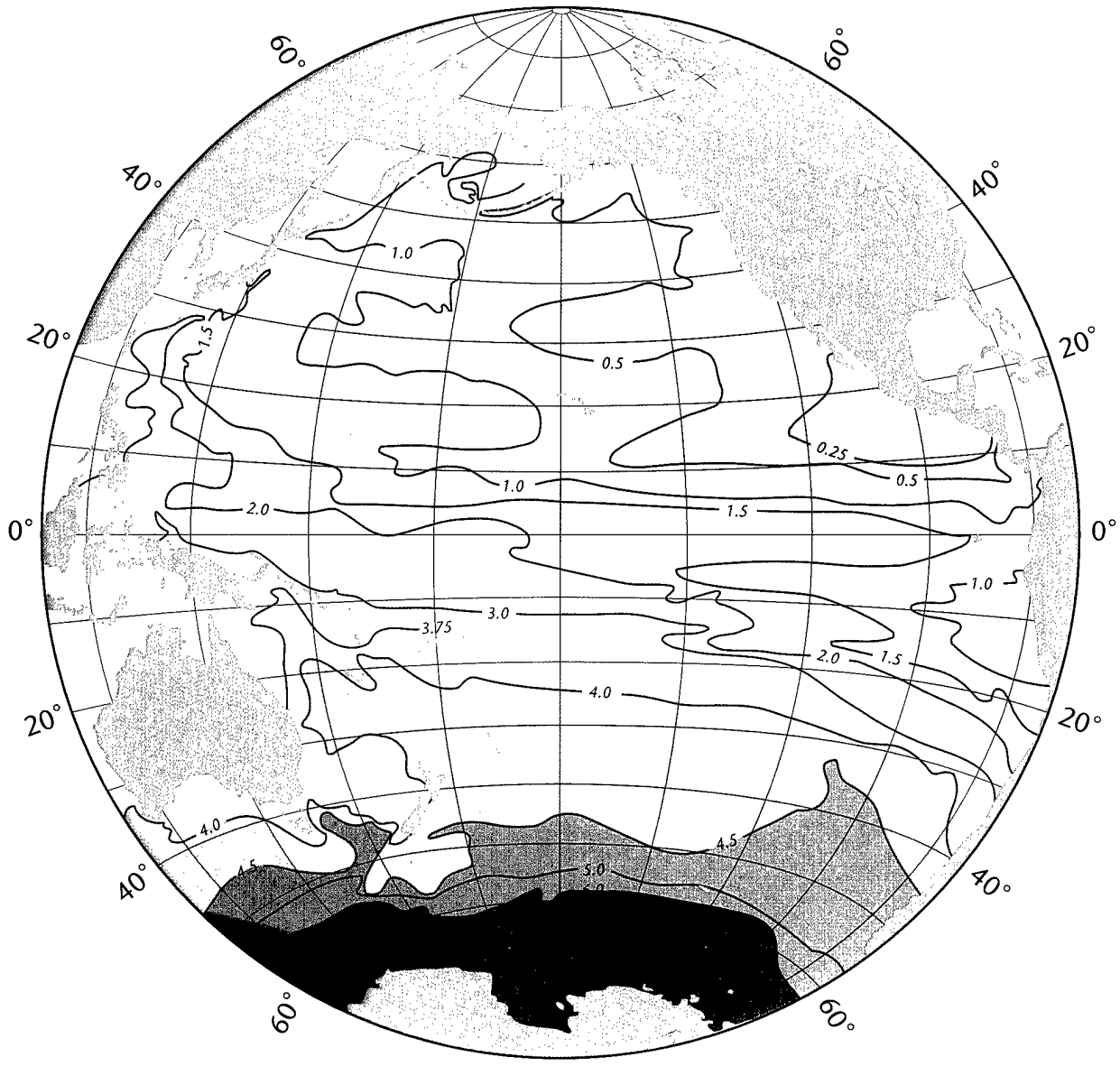

Figure II-63: Oxygen contours (ml L⁻¹) on the σ_t horizon 27.3 (approximately), adapted from Reid (1965, his figure 25).

western boundary of the North Pacific (Reid, 1965; Reid and Mantyla, 1978; Rochford, 1960a; Tsuchiya, 1991).

According to Taft (1963) and Reid (1965), intermediate water enters the South Pacific from the ACCS off the coast of South America, and travels with the South Pacific Subtropical Gyre, flowing west toward the Coral Sea at about 20°S, with the SEC. It is also clear in all maps that intermediate water is headed north of Australia, toward Papua New Guinea as well as toward the Coral Sea. In Taft's (1963) maps the UPIW salinity patterns are even more suggestive in this regard than for LOIW. Tsuchiya (1991) found that about 2–4 Sv of intermediate water was transported toward the equator in the Pacific by a narrow western boundary undercurrent, called the New Guinea Coastal Undercurrent, through Vitiaz Strait and along the coast of Papua New Guinea. According to Tsuchiya (1991, p. S278), after crossing the equator, part of this IW gets caught up in the subsurface NEC along 2°N, but the major part continues northward along the western boundary of the North Pacific. Interesting early articles

Table II-7: Intermediate Water Types, Tasman Sea

Water types on the 27.20 σ_t surface in the Tasman and Coral Seas

Name	Salinity (‰)	Phosphate P (μg-atom/L)
Antarctic Intermediate	34.01	1.88
Pacific Equatorial Intermediate	34.60	3.10
South-West Pacific Intermediate	34.70	0.50

Water types on the 26.80 σ_t surface in the Tasman and Coral Seas

Name	Salinity (‰)	Oxygen (ml/L)	Phosphate P (μg-atom/L)
Upper Equatorial Intermediate	34.80	< 2.00	2.50–3.00
Subtropical	35.20–35.40	5.00–6.00	< 0.50
Upper Antarctic Intermediate	33.80–34.00	6.00–7.00	1.40–1.60

on intermediate water in the Tasman Sea were published by Rochford (1960a, b), see Table II-7. Six intermediate water types were identified, three on the surface σ_t = 27.20 and three on σ_t = 26.80, on the basis of oxygen and phosphate as well as salinity. Burling (1961) identified an indo-pacific type of intermediate water south of New Zealand (also discussed by S95). Fine *et al.* (1994) have made a convincing case that the western equatorial Pacific is a water mass crossroads. I feel that this is true for the upper and intermediate layers of the Pacific Ocean in general at low latitudes (20°S–20°N), not only the equatorial area.

In the eastern segment of the North Pacific subtropical gyre, NPIW is found where fresh subarctic waters spread southward, forming a well-defined $S_{\min}$ at σ_θ = 26.8 (Reid, 1965; Talley, 1993). Bingham and Lukas (1994) have also identified NPIW along the coast of Mindanao, some of which may enter the Indonesian Passages. Reid (1965) suggested widespread subsurface vertical mixing in the subpolar gyre as the source of freshening at NPIW densities, while Talley (1993) advocated mixing with denser Okhotsk Sea water in the straits linking the open North Pacific and the Okhotsk Sea. This point, along with the circulation of NPIW in the western North Pacific, has recently been discussed by Yasuda *et al.* (1996). The circulation of intermediate water in the eastern North Pacific, including the low-latitude eastern Pacific, has recently been discussed by Tsuchiya and Talley (1996).

I have become convinced lately that, from the interbasin circulation point of view, the eastern South Pacific plays a doubly crucial role in the global picture. In the first case, it is clear that this is where the ACCS delivers to the Pacific the SAMW and IW needed to replace the IT, although the details of this path are far from established. The conversion of LSAMW (UPIW) to USAMW is necessary to get the "right" water out through Vitiaz Strait [only 2–4 Sv of the combination of LSAMW (UPIW) and LOIW are so involved] to supply the IT (a further conversion to SLW in equatorial and low-latitude current systems is also necessary). It seems clear that LSAMW and LOIW participate in a subtropical gyre circulation as well, although somewhat south of the SEC perhaps, which could be an upward spiral. But it is also clear that there is a loss of LSAMW in the eastern South Pacific between the 43°S and 28°S Scorpio sections (McCartney and Baringer, 1993), which could imply upward diapycnal conversion in the Peru Current, joining the SEC. I'm definitely not suggesting that most (which I take to be recirculating) of the LSAMW in the South Pacific is converted upward in the

eastern South Pacific, only 5–10 Sv are needed. The conversion could also occur along the boundary of the SEC and the LSAMW tongue. But secondly, the southernmost eastern South Pacific may be a key location for an upward diapycnal transformation of LOIW to UPIW and/or CDW (or even NPDW and IODW) to LOIW that appears to be a necessary component of the global thermohaline circulation. This is the first time I've seen this suggestion made, and I'm aware of minimal evidence for these latter suggestions, other than some numerical model results, maybe, and the observation that there's a lot of LOIW under LSAMW in the 43°S Scorpio section (McCartney and Baringer, 1993) that is not salinity minimum water, but has salinities like "upper" deep water.

2e. The Deep and Near-Bottom Circulation

The abyssal waters in the Pacific Ocean are renewed by flow from the ACCS, primarily as Circumpolar Deep Water (CDW), although possibly including some AABW, and one could perhaps say mostly Lower Circumpolar Deep Water (LCDW); see Johnson (1990), Johnson and Toole (1993), Reid (1986), Roemmich and McCallister (1989), Toole *et al.* (1994b), Wijffels (1993), and Wijffels *et al.* (1996). Circumpolar Deep Water is here taken to be a mixture of converted AABW and transformed NADW, having been modified along excursions north into all the oceans, and homogenized by repeated circulation in the ACCS (schematics of this are in Section 5 below). Defining characteristics of CDW in the Pacific Ocean, relative to the overlying water mass, generally NPDW but perhaps locally in some areas better labeled as "modified CDW" or Pacific Deep Water (PDW) or Upper Deep Water (UDW), include cold temperatures, high oxygen, comparatively low silica, and relatively high salinity. Along 32°S (Figures II-37 and 38), which for this report is the input section to the Pacific Ocean from the ACCS, incoming CDW has silica values of 110–125 and $0.6 \leq \theta \leq 1.2$°C. These silica and potential temperature ranges for CDW along 32°S are similar to those measured many years earlier at 43°S (see for example, Reid, 1986, pp. 16–17). Circumpolar Deep Water entering the Pacific from the south returns to the ACCS, in my opinion both after recirculation with some property changes to PDW or UDW and after some major modification to North Pacific Deep Water (NPDW).

The Samoan Passage (near 10°S, 170°W) has historically been a natural choke point for determining the flow of CDW approaching the North Pacific (Reid and Lonsdale, 1974; Roemmich *et al.*, 1996; Taft *et al.*, 1991), and a region of interesting variability (Johnson *et al.*, 1994). Probably the best existing definition of the flow characteristics of CDW as it moves toward the North from the South Pacific and ACCS occurs at a "new" section (Figures II-35 and II-36) between roughly 150 and 180°W (over the latitude range ~ 15–25°S) from the East Pacific Rise to Fiji (Roemmich *et al.*, 1996), where CDW has silica values ~ 125 and $0.8 \leq \theta \leq 1.2$°C. This recent section by Roemmich *et al.* (1996) crosses the Samoan Passage where previous measurements were concentrated (Reid and Lonsdale, 1974; Taft *et al.*, 1991). This section is a doubly useful "channel" in that both the incoming CDW and a "returning" deep flow that possesses a silica maximum are present. The deep water above and somewhat to the east of the CDW on this section is characterized by a silica maximum near 140 be-

tween 2500 and 4000 m depth. The silica maximum of ~ 140 for deep water at this section is so much lower than the silica maximum of 180 observed for NPDW in the Northeast Pacific Ocean (Talley and Joyce, 1992; Talley, 1995) that I feel there's a better chance we are looking to a large extent at a locally or regionally horizontal recirculation. The generally northward flowing horizontal path of CDW at 4000–4500 m toward the Samoan Passage area in the South Pacific is shown clearly by Reid (1986, his figures 67 and 68).

Moving to the North Pacific, the coldest waters at 10°N (CDW) reside (Wijffels, 1993) in the Central Pacific Basin, which has the deepest channel. The influence of water of circumpolar origin at 10°N is also seen in the East Mariana Basin and over the deepest part of the East Pacific Rise. A silica map for the near bottom (σ_4 = 45.88, near 4500 m depth typically) North Pacific is contained in Figure II-64 (adapted from Talley and Joyce, 1992, and Talley, 1995), which is suggestive of a strong zonal component in the flow of CDW (actually "modified" CDW or Pacific Deep Water might be a more appropriate name). I also feel that Mantyla's (1975) maps and discussion went a long way toward showing us how CDW and "other" deep waters might behave in the Pacific Ocean. The low silica tongue of CDW or modified CDW entering the North from the South Pacific in Figure II-64 appears to wrap around or recirculate around the Hawai-

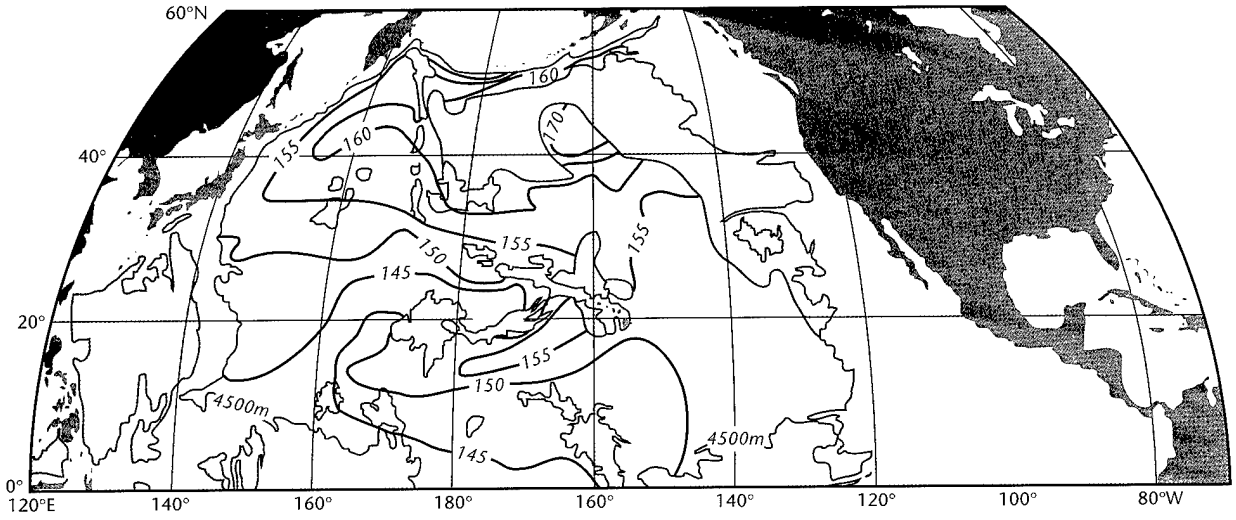

Figure II-64: A silica map for the North Pacific on σ_4 = 45.88, adapted from Talley and Joyce (1992) and Talley (1995). Locations with depths less than 4500 m are darkly shaded. Lighter gray shading identifies areas with depths greater than 4500 m, but where water denser than σ_4 = 45.88 is found.

ian Island chain, as well as propagate farther north to a lesser extent into the North Pacific north of 30°N, all the while increasing in silica along its path, especially north of 30°N or so. Please note for future reference (Section 2f) that for the 24°N section described and discussed by Roemmich *et al.* (1991) and Bryden *et al.* (1991), there is quite a bit of recirculation of modified CDW in this area implied in Figure II-64.

In both the 10°N and 24°N sections, one sees water near the bottom that is somewhat enhanced in silica relative to CDW on the eastern side. This water is notably lower in silica (also comparatively cold) than the overlying deep water. I take this to be evidence for a regional recirculation of modified deep water that occurs without having transited the northernmost Pacific Ocean. The flow pattern by Johnson and Toole (1993) has a recirculation south of the Hawaiian Island chain, and a sizable penetration north (some of which could of course wrap around the Hawaiian Island chain, as in Figure II-64). It could be useful (and this is what I will try to do in Section 2f) to think of a water mass between CDW and NPDW that recirculates at a variety of locations along the incoming path of CDW especially south of, say, 24°N, north of which exists another major horizontal flow pattern where the really large silica maxima that clearly characterize NPDW occur. The horizontal pattern(s) of flow of bottom and deep water north of 24°N are controversial, to say the least (Roemmich and McCallister, 1989; Talley 1995; Talley and Joyce, 1992; Talley *et al.*, 1991; Warren and Owens,

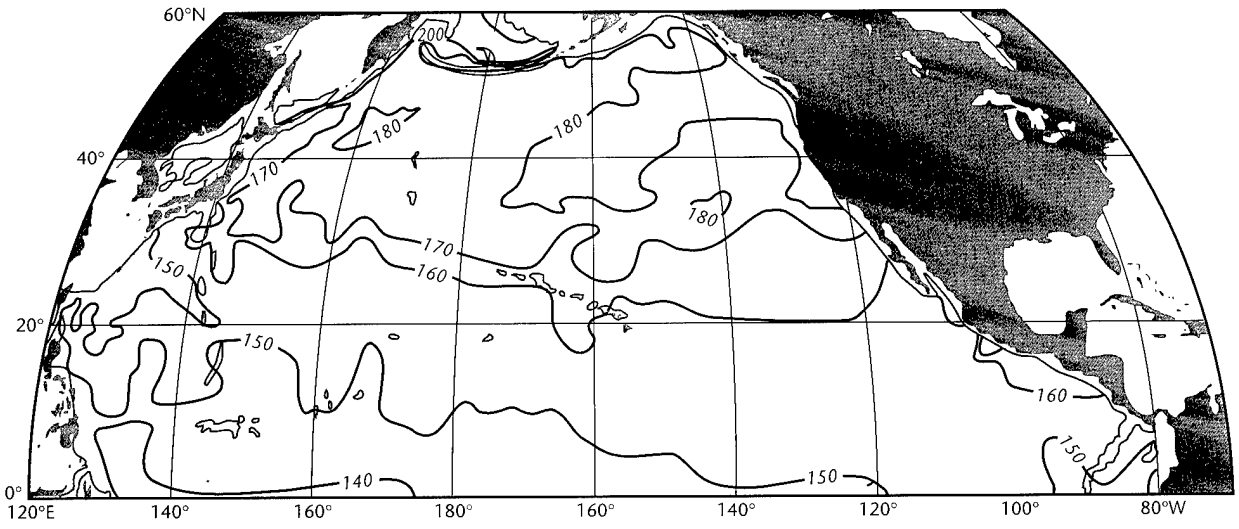

Figure II-65: A silica map for the North Pacific on σ_2 = 36.90, adapted from Talley and Joyce (1992). The shaded areas indicate depths less than 2000 m.

1988). There even exist (Fukasawa *et al.*, 1987) seemingly very good and large mean flow estimates in the northern abyssal Shikoku Basin that, to the best of my knowledge, have never been connected to anything else.

North Pacific Deep Water is conventionally taken to be the end-product of slow warming and freshening (*e.g.*, Mantyla, 1975) of cold dense waters of Antarctic origin,

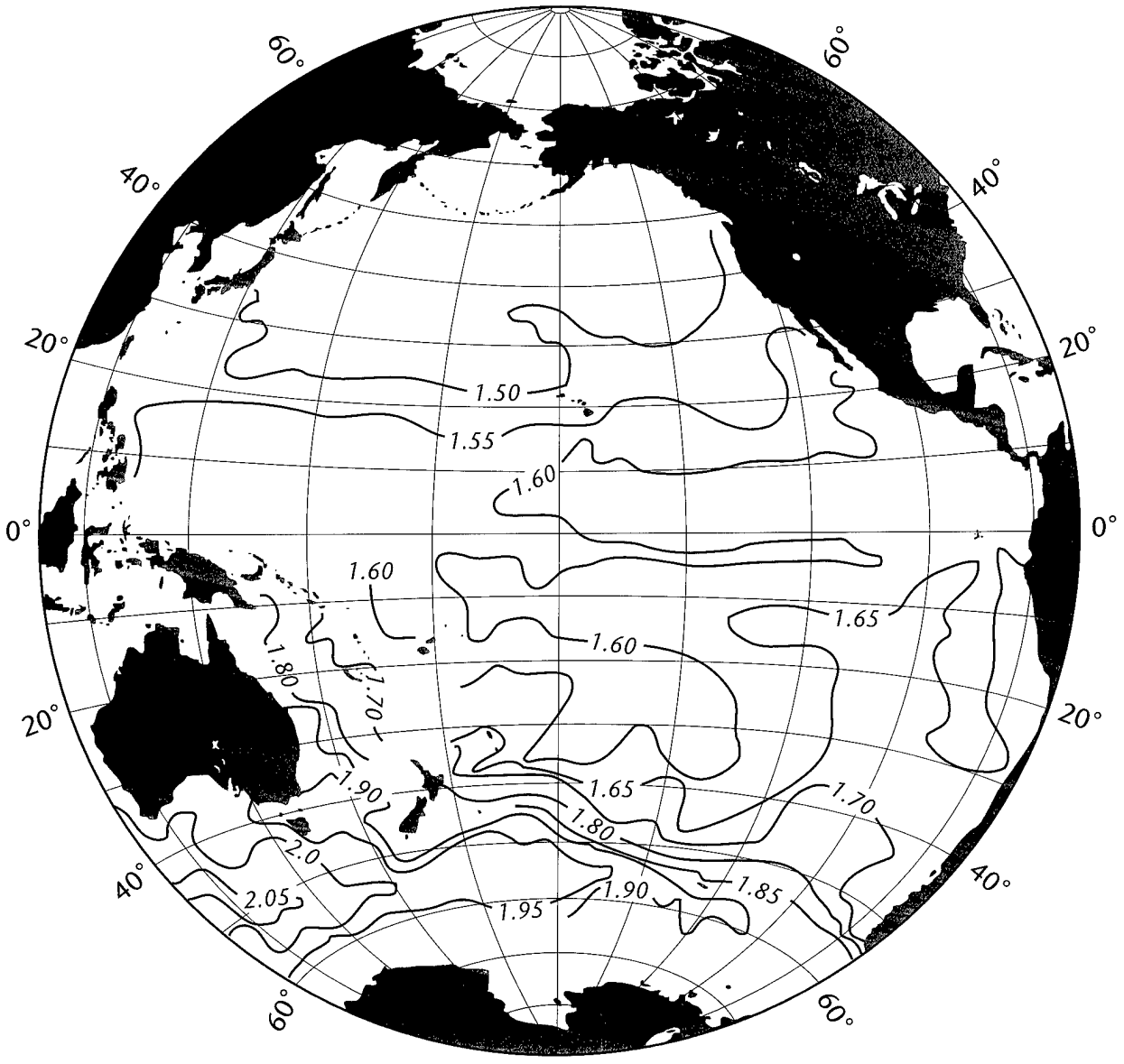

Figure II-66: Potential temperature (°C) on σ_2 = 36.96 (2500 m depth nominal) for the Pacific Ocean, adapted from Talley and Johnson (1994) and Talley (1995).

i.e. CDW (but see Bryden *et al.*, 1991, and below). The defining characteristics of NPDW are high dissolved silica concentrations acquired from long contact with sediments in the northeastern North Pacific and in-situ dissolution (Talley *et al*, 1991;

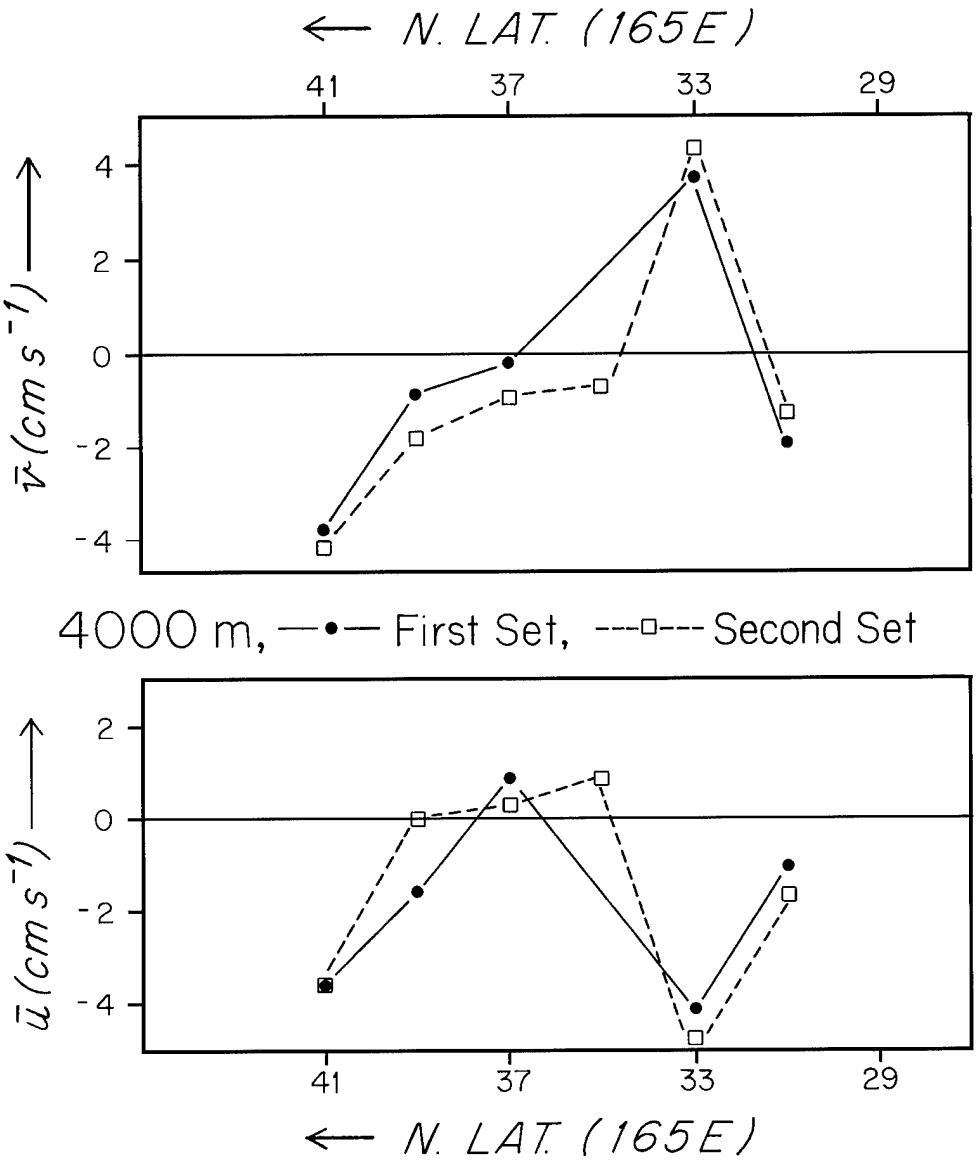

Figure II-67: Estimates of the latitudinal distribution of mean flow at 4000 m depth along 165°E, adapted from Schmitz (1987). These are the most stable time-averaged flows I have ever measured.

Talley and Joyce, 1992), and low oxygen concentrations due to consumption by the oxidation of organic particulate matter in the water column. The highest concentrations of silica along 10°N (> 160 μmol/L) are situated (Figure II-34) between 120°W and 150°W, at the crest of the East Pacific Rise. The silica distributions at a somewhat shallower σ horizon (Figure II-65; $\sigma_2 \doteq 36.9$, ~ 2000 m depth) are notably different than at 4000–5000 m (Figure II-64). In Figure II-65 an anticyclonic cell north of about 25–30°N might be suggested. At the upper end of NPDW is a signature of hydrothermal venting at the crest of the East Pacific Rise (Talley and Johnson, 1994; Talley, 1995). A strong zonality for the flow in upper NPDW (at $\sigma_2 \doteq 36.96$) is indicated by the potential temperature distributions in Figure II-66. A plume of ^{3}He-rich water emanates from the crest of the Rise and spreads westward along the section. A similar plume has been observed extending westward from the Rise at 15°S (Hautala and Riser, 1989, 1993). Both plumes are associated with a warm anomaly on density surfaces (Talley and Johnson, 1994).

In addition to the deep and bottom currents associated with the thermohaline circulation, there are mean flows in the vicinity of the KCS, to some extent associated with rectification of the eddy field, as is the case in the North Atlantic (*i.e.*, Holland, 1978; Schmitz and Holland, 1982, 1986). The deep mean velocity field associated with the Kuroshio Extension from 152°E to 152°W has been directly measured by Schmitz *et al.* (1982, 1987), Schmitz (1987, 1988) and Joyce and Schmitz (1988). Figure II-67 is an example of the most stable mean flows I have ever measured. Most recently, similar measurements have been made near the Izu Ridge but in the Kuroshio Extension by Hallock and Teague (1996), Teague *et al.* (1994), and Shiller *et al.* (1996).

2f. The Large-Scale Meridional Cell in the Pacific Ocean

Our present understanding of the structure of the meridional overturning cell in the Pacific Ocean has recently been nicely summarized by Talley (1995), having been taken a large step forward by Wijffels (1993), Wijffels *et al.* (1996), Toole *et al.* (1994b), and Roemmich *et al.* (1996). At this point I'm going to present what are more or less the first, to my knowledge, data-based transport sections that have been drawn for the zonally-integrated meridional cell in the Pacific Ocean. I propose a figure(s) for the Pacific Ocean analogous to the one for the Atlantic Ocean that I developed in Volume I of my report (Figure I-12 there) and presented in the Introduction to this volume as Figure II-11. The Atlantic meridional overturning cell is probably on firmer ground than is the case for the Pacific, primarily due to the historical concentration of resources in the Atlantic Ocean. At this time, and given the material presented in earlier sections of this report, I see the circulation of intermediate water as the least well-determined element of the picture, followed by NPDW. The incoming CDW seems rather well documented, as the case for the upper level component of the IT, at low latitudes. But I've never seen a data-based explanation of how the ACCS ultimately supplies the IT, and a couple of possibilities that were discussed earlier in this report are presented now. Perhaps surprisingly, there is a numerical-model-based scheme

Table II-8: Transports at 32°S

Layer	Water Types	Net Transport (Sverdrups)
1	Thermocline waters	9.9
2	Antarctic Intermediate Water	6.7
3	Equatorial Water (east), AAIW (west)	–7.0
4	North Pacific Deep Water and Lower Circumpolar Water	–12.0
5	Returning Lower Circumpolar Water	–3.7
6	Densest of the Lower Circumpolar Water (AABW)	16.5
Total		10.5

available to supply the IT (Shriver and Hurlburt, 1996), and there are in fact similarities between these model results and the schemes I present in this report volume.

In the past decade, detailed zonal sections at key latitudes in the Pacific have been completed as noted earlier, and the transport estimates as presented by "individual" authors are contained in Tables II-8, 9 and 10. The 32°S transports (Toole *et al.*, 1994b) are presented in 6-layer format (Table II-8). The 10°N transports (Wijffels, 1993; Wijffels *et al.*, 1996) are summarized in four layers (Table II-9), and the estimates for 24°N by Bryden *et al.* (1991) broken down many ways, Table II-10 being a six-layer condensation that I put together from the detailed data breakdowns that were presented. Transport estimates for various water masses at these three recent zonal hydrographic sections are summarized in a common four-layer format in Table II-11, but since I will work with 6 layers or so, the 10°N 4-layer summary in Table 9 was

Table II-9: Geostrophic transport (10^9 kg s^{-1}) across 10°N in broad water mass classes

Water Mass	θ bounds	Transport (10^9 kg s^{-1})
Thermocline	$\theta > 12.4°$ C	–38.2
Intermediate Water	$2.8 < \theta < 12.4$	–1.0
Deep Water	$1.1 < \theta < 2.8$	–8.3
Bottom Water	$\theta < 1.1$	8.3
Net Geostrophic		–38.1
Ekman Transport		39.0

Table II-10: Geostrophic transports at 24°N

Water Mass	Temperature Range	Transport
Upper Layers	$\theta \geq 5.0°$ C	0
Upper Intermediate Water	$3.0°C \leq \theta \leq 5.0°C$	1.9
Lower Intermediate Water	$1.9°C \leq \theta \leq 3.0°C$	1.8
NPDW	$1.20°C \leq \theta \leq 1.9°C$	–4.3
UCDW	$1.05°C \leq \theta \leq 1.120°C$	–4.1
CDW	$\theta \leq 1.05°C$	4.8

expanded upon in order to produce the meridional cell figures discussed below. There is also some variability in layer definition between Tables 8-11. The IT will be taken to be 10 Sv throughout. This is consistent with RT96 (my benchmark) and the approximate average of Fieux *et al.* (1994) and Fieux *et al.* (1996a). But I do examine a couple of possible variations of the distribution of this 10 Sv in density parameter space at various stages of its path.

Table II-11: Pacific Ocean Transports (Sverdrups) for indicated zonal sections

	32°S Toole *et al.* (1994b)	10°S Wijffels *et al.* (1996)	24°N Bryden *et al.* (1991)
Ekman	n.e.*	39.0	12
WBC	n.e.	n.e.	28.3
Upper Layers	9.9	–38.1	–40.3
Intermediate Water	–0.3	–1.0	4.3
NPDW	–12.0	–8.3	–8.4
CDW	12.8	8.3	4.9

*n.e.: estimate not provided

A guess at the qualitative (no transport estimates) structure of the large-scale meridional cell in the Pacific Ocean in a global context was shown as a part of Figure II-8. A more detailed picture, so even more of a guess (#1), involving six layers (plus a throughflow "layer" or box) and including transport estimates, is shown in Figure II-68. This 6-layer picture uses layers that I have found useful, and the layer structure in Tables 8 through 11 has been reconfigured to these layers for Figure II-68. I've extrapolated a lot in Figure II-68, primarily because I believe (gut feeling) that the IW and SAMW component of the large-scale Pacific meridional cell needs more scrutiny, at least with regard to how the IT is supplied. Also, it seems to me that the "conventional" CDW/NPDW cell really involves at least a couple of regional recirculations [one has

been described by Johnson and Toole (1993), and another implied by Talley (1995), Talley and Joyce (1992), and perhaps by Bryden *et al.* (1991)].

In Figure II-68 I am taking the deep/bottom cell to be closed, that is, not involved with intermediate water. I'm suggesting three regional recirculations of CDW south of, say, 30°N (one right at the 24°N section). The total incoming Circumpolar Deep Water and outgoing UCDW (U, upper, or "modified" CDW) transports at 32°S are taken from Toole *et al.* (1994b), rounded off to the nearest Sverdrup. Most of the source for the IT (8 out of 10 Sv) is taken to be LOIW that is supplied from the ACCS in the eastern South Pacific, with 3 Sv of this supplied from the meridional cell in the Indian Ocean via the Agulhas Current System, AF and SFZ. Two Sverdrups of USAMW are also shown as being directly supplied to the South Pacific from the Subantarctic Frontal Zone. Five Sverdrups of lower intermediate water are shown having their ultimate origin in the PFZ, presumably as UCDW. Six Sverdrups of this LOIW are converted to UPIW (LSAMW) off the coast of Chile south of the 43°S Scorpio section, and further transformed to USAMW in the Peru Current by 28°S. Figure II-68 shows 4 Sv of intermedi-

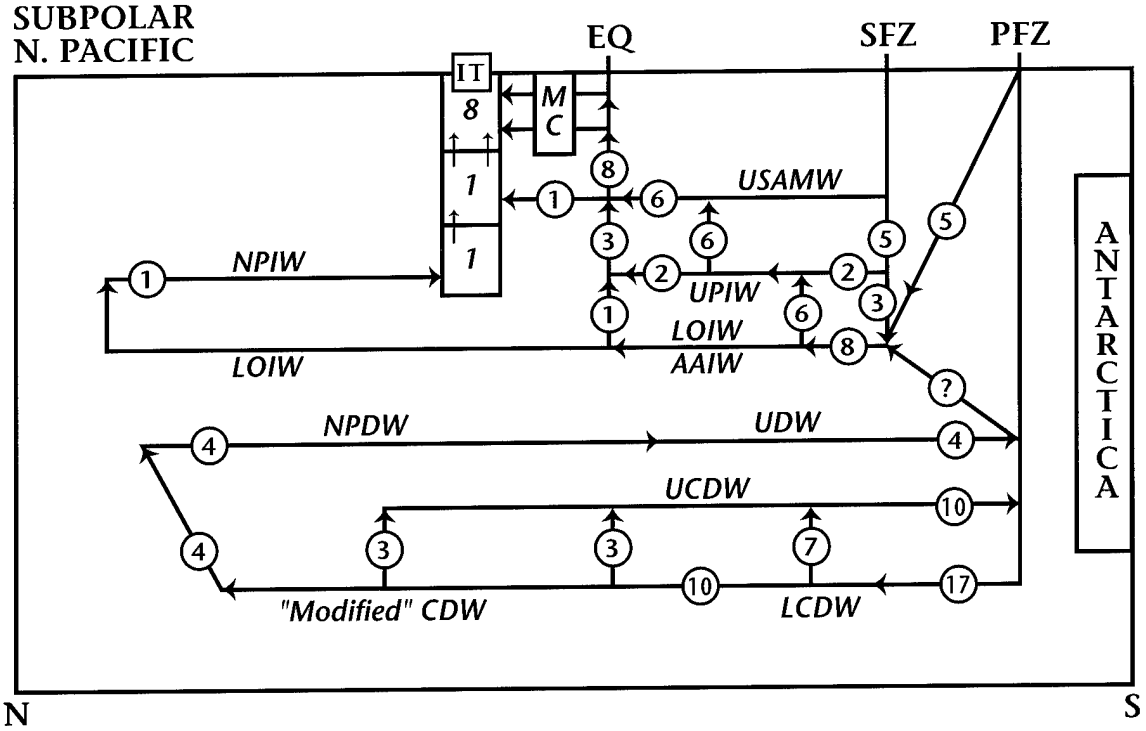

Figure II-68: A first cut at a schematic transport configuration for the large-scale meridional cell in the Pacific Ocean.

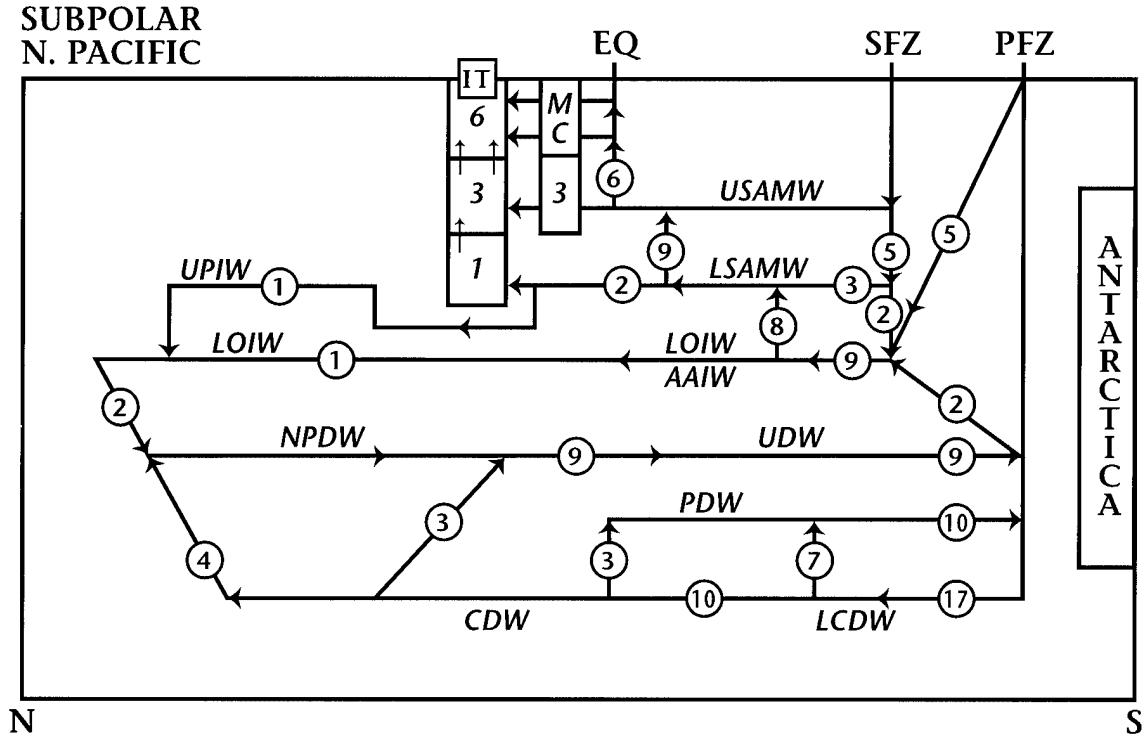

Figure II-69: My second guess at an idealized transport scheme for the large-scale meridional cell in the Pacific Ocean.

ate water (2 UIPW and 2 LOIW) going through Vitiaz Strait (or nearby), 3 upwelled at the equator and 1 continuing on into the North Pacific, eventually supplying the IT after diapycnal modification to the NPIW density parameter range. This 1 Sv is shown to be diapycnally modified upward through NPIW to Upper Subantarctic Mode Water to SLW in the IT. Three Sverdrups of UPIW are also shown being modified to USAMW at the equator for a total of 9 Sv USAMW there. Most of this USAMW (8 Sv) is converted to surface layer water at the equator and eventually supplied to the Indonesian Throughflow through the Mindanao Current (MC). One Sverdrup of USAMW is shown entering the IT and being diapycnally modified upward to SLW.

A second guess at a Pacific meridional cell configuration is presented in Figure II-69, a considerably more complicated scenario than presented in Figure II-68. In both Figures II-68 and II-69, 5 Sv of the lower intermediate water supplied by the ACCS in the southeastern South Pacific is taken to arrive via the PFZ, perhaps as a result of the "conventional" mechanism. On the other hand, if transformation from Circumpolar Deep Water to LOIW takes place off the coast of Chile, in the latitude range 40–50°S,

say, then CDW might be eroded upward to LOIW by convection. This would perhaps be consistent with the salinity distribution at 32°S (Figure II-53) where LOIW is below a salinity minimum of 34.3, at salinities of 34.4 and 34.5. In Figure II-69 the bottom/deep cell transports are coupled with 2 Sv of lower intermediate water, taken to be resupplied to the SFZ from NPDW (CDW) near the Polar Frontal Zone. So a total of 9 Sv of LOIW is supplied to the southernmost eastern South Pacific via the ACCS in Figure II-69, 8 Sv then being transformed to LSAMW (UPIW) off the coast of Chile. Please note that by 32°S (Figures II-52, 53 and 54) the intermediate water density parameter range is dominated by LSAMW with both the salinity minimum and oxygen maximum located there.

One Sverdrup of lower intermediate water is shown entering the North Pacific (via Vitiaz Strait). In Figure II-69, 3 Sv of LSAMW (UPIW) enter the Peru Current from the ACCS and join the 8 Sv of upward converted LOIW. Nine Sverdrups of LSAMW are then transformed to USAMW in the low-latitude (~ 28°S) segment of the Peru Current. The remaining 2 Sv of UPIW flow through Vitiaz Strait with 1 going into the IT where it is modified to USAMW, perhaps in the Banda Sea. The other 1 Sv joins 1 Sv of lower intermediate water in interacting with NPDW formation. Nine Sverdrups of USAMW flow into the equatorial Pacific with 3 entering the IT as USAMW and 6 being modified to SLW before entering the IT through the MC. Although the net LOIW supplied to the Pacific by the ACCS is 1 Sv larger in Figure II-69 than in II-68, there are only 2 instead of 3 Sv supplied from the Indian Ocean via the AF and SFZ. The transport of intermediate water in Vitiaz Strait is now 3 Sv instead of 4.

In Figure II-69 17 Sv of LCDW enter the South Pacific from the Antarctic Circumpolar Current System and 10 Sv are returned to the ACCS by two recirculations, one, of 7 Sv in the South Pacific south of the Roemmich *et al.* (1996) section, another (3 Sv) near the equator. The direct recirculations of CDW in II-69 have been collectively called Pacific Deep Water (PDW) rather than UCDW as in Figure II-68. Four Sverdrups are modified to NPDW in the northern North Pacific, along with 2 Sv IW, with these 6 Sv merging with 3 Sv of highly transformed CDW in the northern hemispheric tropics to form a composite of 9 Sv of deep water, eventually joining the ACCS as upper deep water (UDW), where 2 Sv are re-converted to lower intermediate water. The meridional overturning cell in the Pacific Ocean is described in a global context in Section 5 of this report.

2g. The Mesoscale Eddy Field

The data base for describing the eddy field in the North Pacific Ocean can be thought of as having four or five sources. There were various surveys early on, primarily hydrographic, some by geomagnetic electrokinetograph (GEK), before the explosion of eddy-related field programs in the 1970s onward. There were a small number of "early" moored instrument results (Taft *et al.*, 1973). Maps of K_E based on ship drift by Wyrtki *et al.* (1976) were very influential. Then there were XBT-of-opportunity programs (notably the TRANSPAC Program; *e.g.*, Bernstein and White, 1974, 1977, 1981; White and Bernstein, 1979). Talley and White (1987) have presented results from this XBT exploration of the upper layer temperature field in the North Pacific. Then, in the 1980s and continuing until the present, a variety of moored arrays were set and retrieved in the North Pacific (*e.g.*, Schmitz *et al.*, 1982, 1987; Schmitz, 1987, 1988; Hallock and Teague, 1996). Taft *et al.* (1981) demonstrated that the eddy field in the abyssal interior of the North Pacific was very weak. Most recently, floats are being deployed in the Pacific Ocean to determine eddy statistics and mean flows. Riser (1995) has demonstrated that K_E near 1000 m depth in the vicinity of the Kuroshio

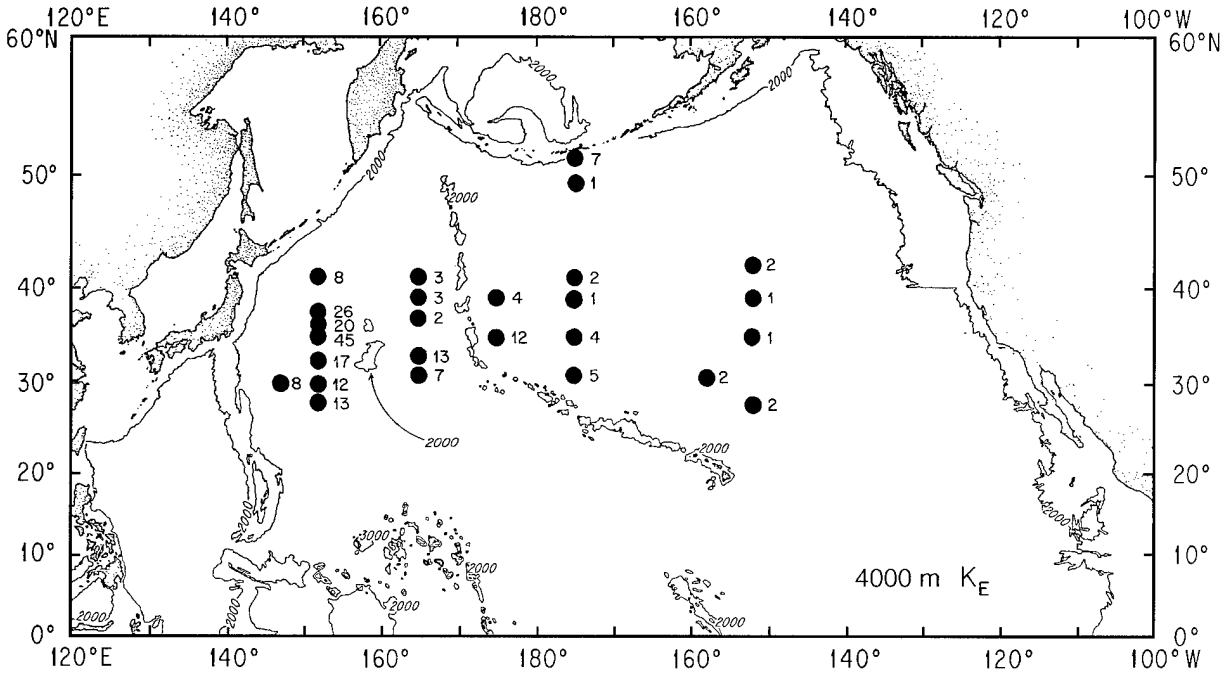

Figure II-70: Estimates of abyssal (~ 4000 m depth) K_E in the mid-latitude North Pacific, taken from Schmitz (1988).

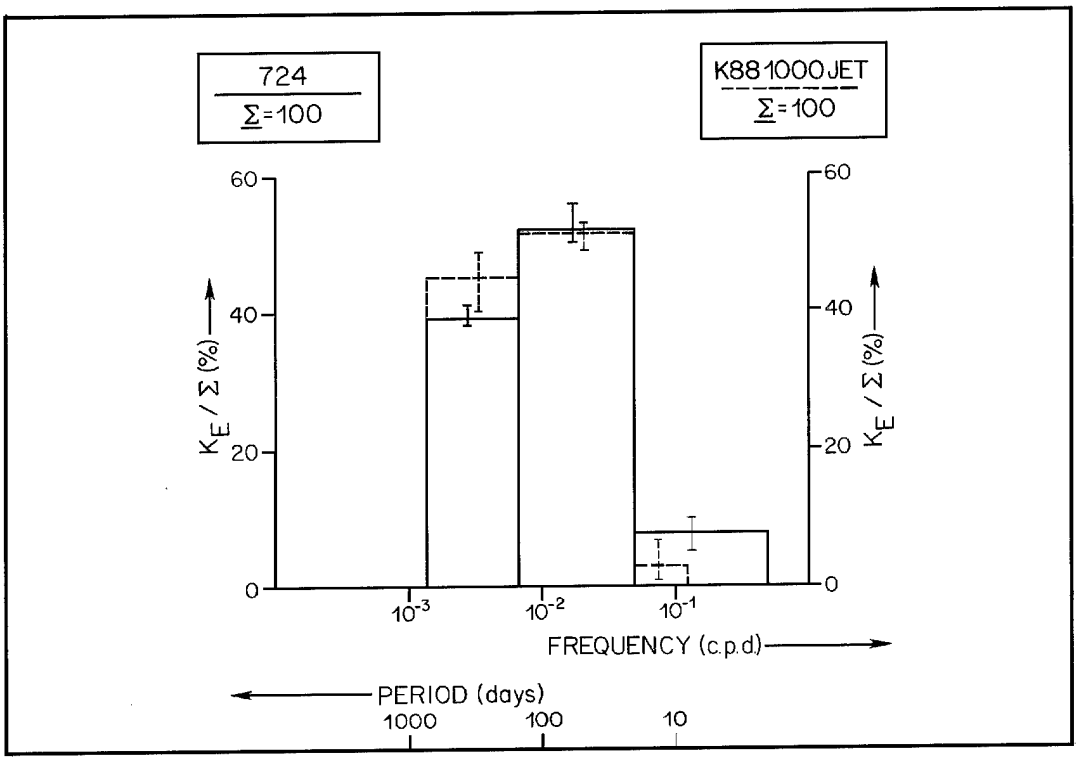

Figure II-71: Vertically averaged and normalized (percentage) frequency distributions of K_E. The solid line and error bars are for mooring 724 from 152°E in the Kuroshio Extension. The dashed line and error bars are from an 8-layer numerical experiment.

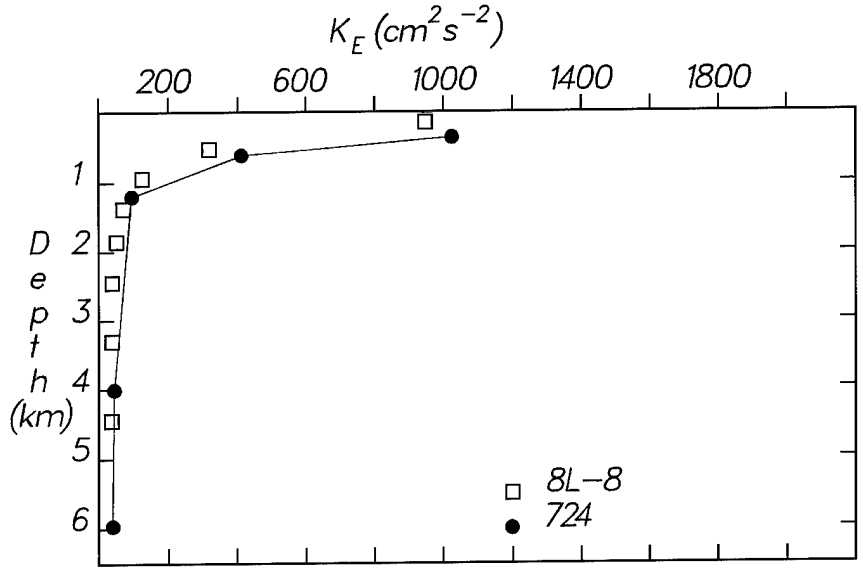

Figure II-72: Vertical distributions of eddy kinetic energy, adapted from Schmitz and Holland (1986). Solid dots denote data from the North Pacific along 152°E, and open squares denote model results from the equivalent longitude of an 8-layer numerical experiment.

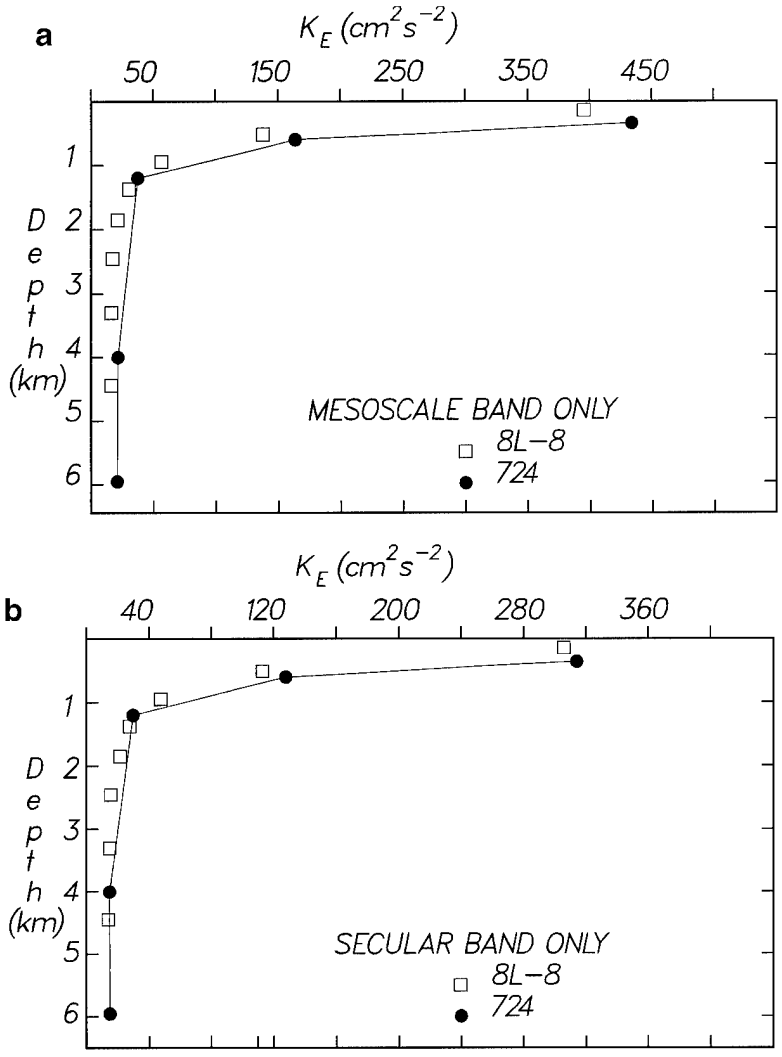

Figure II-73: Vertical distributions of K_E at mooring 724 (solid dots), and for a particular 8-layer numerical experiment, for specific frequency bands: (a) the mesoscale, periods 20–150 days; and (b) secular scale, periods 150–720 days. Adapted from Schmitz and Holland (1986).

Extension is ~ 100–120 cm^2 s^{-2} near 145°E, decaying to about 80 at 152°E, then to about 50 at 165°E, and about 10 near the dateline. The mean flows observed in the entire area of operation are mostly, but not entirely, eastward.

The first long-term moored instrument array across a sizable section of the mid-latitude North Pacific (Schmitz *et al.*, 1982) was initially set in 1980 and recovered for the last time in 1982. Observations were made along 152°E from 28° to 41°N across the Kuroshio Extension, in two deployments of ten moorings for roughly a year each. Results from this array and associated XBT and CTD measurements have been presented by Koblinsky *et al.* (1984), Niiler *et al.* (1985), Schmitz *et al.* (1982, 1987), and Schmitz (1984a, b); see also Schmitz and Holland (1986), Bradley (1982), and Levy and Tarbell (1983). An additional two-year moored instrument data acquisition cycle was initiated in the fall of 1983 to extend this type of data base zonally at mid-latitudes. Fourteen moorings were

deployed across the North Pacific east of 152°E to 152°W, with each site occupied for about 2 years. Results from this array and associated CTD measurements were presented by Joyce and Schmitz (1988) and Schmitz (1987, 1988). Niiler and Hall (1988) and Hu and Niiler (1987) have published results from a moored instrument and CTD exploration at 152°W.

Various observational descriptions for the eddy field along 152°E were published by Schmitz (1982, 1984a, b). Abyssal K_E is contained in Figure II-70, an update of figure 8 from Schmitz (1988). Schmitz (1988) also presented a variety of vertical structure distributions for the eddy field in the North Pacific. In summary, the vertical, horizontal and temporal statistical scales of the eddy field in the mid-latitude North Pacific are now reasonably well known at zero order. The eddy field in the Kuroshio Extension is less energetic than in the Gulf Stream, especially near 4000 m depth, and decays much more abruptly zonally moving away from the western boundary. Results from an early intercomparison (Schmitz and Holland, 1986) of numerical model results in the North Pacific with data from long-term moorings in the Kuroshio Extension are contained in Figures II-71 to II-73. In summary, two numerical experiments were found that have realistic temporal, zonal and vertical distributions in the vicinity of the Kuroshio Extension.

The dynamics of the Kuroshio/Oyashio current system were recently investigated in detail using a set of eddy-resolving simulations of the Pacific Ocean north of 20°S, along with model–data comparisons, by Hurlburt *et al.* (1996). In the principal simulations the horizontal resolution is 1/8° for each variable and the vertical resolution ranges from 1.5-layer reduced gravity to 6 layers with realistic topography. It was possible to extend one of the 6-layer simulations with realistic topography to 1/16° resolution and two different eddy viscosities. These results were supplemented by 1/16° two-layer simulations of the Pacific subtropical gyre (closed boundaries). Both the 2- and 6-layer simulations are able to simulate the meander path and the straight path south of Japan, the prominent mean meander path just east of Japan, and the separation of the connecting flow from the Kuroshio to the subarctic front from the east coast of Japan. These results are directly linked to the combined effects of baroclinic instability and several specific topographic features. In essence, the topography regulates the location and strength of the baroclinic instability.

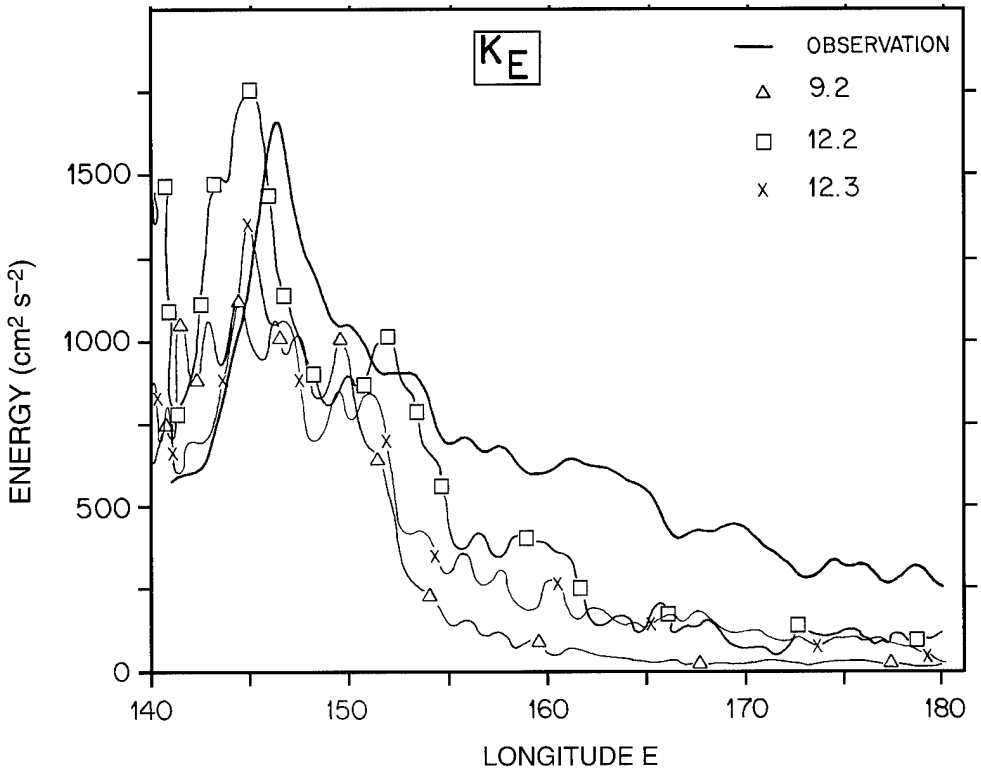

Figure II-74: K_E at the sea surface as a function of distance along the axis of the Kuroshio Extension. The solid line denotes the data, symbols various 6-layer numerical experiments.

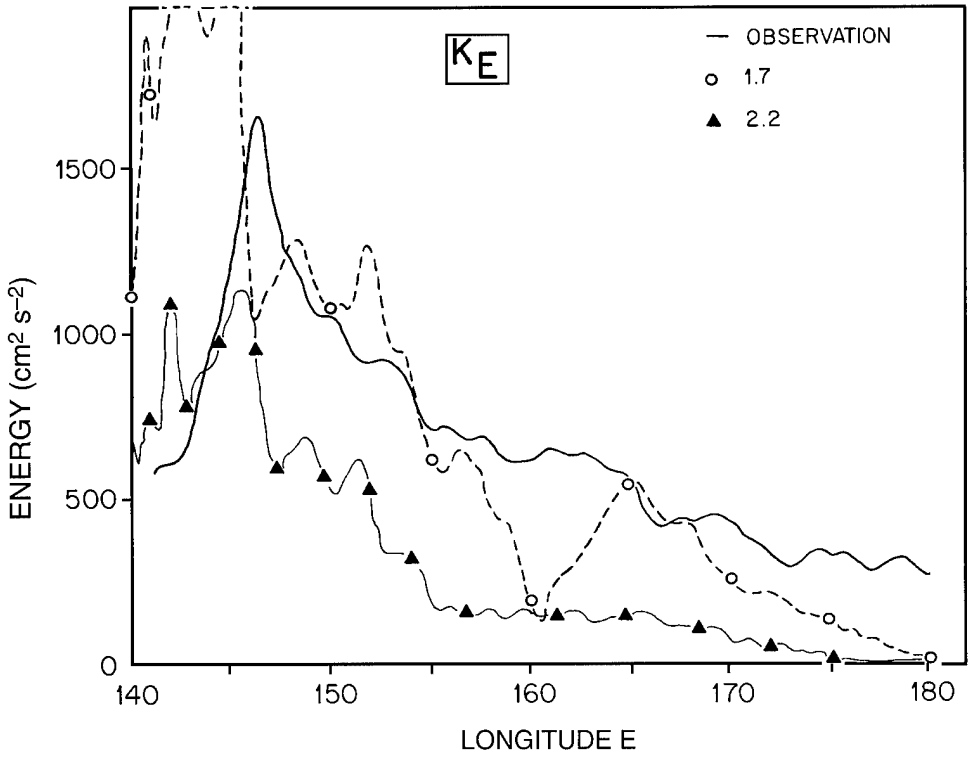

Figure II-75: K_E at the sea surface as a function of distance along the axis of the Kuroshio Extension. The solid line denotes the data, symbols indicate the results of various 2-layer numerical experiments.

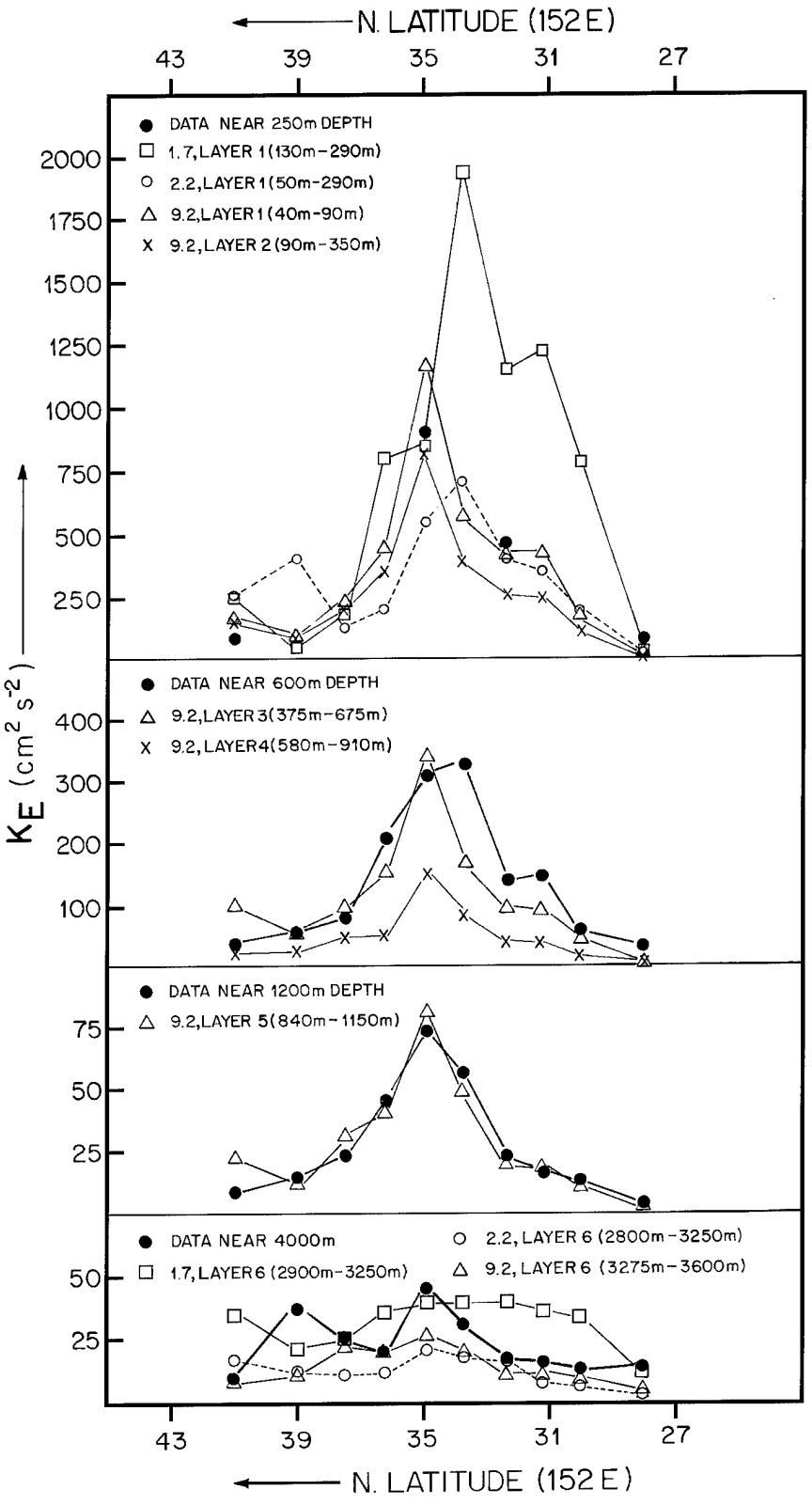

Figure II-76: K_E as a function of latitude for 152°E and depth ranges. Solid black circles denote data, other symbols various numerical experiments.

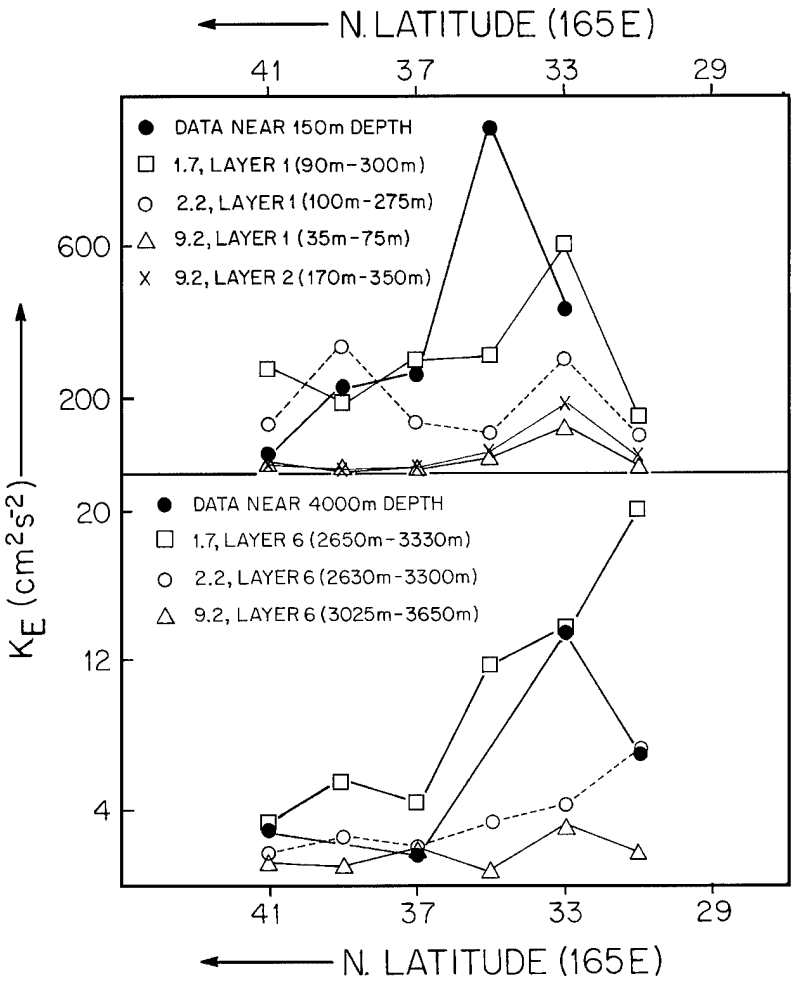

Figure II-77: K_E as a function of latitude along 165°E for indicated depth ranges. Solid black circles denote data, other symbols various numerical experiments.

Comparisons with observations from Geosat altimetry and current meters ranging in depth from 150 to 4000 m show that increasing the grid resolution from 1/8° to 1/16° for each variable yields substantial improvements in the simulation of the Kuroshio Extension, especially east of the Shatsky Rise. These include increased eastward penetration of the inertial jet and associated high K_E. Selected results of this intercomparison are shown in Figures II-74 through II-77. Eastward penetration of an inertial jet from a western boundary is a canonical problem in ocean modeling (Schmitz and Holland, 1982; Holland and Schmitz, 1985; Schmitz and Thompson, 1993).

The statistics of the eddy field in the South Pacific are relatively unexplored compared to most other oceans. However, the mechanism for formation of EAC (warm core) rings has been sorted out in a nice piece of work by Nilsson and Cresswell (1981). Their summary sketch of the kinematics of EAC ring development in a somewhat modified form is used here as Figure II-78. This "sock" mechanism is similar to ring or eddy development in the Agulhas Retroflection (Section 3g below) and in the North Brazil Current.

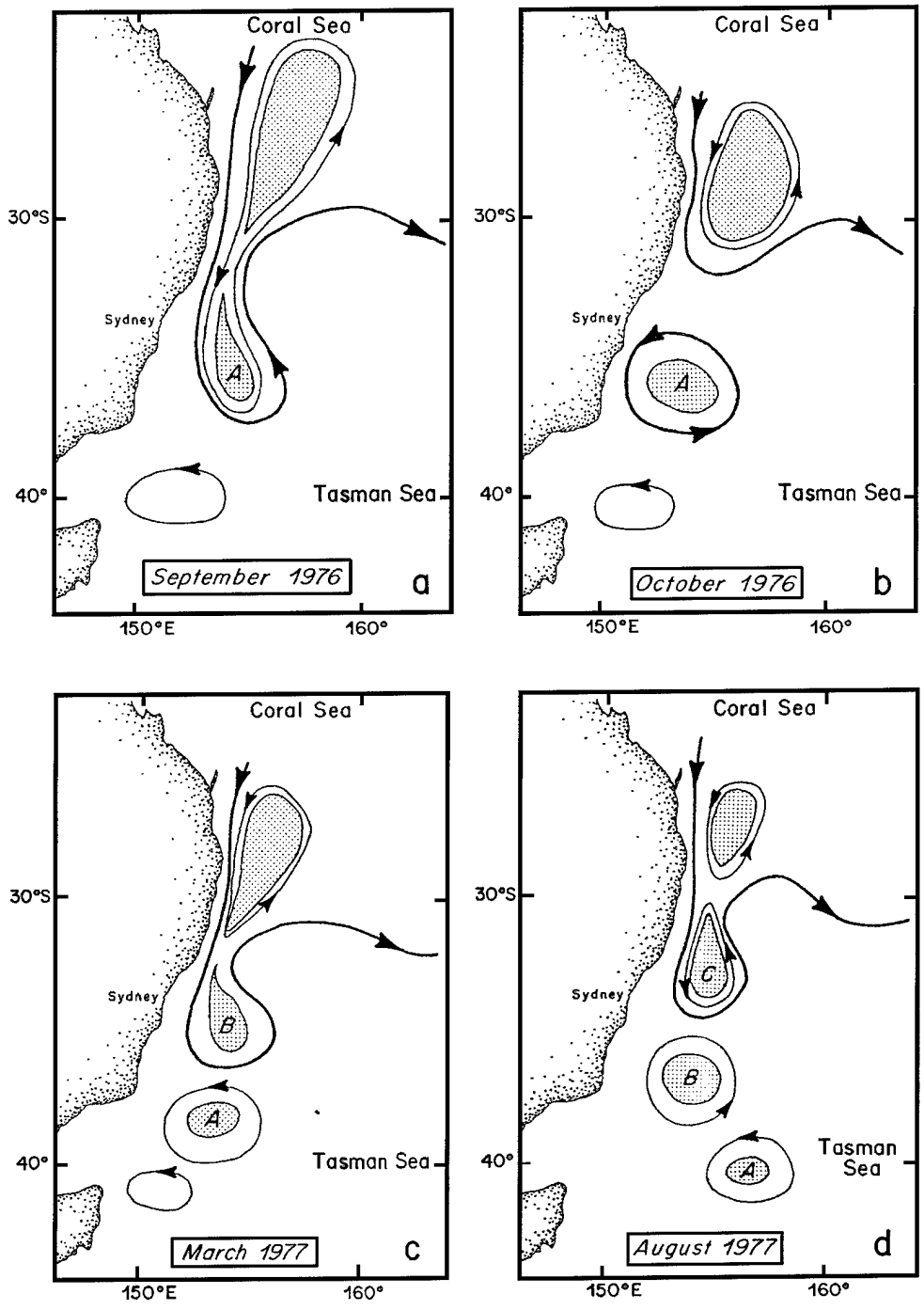

Figure II-78: A summary schematic of the kinematics for warm core ring formation in the EACS, adapted from Nilsson and Cresswell (1981). Each frame (a–d) represents a different (noted) time of observation.

3. The Indian Ocean

In the last decade or so, an especially popular topic relative to the Indian Ocean has been the Indonesian Throughflow (IT) and associated circulation patterns with a connection (Gordon, 1986) to conveyor belt ideas concerning the replacement path for North Atlantic Deep Water. Field programs and consequent analyses since circa 1986 have tended to be concentrated in the Indonesian Seas and Passages (Bray *et al.*, 1996; Ffield and Gordon, 1992; Fieux *et al.*, 1994, 1996a, b; Fine, 1985; Hautala *et al.*, 1996; please see Godfrey, 1996, for a review) and near South Africa (Duncome Rae, 1991; Duncombe Rae *et al.*, 1996; Garzoli and Gordon, 1996; Gordon *et al.*, 1992; Lutjeharms *et al.*, 1992). Although these areas are interesting in their own light, my general objective in this report is to determine the composite path for the replacement flow for NADW (S95), which has to include CDW and its excursions into the Pacific and Indian Oceans and return to the ACCS, as well as the role of intermediate water in this process, including the sources and compound path for the IT. Since the water mass properties and transport of the IT regime are important to the global interbasin exchange picture, this topic is described briefly in a separate section below (3b). Please refer to Appendix D for a list of abbreviations.

Gordon (1986) suggested an order 10 Sv upper-layer replacement flow for NADW from the Indian Ocean around the tip of South Africa, roughly 50% of which was supplied by the IT, which was itself the result of ~ 5 Sv uniform upwelling through the thermocline from the abyssal to upper layers in the interior Pacific Ocean. This 5 Sv was hypothesized to join ~ 5 Sv uniformly upwelled from the interior abyssal Indian Ocean (the other 50% of the replacement flow from the ACS) into the thermocline. The observational case for uniform upwelling from the abyssal ocean up through the thermocline in the ocean interior to get the needed upper-layer replacement flow for NADW formation is doubtful at best (Toole *et al.*, 1994b). In my opinion, the upward limbs of large-scale meridional cells are located in a variety of special places depending on situation and mechanism. Gordon's (1986) scheme to replace NADW by an upper layer flow from the ACS was to some extent motivated by the comparative high salinity and temperature of the Benguela Current System (or the subtropical South Atlantic in general), compared to the salinity of the flow of circumpolar water through Drake Passage. The dilemma associated with explaining how water of circumpolar "origin," as part of the flow through Drake Passage, enters the BCS with a salinity of ~ 34.5 to

34.7, much higher than the upper level flow salinities in Drake Passage, has not clearly been resolved. This point is addressed further below. I have argued in Section 1 above, and will continue to build the case in Sections 4 and 5, that the Malvinas or Falkland Current that carries UPIW from Drake Passage interacts strongly with the Brazil Current and South Atlantic subtropical gyre in general to increase its *T/S* characteristics along its path in the SFZ and eventually, perhaps, the Subtropical Front (STF).

Only a few Sverdrups of intermediate water were taken by Gordon (1986) to possibly exit eastward through Drake Passage and thence into the South Atlantic and north (in the BCS I guess) to contribute to NADW replacement (please also see the discussion of these points by S95, and/or in Volume I and/or in the Introduction to this volume). On the other hand, Rintoul (1991) found about 10 Sv of intermediate water flowing eastward through Drake Passage and not eastward between the tip of Africa and Antarctica, therefore into the South Atlantic (into the BCS). Since this was a net transfer (actually of UPIW, $26.8 \leq \sigma_\theta \leq 27.2$; S95), presumably this flow is ultimately part of the replacement for NADW. Rintoul's (1988, 1991) results showed very little net transport into the Atlantic of LOIW $27.2 \leq \sigma_\theta \leq 27.5$ (but a sizable recirculation was not disallowed). Given the differing results by Gordon (1986) and Rintoul (1991), it seemed like fun to try and track down, to the extent possible, the sources of both of these ideas (S95), and I'm continuing to examine this topic. The Indian Ocean's contribution to the global thermohaline (interbasin) circulation needs to be clarified in order to resolve the outstanding questions concerning the replacement flow for NADW. The result (S95) is a bit of a surprise, in that the role of the Indian Ocean in NADW replacement could be, along with leakage around the tip of Africa, a source of intermediate water via its meridional overturning cell, at least some of which, after modification, flows out of Drake Passage and into the BCS as a component of the Rintoul Picture. All in all, the Indian Ocean is a fascinating area.

North Atlantic Deep Water joins the ACCS and has a long history as CDW and as various brands of deep water after excursions into the Pacific and Indian Ocean basins before returning to the ACCS (Lynn and Reid, 1968; Reid and Lynn, 1971; Mantyla and Reid, 1983, 1995; Toole and Warren, 1993; RT96). An essential (S95) question relative to the pictures presented by Gordon (1986) and/or Rintoul (1991) would be how CDW might be transformed into either IW before flowing through Drake Passage and into the South Atlantic or how it might really get to be upper layer water (or IW) before flowing

around the tip of South Africa from the Agulhas Current into the South Atlantic. It turns out (S95) that the various exchanges (Mantyla and Reid, 1983) between deep and bottom (or near bottom) water in all of the ocean basins need to be taken into account in order to develop fully our picture of NADW replacement. And, it also turns out to be necessary to develop our picture of the various transformations involving IW, since deep water has to go through this density range somehow to get to be upper layer water.

Of the several options available, S95 estimated, by a version of global mass conservation, that a few (~ 3–5) Sverdrups were advectively supplied by the IT and consequent flow around Africa to replace NADW [subsequently, Garzoli and Gordon (1996) directly measured a 2–4 Sv time-averaged, advective, upper layer transfer from the ACS to the South Atlantic and an associated 5–10 Sv flow of water of possible circumpolar origin into the eastern South Atlantic]. The role of cut-off Agulhas eddies in this process is also interesting in the context of supplying mass, heat and salt to the South Atlantic. The estimates by Duncombe Rae (1991) and Duncombe Rae *et al.* (1996) suggest that 3–4 Sv of volume flux are supplied to the South Atlantic by cut-off rings from the Agulhas Retroflection Regime, about the same size as the advective "leakage" around the tip of Africa. The net flow of the IT that also makes it around Africa could be replaced (S95) by a few Sverdrups of upwelling of NADW in the ACCS and consequent northward flow in the eastern South Pacific, a mechanism discussed to some extent in this report volume and recently emphasized by Shriver and Hurlburt (1996).

Schmitz (1995) suggested for the first time a possible link between NADW replacement and meridional overturning from CDW to IW in the Indian Ocean. Toole and Warren (1993) found a net southward transport of 9–10 Sv of intermediate water (their selection of σ space for this was: $27.5 \geq \sigma_\theta \geq 27.0$) across 32°S, presumably in the ACS (Figure II-79; there is a more complete discussion of this point in the appendix to S95). About 10 Sv of intermediate water of circumpolar origin was found to move northward across 32°S east of the Agulhas Current (about 3 or 4 in the recirculation and 6–7 farther east). This "conventional" intermediate water was then joined by 10 Sv of water diapycnally transformed to the IW density range north of 32°S east of the Agulhas Current to yield a flow of 19–20 Sv of, on the average, saltier and higher silica intermediate water southward in the Agulhas Current along 32°S. According to S95, this ~ 10 Sv of excess IW in the Agulhas Current might be transformed from deep and

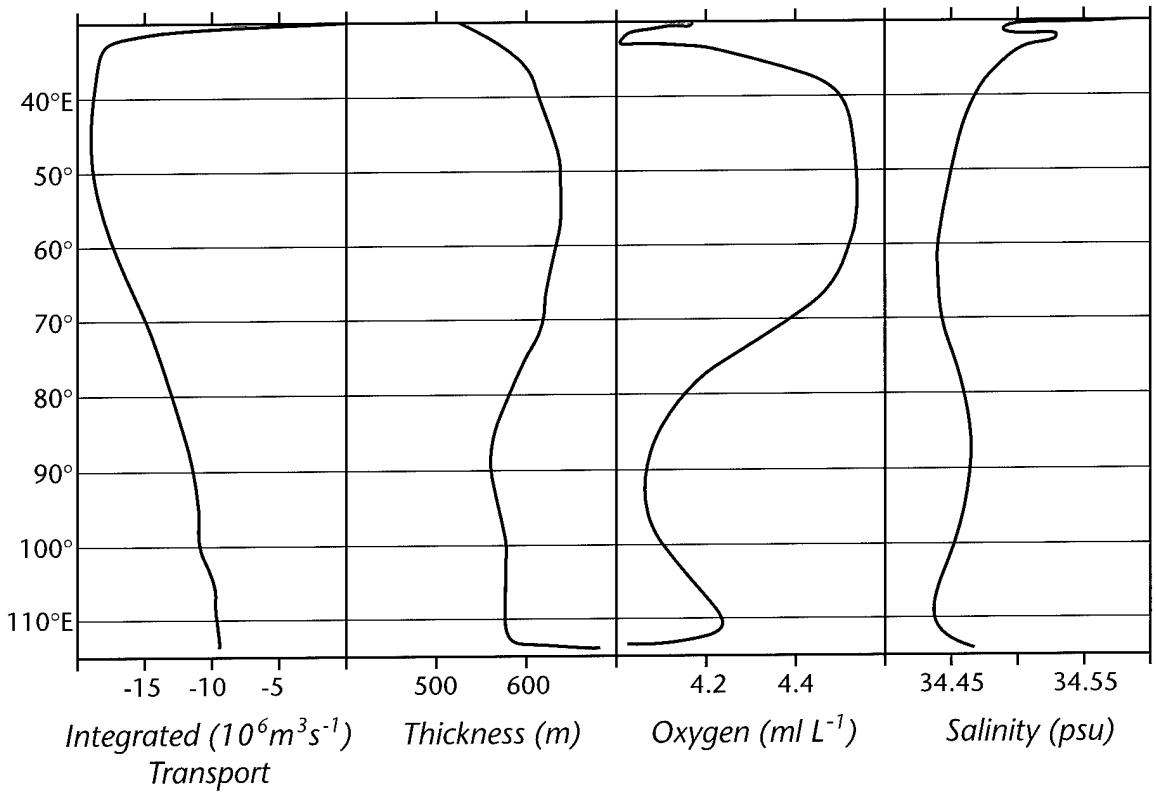

Figure II-79: The characteristics and transport along 32°S in the Indian Ocean for intermediate water, defined in this figure as the layer where $27.0 \leq \sigma_\theta \leq 27.5$, adapted in smooth form from Toole and Warren (1993, their figure 5).

bottom water to intermediate water in the Indian Ocean and flow south in the Agulhas Current, and thence into the STF where these fronts merge in the Crozet Basin, and eventually the SFZ south of Australia, where it is further modified by convection, and flows out of Drake Passage into the South Atlantic, a mechanism involving replacement of NADW not previously suggested as far as I know. A possible area where the merger of the AF, STF, and Subantarctic Front (SAF) occurs (Park *et al.*, 1991) is indicated in Figure II-80, adapted from Belkin and Gordon (1996). Recently, the transport estimates by Toole and Warren (1993) have been modified by new ideas and calculations (RT96). In the following I will present an updated scheme for NADW replacement, involving modification of the picture presented by S95, strongly influenced by RT96, and by Shriver and Hurlburt (1996).

It is also interesting to investigate further how the water entering the Indonesian Passages from the Pacific and flowing out into the Indian Ocean (or vice versa) is

resupplied to and from the ACS and ACCS, south of Australia and into the South Pacific (Schmitz, 1995; Godfrey, 1996; Shriver and Hurlburt, 1996): that is, to determine the return path for the IT from the Indian Ocean through the ACCS and then the Pacific Ocean, both that component involved in NADW replacement as well as the recirculation from the Indian Ocean. I am assuming that Toole and Warren (1993, who have an IT transport of 7 Sv) and especially RT96 (who have an IT transport of 10 Sv) demonstrate more or less conclusively that water supplied to the Indian Ocean (when this is the flow direction) by the IT is flowing south in the upper layers of the Agulhas Current at 32°S.

The Indian Ocean beyond the IT and its linkage to NADW replacement has received "new" attention in the last few years (Mantyla and Reid, 1995; RT96; S95; Stramma, 1992; Stramma and Lutjeharms, 1996; Toole and Warren, 1993); a few of these studies have been focused on the large-scale meridional cell. The eddy field in the ACS has also been a very active research area in the past decade or two (Gründlingh, 1983; Holland *et al.*, 1991; Lutjeharms, 1988; S96). To me, the most exciting new result(s) concerned with both the general circulation and the mesoscale eddy field is (are) connected to the interbasin circulation associated with the large-scale meridional cell in the Indian Ocean, as well as the IT. The

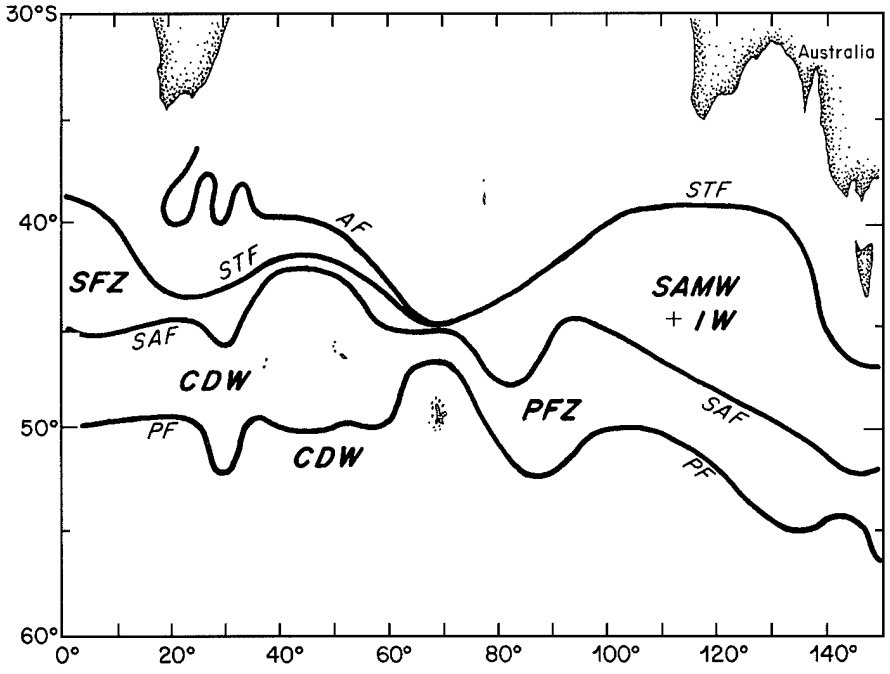

Figure II-80: A schematic map of the frontal structure south of the Indian Ocean, adapted from Belkin and Gordon (1996). AF denotes Agulhas Front, PF Polar Front, PFZ Polar Frontal Zone, SAF Subantarctic Front, SFZ Subantarctic Frontal Zone, and STF Subtropical Front. CDW, IW, and SAMW are water masses defined in the text; please also see Table II-1.

strength of this meridional cell and the water-mass components that contribute have recently been described rather definitively by RT96. Other results relative to both the eddy field in the ACS and in comparison with the global eddy field have been described by S96, and these results relate in the ACS, and even globally, to meridional cells such as described by RT96 and specifically to interbasin exchange.

The 8-layer (Figure II-81) net meridional transports (RT96) across approximately 32°S for the entire South Indian Ocean are listed in Table II-12. It is interesting to look at how these transports are partitioned between the ACS, its recirculation, and the interior of the South Indian Ocean. This has been made possible by personal communication to me by Robbins and Toole of their layer-by-layer transport streamfunction plots. I have somewhat arbitrarily defined the Agulhas Current, its recirculation, and interior values, and entered them in the indicated columns of Table II-12 (where all transports are rounded off to the nearest Sverdrup). The upper layer components of the circulation in the ACS (according to RT96, again possible for me to do since they kindly made their layer streamfunctions across 32°S available by personal communication) were shown by Schmitz (1996) to agree to within a few Sverdrups with similar results off Durban from data (Harris, 1972) taken almost 30 years earlier (please see below and also Stramma and Lutjeharms, 1996). The hydrology and ocean circulation in the vicinity of South Africa, including interesting discussions of IW and interchanges between the ACS, the BCS, and the ACCS, were summarized early on by Clowes (1950).

The hydrography of the deep Indian Ocean, focusing on implications for the meridional thermohaline circulation, has been described by Mantyla and Reid (1995); see also Johnson *et al.* (1991a, b), Park *et al.* (1993), RT96, and Toole and Warren (1993). The work by Mantyla and Reid (1995) is my main source for the distribution of properties in the deep and abyssal Indian Ocean, and RT96 the essential source for the transports associated with the meridional cell in this ocean. The Indian Ocean Atlas (Wyrtki, 1971) is my principal reference for upper layer property distributions. Robbins and Toole (1996) found (Table II-12 and Figure II-82) 13 Sv flowing northward across approximately 32°S below a σ_2 of 36.92, including lower deep water (NADW characteristics) and both upper and lower bottom water, their layers 6 → 8. Above σ_2 = 36.92, in layers 1–5 (RT96, Table II-12) there are 23 Sv flowing southward, 13 to replace the northward flow below σ_2 = 36.92 and 10 Sv associated with the IT. In Figure

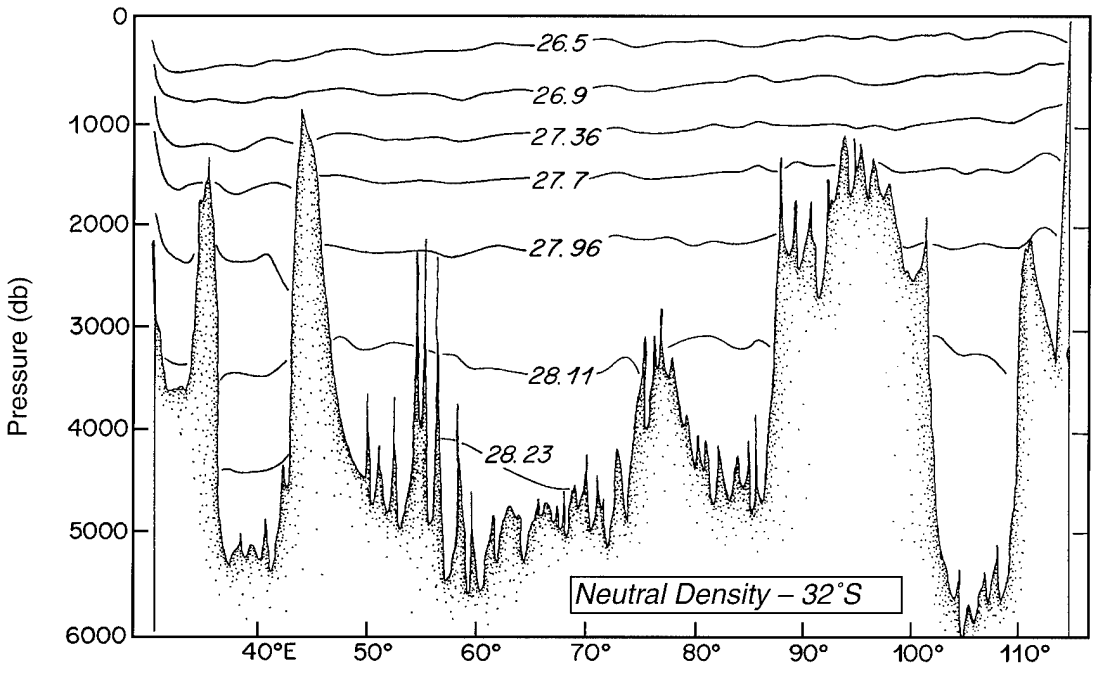

Figure II-81: Contours of neutral density along latitude 32°S (nominal) in the Indian Ocean, taken from Robbins and Toole (1996).

II-82, adapted from RT96 figure 3, mass transport stream functions are presented for two different determinations of the net transports in the combination of layers 6–8 (upper panel of the figure) and layers 1–5 (lower panel). The dashed line represents the estimates by Toole and Warren (1993) and the solid line estimates by RT96, a silica-conserving (Figure II-83) solution (a meridional silica section to compare with the zonal section in Figure II-83 is shown in Figure II-84). Robbins and Toole (1996) found 4 Sv of the incoming 13 Sv in layers 6–8 returning to the ACCS as (their layer 5) upper deep water [or perhaps Indian Ocean Deep Water (IODW), see Park *et al.* (1993)]. Of the remaining 9 Sv, 2 are returned as upper layer (a combination of their layers 1 and 2) water and 7 Sv [rows (layers) 3 and 4 in Table II-12] are returned as intermediate water (4 UPIW, 3 LOIW). The flow out of the Indonesian Passages (~ 10 Sv by RT96, ~ 7 Sv by Toole and Warren, 1993) is presumably carried south with the ACS mostly in layer 1.

My discussion of the Indian Ocean in the following will be concentrated on the meridional cell and on the implications of interbasin circulations for the eddy field in the Agulhas Current, and globally. Other features of the physical oceanography of the

Table II-12: The Meridional Cell in the Indian Ocean at 32°S, adapted from Robbins and Toole (1996, and personal communication)

Layer Number and Name	Gamma (kg m^{-3})	Sigma (kg m^{-3})	Theta (°C)	Transports* (kg s^{-1}) across 32°S	Transports (kg s^{-1}) S.A. coast to 50°E	Transports (kg s^{-1}) ACS	Transports (kg s^{-1}) Recirculation	Transports (kg s^{-1}) Interior
	ocean surface	ocean surface	ocean surface					
1: Surface Water				–16	–23	–33	10	7
	26.50	σ_θ = 26.45	14.1					
2: Subantarctic Mode Water				4	–18	–22	4	22
	26.90	σ_θ = 26.80	9.85					
3: Upper Antarctic Intermediate Water				–4	–16	–19	3	12
	27.36	σ_θ = 27.20	4.65					
4: Lower Antarctic Intermediate Water				–3	–7	–10	3	4
	27.70	σ_2 = 36.65	3.26					
5: Upper Deep Water				–4	–2	–6	4	–2
	27.96	σ_2 = 36.92	2.20					
6: Lower Deep Water (NADW influence)				2	8	2	6	–6
	28.11	σ_4 = 45.89	1.28					
7: Upper Bottom Water				10	3	0	3	7
	28.23	σ_4 = 46.01	0.43					
8: Lower Bottom Water				1	0	0	0	1
	sea floor	sea floor	sea floor					
				Σ = –10	–55	–88	33	45

*Minus signs indicate southward flow throughout this table.

Indian Ocean will be mentioned only in passing. I do however feel that the low-latitude and northern Indian Ocean (a region I am unfortunately ignorant about) is important in determining how the upward limb of the meridional cell works, keeping in mind that the diapycnal transfer of 9 Sv of water denser than $\sigma_2 = 36.65$ (or, roughly, $\sigma_\theta \doteq 27.5$) according to RT96 is dominated by the transfer from upper bottom water ($46.01 \geq \sigma_4 \geq 45.89$) to 7 Sv intermediate water mostly in the North Indian Ocean, presumably through some form of deep water as a necessary step along the way. The Wyrtki (1971) Indian Ocean Atlas contains a wealth of information about the hydrographic properties of this ocean. Some of the atlas figures were presented in Section 1 of this report, in order to suggest a possible role for the North and Equatorial Indian Ocean in the upper

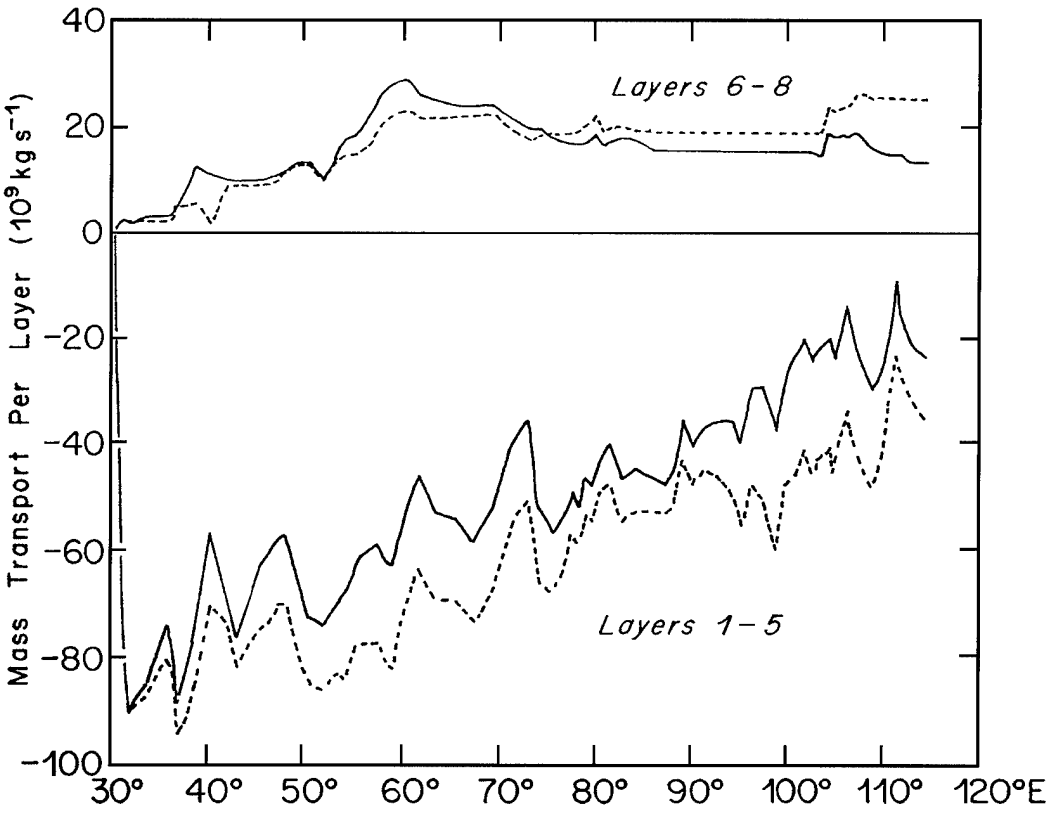

Figure II-82: Cumulative mass transports (starting at the western boundary) for the shallow and deep portions of the flow across 32°S, adapted from RT96. Layers 1 through 5 include water above a neutral density of 27.96 (kg s^{-1}) while 6 through 8 are below. The circulation due to Toole and Warren (1993) is represented by the dashed line while the silica-conserving circulation by RT96 is indicated by the solid line.

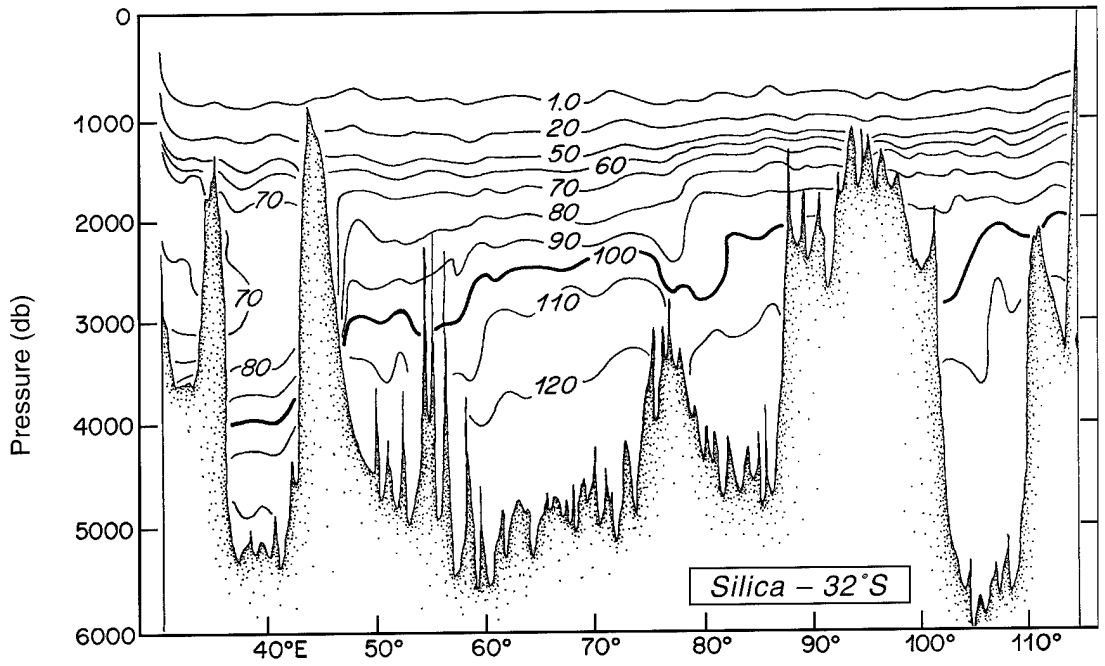

Figure II-83: Contours of dissolved silica (μmol kg^{-1}) along 32°S, adapted from Robbins and Toole (1996).

limb of the meridional cell; others are presented below in this context. Determination of the upward limbs of meridional cells and interbasin exchanges is one of the major tasks facing physical oceanographers, a much more difficult problem than water mass formation. Since my agenda for the Indian Ocean is different from that for the Pacific, this section of my report is organized with the intermediate circulation following the deep circulation (please see the table of contents).

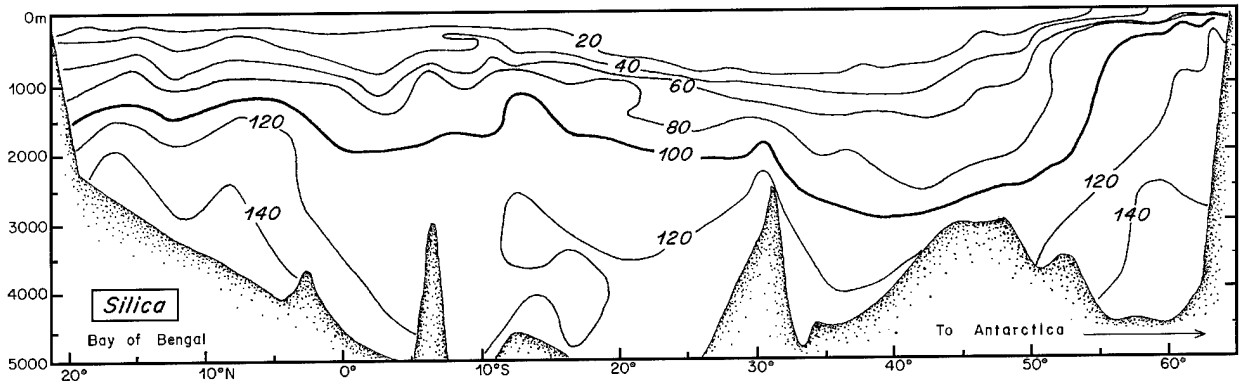

Figure II-84: A silica section from the Bay of Bengal to Antarctica, adapted from p. 414 in the Indian Ocean Atlas (Wyrtki, 1971).

3a. Short Notes on the Upper-Layer Subtropical Gyre in the South Indian Ocean

Various characteristics of this flow field are shown in Figures II-85 and II-86, adapted from Stramma and Lutjeharms (1996) and Stramma (1992), respectively. Figure II-85 is a map of the volume fluxes associated with the upper 1000 m (or so) for the subtropical gyre in the South Indian Ocean, and Figure 86 emphasizes the South Indian Ocean Current (Stramma, 1992) and upper layer flows in the SFZ (see also Read and Pollard, 1993). According to Wyrtki (1971) the $\sigma_\theta = 27.2$ surface is at roughly 1000 m depth in the interior of the South Indian Ocean. So the Stramma and Lutjeharms (1996) upper (1000 m) layer flow also contains what I call UPIW. But the probable complex interaction of this flow (the SEC component) with the low latitude circulation, including the IT, even in the South Indian Ocean (0–20°S, say), isn't really accessible in Figure II-85. The area between 0° and 20°S contains a frontal regime in both upper and intermediate layers, so prominent in the Indian Ocean Atlas (Wyrtki, 1971) and emphasized by Wyrtki (1973). For example, the idea that the SEC in the Indian Ocean is larger than expected from the Sverdrup relation because of the IT (Godfrey and Golding, 1981) could also be related to the addition of meridional cell components to the SEC from the North Indian Ocean.

Articles on the Agulhas by Clowes (1950), Harris (1972), Visser and Van Niekerk (1965) and Wyrtki (1971, 1973) provide interesting early-on background material on

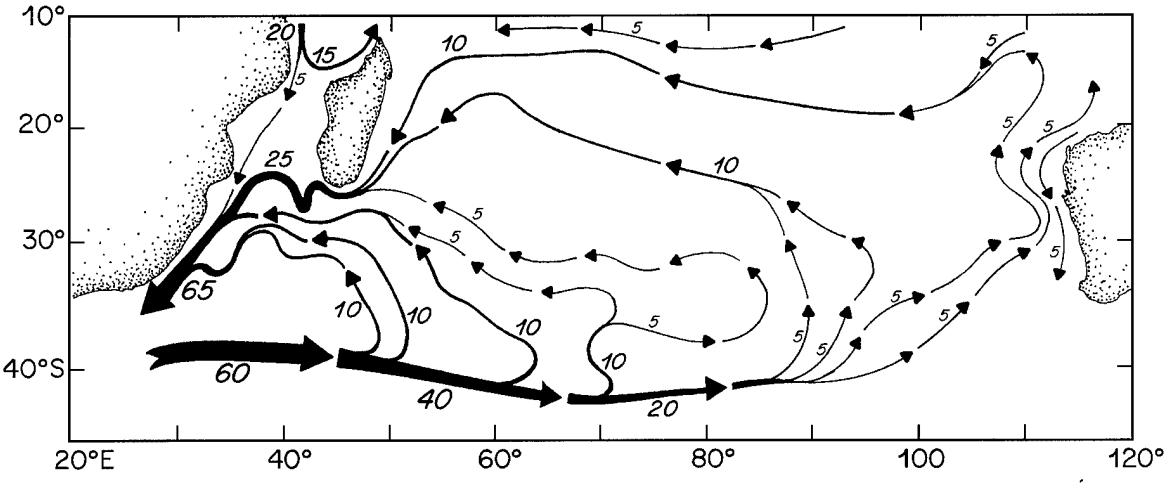

Figure II-85: Schematic illustration of the flow field in the upper 1000 m of the South Indian Ocean, adapted from Stramma and Lutjeharms (1996).

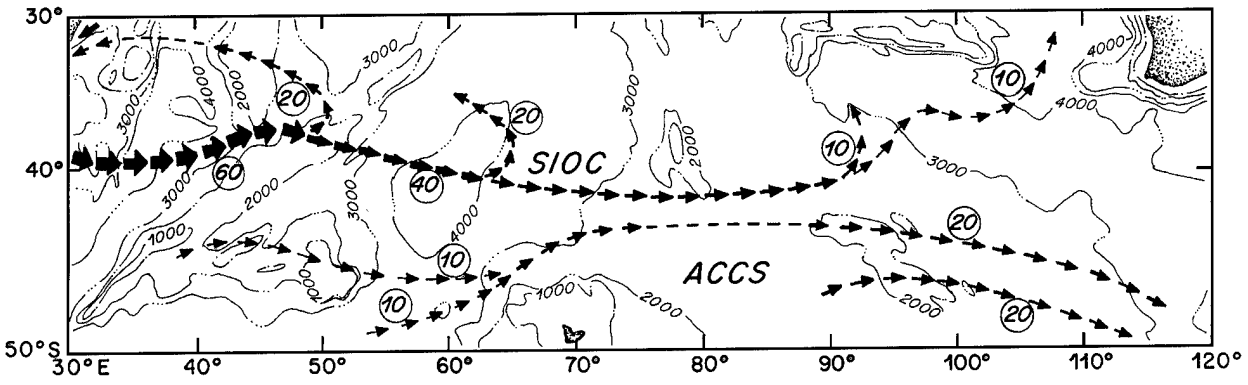

Figure II-86: The South Indian Ocean Current and the upper layer flow in the Antarctic Circumpolar Current, according to Stramma (1992).

this area of the ocean. One may favorably compare the Agulhas Current transport of 60–65 Sv in the upper 1000 m of Figures II-85 and 86 with about 65 Sv found by S96 based on the Harris (1972) results or with 74 Sv by RT96, the latter two transport estimates being from above 27.2 σ_θ. Robbins and Toole (1996, Table II-12) have a recirculation of 17 Sv by 50°E above 27.2 σ_θ to compare with ~ 20 by Stramma and Lutjeharms (1996). The ship-drift-data-based surface currents in Figure II-3, for the South Indian Ocean, only barely define a subtropical gyre there. Two paragraphs on the subtropical gyre in the South Indian Ocean constitute cursory treatment indeed. But for now, not only am I out of time but also the reader may pursue the details of this flow regime further in the references already noted throughout this report. The Indian Ocean Atlas (Wytrki, 1971) is very useful.

3b. The Indonesian Throughflow

The Indonesian Throughflow (Wyrtki, 1987) is a hot topic (Bray *et al.*, 1996; Ffield and Gordon, 1992; Fine, 1985; Fieux *et al.*, 1994, 1996a; Godfrey, 1996; Godfrey and Golding, 1981; Godfrey *et al.*, 1993; Gordon, 1995; Hautala *et al.*, 1996; Hirst and Godfrey, 1993). A recent review paper on the IT by Godfrey (1996) has been very helpful in writing my report, and a modification of his summary table of observed transports is included here as Table II-13. The latest word (Table II-13, last two entries) is the existence of very large temporal variability in the IT, and Meyers *et al.* (1995) discuss this in terms of El Niño–Southern Oscillation (ENSO) phenomena.

Table II-13: Estimates of the Indonesian Throughflow Transport*

Reference	Method	Result, 10^6 m^3 s^{-1}	Remarks
Wyrtki (1961)	geostrophy	–1.7	top 200 m
Godfrey and Golding (1981)	geostrophy	–10	sections unclosed
Wunsch *et al.* (1983)	inverse calculation, 43°S and 28°S Pacific sections	$\ll$ –10	
Piola and Gordon (1984)	freshwater budget, Pacific and Indian Oceans	–14	
Fine (1985)	tritium budget	–5	top 300 m
Toole *et al.* (1988)	Salinity budget, West Pacific	< –5	sensitive to IT salinity
Godfrey (1989)	geostrophy, Australia–Sumatra, Levitus (1982) annual mean data	< –12	boundary currents unresolved
Toole and Warren (1993)	geostrophy	–7	Indian Ocean 32°S
Meyers *et al.* (1995)	time series from expendable bathythermograph sections	–5	top 400 m
Fieux *et al.* (1994)	geostrophy, Australia–Bali, plus current meters	–18.6 ± 7	August 1989 snapshot
Fieux *et al.* (1996a)	geostrophy, Australia–Bali, plus current meters	+2.6 ± 7	February–March 1992 snapshot

*Minus signs indicate westward flow. Adapted from Godfrey (1996).

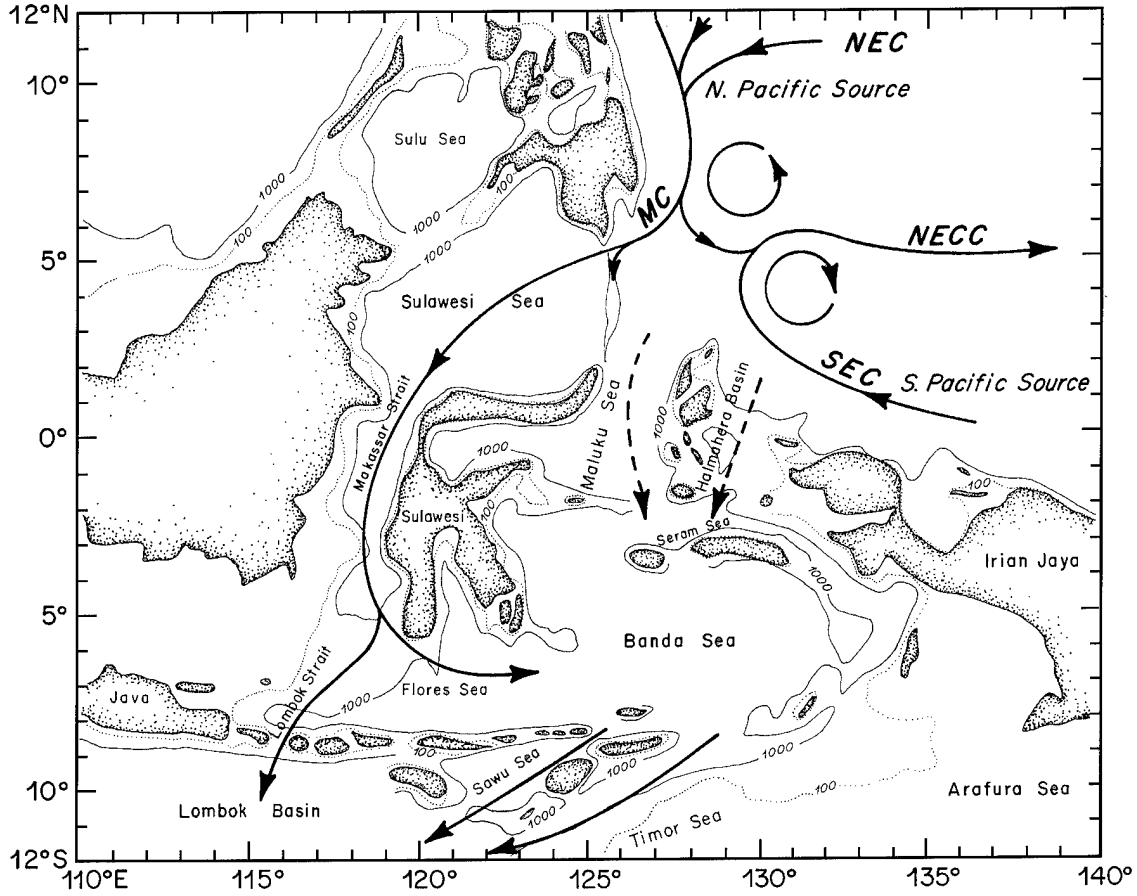

Figure II-87: Map of the flow pathways in the vicinity of the Indonesian Passages, adapted from Ffield and Gordon (1992).

Topographic features for, and possible flow pathways in, the Indonesian Archipelago are shown in Figure II-87. Water from the IT can be traced as a tongue of low salinity extending westward in the South Equatorial Current of the Indian Ocean (Rochford, 1966). Godfrey's (1996) map of the regional source of the IT was shown in Figure II-26, with another summary map shown in Figure II-9, the latter adapted from Lukas *et al.* (1991). Also, a similarly oriented schematic by Wijffels (1993) was presented as Figure II-55. A possible connection of the IT to the global interbasin circulation was shown in S95, has been discussed throughout this report, and will be updated below. Another intriguing possibility associated with the "IT area" and the global thermohaline circulation lies in the role of the composite circulation of the IT plus other flow components (Meyers *et al.*, 1995) associated with the North Australian Bight (NAB). Here the NAB is taken to be the area bounded by the line from Shark Bay to

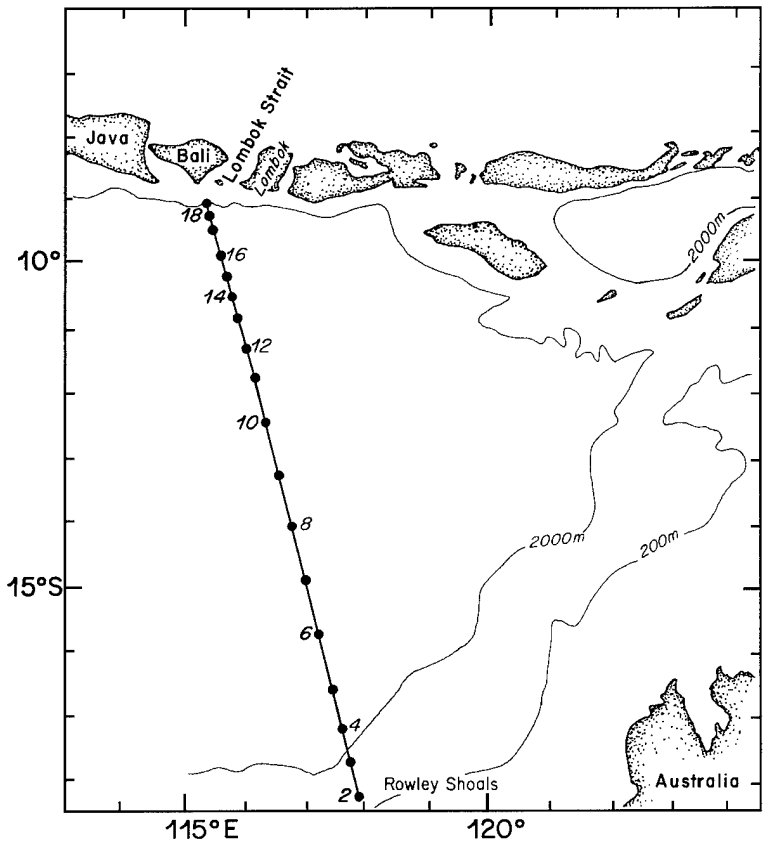

Figure II-88: Location of stations in the throughflow regime along a section from Australia to Bali, after Fieux et *al.* (1994).

Table II-14: Australia–Bali Section Transports (in Sverdrups; adapted from Fieux *et al.*, 1994)

Layers	Transport*
0–200 db	–23.1
200–500 db	–2.7
Total 0–500 db	–25.8
500–2000 db	+9.6
Total 0–2000 db	–16.2

*Minus signs indicate westward flow.

Sumatra and into the Timor Sea. It looks like some components of the diapycnal upper limb of the meridional cell in the Indian Ocean converge with the IT in the NAB. But since my main interest in the NAB is for the IW picture, further discussion of this area is contained in Section 3d.

Sections from Australia to Bali in August, 1989 (Figure II-88), by Fieux *et al.* (1994) of T, S and σ_θ (Figures II-89 to II-91) are shown here for background information. A breakdown in vertical layers of the Australia to Bali transports as observed by Fieux *et al.* (1994) is shown in Table II-14. Most of the transport of the IT occurs in the top 200 to 500 m of the Australia–Bali section presented by Fieux *et al.* (1994), at σ_θ values (Figure II-91) less than 25.5 for 200 m or 27.0 for 500 m. Further observations of a similar type from February–March, 1992, are now available (Fieux *et al.*, 1996a). There turns out to be a wide dynamic range in transport

estimates in the Australia–Bali data of 1989 and 1992 (–18.6 → +2.6 Sv, Table II-13), but the average is the canonical 10 Sv. This variability could be connected (Meyers, 1996) to El Niño–Southern Oscillation (ENSO). Fieux *et al.* (1994, their figures 7 and 9) also present some extremely interesting pictures of the possible flow path and distribution of salinity and oxygen on σ_θ surfaces 26.8 and 27.2. They show a boundary current flowing from the North to the South Indian Ocean along the coasts of Sumatra and Java, turning west in the NAB. Since this is for UPIW, a more detailed discussion will be postponed to Section 3d. These flows are underneath the seasonally varying South Java Current (Quadfasel and Cresswell, 1992).

Water masses in the generalized IT area have been described by Hautala *et al.* (1996). Temperature/salinity curves adapted from Hautala *et al.* (1996) are shown in Figure II-92 and σ_θ/O_2 curves in Figure II-93. Property maps on selected σ_θ surfaces are shown in Figures II-94 through II-96, adapted from Hautala *et al.* (1996). The incoming (North) Pacific water masses on σ_θ = 24.5, which presumably represents the bulk of the IT, are said to be freshened inside the archipelago. It is the uniform salinity water of the central Banda Sea, with salt content in the top 200 m diluted by precipitation and runoff, that flows out into the Indian Ocean. On σ_θ = 26.0 (Figure II-95), at depths of 200–300 m, the salinity inside the archipelago is much closer in value to the North Pacific source than to the South Pacific source. Continuity of $S < 34.5$ can be seen all the way from the Mindanao Current to southern Makassar Strait. On σ_θ = 26.5, corresponding to the North Pacific Intermediate Water salinity minimum at depths of 300–400 m, salinity values are more intermediate between the two Pacific sources. On σ_θ = 27.0, at

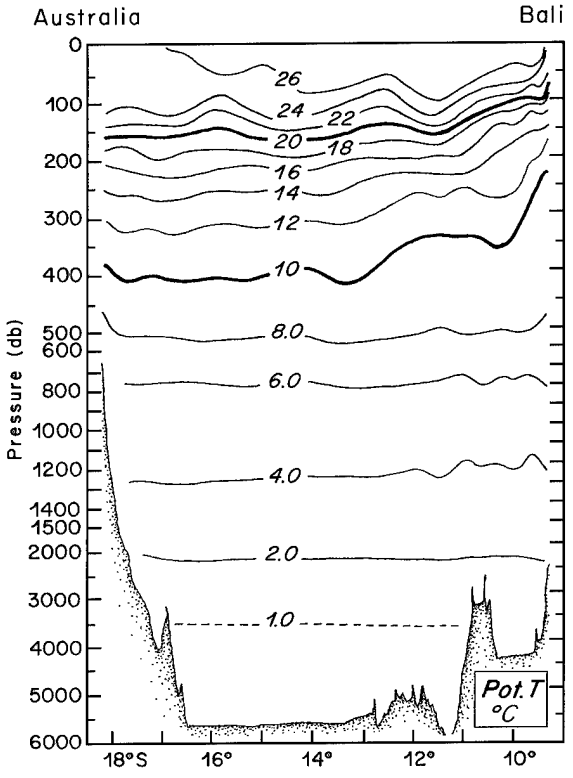

Figure II-89: A simplified temperature (°C) section, Australia to Bali, station locations in Figure II-88, selected contours from Fieux *et al.* (1994).

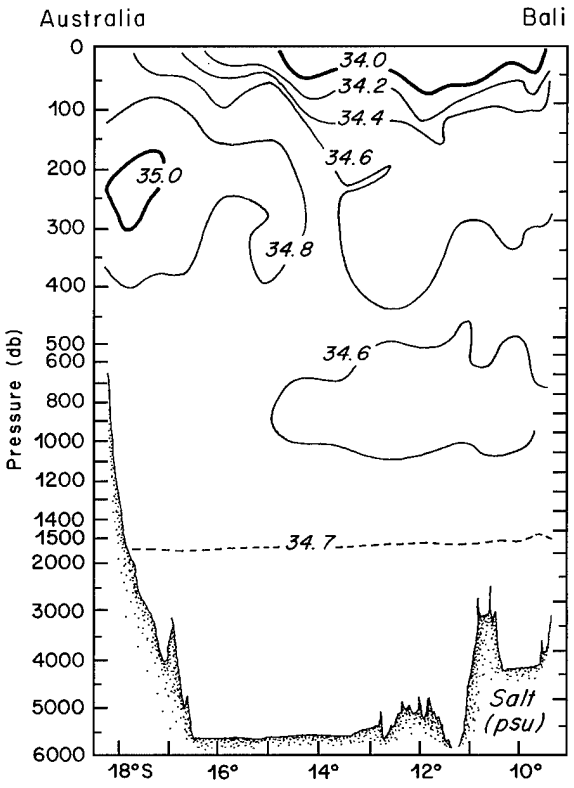

Figure II-90: A simplified salinity (psu) section, Australia to Bali, station locations in Figure II-88, selected contours from Fieux *et al.* (1994).

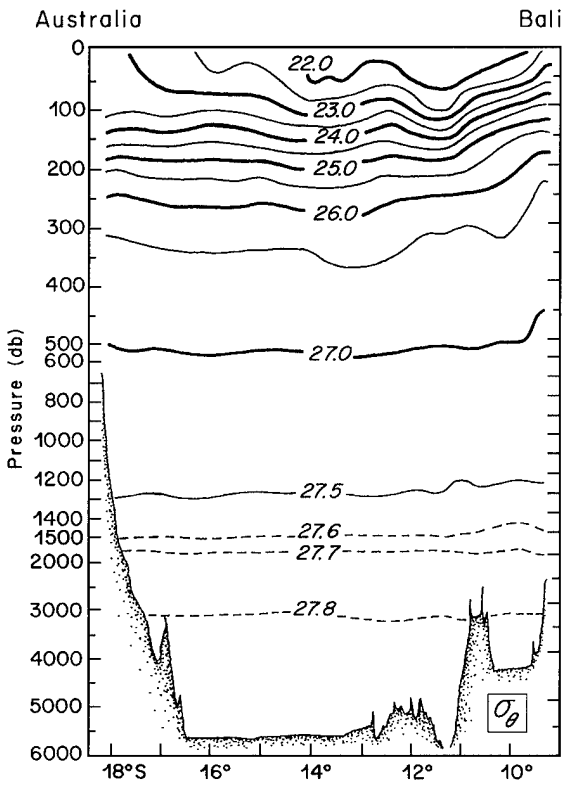

Figure II-91: Potential density parameter (σ_θ, kg m^{-3}) section, Australia to Bali, station locations in Figure II-88, selected contours from Fieux *et al.* (1994).

500–600 m depth (Figure II-96) an isolated salinity maximum is centered on the Seram Sea. This feature shifts southward into the Banda Sea proper with depth and the pattern of isohalines supports an anticyclonic gyre. Such high salinities in the Pacific source regions are found only on much deeper isopycnals ($\sigma_\theta > 27.50$).

Although the Leeuwin Current is potentially a connection in the interbasin circulation associated with IT, it is not really clear to me what its exact role is or what its transport characteristics are. Articles on this current system are available, however (Church *et al.*, 1989; Cresswell and Golding, 1980; Cresswell *et al.*, 1978; Godfrey and Ridgway, 1985).

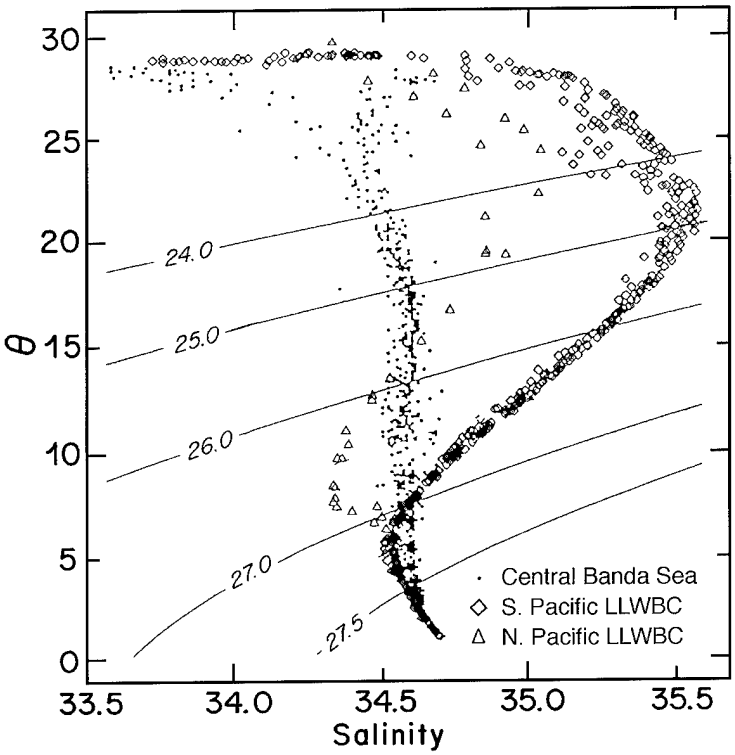

Figure II-92: Potential temperature (θ) vs salinity (S) curves for the Banda Sea and for possible sources from the Low-Latitude Western Boundary Currents (LLWBCs) in the South and North Pacific.

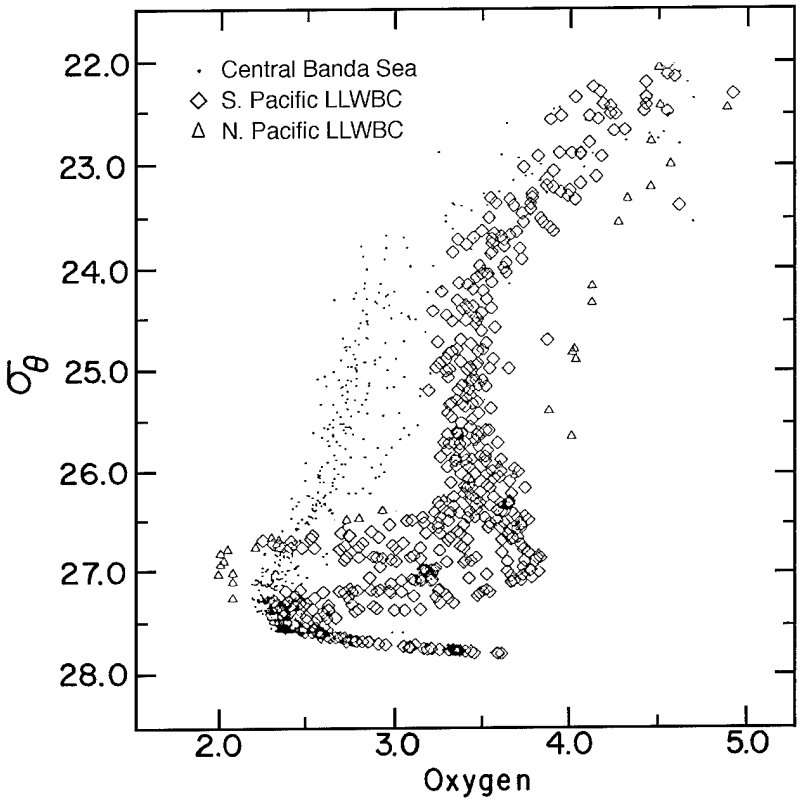

Figure II-93: Potential density (σ_θ, kg m^{-3}) vs oxygen (O_2, ml L^{-1}), to accompany Figure II-92.

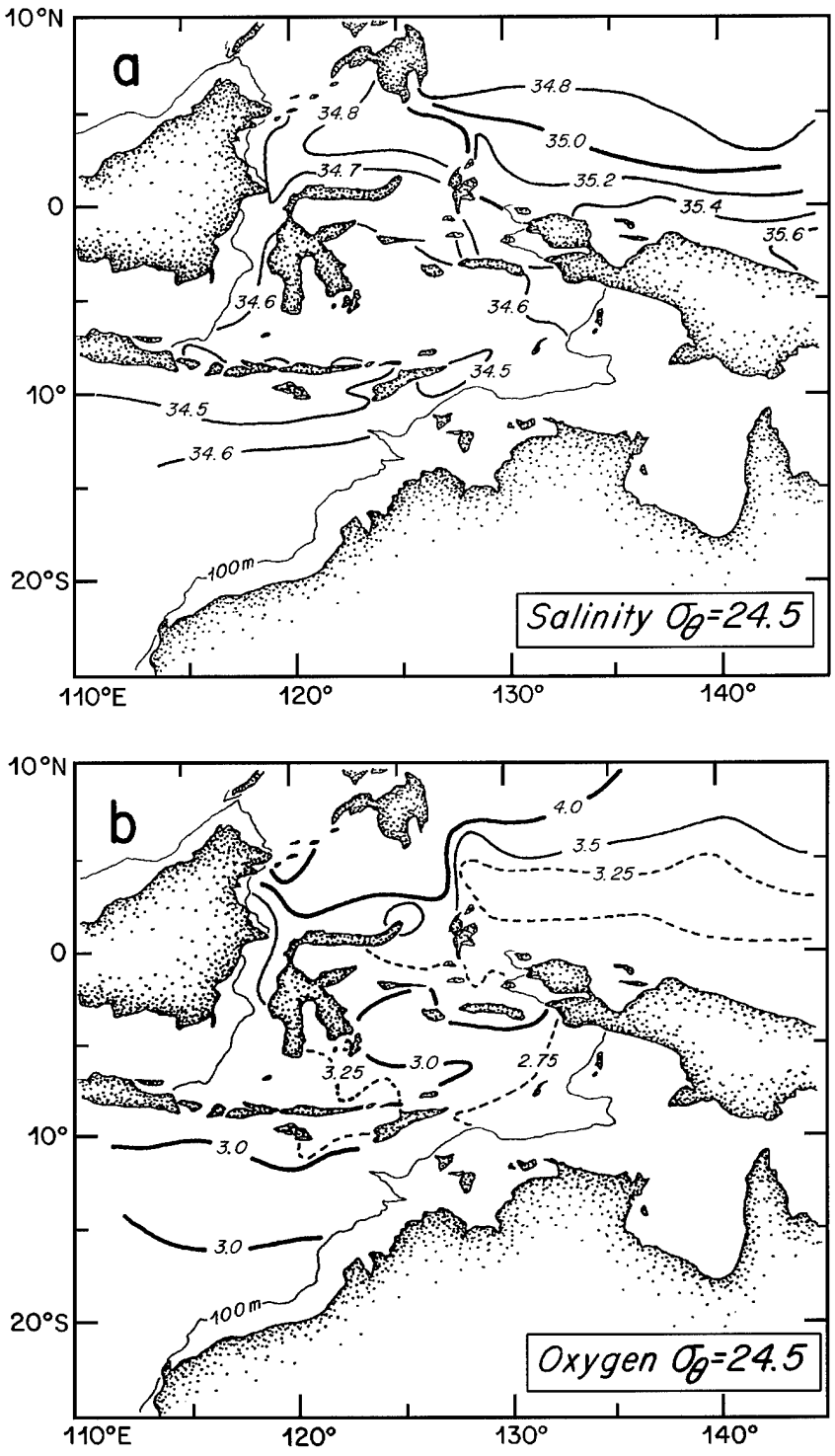

Figure II-94: Maps of (a) salinity (psu) and (b) oxygen (ml L^{-1}) contours on σ_θ= 24.5, adapted from Hautala *et al.* (1996).

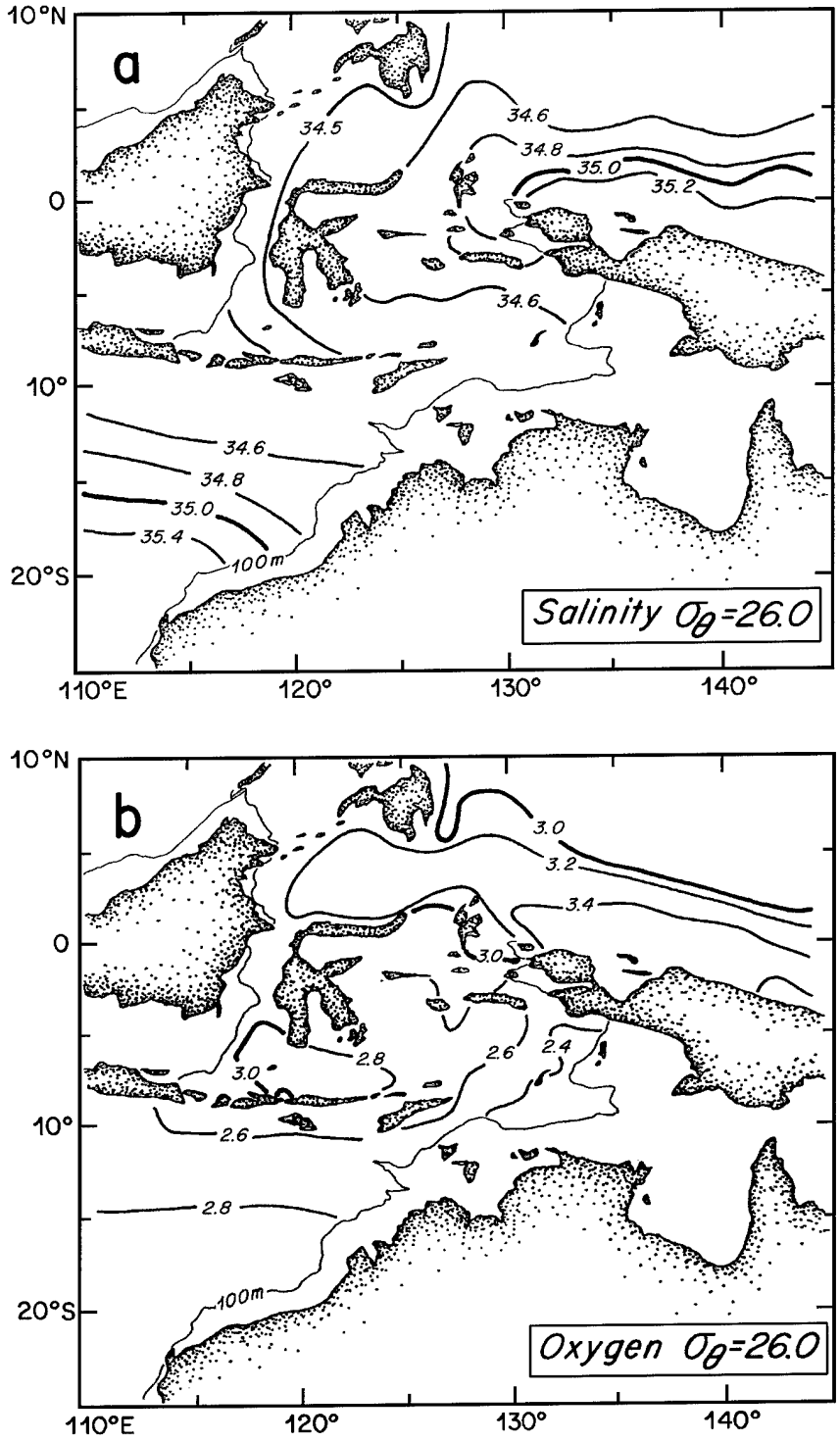

Figure II-95: Maps of (a) salinity (psu) and (b) oxygen (ml L^{-1}) contours on σ_θ = 26.0, adapted from Hautala *et al.* (1996).

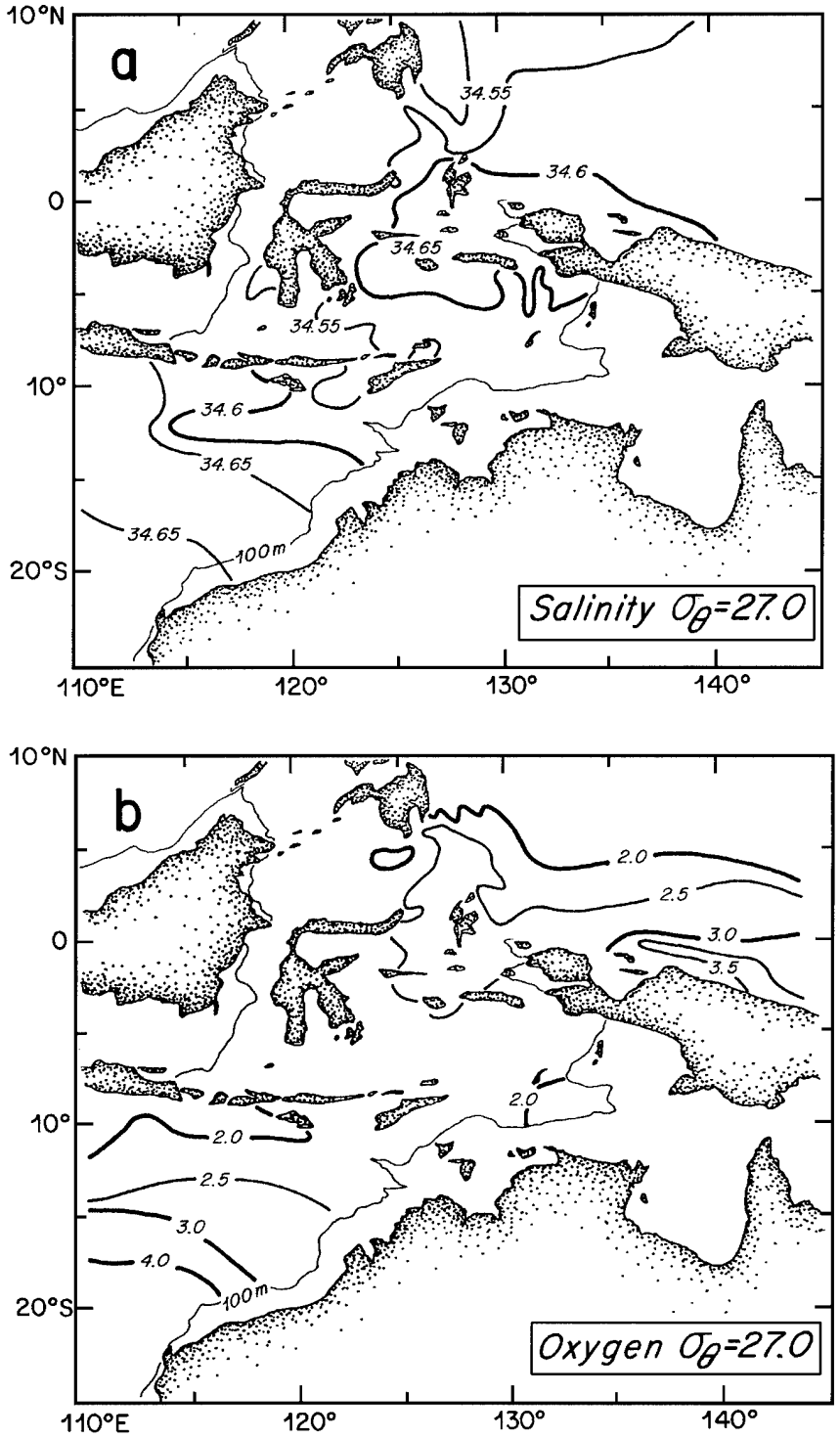

Figure II-96: Maps of (a) salinity (psu) and (b) oxygen (ml L^{-1}) contours on σ_θ = 27.0, adapted from Hautala *et al.* (1996).

3c. The Deep and Near-Bottom Circulation of the Indian Ocean

According to Mantyla and Reid (1995) the general pathways of bottom water circulation in the Indian Ocean have been understood for some time, with progressive refinement in detail as more observations have become available. A topographic schematic with some feature names is shown in Figure II-97, and a map of σ_4 at the bottom of the Indian Ocean is shown in Figure II-98 (adapted from Mantyla and Reid, 1995, their figure 2a; a version of this figure in color was kindly provided by personal communication). The bottom flow into the western Indian Ocean enters from the Weddell–Enderby Basin, and the bottom flow into the eastern Indian Ocean enters from the

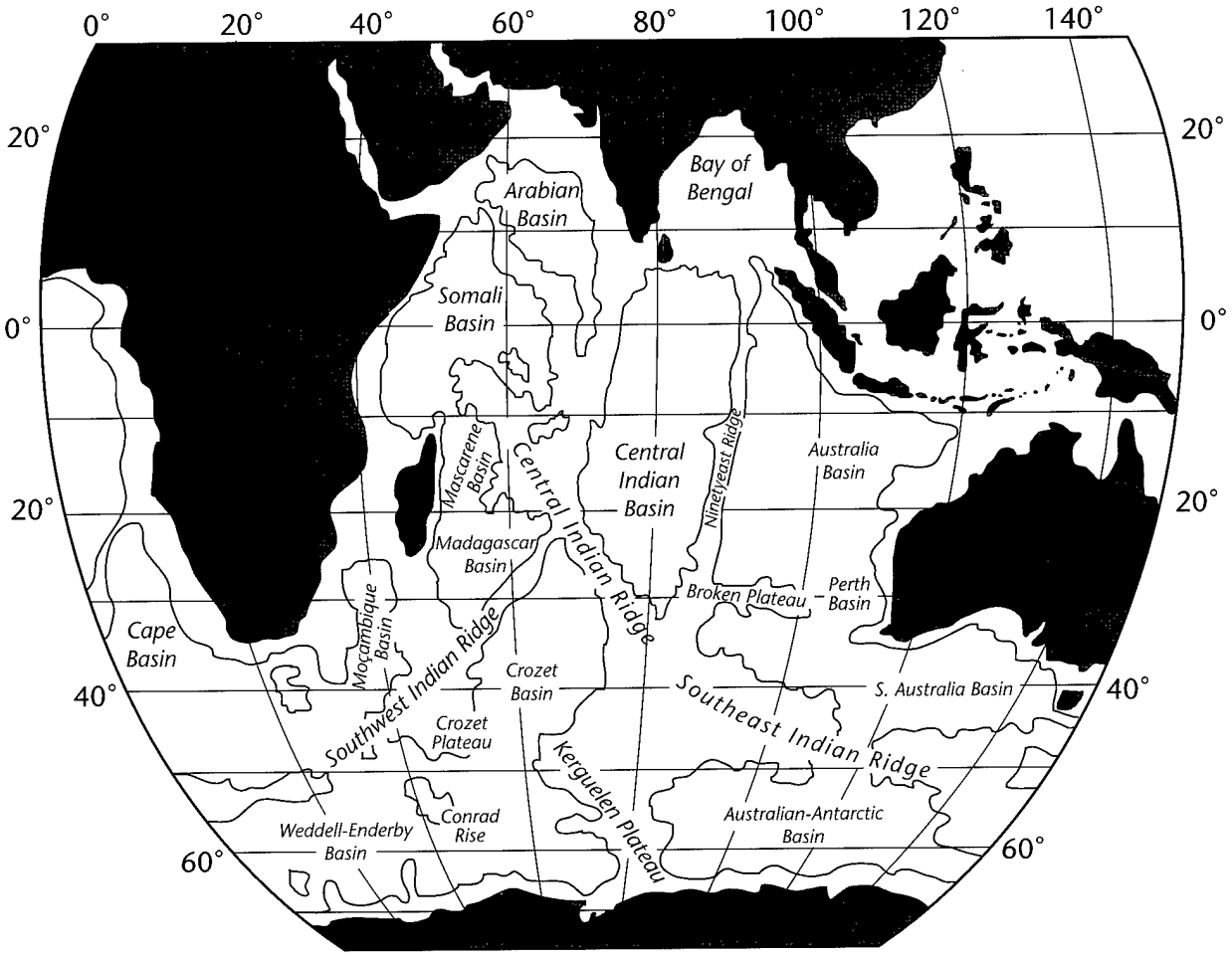

Figure II-97: A map containing selected topographic features of the Indian Ocean.

Australian–Antarctic Basin. The characteristics of the Weddell–Enderby Basin are derived from the Weddell Sea. The bottom waters of the Australian–Antarctic Basin are derived primarily from the Ross Sea, as indicated by the higher salinity there, and secondarily from the Adèlie Coast (140°E), seen best in the dissolved oxygen data.

The primary northward path of bottom water in the western Indian Ocean (Mantyla and Reid, 1995) is through the discordance zone in the Southwest Indian Ridge at about 30°S, 60°E by way of the Crozet Basin, in the eastern segment of which there also appears to be a substantial recirculation in Figure II-98 (as calculated by RT96 for their layers 6 and 7, a total of about 7 Sv in this location). In Figure II-98, there also appears to be a southward and then southeastward flow (as one scans this

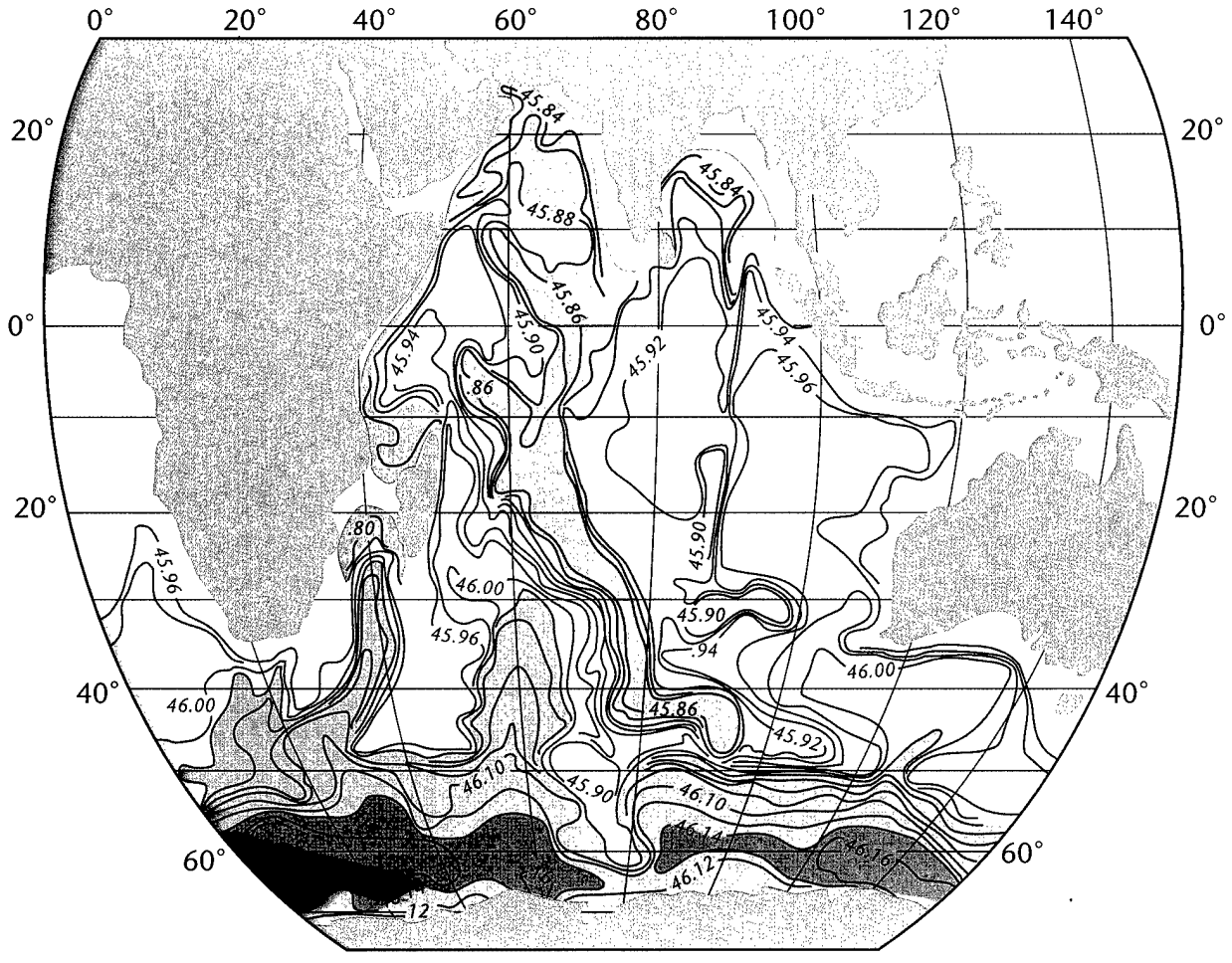

Figure II-98: σ_4 (kg m^{-3}) at the bottom of the Indian Ocean, adapted from Mantyla and Reid (1995, and personal communication).

figure from northwest toward the southeast), along the Central and Southeast Indian Ridges of water with σ_4 values of approximately 45.86, from the northern Indian Ocean to the ACCS. A recirculation of about 5 Sv occurs in this location according to figure 8 by RT96, their layer 6; please note the decrease in transport streamfunction from 60 to 85°E. Near-bottom water in the western Indian Ocean flows northward into the Madagascar Basin, into the shallower Mascarene Basin, through the Amirante Trench to the Somali Basin, and through the Owen Fracture Zone to the Arabian Basin (Johnson *et al.*, 1991a, b; Mantyla and Reid, 1995; please also see pp. 471–473 in the Indian Ocean Atlas, Wyrtki, 1971). Along this western abyssal spreading path, the near-bottom potential-density anomaly decreases from $\sigma_4 = 46.18$ in the Weddell–Enderby Basin to $\sigma_4 \doteq 45.86$ in the Arabian Basin; potential temperature increases from –0.8° to about 1.4°; salinity increases from 34.66 to 34.74; and dissolved oxygen decreases from more than 5.8 to about 3.6 ml L^{-1}. Since these changes are all towards the values of the overlying water column, vertical mixing is suggested as the mechanism of water mass transformation along this path (Mantyla and Reid, 1995).

The spreading of abyssal waters in the eastern Indian Ocean according to Mantyla and Reid (1995) is by way of the South Australia Basin through a gap near 33°S, 105°E between the Broken and Naturaliste Plateaus into the Perth Basin, then to the deeper Australian and Cocos Basins and finally to the Central Indian Basin through a gap in the Ninetyeast Ridge at about 10°S. Along the eastern abyssal spreading path, where there are also indications of recirculation at the eastern boundary of the Perth Basin (a recirculation of 4–5 Sv in layer 6 was calculated by RT96 at this location), θ increases from about 0 to 1°C, salinity from 34.70 to 34.72, and oxygen from about 5.0 to 3.6 ml L^{-1} (Mantyla and Reid, 1995, their figure 2). According to RT96, a net 11 Sv (Table II-12) of bottom water (CDW) exits north from the ACCS across 32°S, along with 2 Sv of Lower Deep Water ("recently" NADW; their layer 6). Robbins and Toole (1996) define two types of bottom water (Upper, Lower) and the bulk (10 Sv) of their northward flow is in Upper Bottom Water (layer 7, $45.89 \leq \sigma_4 \leq 46.01$). In their layer 7, RT96 have about 7–8 Sv flowing northward on the western side of the Crozet Basin, with a recirculation of 3–4 Sv on the eastern side, for a net of 4 Sv north as a Deep Western Boundary Current, presumably along the path suggested by Mantyla and Reid (1995). The recirculation of a total of about 14–15 Sv in layers 6 and 7 as found by RT96 is the principal difference between their estimate and the previous estimate by Toole and

Warren (1993). Robbins and Toole (1996) also have about 4 Sv flowing north into the Perth Basin in their layer 7. The remaining 2 Sv of 10 in layer 7 according to RT96 "leaks" across the ridge and basin system west of 50°W.

A map of the depth of the surface defined by σ_4 = 45.96, adapted from Mantyla and Reid (1995) is shown in Figure II-99. This map is from the middle of the upper bottom water layer (RT96), carrying the bulk of the bottom water transport north. At this σ_4, the two main pathways for the flow of bottom water north (Figures II-98 and 99) are into cul-de-sacs. At σ_4 = 45.89, at the top of upper bottom water as defined by RT96, the salinity distribution (Figure II-100; adapted from Mantyla and Reid, 1995, their figure 5b) indicates that CDW has penetrated into essentially all of the deep basins of the Indian Ocean, including those north of the equator. It is in layer 6 (lower deep water, with "recent" NADW influence) that RT96 find the largest difference in net

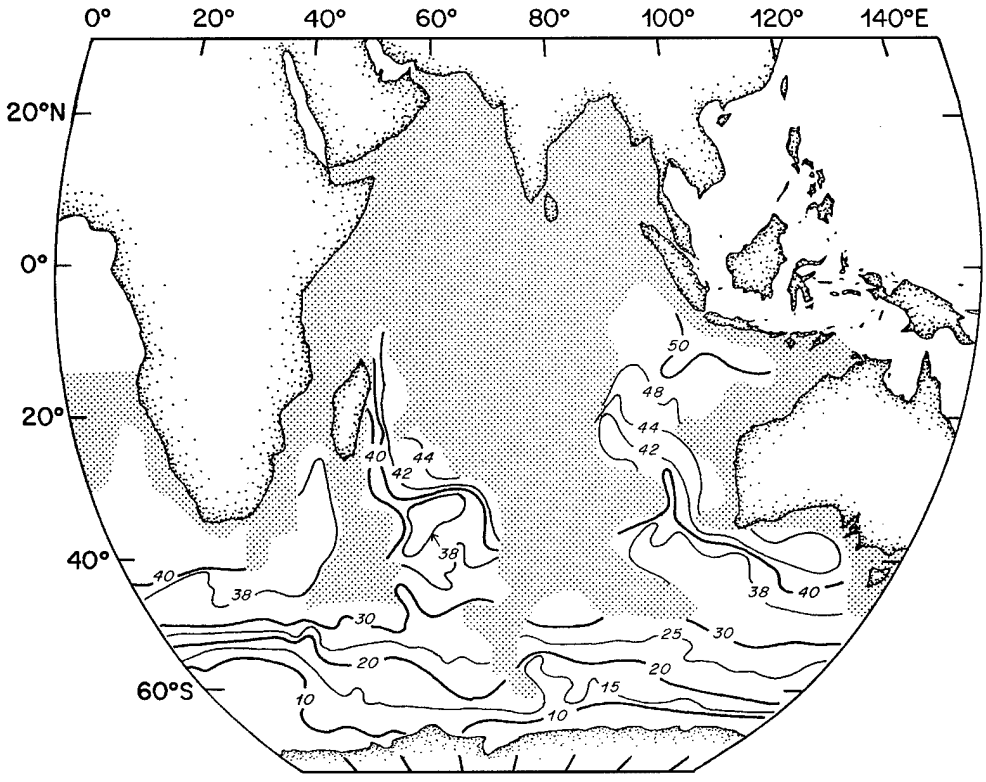

Figure II-99: Depth of σ_4 = 45.96 (kg m^{-3}) for the Indian Ocean, adapted from Mantyla and Reid (1995, their figure 4a). Area is shaded where the bottom is shallower than this isopycnal depth.

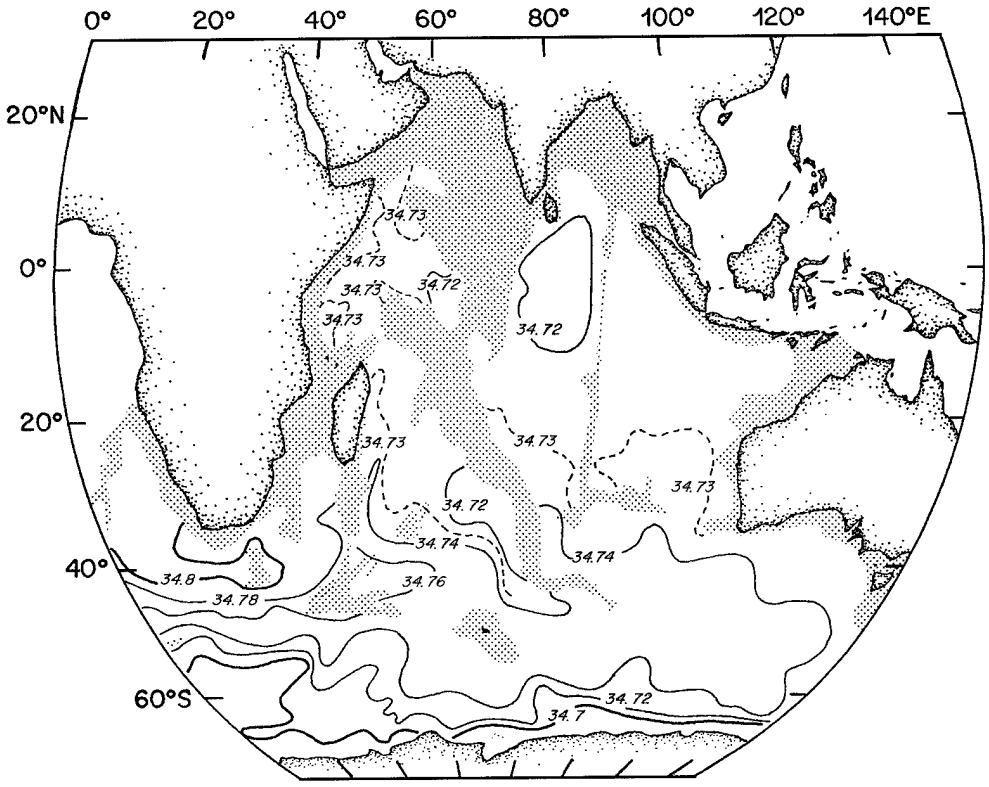

Figure II-100: Salinity on σ_4 = 45.89, adapted from Mantyla and Reid (1995, their figure 5b). Area is shaded where the bottom is shallower than this isopycnal depth.

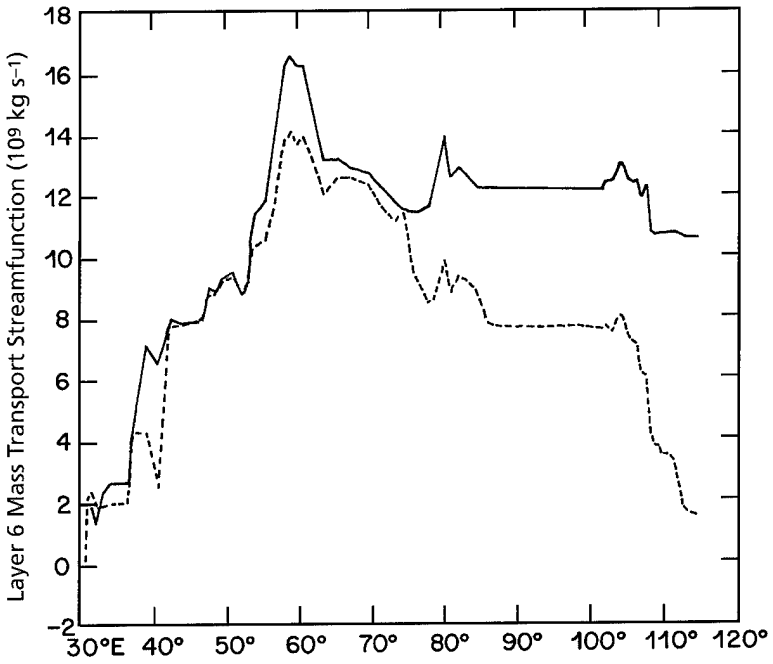

Figure II-101: Meridional mass transport streamfunction for layer 6 (core of NADW) for Toole and Warren (1993) circulation (solid line) and revised (RT96) circulation (dashed line), adapted from RT96 (their figure 8). The magnitude of the northward flow of layer 6 in the western half of the ocean is relatively unchanged, however, the revised transport has much larger southward transport across the interior of both the Crozet Basin (60° to 76°E) and Perth Basin (101° to 111°E).

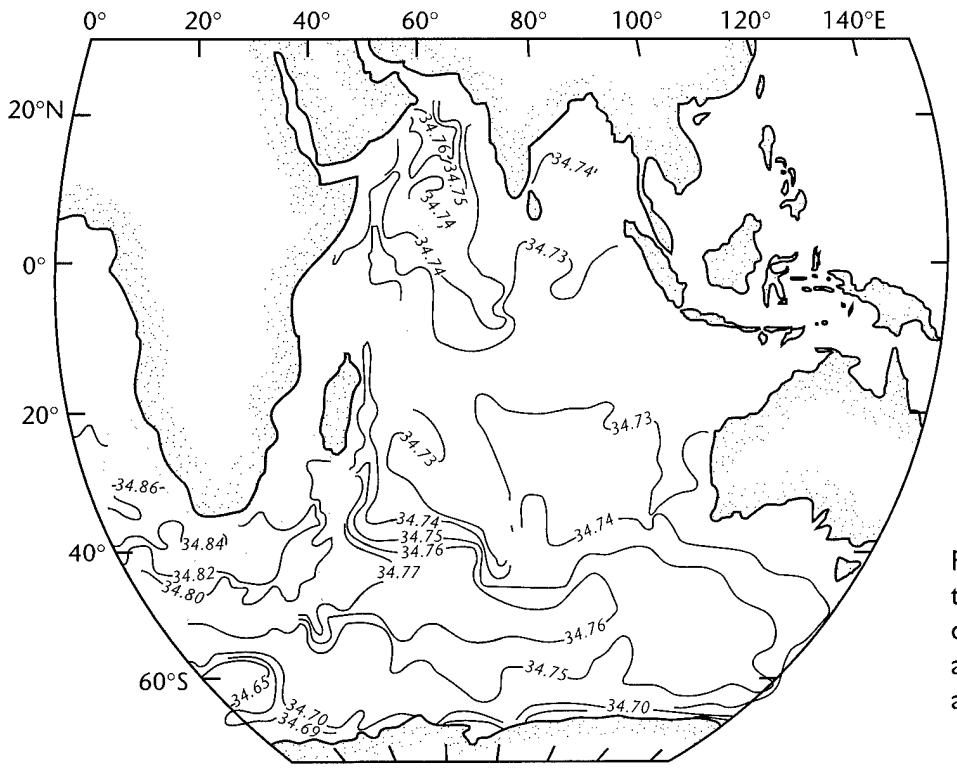

Figure II-102: Salinity on the 41.495-σ_3 potential-density anomaly surface, adapted from Mantyla and Reid (1995).

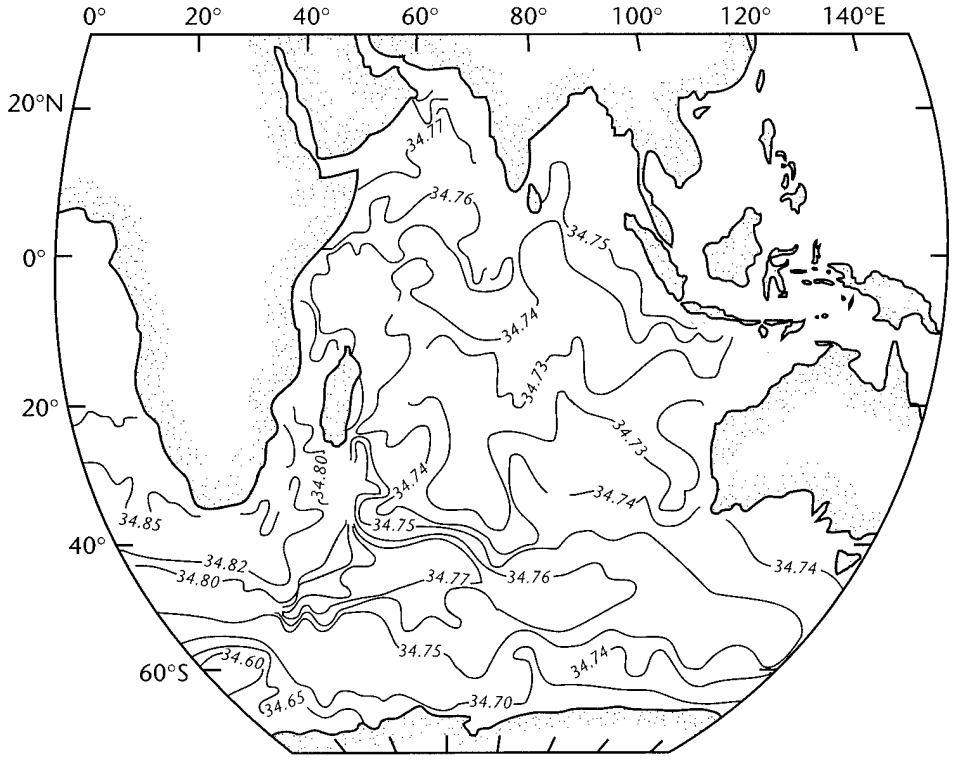

Figure II-103: Salinity on the 37.00-σ_2 potential-density anomaly surface, adapted from Mantyla and Reid (1995).

northward transport (2 Sv vs 11 Sv) between their silica-conserving model and the Toole and Warren (1993) results (Figure II-101), due to large recirculations of this water type (~ 5 Sv in the Crozet Basin and ~ 4 Sv in the Perth Basin). The existence of this path segment for "recent" NADW may be an element of the process by which NADW "becomes part of CDW."

As is generally the case throughout the oceans (S95), our knowledge of abyssal water mass formation and spreading in the Indian Ocean is superior to our ability to identify the characteristics of the upward limb(s) of the meridional cell. In Section 1, I introduced a few figures from the Indian Ocean Atlas (Wyrtki, 1971) that could point to a couple of possibilities, the first as suggested, for example, by Mantyla and Reid (1995). That is, CDW is modified by vertical mixing in its journey through the Indian Ocean and returns to the south from the northern Indian Ocean as a low oxygen tongue of "comparatively" high salinity, as is very clearly indicated in the sections in the Indian Ocean Atlas (Figures II-12 through 15 are the examples presented in Section 1 of this report). The low oxygen, "high" salinity tongue in Figures II-12 and 13 also extends across the intermediate water potential density range, possibly suggesting diapycnal conversion (see below). A clue relative to another process possibly connected to the meridional cell in the Indian Ocean may lie in some of the salinity maps on σ surfaces presented by Mantyla and Reid (1995), specifically their figures 6b and 7b, shown here in simplified form as Figures II-102 and 103. In these figures, there are areas of low salinity surrounded by areas of high salinity only, which might imply vertical mixing or diapycnal transformation by/of the abyssal waters below these surfaces.

3d. Intermediate Water

There is a strong flow of intermediate water (15–30 Sv, depending primarily on its definition in σ space and somewhat on data set and analysis techniques) in the Agulhas Current (Clowes, 1950; Harris, 1972; RT96; S95; Toole and Warren, 1993; Visser and Van Niekerk, 1965). Although this characteristic of the ACS had been known for quite a while, the first definitive indication insofar as I know that the IW flowing south in the ACS exceeded the intermediate water flowing north into the South Indian Ocean east of the ACS was due to Toole and Warren (1993), who found a net imbalance of 9–10 Sv southward across 32°S (Figure II-79). They found about 18–20 Sv of IW (defined by $27.0 \leq \sigma_\theta \leq 27.5$) going south in the Agulhas Current at 32°S, with roughly 9–10 Sv flowing northward across the rest of the South Indian Ocean along 32°S, the latter transport cited including 3–5 Sv recirculating northward by approximately 70–80°E (Figure II-79).

This IW imbalance has recently been revised by RT96 to 7 Sv, using the same data as Toole and Warren (1993) with a different technique for choosing reference level, and including a redefinition for IW (an enlargement of σ space; $26.8 \leq \sigma_\theta \leq 27.5$). According to RT96 (Table II-12) about 29 Sv of IW flows southward in the Agulhas Current at the 32°S section, and 22 Sv flows northward across the rest of the South Indian Ocean along 32°S, with about 10 Sv of the latter recirculating northward by 70–80°E. Schmitz (1995) suggested that the "excess" intermediate water in the ACS at 32°S might eventually flow eastward below the STC (or Agulhas Front; abbreviated AF by Belkin and Gordon, 1996; please see Figure II-80) in the South Indian Ocean, merging with the SFZ there; in Figure II-80 the STC and SFZ and Agulhas Front (AF) merge near the Crozet Basin; please also see Park *et al.* (1991). According to S95 this "excess" IW from the upward limb of the meridional cell in the Indian Ocean could constitute a source for the intermediate water flowing south of Australia across the South Pacific, through Drake Passage and exiting to the South Atlantic (R8891; S95) and thence the North Atlantic (Schmitz and Richardson, 1991; Schmitz and McCartney, 1993; S95; Volume I of this report) to act as part of the replacement flow for NADW. Alternatively, some of the excess of IW in the ACS could also be a source for the IT, to go along with that part of the upper layer IT that flows from the Agulhas into the AF, merges with the SFZ in the Crozet Basin, and is eventually converted to SAMW. In transiting the area from south of the Indian Ocean to south of Australia to the eastern

South Pacific, all in the SFZ, considerable upper layer water mass modification is probable (McCartney, 1977, 1982), at least to SAMW, and especially in the South Pacific east of the longitude of New Zealand to LSAMW and/or LOIW where the latitude of the SFZ increases significantly, from ~ 45°S in the Crozet Basin to 55°S approaching Drake Passage.

Interesting results and ideas concerning IW in the Indian Ocean have been published by Fine (1993), Piola and Georgi (1982), Read and Pollard (1993), Reid (1981), Rochford (1961, 1963, 1964, 1966), RT96, Taft (1963), and Toole and Warren (1993). I believe that critical clues to the exceptional nature of the IW in the Indian Ocean, providing me the opportunity to speculate on its role in the upward limb of the meridional cell in the Indian Ocean at this time, lie in the works by Rochford (1961, 1963, 1964, 1966). Basically Rochford found three types of intermediate water in the southeast Indian Ocean, that is, his area of operation in the 1950s and '60s. These varieties were called Antarctic, Banda, and Northwest Indian Intermediate Waters, the latter two in my opinion "associated" with the meridional cell (discussed further below). It is also possible of course that west and south of Rochford's area of operations some IW of circumpolar origin could mix with deep water (Figures II-102 and 103), or Banda/Northwest Indian Intermediate Water, and such mixtures could be IW "connected" to the large-scale meridional cell.

The largest component of the flow of IW in the Agulhas Current is "modified" IW of circumpolar origin (*i.e.*, the return flow of the 22 Sv found by RT96 to be flowing northward across the 32°S section east of the Agulhas Current). The intermediate water entering the South Indian Ocean in the east (Toole and Warren, 1993) and that in the Agulhas recirculation both have the low salinity characteristics of IW of circumpolar origin. Fine *et al.* (1994) point out that the IW entering at the Agulhas recirculation also has comparatively high oxygen. The IW flowing south in the Agulhas Current is of higher salinity and silica than intermediate water of circumpolar origin (RT96; Toole and Warren, 1993; for salinity please see Figure II-79 as well as Figures II-104 and 105). The silica contours associated with the ACS in Figure II-83 below 2000 m are lower than those in the interior, with the opposite tendency above 2000 m depth. The situation with respect to potential density surfaces, which is more subtle than the distribution of silica with depth, is discussed below.

It has long been known (Piola and Georgi, 1982) that one may find different brands of intermediate water in different oceans, with the Indian Ocean IW being notably saltier than that for the Atlantic, and Pacific IW being in between (Figure II-105). There is also IW south of Australia that is similar to Indian Ocean IW (curves denoted 10–11 in Figure II-105, please see a detailed dicussion in the appendix of S95). This point was used by S95 to infer a transfer of IW from the Agulhas Current to the SFZ south of the Indian Ocean that propagates south of Australia and across the Pacific. Banda Intermediate Water (BIW; as originally described by Rochford, 1961, 1963, 1966; see below) salinities are slightly lower than for CDW, possibly indicating mixing with IW of Pacific origin in the Banda Sea, or with IW of circumpolar origin in the southeastern Indian Ocean. But, as discussed in detail later in this section, I don't think that the Banda Sea is necessarily the source of all BIW, which is LOIW, occurring in the σ_θ range 27.2 → 27.6, say. The Northwest Indian Intermediate Water (NIIW), as the name implies, apparently "originates" in the North Indian Ocean, and appears to reach the low-latitude southeastern Indian Ocean by cross-equatorial flow near Sumatra (Rochford, 1961, 1964; Fieux *et al.*, 1994), but with lower salinities (34.7–35.0) than when in the Arabian Sea (35.2–35.6).

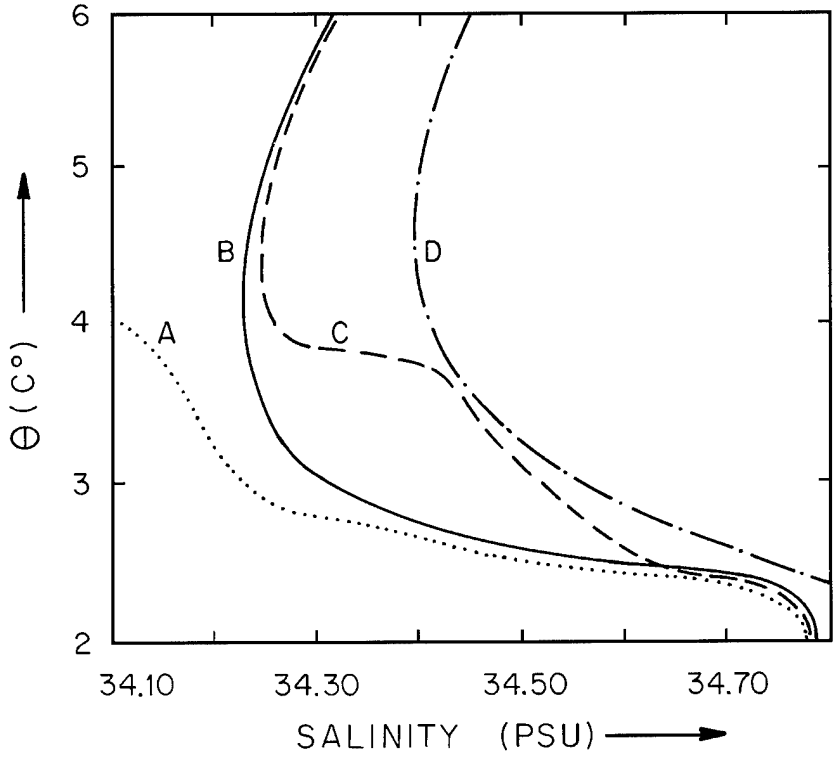

Figure II-104: Potential Temperature/Salinity (θ, S) profiles for Intermediate Water across the Agulhas return flow and the Southern Ocean, adapted in smoothed form from Read and Pollard (1993). Antarctic Surface Water is depicted in curve A, AAIW from the south in curve B, Intermediate Water from the north in curve D, and interleaving between B and D in curve C.

The biggest question mark relative to the conversion of 7 Sv of CDW plus "NADW" from the ACCS to intermediate water in the Indian Ocean is where and how this might occur. The transformation processes from CDW and NADW to "upper" deep water occur to some extent within the deep basins of the South and to a large extent in the North Indian Ocean (Johnson *et al.*, 1991a, b; Mantyla and Reid, 1995). Water mass conversion processes in equatorial currents could also play a role in these transformations and perhaps be a factor in selecting the σ distribution of the IW crossing the equator in the boundary current off Sumatra. Red Sea Water (RSW) is a well-known source of IW that has a σ_θ range of about 27.0–27.3 in the Arabian Sea and western North Indian Ocean in general (Quadfasel and Schott, 1982; Rochford, 1964; Shapiro and Meschanov, 1991). There are indications of RSW at lower density horizons in the western South Indian Ocean near 25–30°S, in the σ_t range 27.0–27.7, between 800 and 2000 m depth (Gründlingh, 1985). Sharma (1976) states that there is no large flow of RSW across the equator except very near the African coast. Sætre and da Silva (1984) find RSW in the Mozambique Channel.

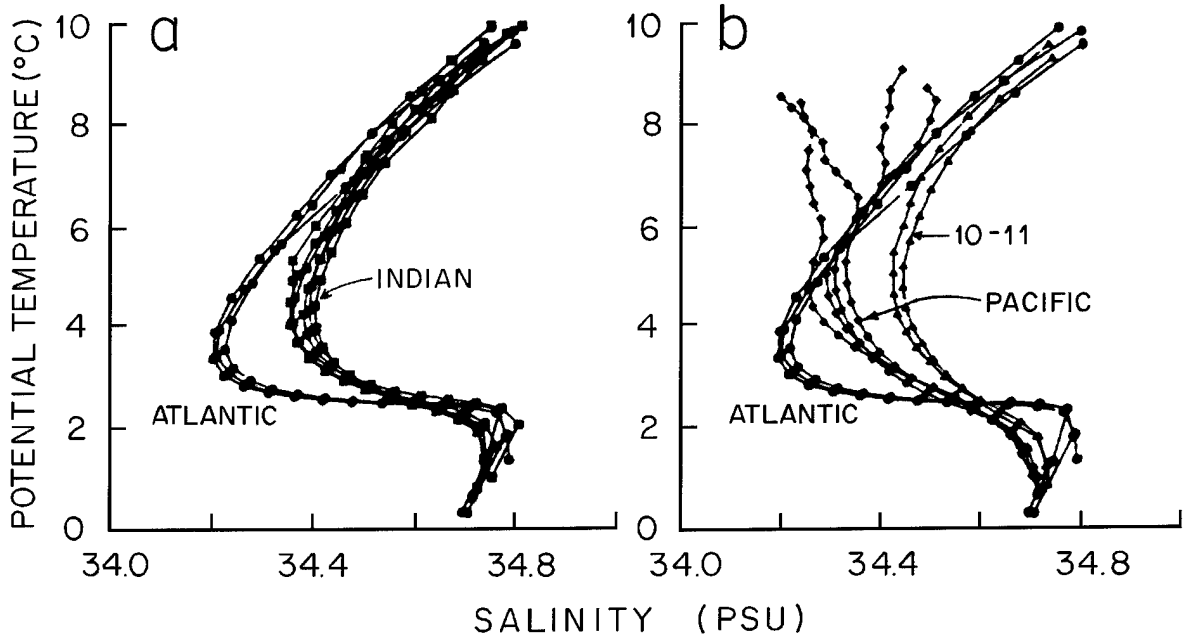

Figure II-105: Potential Temperature/Salinity (θ–S) diagrams for intermediate water in the southern hemispheric oceans, adapted from Piola and Georgi (1982, their figure 8; see also Schmitz, 1995). Each θ–S curve is from a zonal sector of the ACCS, grouped by ocean basin except that curves labeled 10 and 11 are south of Australia: (a) Atlantic vs Indian Ocean sectors, (b) Atlantic vs Pacific and Austral Pacific (curves 10–11) sectors.

Red Sea Water helps to account for the comparatively high salinity of some of the meridional cell components (which start out at a salinity of 34.7–34.8 as CDW and "NADW"), but it is not by itself sufficient to explain the excess transport of 7 Sv of intermediate water in the ACS associated with a large-scale meridional cell, because RSW transports a fraction of a Sverdrup as it exits the Red Sea. The very low oxygens at deep and IW density horizons probably relate to the gradual loss of O_2 by the deep meridional cell components. It is clear that the North Indian Ocean is a location of "high" salinity and "low" oxygen at deep and intermediate levels, and in my opinion the source of Rochford's (1961, 1963) NIIW. Is NIIW also affected by diapycnal modification in deep equatorial jets in its transit to the eastern Indian Ocean? In any event, equatorial and low-latitude current systems play a key role in the flow of NIIW. Sharma (1972, 1976) noted that the upper and intermediate layer flow patterns in the equatorial Indian Ocean were primarily zonal except at the eastern and western boundaries, and Sharma (1976) pointed out that a southward cross-equatorial transport at the eastern boundary was common to a variety of density horizons.

Rochford (1961, 1963, 1964, 1966) demonstrated that the circulation in the southeastern Indian Ocean for $27.0 \leq \sigma_t \leq 27.5$ was characterized not only by intermediate water of circumpolar origin (the dominant type south of 20°S). Two other distinct, in *T/S* characteristics, types of intermediate water were found between about 0 and 20°S in the eastern South Indian Ocean. A frontal distribution of properties in IW between 0 and 20°S can readily be seen for various sections in the Indian Ocean Atlas, including western and central sectors of the Indian Ocean as well as the eastern. Potential density values of 26.8–27.4 tend to deepen sharply toward the south between 5 and 20°S under the surface expression of the SEC, as the boundary between IW with North Indian Ocean characteristics and IW with circumpolar-derived characteristics. The S and O_2 isopleths in the intermediate water σ_θ range ($26.8 \leq \sigma_\theta \leq 27.5$) are somewhat vertical over this σ_θ interval from, say, 10°N to 10°S for S, and 10°N to 20°S for O_2, in most of the cross-equatorial sections plotted in Chapter 10 of the atlas (Wyrtki, 1971; pp. 477–520). From another viewpoint, most of Taft's (1963) salinity and oxygen contours for various intermediate water horizons at and below $\sigma_\theta \doteq 26.8$ in the Indian Ocean are strongly zonal and compact between 0 and 20°S, except at the western and eastern boundaries where the cross-equatorial exchanges take place.

In Section 1 of this report volume a couple of meridional–vertical distributions from the Indian Ocean Atlas were shown that could imply a general southward and upward spreading of comparatively saline and low oxygen upper deep and intermediate water from the North toward the South Indian Ocean, possibly as part of the diapycnal upper limb of the meridional cell in the Indian Ocean. Sections across and along the

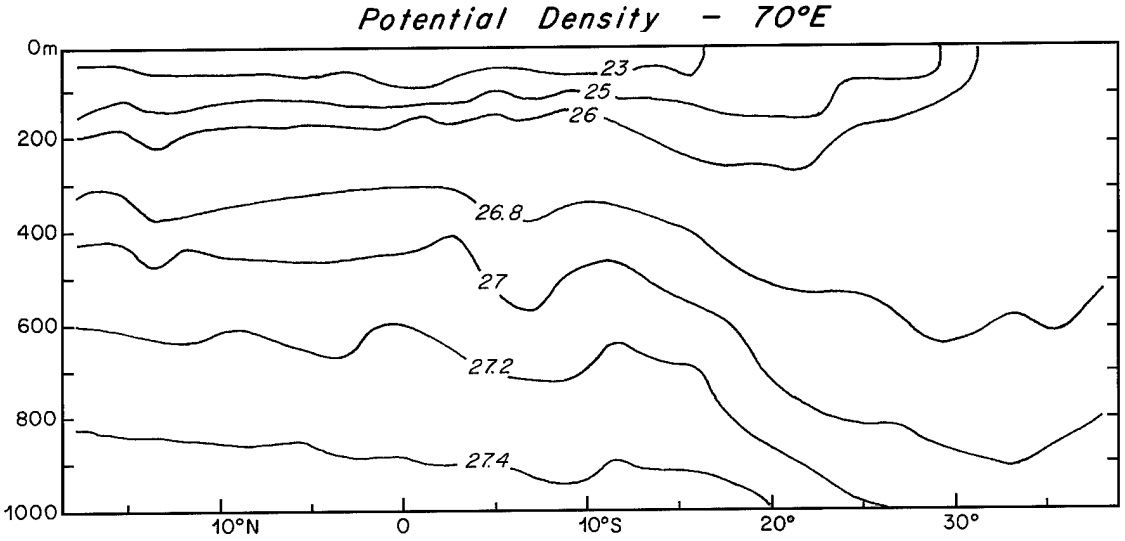

Figure II-106: Potential density in the upper 1000 m along a section down 70°E off Bombay to 37°S, adapted from Wyrtki (1971, p. 500).

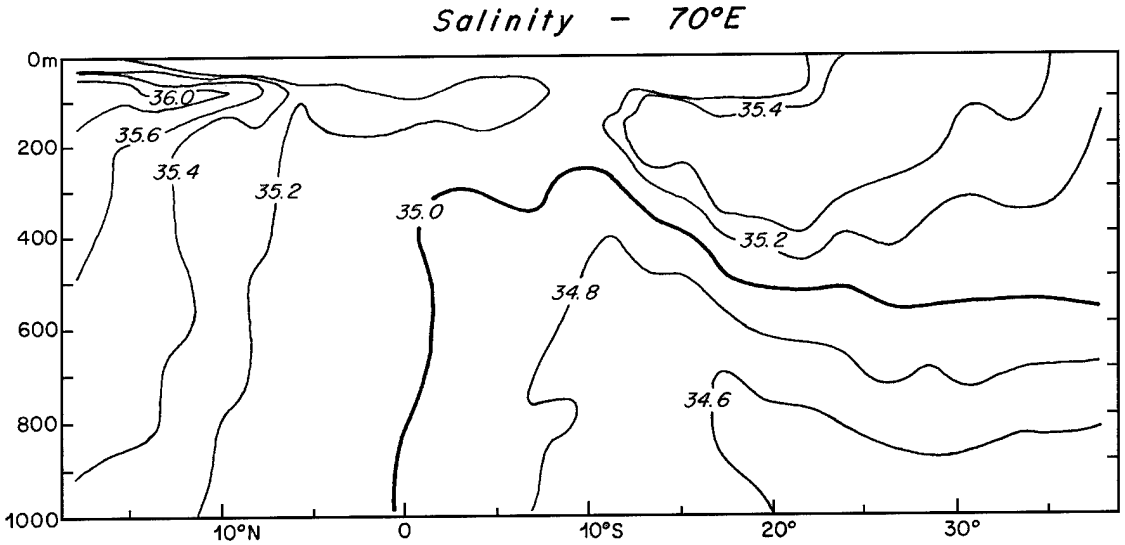

Figure II-107: Salinity in the upper 1000 m along a section down 70°E off Bombay to 37°S, adapted from Wyrtki (1971, p. 501).

equator (Wyrtki, 1971) for intermediate and upper layer depth ranges are now shown in Figures II-106 through 116. In Figure II-106, the potential density range $26.8 \leq \sigma_\theta \leq 27.4$ occupies the water column from about 10°N to 10°S in the nominal depth range 350 to 1000 m, and in this area (Figures II-107 and 108) the salinities are comparatively high and oxygens relatively low. South of 10°S σ_θ surfaces deepen and by 20–

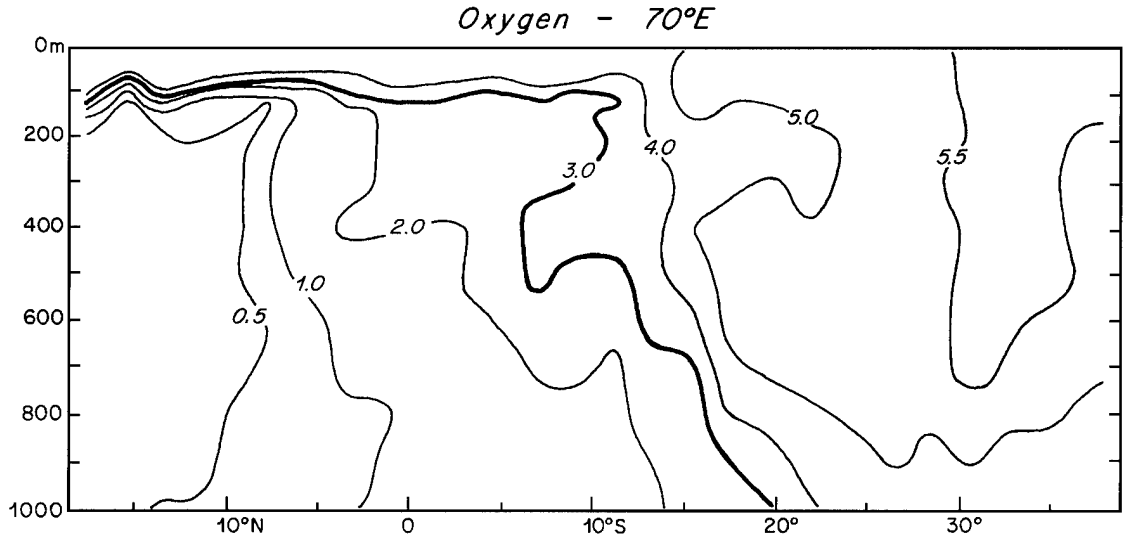

Figure II-108: Oxygen in the upper 1000 m along a section down 70°E off Bombay to 37°S, adapted from Wyrtki (1971, p. 502).

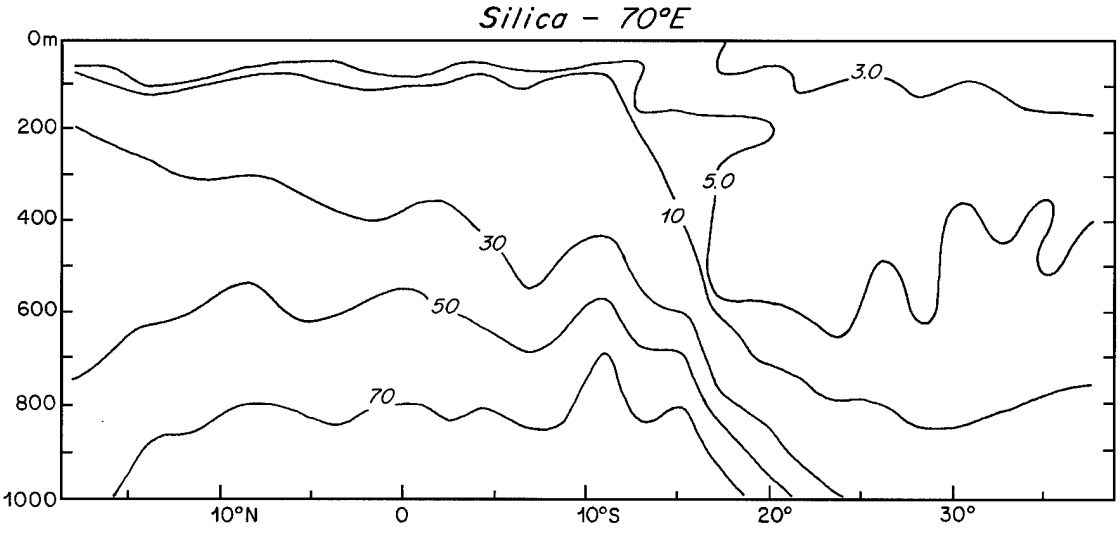

Figure II-109: A silica section for the upper 1000 m along a section down 70°E off Bombay to 37°S, adapted from Wyrtki (1971, p. 503).

30°S salinities and oxygens become like those of intermediate water of circumpolar origin (relatively low salinity and high oxygen). The distributions in Figures II-106–109 are from the "western" Indian Ocean at 70°E, the same location used by Wyrtki (1973; his figure 3) to call attention to frontal variability. Here I first want to emphasize that the variations in properties are strongest in the intermediate water potential density range. Then there is also an interesting feature of the silica distribution in Figure II-109 that I would like to draw attention to, especially in light of the RT96 silica balance. That is, the silica contours approximately follow σ_θ contours for LOIW, but for UPIW ($27.2 \leq \sigma_\theta \leq 26.8$) the silica carried in the front is at least a factor of 2 larger (30–50 vs 5–30) than for similar σ_θ horizons south of 20°S (Figure II-110, which is a joint plot of selected silica and σ_θ contours).

Meridional sections similar to those plotted in Figures II-106–109 but from the easternmost Indian Ocean along 94°E are shown in Figures II-111–114, and along the equator in Figures II-115 and 116. Figures II-111 through II-114 are respectively potential density, salinity, oxygen and silica sections from the Nicobar Islands to 20°S, taken from Wyrtki (1971). This section is close to Sumatra, at the eastern boundary of the low-latitude North Indian Ocean. The flow characteristics shown in Figures 111 through 114 (and 115, 116) are those impinging on the Indonesian Archipelago, and

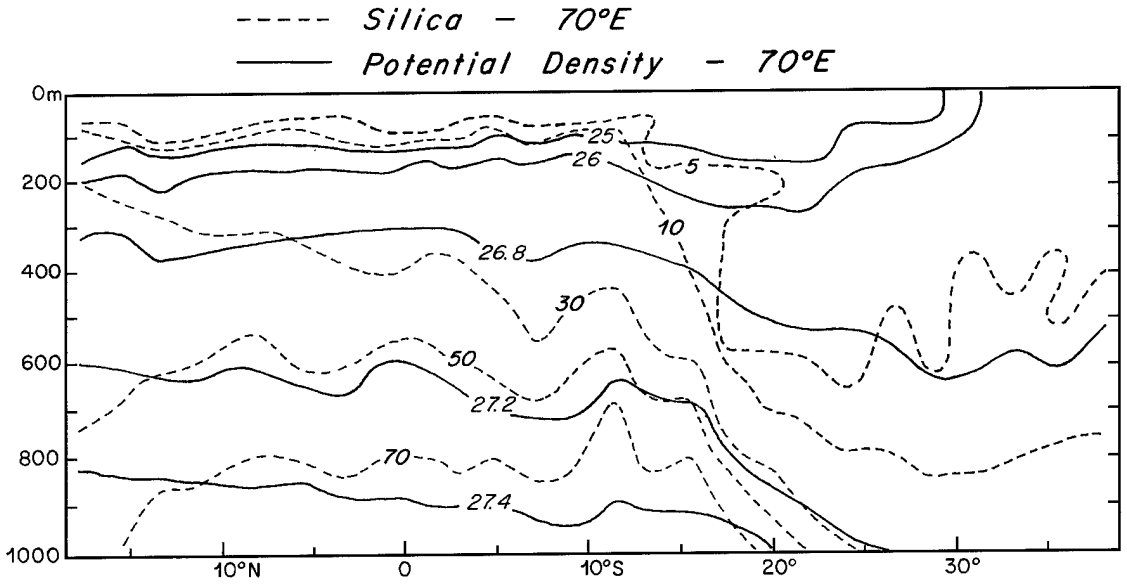

Figure II-110: Selected silica contours from Figure II-109 are superimposed on potential density contours taken from Figure II-106.

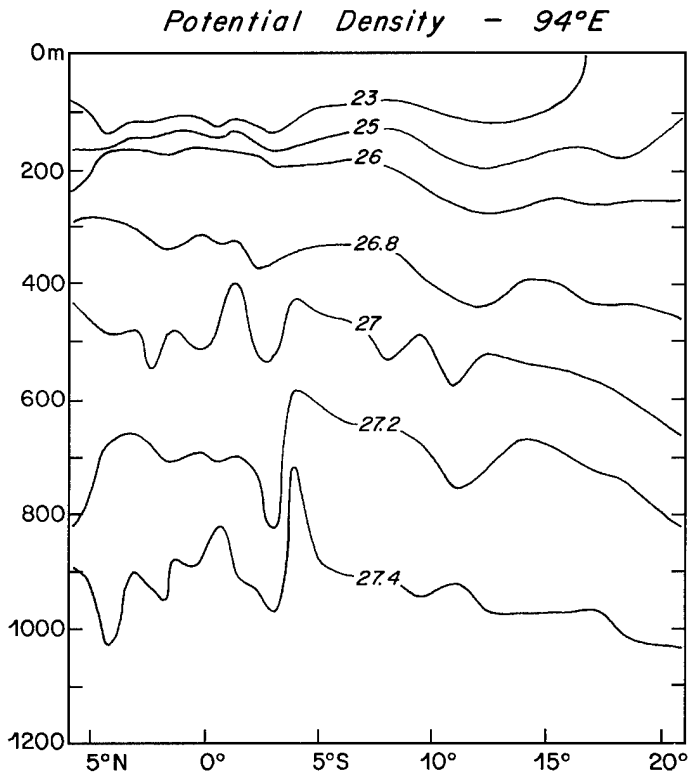

Figure II-111: A potential density section along 94°E from the Nicobar Islands to 20°S, adapted from Wyrtki (1971, p. 512).

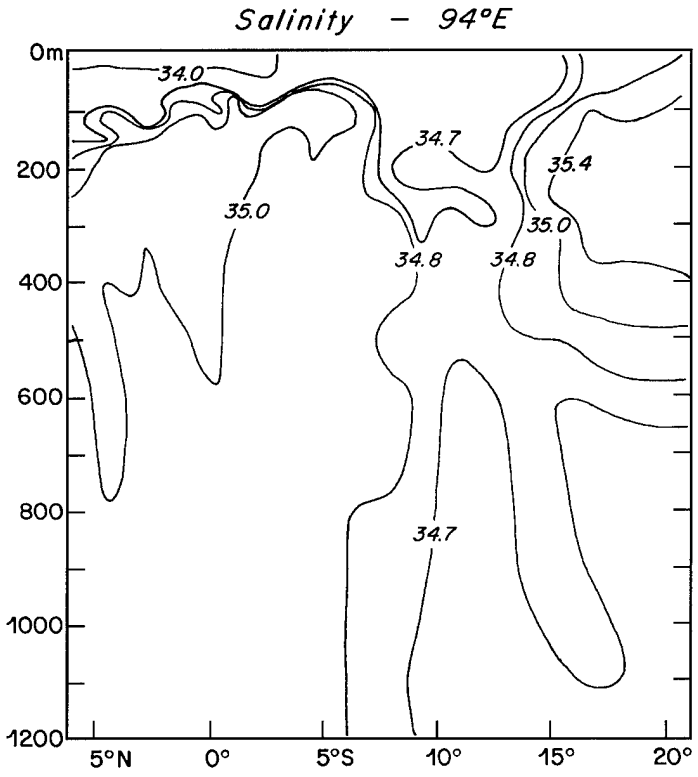

Figure II-112: A salinity section along 94°E from the Nicobar Islands to 20°S, adapted from Wyrtki (1971, p. 512).

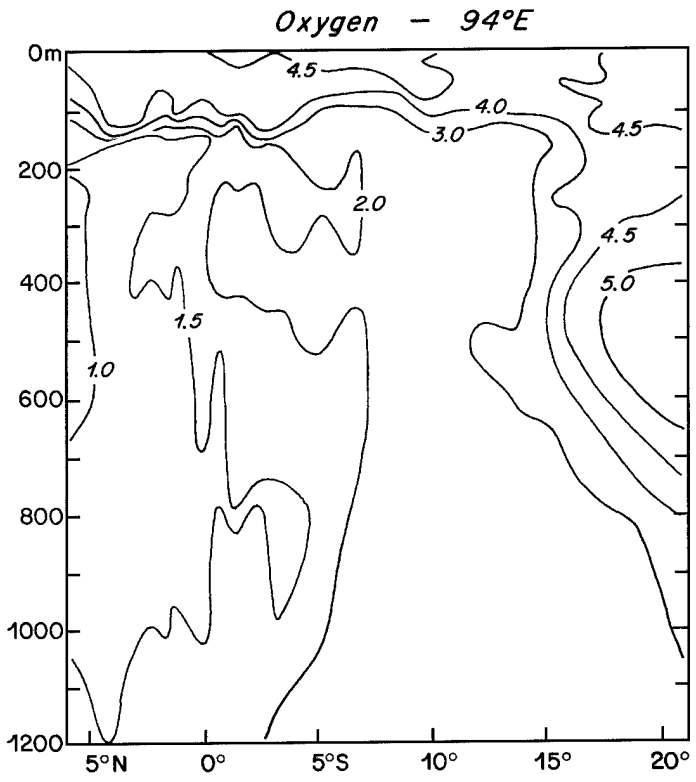

Figure II-113: An oxygen section along 94°E from the Nicobar Islands to 20°S, adapted from Wyrtki (1971, p. 513).

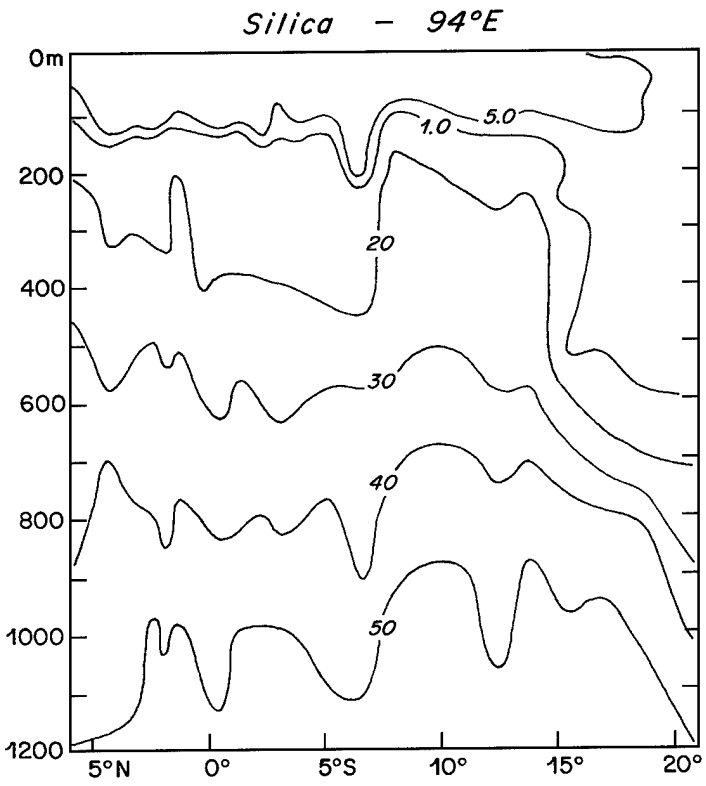

Figure II-114: A silica section along 94°E from the Nicobar Islands to 20°S, adapted from Wyrtki (1971, p. 513).

that to some extent drop south to the latitude of the north coast of Australia (see below). So this is the "upstream section" for flow impinging on Sumatra and the downstream section for the flow associated with the cul-de-sac between Australia and Java. In the latter context, please note the uplifted silica (10–50) contours between 5 and 15°S in Figure II-114, which I take to be possibly associated with the BIW identified by Rochford (1961), as discussed in the next and following paragraphs. Intermediate water from the Pacific that enters the Indian Ocean through the IT could also be a source of high silica. Figures 115 and 116 are potential density and salinity sections along the equator from Somalia to Sumatra, also taken from Wyrtki (1971). Please note the vertical homogeneity of salinity in the IW depth range, ~ 300–1000 m along the equator (Figure II-116).

Rochford (1961, 1963, 1966) identified three types of intermediate water for the σ_t range 27.0–27.5 in the southeastern Indian Ocean in terms of salinity maxima or minima. These three types of intermediate water and their properties in *T/S* space (Figures II-117, 118 and 119) according to Rochford (1961, his abstract) are: (1) intermediate water of circumpolar origin, but possibly somewhat enhanced in salinity (reminiscent of Figures II-104 and II-105), characterized by a salinity minimum in the range 34.3–34.6, in the σ_t range 27.0–27.3, (2) Banda Intermediate Water (BIW), characterized by salinity minima in the range 34.6–34.7, with σ_t values in the range 27.3–27.6, that are distinct in temperature from AAIW except at the least dense end of BIW, (3) Northwest Indian Intermediate Water (NIIW), having a salinity maximum in the σ_t range 27.2–27.5 (I think that this σ_t range and definition should be extended to less dense σ_t, or σ_θ, and associated with a salinity range rather than extremum, see below). Figures II-117, 118 and 119 are adapted from Rochford with minor modification, and the numbers 1 → 3 relative to type of IW as described above correspond to the numbers on Figure II-118. Later in this report, "updated" versions of II-118 will be described, where modifications involving both NIIW and BIW are suggested. A couple of maps of the distribution of these intermediate water masses are presented in Figures II-120 and 121. Figure II-120 depicts depth contours for the salinity minimum associated with AAIW, and basically restricts this water to the south of 15–20°S, in agreement with the sections in the Indian Ocean Atlas (Wyrtki, 1971). Figure II-121 is a simplified schematic of the salinity contours for the salinity maximum identifying NIIW according to Rochford (1961). It is clear that NIIW originates in the northern Indian Ocean and

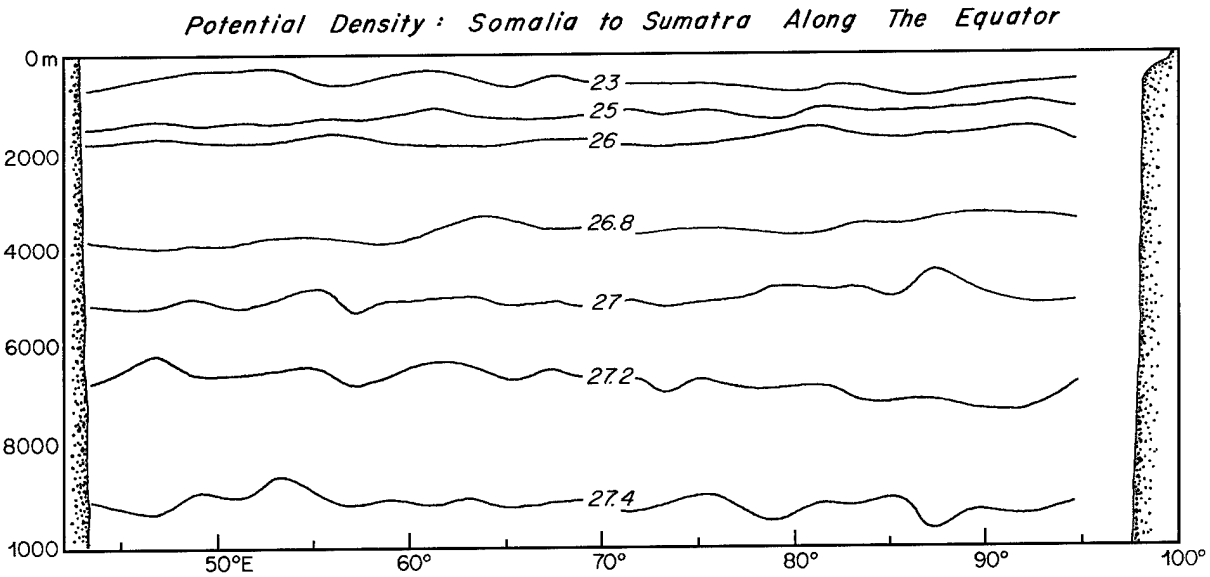

Figure II-115: A potential density section along the equator in the Indian Ocean from Somalia to Sumatra, adapted from Wyrtki (1971, p. 514).

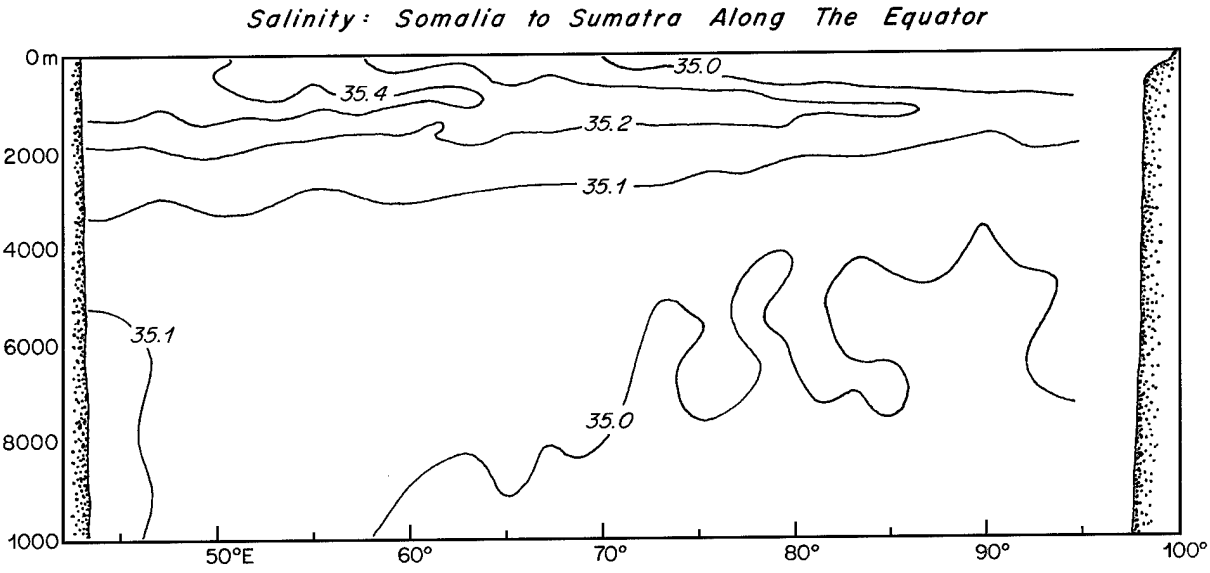

Figure II-116: A salinity section along the equator in the Indian Ocean from Somalia to Sumatra, adapted from Wyrtki (1971, p. 515).

crosses the equator along the coast of Sumatra, and the extension of NIIW in Figure II-118 to low salinities is questionable in my opinion, as is the southward extension in Figure II-121.

Intermediate water of circumpolar origin has been studied in a lot of detail, for decades. But what are the sources for and distribution of BIW and NIIW? Could Banda and NIIW be meridional cell components? These points are discussed next, BIW first, then NIIW. Rochford (1963) was clear about the separation of BIW from IW of circumpolar origin geographically and in *TS* space, especially in the latter case for the AAIW σ_θ range. In Figures II-116 and 117 (Rochford, 1961), BIW is characterized by a salinity minimum for $27.2 \leq \sigma_t \leq 27.5$, distinct from the salinity minimum associated with AAIW. In Figure 119, the separation between AAIW and BIW is made even more clear by using the modes of salinity histograms (Rochford, 1963). This separation was also shown geographically in figures 13–16 by Rochford (1963), where it is clear that the area between Australia and Java projected out to about 100°E is the prime location of BIW in the southeastern Indian Ocean. But is the Banda Sea "the source" of BIW? According to Fieux *et al.* (1994), Wyrtki (1961) took Banda Sea Water to be formed by mixing of North Pacific Subtropical Water and Pacific Intermediate Water and some water from the shallow and low salinity Java Sea. Hautala *et al.* (1996) conclude that the relevant density range in the Banda Sea shows the influence of the deep Indian Ocean. Please see their map of *S* and O_2 on $\sigma_\theta = 27.25$, shown here as Figure II-122, and compare Figure II-122 with their other maps in Figures II-95 and 96. Fieux *et al.* (1994) make a similar comment and have observed the flow in the Timor Passage toward the Banda Sea below 1200 m. Figure II-123 is a plot of the east–west component of flow in Timor Passage from Fieux *et al.* (1994). A somewhat similar conclusion was reached by Cresswell *et al.* (1993), who identified flow into Timor Passage from the Indian Ocean below 1700 m instead of 1200 m.

The silica distribution at $\sigma_\theta = 27.4$ from the Wyrtki (1971) Atlas is shown in Figure II-124. There is a silica maximum in the area between Java and Australia, a potential source region for BIW as determined by Rochford. This silica maximum is surrounded regionally by lower silica values, so the area below $\sigma_\theta = 27.4$ is the "only" local source for this water, unless "high" silica IW of Pacific origin is involved, possibly connected to flow through and mixing within the Banda Sea. Perhaps both sources are present: could BIW be formed locally, at least in part, by diapyncal uplift of Indian Ocean Deep Water (CDW-derived upper deep water) as well as a mixture of South Pacific Water perhaps, by sloshing back and forth between the North Australian Bight and the Banda Sea? In any event, Fieux *et al.* (1994) conclude that any transport across their Austra-

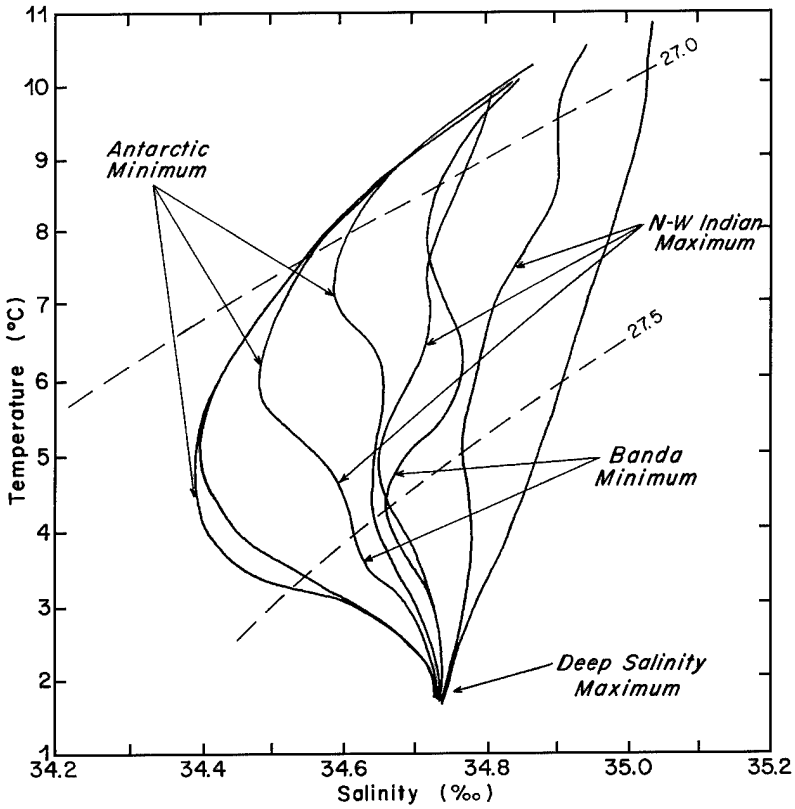

Figure II-117: *T/S* curves for various hydrographic stations in the southeastern Indian Ocean, adapted from Rochford (1961).

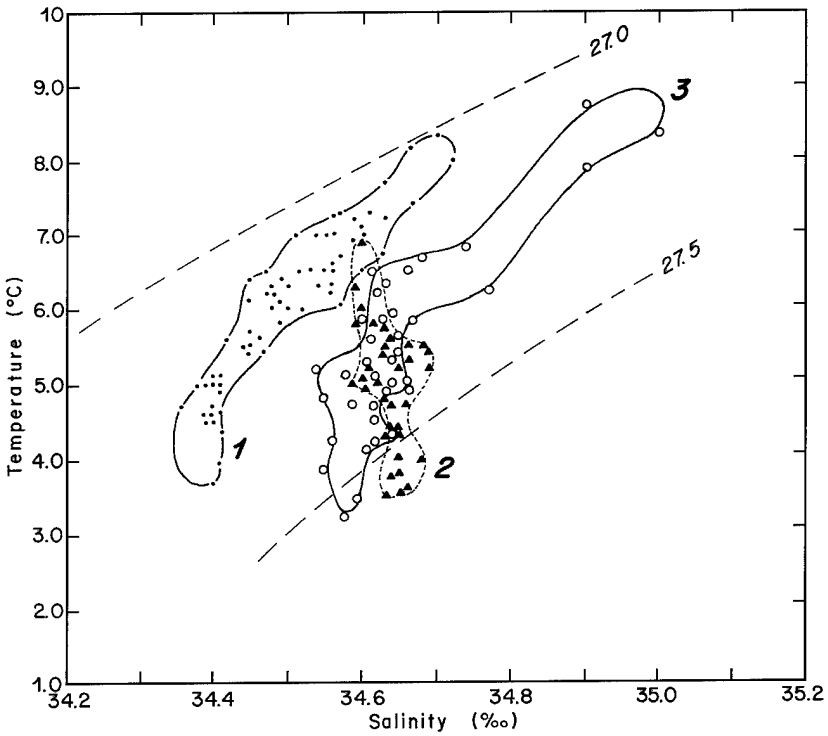

Figure II-118: Areas in the *TS* plane for three types of intermediate water, adapted from Rochford (1961). (1) denotes intermediate water of circumpolar origin, solid dots; (2) BIW, solid triangles; and (3) NIIW, open circles.

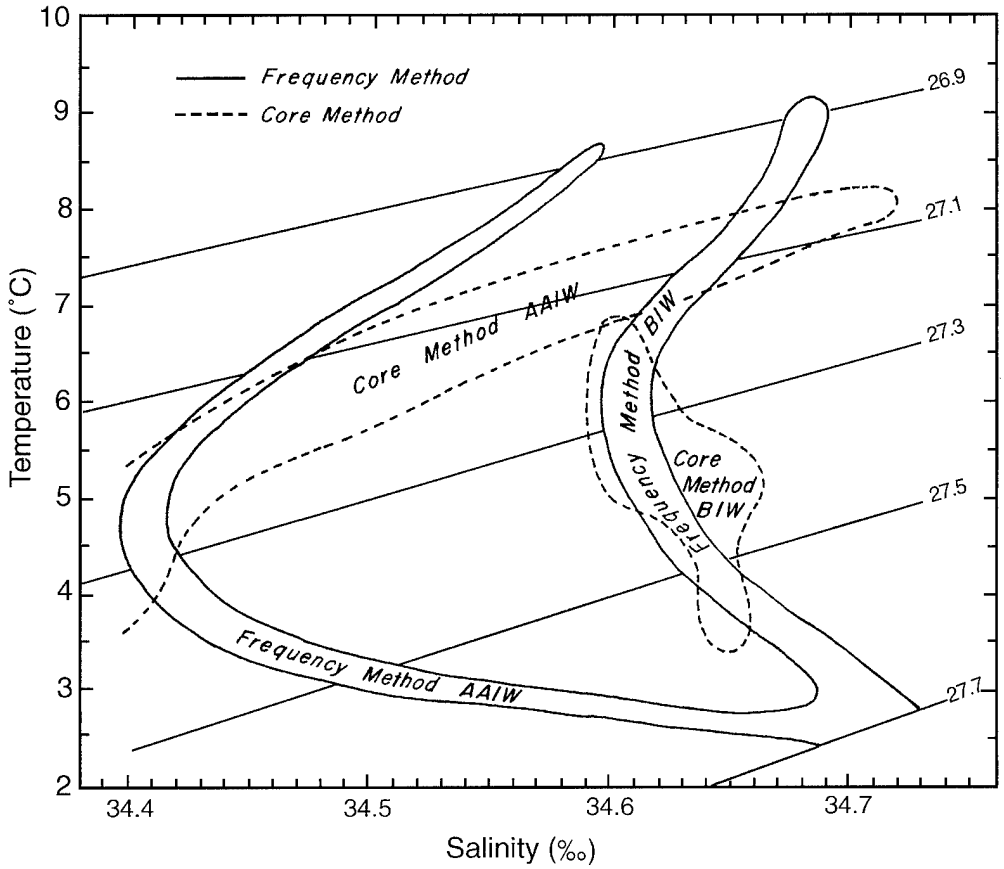

Figure II-119: Modal *T/S* curves, with areas defined by the location of salinity minima superimposed, adapted from Rochford (1963, his figure 27).

lia–Bali section below 500 m is of the order of the uncertainty of the measurement! But could a case for recirculation be made? Some of Rochford's *T/S* points in BIW (at the lower salinities) could be associated either with the Banda Sea or with mixing with AAIW. Much work needs to be done to sort out the situation for BIW. For now I assume that 1–3 Sv of IODW impinges on the NAB and is modified to BIW there, and to some extent traverses the NAB into the Banda Sea, is modified to BIW there, and recirculates back, perhaps accompanied by IW of Pacific origin.

As the name implies, the origin of NIIW is north of the equator, and it presumably "leaks" across the equator in the east (Figure II-121). Water of these characteristics is "strongest" in Figures 117 and 118 from stations used by Rochford (1961) that are closest to Sumatra and Java. There are indications that this brand of IW could extend

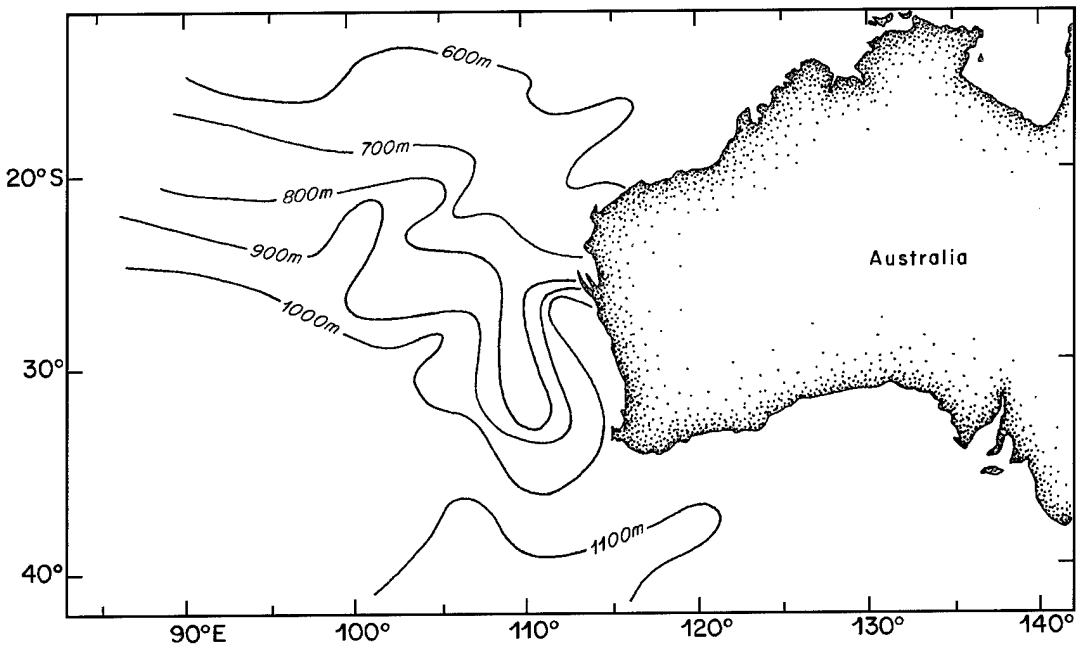

Figure II-120: Depth contours for AAIW in the southeastern Indian Ocean according to Rochford (1961), adapted with considerable simplification from his figure 4.

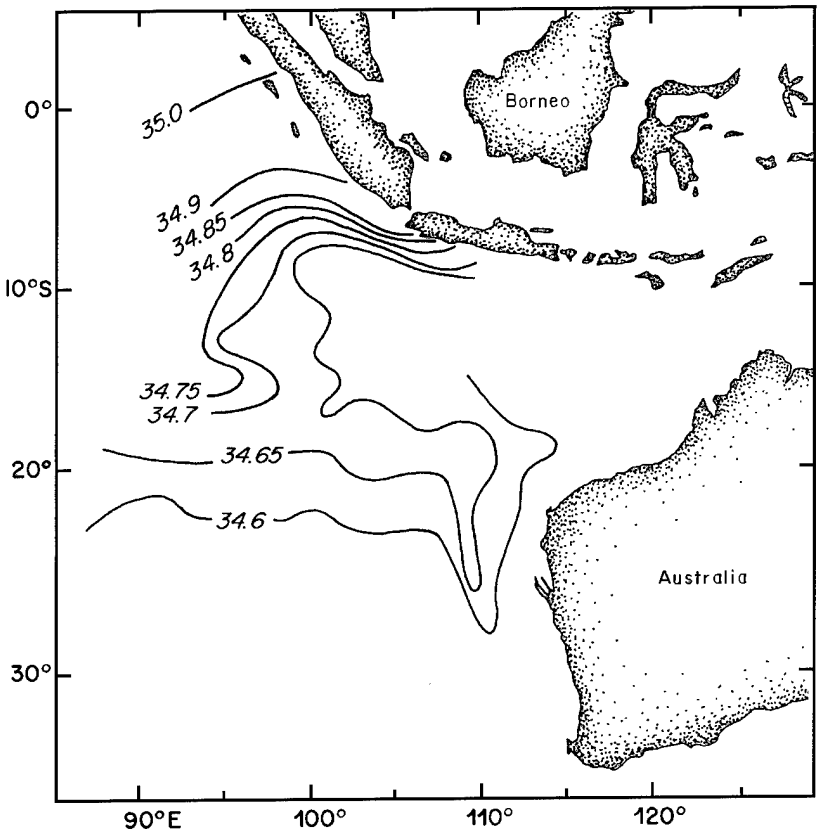

Figure II-121: Salinity contours for NIIW in the southeastern Indian Ocean according to Rochford (1961), adapted from his figure 9.

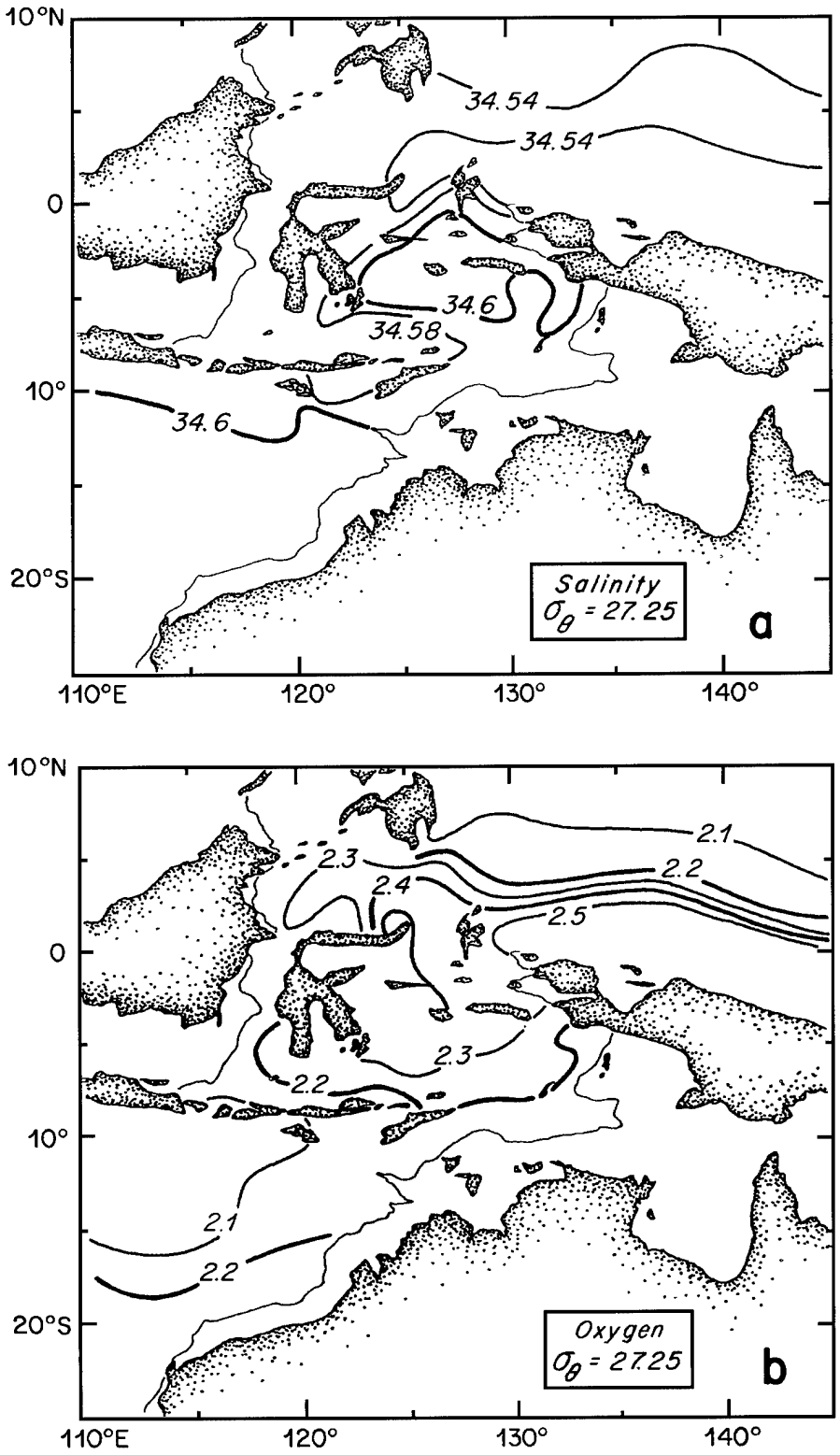

Figure II-122: Maps of (a) salinity (psu) and (b) oxygen contours on $\sigma_\theta = 27.25$, adapted from Hautala *et al.* (1996).

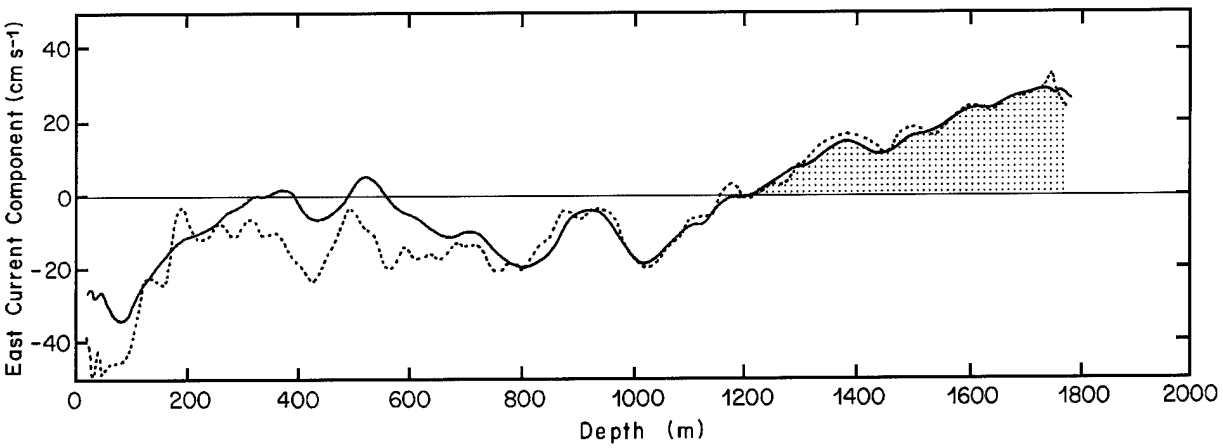

Figure II-123: Two current profiles on the sill of the Timor Trench in August 1989, adapted from figure 11 by Fieux *et al.* (1994). The east–west velocity component, positive eastward, is shown as a function of depth, with the eastward flow into the Banda Sea area below 1200 m stippled.

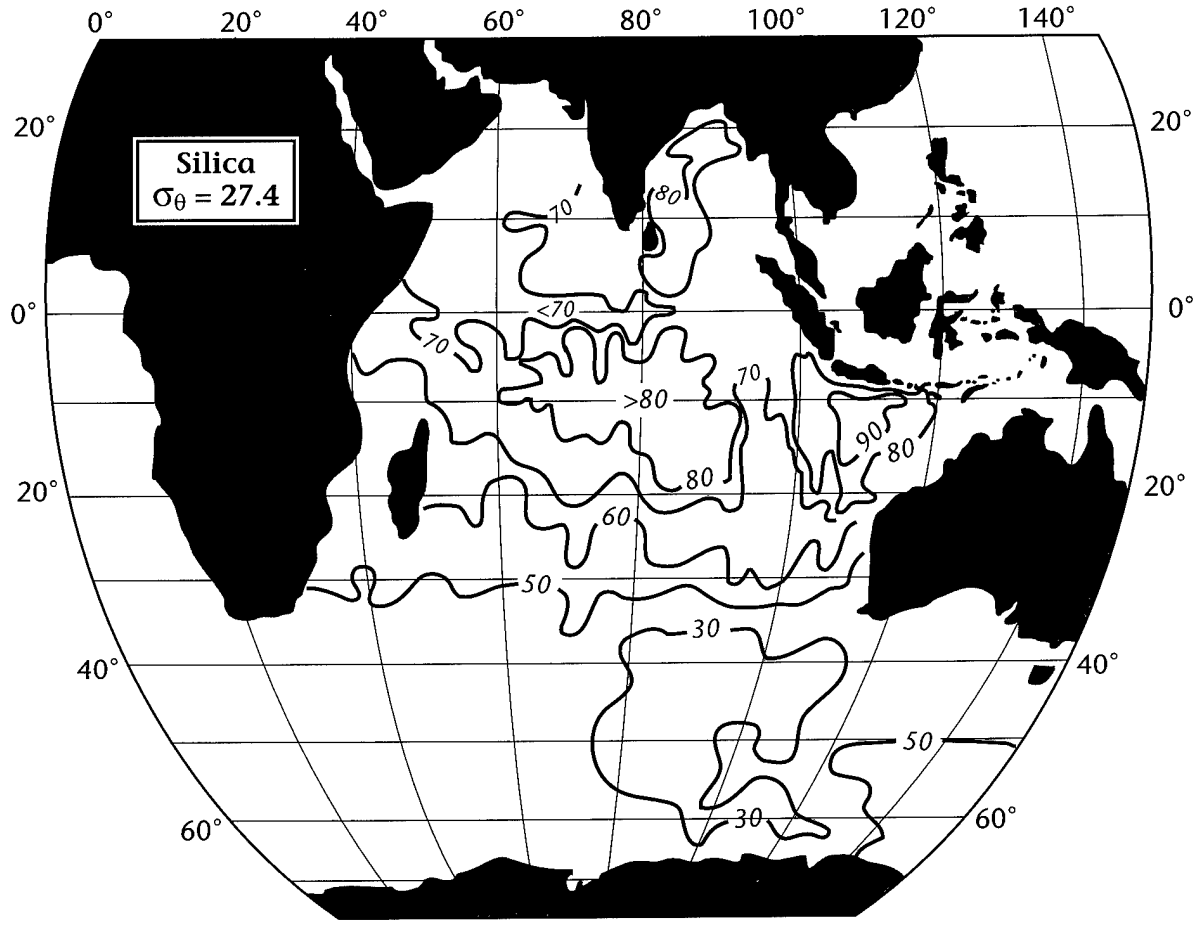

Figure II-124: A simplified map of silica on $\sigma_\theta = 27.4$, adapted from the Indian Ocean Atlas (Wyrtki, 1971).

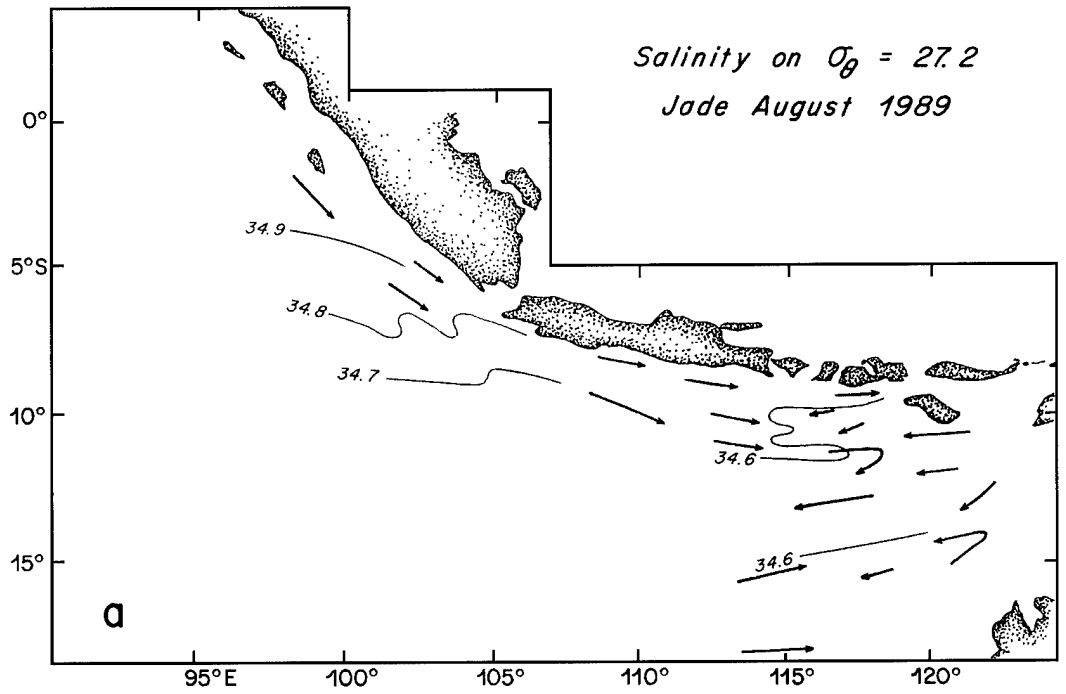

Figure II-125: Maps of (a) salinity and (b) oxygen on $\sigma_\theta = 27.20$, adapted from Fieux *et al.* (1994, their figure 9).

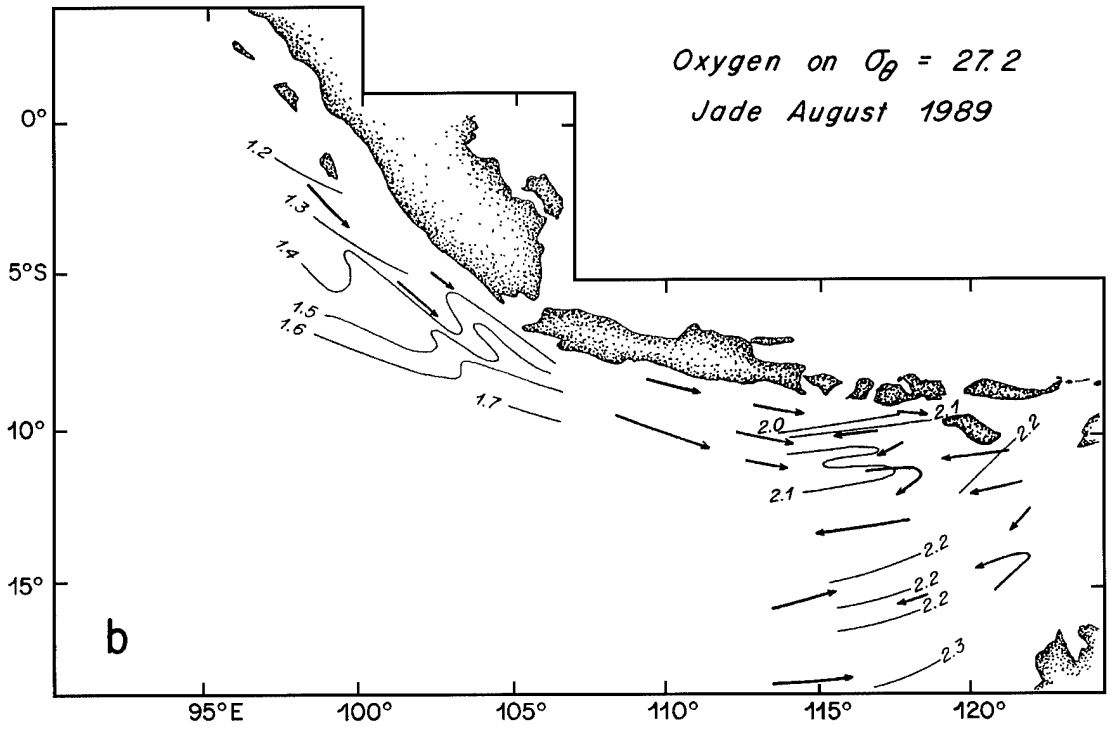

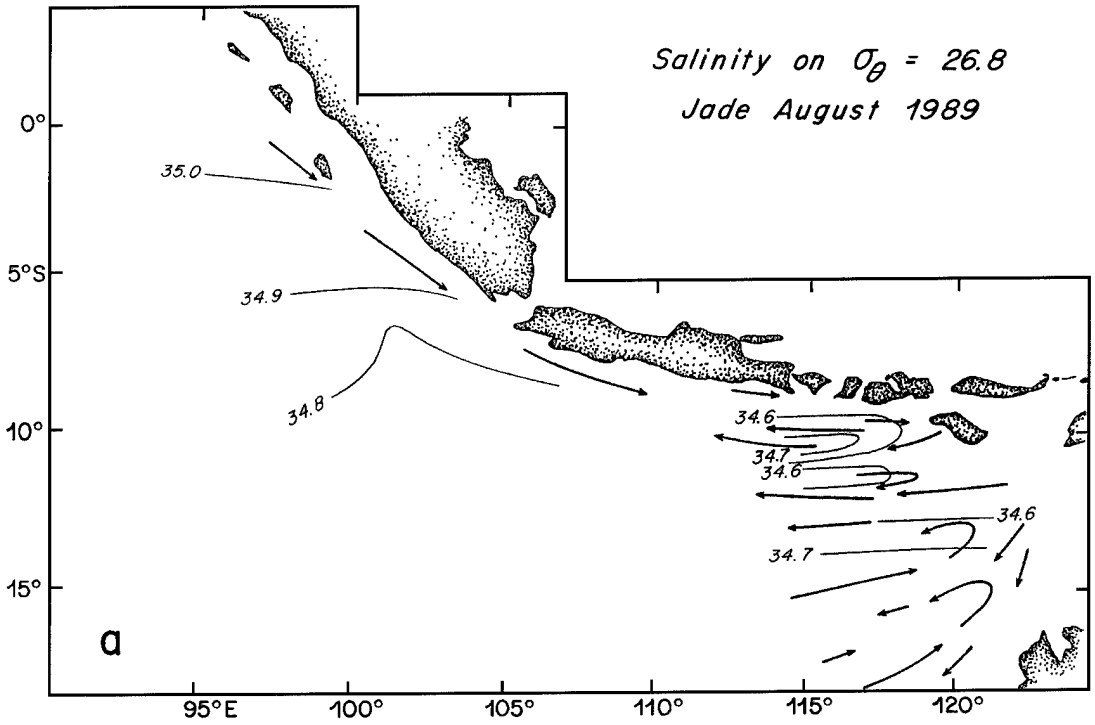

Figure II-126: Maps of (a) salinity and (b) oxygen on $\sigma_\theta = 26.80$, adapted from Fieux *et al.* (1994, their figure 10).

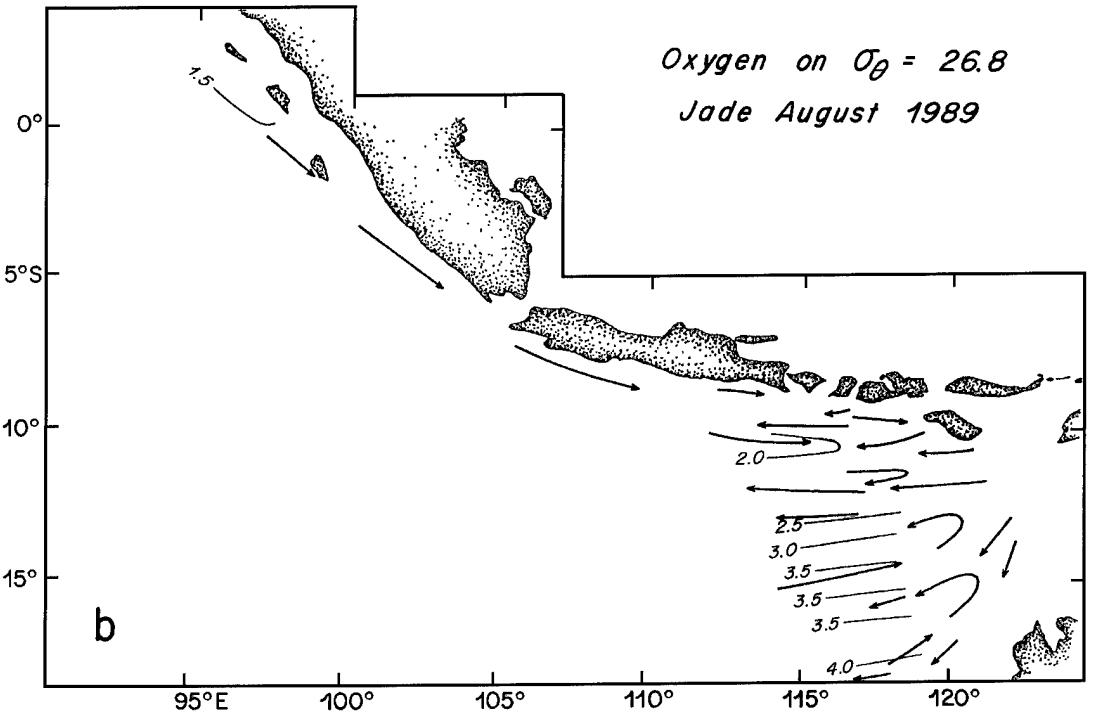

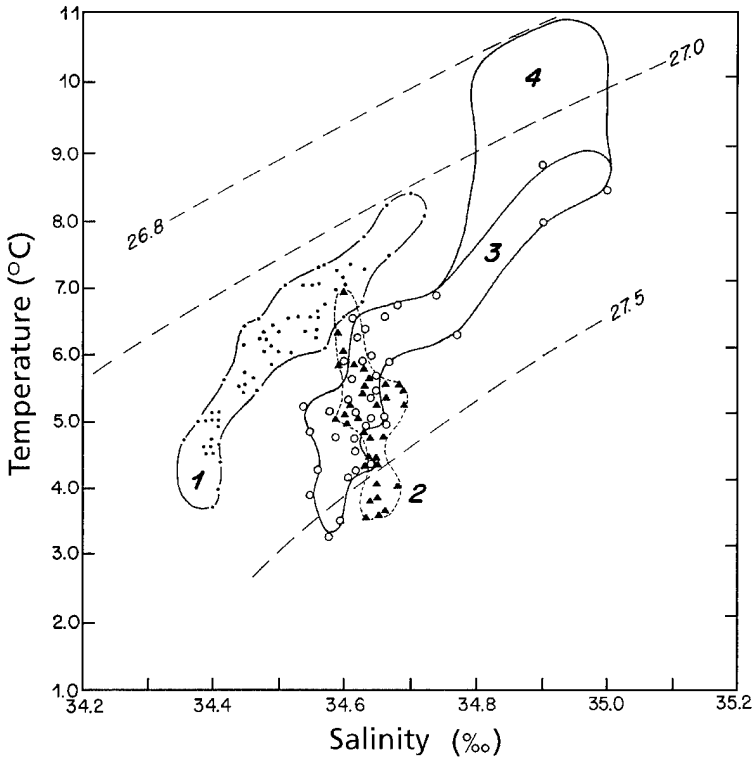

Figure II-127: A modification as described in the text of Rochford's (1961) *TS* plot, previously shown in Figure II-118. Relative to Figure II-118, a new area (numbered 4 in Figure II-127) has been added, extending the definition of NIIW.

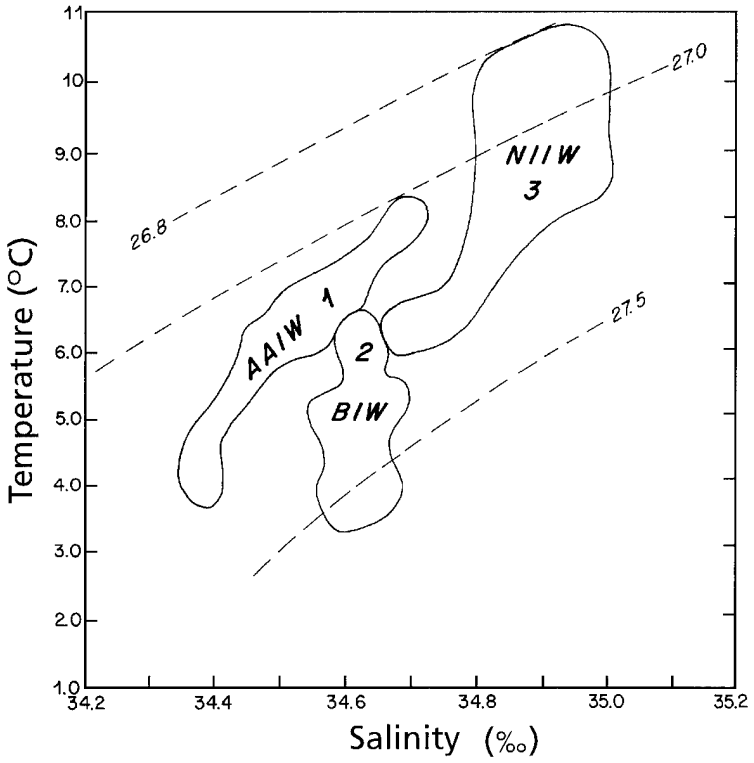

Figure II-128: A modification of the *T/S* plot in Figure II-127. Relative to Figure II-127, the low salinity end of NIIW has been incorporated into BIW (2), and the "new" or resulting area in *TS* space for NIIW has been labeled by the number 3.

up into $27.2 \leq \sigma_\theta \leq 26.8$ (not shown by Rochford) as indicated in Figures II-125 and 126 by Fieux *et al.* (1994), in an eastern boundary current along the coast of Sumatra and Java. It makes sense that this is the primary route of injection of NIIW, derived in *T,S* properties to a large extent from Red Sea Water, into the South Indian Ocean. Fieux *et al.* (1994) note that, near the Java and Sumatra coasts, their data in the 300–800 m depth range ($26.7 \leq \sigma_\theta \leq 27.25$) shows a water mass with comparatively high salinity and low oxygen that cannot come from the Indonesian Seas. They call this water mass North Indian Ocean Water, NIW, but I prefer NIIW as indicated above. I feel that it is crucial that Fieux *et al.* (1994) point out that NIIW extends up to $\sigma_\theta = 26.8$, as discussed in the next paragraph.

Having reviewed Rochford's (1961, 1963, 1966) results, in conjunction with other observations, especially Fieux *et al.* (1994), but also including my understanding of some of Rochford's own data, I would like to propose a re-configuration and re-interpretation of the *T/S* information relevant to NIIW. I first take Rochford's (1963) *T/S* plot in Figure II-118 and add to it an extension of the *T/S* space for NIIW to include $26.8 \leq \sigma_\theta \leq 27.2$ as indicated in Figure 127 by the area encompassing the number 4, in addition to the three types of IW in Figure II-118. The area labeled 4 in Figure II-127 is basically defined by the salinities presented by Fieux *et al.* (1994) in the upper frame of Figures II-125 and 126, especially the latter. The temperature range to go with these salinities was kindly made available by Susan Wijffels (personal communication, 1996). So Figure II-127 extends the definition of NIIW to less dense σ_t or σ_θ horizons. I would also like to suggest a second modification to Rochford's *TS* summary in Figure II-118 (and to Figure II-127), this one primarily affecting BIW, but also to some extent NIIW, as indicated in Figure II-128. Here the very low salinities (below 34.7) that Rochford included with NIIW in Figure II-118 are assigned to BIW. So NIIW (area 3 in Figure II-118 and areas 3 + 4 in Figure II-127) is redefined in Figure II-128 to include only salinities ≥ 34.7, and the definition of BIW is extended a bit. In Figure II-128, NIIW is redefined to extend from $\sigma_t = 26.8$ to 27.3 (or so), as opposed to Rochford's (Figure II-118) inclusion of NIIW with low salinities from ~ 27.3 to 27.5(6) σ_t. In Figure II-128, BIW now also occupies these lower salinities that were previously identified with NIIW in Figure II-118. It is a pleasure to note that Sue Wijffels played a key role in helping me develop my ideas about Rochford's intermediate water picture, but of course she is not responsible for any errors in my interpretation, etc.

3e. The Large-Scale Meridional Cell in the Indian Ocean

The basis for determining the structure of the large-scale meridional cell in the Indian Ocean has progressed significantly in the past few years (Toole and Warren, 1993; Mantyla and Reid, 1995; S95; RT96). In particular, RT96 have produced an estimate of the properties and transports of this cell at 32°S in eight layers, with overall amplitude about half of that suggested by Toole and Warren (1993), and in line to some extent with estimates by Macdonald (1993) and S95. One guess at a transport section for the large-scale meridional cell in the Indian Ocean is shown in Figure II-129, with a second option depicted in II-130. In preparing Figures II-129 and 130, the RT96 layers (Table II-12) were used, with their transports in circles in the vicinity of the 32°S locater on these figures. The Subtropical Front (STF) or South Indian Ocean Current (Stramma, 1992) is located about 40°N. The SFZ (or SAF) and PFZ (or PF) are conventional abbreviations, and their relative locations on Figures II-129 and 130 vary quite a

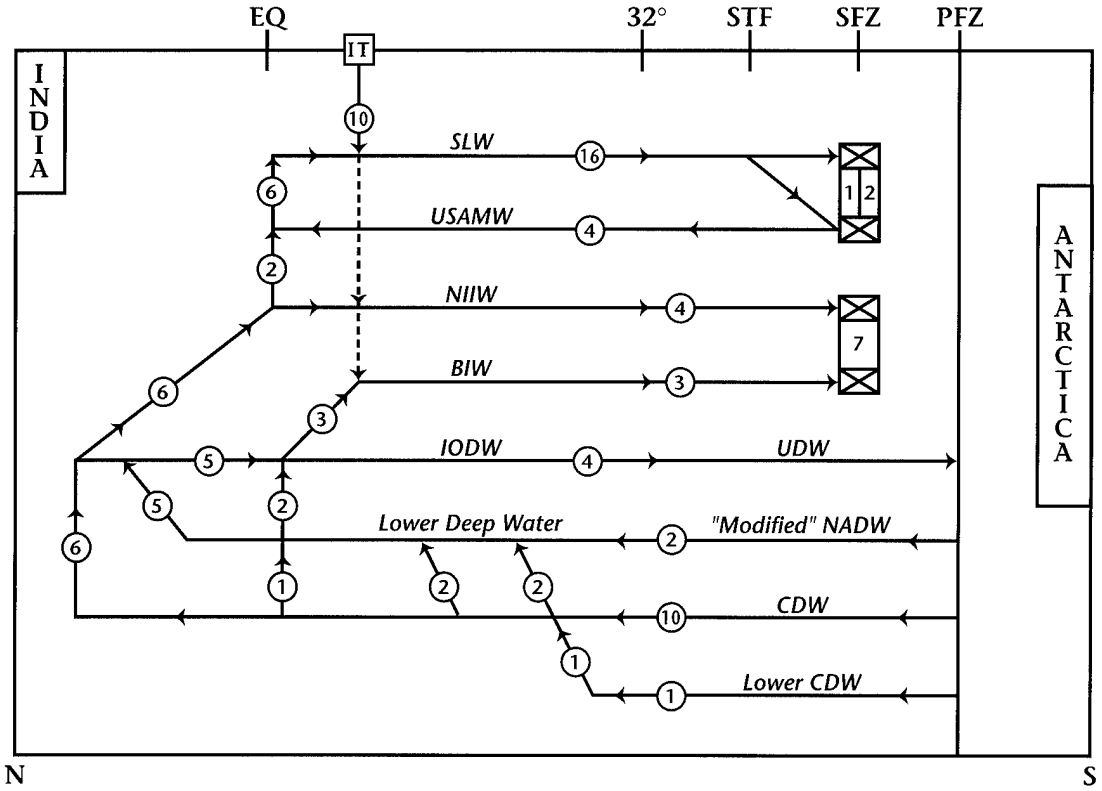

Figure II-129: An idealized meridional section of the large-scale thermohaline flow in the Indian Ocean, version 1.

bit south of the Indian Ocean (Figure II-80). In both figures, the layer called upper deep water by RT96 is also called Indian Ocean Deep Water (IODW), with the relative role played by IODW in the formation of BIW varied between Figures II-129 and II-130.

Figure II-129 represents a view of the meridional cell that uses only BIW and NIIW as the direct IW components of the cell, and minimizes the exchange of IW through the IT, which is indicated only by a dashed line as possibly having some influence on the Indian Ocean. Banda Intermediate Water is diapycnally modified IODW. Northwest Indian Intermediate Water derives from deep water in the North Indian Ocean, where the salinity of NIIW is strongly affected by RSW, not explicitly shown in Figure II-129, but an integral part of Figure II-130, and in one of the summary maps in Section 5 below. Two Sverdrups of water from the deep North Indian Ocean (as "required" by RT96) plus 4 Sv USAMW are converted to SLW at the equator and join 10 Sv SLW from the IT to complete the loop. In Figure II-129 (also II-130), most of the net

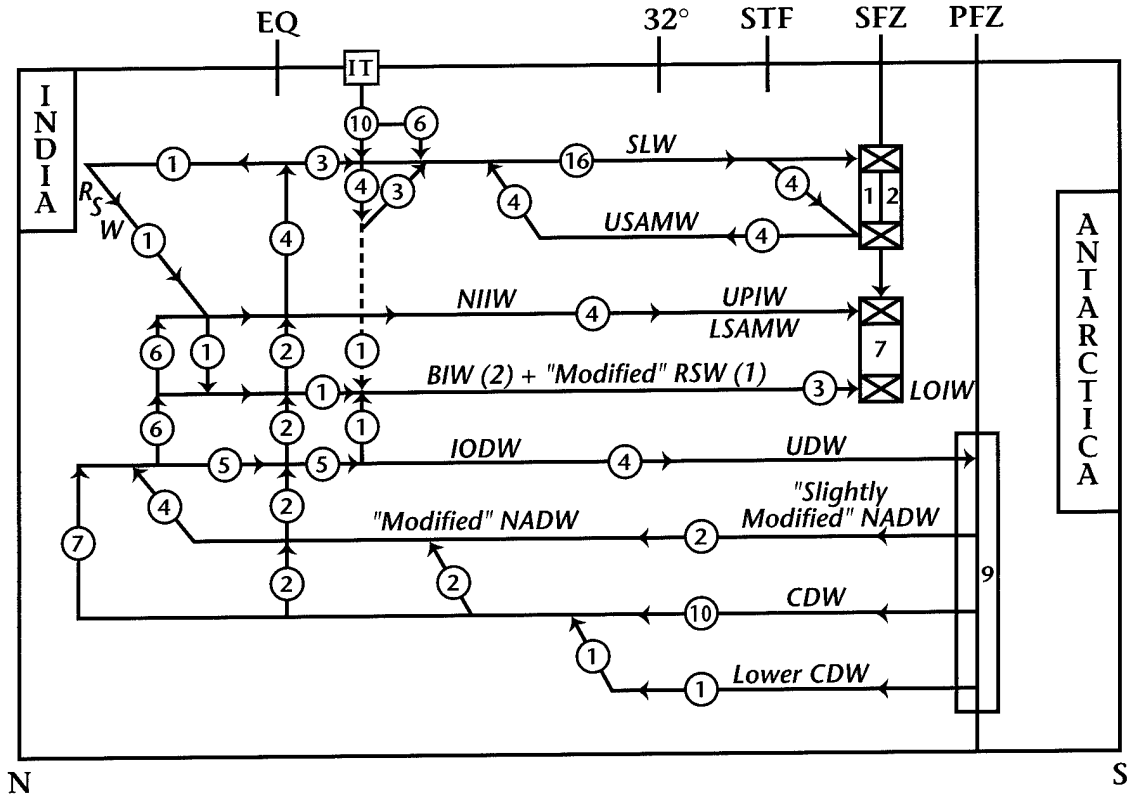

Figure II-130: A schematic meridional section of the large-scale thermohaline flow in the Indian Ocean, version 2.

bottom/deep circumpolar water entering the Indian from the ACCS across 32°S is eventually converted to IODW in the North Indian Ocean (Barton and Hill, 1989; Edmond *et al.*, 1979; Johnson *et al.*, 1991a, b; Mantyla and Reid, 1983, 1995; Park *et al.*, 1993; Wyrtki, 1971). This IODW (which seems similar to the North Indian Deep Water discussed by Park *et al.*, 1993) either returns south to the ACCS (4 Sv) or is upwelled to IW (7 Sv) or SLW (2 Sv) in the northern or low-latitude Indian Ocean. Figure II-129 is about the simplest view of the meridional cell structure that I can envision.

In Figure II-130, the lowest layer structures are only slightly changed from Figure II-129. But the IW, IT, and upper layer configurations are much different, coupled to the individual cell #2 for the Pacific Ocean shown in Figure II-69. The North Indian Ocean part of the meridional cell above IODW is the source of 4 Sv NIIW. Two Sverdrups of deep water and 4 Sv of IW are upwelled at the equator. Upper SAMW (4 Sv) in the South Indian Ocean is converted to SLW in the tropics, as is the 3 Sv of USAMW that entered the Indian Ocean through the IT. One Sverdrup from the North Indian Ocean enters the ACS in the western Indian Ocean as RSW. In Figure II-130, 2 Sv of BIW is shown being formed from 1 Sv IODW from the North Indian Ocean (modified upward) along with 1 Sv UPIW from the IT, with some implied recirculation in the IT. The remaining 6 Sv of SLW entering the Indian Ocean through the IT exits 32°S in the Agulhas Current.

3f. Incredibly Brief Remarks on the Upper-Layer North and Low-Latitude Indian Ocean

In addition to being interesting in its own light, this area is a likely location for various elements of the upward limb of the large-scale meridional cell in the Indian Ocean, as discussed in previous sections of this report volume. The upward limb appears to be dominated (RT96; S95) by a transfer of abyssal water to upper deep water and intermediate water, topics also discussed in Sections 3d, 3e, and 3f. One might also wonder if deep equatorial jets (Luyten and Swallow, 1976; Luyten *et al.*, 1980; Eriksen, 1980, 1982; Ponte and Luyten, 1990) are somehow involved in this upward conversion process.

A schematic of the circulation in the western segment of this regime is indicated in Figure II-131, adapted from Morales *et al.* (1996); see also Figures II-1, II-3, and II-4.

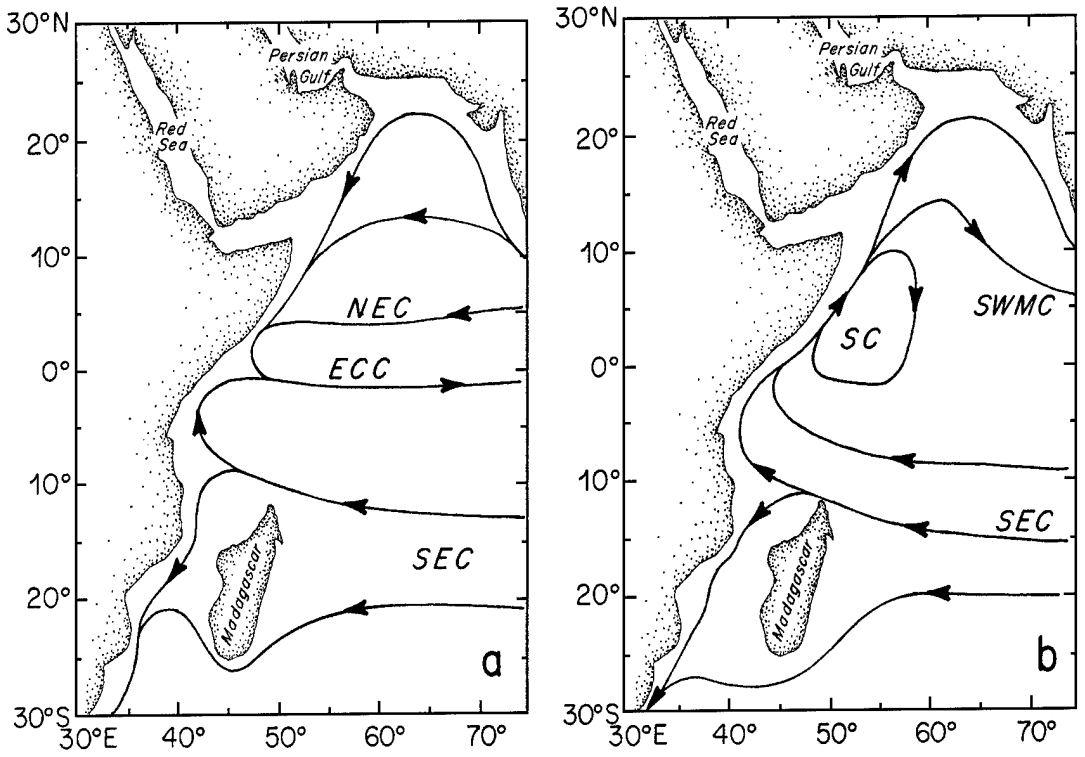

Figure II-131: A schematic of the circulation in the western North and low-latitude Indian Ocean, adapted from Morales *et al.* (1996): (a) NE Monsoon, and (b) SW Monsoon. SEC denotes South Equatorial Current; ECC, Equatorial Countercurrent; NEC, North Equatorial Current; SC, Somali Current; SWMC, Southwest Monsoon Current.

The monsoonal current regimes (for an early overview, see Wyrtki, 1973) in this area have recently been studied extensively by, for example, Hastenrath and Greischar (1991). The Indian Ocean Atlas (Wyrtki, 1971) is clearly an important source of data for this area. Other articles that could be examined to start getting familiar with this region include those of Bruce, 1979; Cane and Sarachik, 1983; Fieux and Levy, 1983; Hurlburt and Thompson, 1976; Kindle and Thompson, 1989; Knox and Anderson, 1985; Quadfasel and Schott, 1982; Rochford, 1964; Schott, 1983; Schott *et al.*, 1988; Sharma, 1972; and Stramma *et al.*, 1996.

3g. The Mesoscale Eddy Field in the Agulhas Retroflection, and Globally

The kinematics of ring formation in the retroflection are shown in Figure II-132. The fate of pinched-off rings from the Agulhas Retroflection in the South Atlantic has been described by Duncombe Rae (1991), Duncombe Rae *et al.* (1996), and Van Ballegooyen *et al.* (1994). A schematic of the structure of the ACS may be found in Figure II-133. Schmitz (1996) has described the results from a moored array deployed in the Agulhas Retroflection (Figure II-134). Vertical distributions of eddy kinetic energy [denoted $K_E(z)$] for all moorings (Figure II-135) tend to separate out into two groups (with some overlap), the more energetic set encompassing moorings 834, 835, 837 and 838. The ACS moorings with the most energetic upper ocean eddy field (835 and 838) are located in the western segment of the retroflection (Lutjeharms and Van Ballegooyen, 1988) where rings typically pinch off (*e.g.*, Duncombe Rae, 1991; Duncombe Rae *et al.*, 1996). However, 835 is noticeably less energetic than 838 at depths greater than 1 km. Mooring 834 is comparable to 838 $K_E(z)$ at common depths, and 837 is like 838 at two depths, but weaker near 4000 m. 834 and 837 are the two moorings in addition to 835 and 838 that are deployed at the western segment of the retroflection where rings typically pinch off. So the more energetic $K_E(z)$'s in Figure II-135 are all in the western part of the retroflection area.

The $K_E(z)$ distribution for the most energetic Agulhas site (838) is almost identical to the $K_E(z)$ associated with the Gulf Stream System (GSS) at 55°W (Figure II-136). In Figure II-136, $K_E(z)$ from ACS moorings 835 and 838 are compared with a summary of the available data from 55°W in the GSS east of the New England Seamounts, with mooring 771 (~ 68°W) in the GSS west of the New England Seamounts, mooring 780

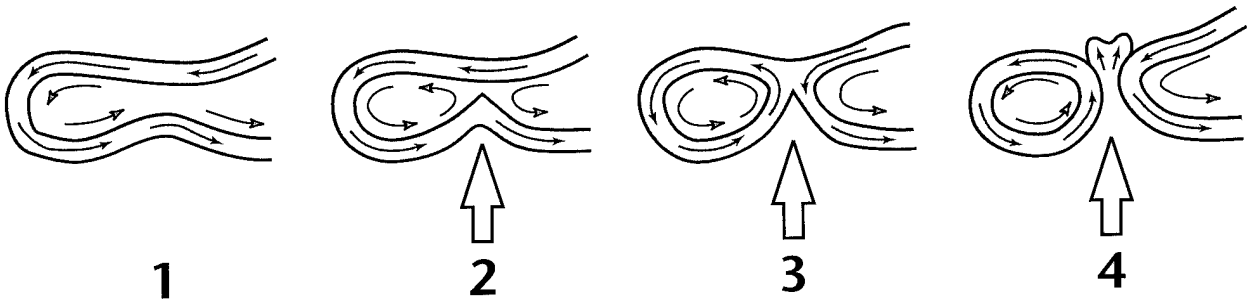

Figure II-132: A conceptual image of the initiation (2), development (3), and separation (4) of an Agulhas ring from the Agulhas Retroflection (1), with the accompanying inflow of subantarctic water. Taken from Duncombe Rae (1991, his figure 5).

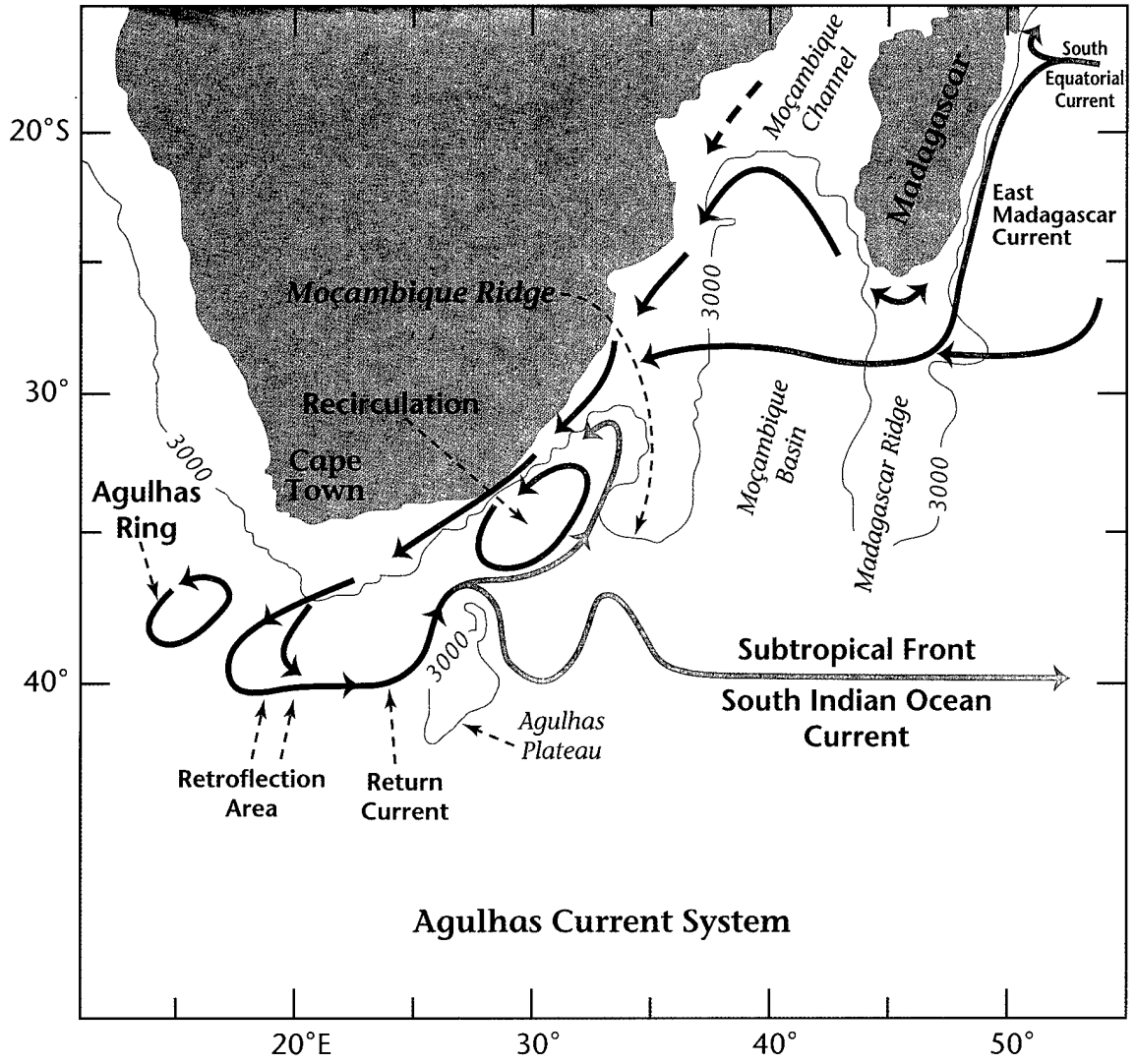

Figure II-133: A schematic diagram and nomenclature for the diverse elements of the Agulhas Current System (ACS), taken from S96.

deployed near the New England Seamounts in the GSS, and mooring 724 from the Kuroshio Current System (KCS). These GSS and KCS data have been discussed previously, for example, by Schmitz and Holland (1986). Note, however, that whereas 835 and 838 have nearly the same energy in the upper 1000 m, 835 is notably (~ 50%) less energetic at depth. This is somewhat reminiscent of the comparison between GSS locations 771 and 55°W, or between 724 (KCS) and 55°W. In Figure II-136, these similarities and differences are highlighted by the difference between the open and

closed symbols. We could also, of course, find moorings near the KCS or GSS that would tend to be like those least energetic ACS moorings (836, 841, 842, 843), by choosing locations that experience fewer meander excursions or ring passages. The normalized frequency distributions (Figure II-137) for the most energetic Agulhas moorings, 835 and 838, are weakly depth-dependent and peaked at the mesoscale, fitting into a typical K_E vs frequency or period range plot for energetic oceanic areas (Figure II-138, adapted from Schmitz and Luyten, 1991).

The similarities between the eddy fields in the GSS and in the ACS may suggest an analogous mechanism of eddy generation (a mixed barotropic/baroclinic instability; see, for example, Schmitz *et al.*, 1983), in comparably structured mean flow regimes. Some version of this notion has been used to explain numerical model results in a variety of western boundary current regimes, including the ACS (Holland *et al.*, 1991; see also Boudra and Chassignet, 1988; Chassignet and Boudra, 1988; Chassignet *et al.*, 1990). If, at finite amplitude, the upper ocean eddy field at locations near the strong current regime is primarily determined by meander and ring passage (65–75%, say, ~ 50% at abyssal depths, *e.g.*, Hogg and Johns, 1995), then some integrated measure of the mean flow plus the proximity of the site in question to a strong current (or relative frequency of meander/ring passage) would be key parameters in estimating the resulting eddy signal. Agulhas Rings are known to be numerous and energetic, much as in the GSS (Duncombe Rae, 1991). Schmitz and Holland

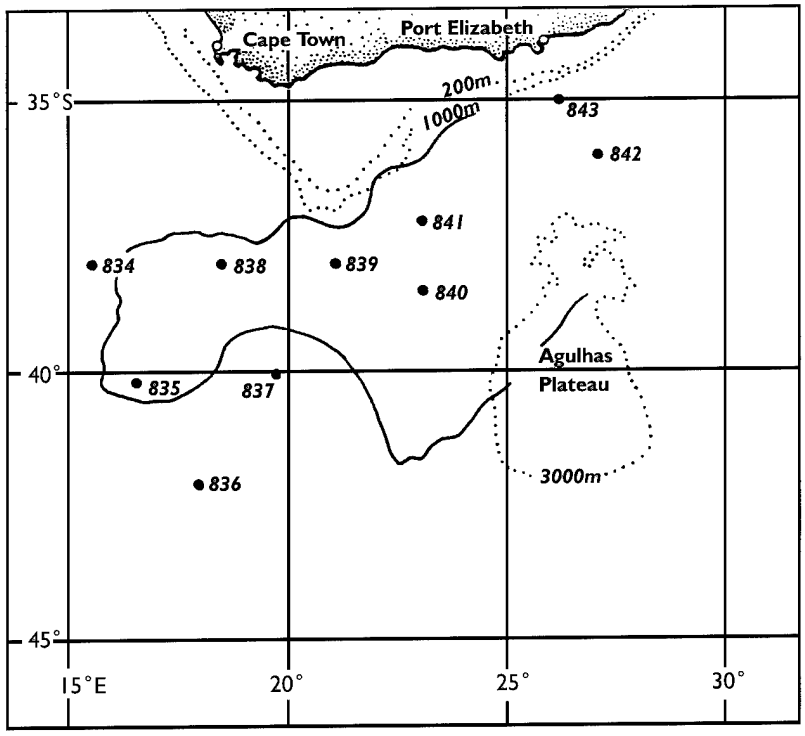

Figure II-134: Agulhas Current System mooring locations, with the path of the current at deployment time superimposed, taken from S96.

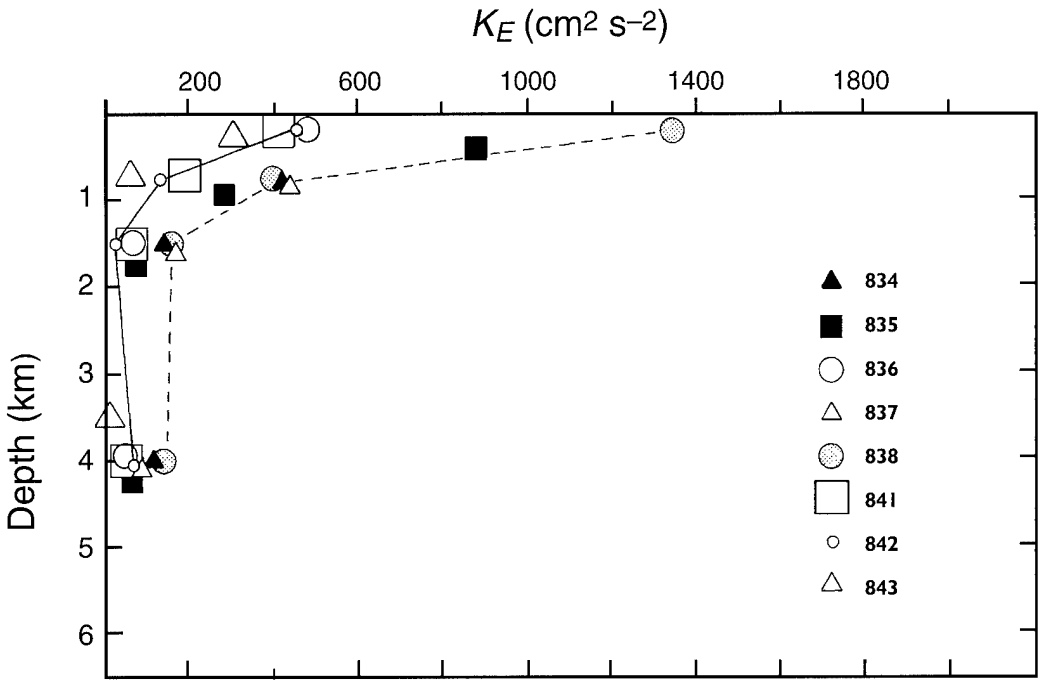

Figure II-135: A composite of the vertical distribution of K_E for the ACS moorings, adapted from S96.

(1986) and Schmitz and Thompson (1993) have presented energy budget diagrams for various model results where the primary upper layer energy transfer is mean kinetic energy to K_E, with abyssal or deep K_E coming mostly from available potential energy. In the following, the integral current structures (transports) for the upper 1000 m or so will be intercompared with the overall strength of $K_E(z)$ distributions over the same depth or potential density intervals.

But in what way could the general circulation flow regimes in the ACS and GSS be alike? In both the ACS and GSS the mean flow in the boundary current includes both a contribution of 20–30 Sv from a wind-driven gyre on basin scale and a strong recirculation regime on sub-basin scale (~ 500 km) [*i.e.*, Figure II-133 for the ACS; Hogg and Johns (1995) for the GSS, see also RT96 and Stramma and Lutjeharms (1996)]. Various key features (*i.e.*, strong boundary current, retroflection area, recirculation and return currents) were assimilated into the numerical experiments performed by Holland *et al.* (1991) by specifying dynamic heights calculated from the Southern Ocean Atlas by Gordon (1982).

There is also evidence that both mean flow regimes contain upper layer thermohaline renewal components, even at similar depths or density horizons (S95). These are a near-surface contribution from the Indonesian Throughflow (Fieux *et al.*, 1994) in the case of the Agulhas and a thin warm upper layer flow across the equator into the Caribbean and thence the Gulf Stream System [Schmitz and Richardson (1991), where an ~ 5 Sv flow of intermediate water was also found]. This structure for the thermohaline replacement flow in the low-latitude Atlantic Ocean has recently been independently determined by Johns *et al.* (1997). A strong flow of intermediate water in the ACS (S95) has been known for some time (Harris, 1972; Visser and Van Niekerk, 1965), and is also a feature of recent investigations (Macdonald, 1993; RT96; Toole and Warren, 1993).

To pursue these ideas further, the transports [TR(σ); σ denotes a generalized density parameter] as a function of σ_t (Agulhas) or σ_θ (GSS) range were estimated

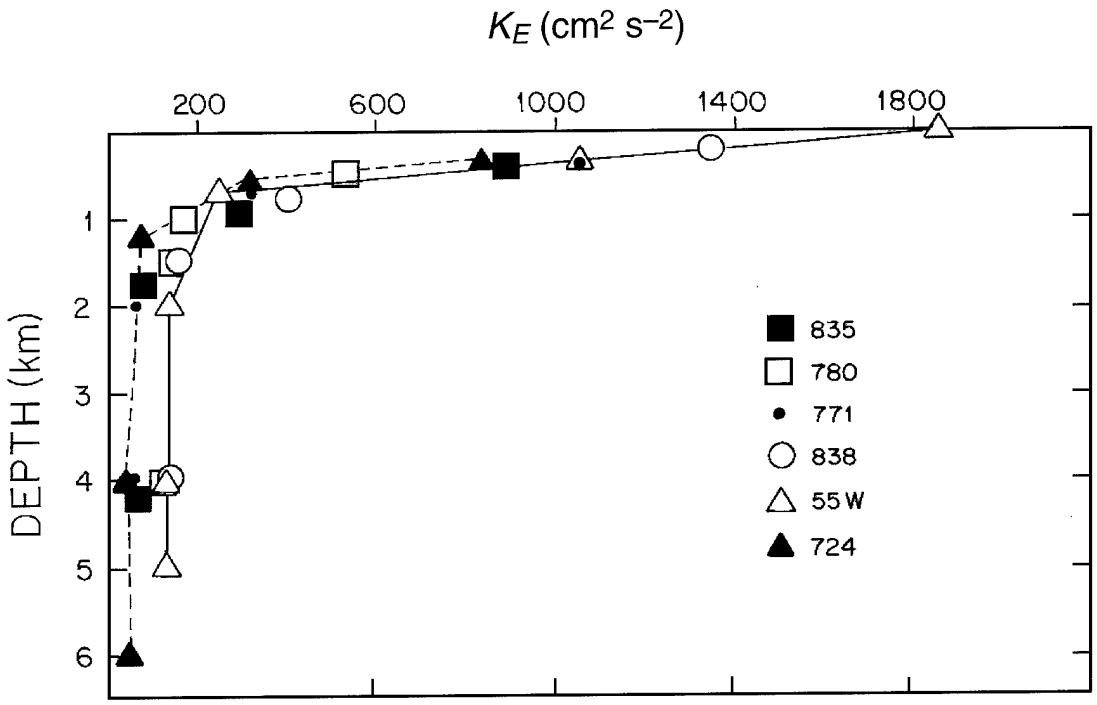

Figure II-136: A comparison of $K_E(z)$ for a variety of comparatively energetic locations in three western boundary current systems of the World's Oceans, from S96. Moorings 835 and 838 are from the ACS, 771 and 780 from the GSS, and 724 from the KCS. 55°W is an average over that longitude for the GSS, and includes surface drifter, neutrally-buoyant float, and current meter mooring data.

respectively by integrating the Harris (1972) data (for details see S96) for the former and from the results of Hall and Fofonoff (1993, their table 3a) for the latter. The distributions of transport [TR(σ)] with σ_θ (or σ_t) interval for the ACS and GSS in Table II-15 are remarkably similar. The specific layers selected for Table II-15 were determined by those chosen by Hall and Fofonoff (1993). So to the extent that the upper layer $K_E(z)$ observed in the Agulhas Retroflection Area is due to the passage of meanders (see, for the GSS: Halkin and Rossby, 1985; Hogg, 1994; Kelly, 1991) and pinched-off rings (Duncombe Rae, 1991; Duncombe Rae *et al.*, 1996; Olson, 1991), perhaps Table II-15 suggests why these $K_E(z)$, or $K_E(\sigma)$, are so similar (see also Holland *et al.*, 1991, p. 416). Recirculations are related to eddy rectification (Hogg and Johns, 1995; Holland, 1978). So all that remains to be similar are the "upper layer" thermohaline components of the ACS vs the GSS.

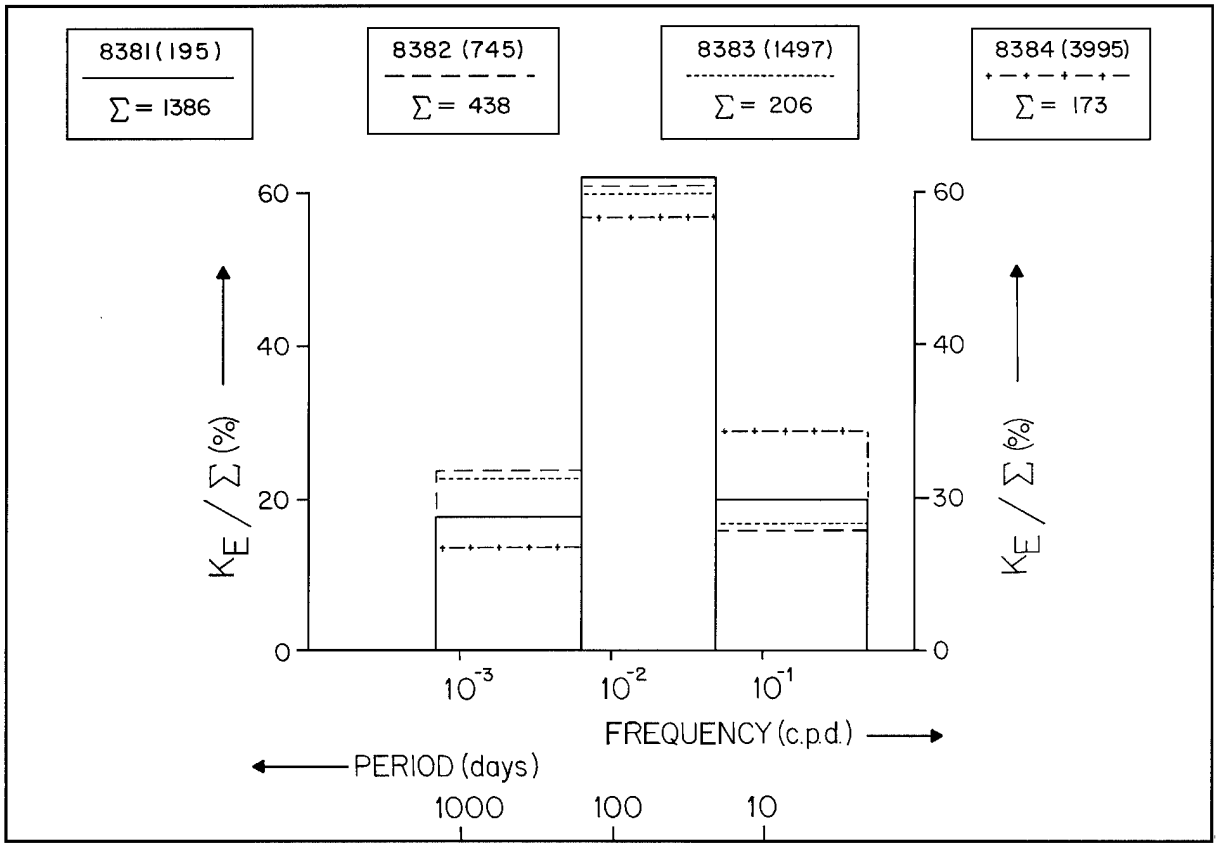

Figure II-137: Normalized frequency distributions for the most energetic ACS mooring, adapted from S96.

How could TR(σ) be similar in the western boundary currents at ~ 30°S in the southern Indian Ocean and 68°W in the North Atlantic? As demonstrated by Toole and Warren (1993), RT96, and Stramma and Lutjeharms (1996), the wind-driven and recirculating components of the upper ocean subtropical circulation of the South Indian Ocean are of comparable magnitude to those in the North Atlantic (see Hogg and Johns, 1995, or Schmitz and McCartney, 1993). So all that is needed in addition is to consider the thermohaline-related upper layer replacement flow components of the GSS vs the ACS. As discussed above, the types of interbasin transport contribution in the upper ~ 1000 m that make up the ACS and GSS are similar. The GSS data in Table II-15 are from 68°W, in the Gulf Stream east of Cape Hatteras but west of the New England Seamounts, whereas the ACS results are from offshore of Durban (~ 30°S). For the North Atlantic, sections off Cape Hatteras or Cape Fear might be more analogous to those off Durban. But Hall and Fofonoff (1993, their figure 6) demonstrate that the upper level velocity (transport) structure is essentially identical near Hatteras [at

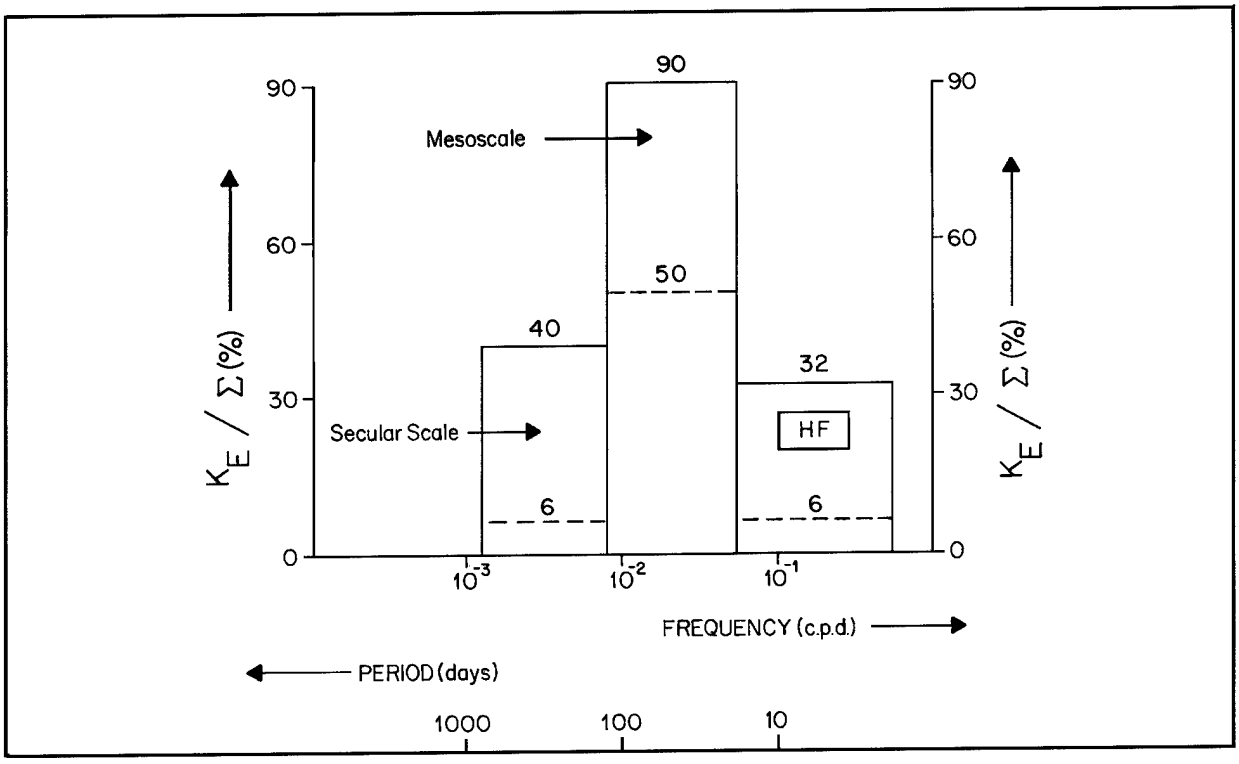

Figure II-138: A standard spectral range plot for the eddy field in a variety of strong-current regimes, taken from S96.

Table II-15: Transports (Sverdrups) for the indicated currents in density parameter (σ) intervals, taken from Schmitz (1996)

σ Range	Gulf Stream (68°W)	Agulhas (Durban)	Agulhas (32°S)	Kuroshio (152°E)	North Brazil Current (~ 4°N)
< 26.65	38	36	37	30	32
26.5 → 26.75	12	11	15	5	12
→ 27.00	12	11	13	5	5
→ 27.4	12	14	16	9	3
Σ	74	72	81	49	52

73°W, see Halkin and Rossby (1985) and Leaman *et al.* (1989)] to their results at 68°W. There is a thermohaline component involving intermediate water transfer from the South Pacific to the KCS (Reid, 1965; Reid and Mantyla, 1978; Tsuchiya, 1991), but seemingly with a transport that is noticeably less than in the GSS or ACS. Net upper layer flow from the South Pacific to the North Pacific mostly exits through the Indonesian Passages (Bray *et al.*, 1996; Fine *et al.*, 1994; Godfrey, 1996; Hautala *et al.*, 1996; Shriver and Hurlburt, 1996) rather than joining the KCS.

A crude breakdown of TR(σ) for the KCS near 152°E (Hall, 1989) is also listed in Table II-15. This distribution is uniformly lower by about 5 Sv for each of the four σ classes shown. If we plot $K_E(z)$ for the KCS from Figure II-136, but with a barotropic contribution of 100 $cm^2\ s^{-2}$ added, against $K_E(z)$ for the GSS at 55°W and 838 for the ACS, the correspondence is remarkable (Figure II-19). If we imagine that K_E could be roughly proportional to a transport or "average speed" squared, and that the missing 5 Sv of intermediate water is distributed over about 500 m in depth and 10^2 km in width, then the resulting typical speed is 10 cm s^{-1} or 10^2 $cm^2\ s^{-2}$ for the square, possibly an accidentally favorable comparison, but the needed order of magnitude. On the other hand, the preceding argument, which only involves the influence of a barotropic instability without regard to the influence of baroclinic energy transformations, does not

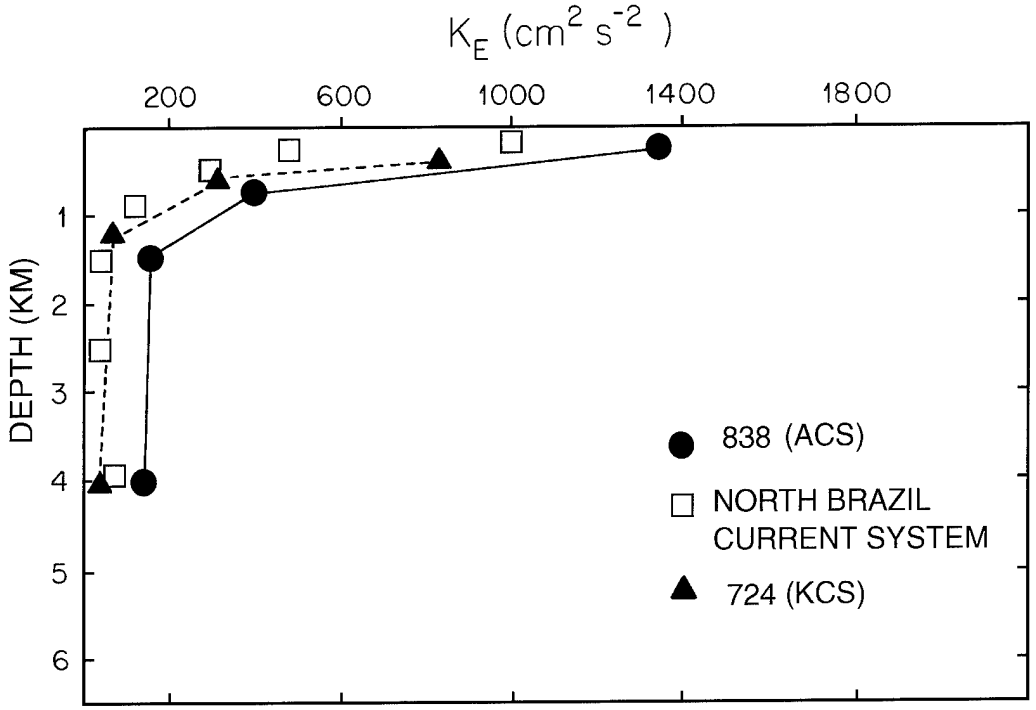

Figure II-139: The vertical distribution of K_E for the ACS, as compared with the KCS and NBCS, taken from S96.

adequately account for the differences in deep K_E. Figure II-139 includes recent $K_E(z)$ data (Johns *et al.*, 1990) from the vicinity of the North Brazil Current System (NBCS), another boundary current dominated by retroflection. This location is both comparatively distant horizontally from the NBCS retroflection area and experiencing (Flagg *et al.*, 1986) a TR(σ) more like that found at mooring 724 (KCS) than mooring 838 (ACS). Near the NBCS (Figure II-139), $K_E(z)$ is more like the KCS than the ACS. Similar transport and K_E data from the Brazil and/or East Australian Current Systems have not yet been located.

Numerical experiments for the low-latitude Indian Ocean have been presented by Kindle and Thompson (1989). They find strong responses at ~ 75 days and ~ 50 days, and relate these model results to data in a positive way. The longer period variability is the result of an instability mechanism and the shorter period fluctuations to wind-forced waves. It could be worth some effort to determine if equatorial jets, especially deep ones, might lead to water mass transformation (diapycnal mixing) somehow.

4. The Southern Ocean(s)

I use the term "Southern Ocean(s)" to include the Antarctic Circumpolar Current System (ACCS) along with its interactive circulation with all of the southern hemispheric ocean basins (South Atlantic, South Indian, South Pacific). A noteworthy pioneer relative to the physical oceanography of the Southern Ocean was Sir George Deacon, and his modern summary article on the topic (Deacon, 1963) and its references are a starting point for getting spun-up on this area. A recent map of the various fronts in the Southern Oceans (Belkin and Gordon, 1996) is adapted for use here as a generalized sketch (Figure II-140). For my purposes, the Polar Front (PF) and Polar Frontal Zone (PFZ) are primarily where CDW, and especially LCDW, reside and where the bottom layer exchanges with other ocean basins originate. Similarly the SAF (Subantarctic Front) and the SFZ are here taken to be where IW and SAMW are located and transferred back and forth. But it might turn out to be of significance to the global interbasin flow picture that the various least dense products associated with the deep/bottom meridional cells, such as UNADW, upper IODW and upper NPDW, reside for a time in the SFZ "under" IW and may be "there converted" to LOIW. Since I just reviewed the circulation, including exchanges with the ACCS for the (South) Pacific and (South) Indian Oceans, Section 4 will include only a cursory summary of the circulation of the South Atlantic Ocean, briefly emphasizing at first its interaction with the North Atlantic, followed by a short account of its interactions with the ACCS.

For present purposes the South Atlantic and ACCS circulations are rather well documented (*e.g.*, Clement and Gordon, 1995; Deacon, 1933, 1937, 1963; Garzoli and Gordon, 1996; Gordon, 1971, 1975; Hogg *et al.*, 1996; Mantyla and Reid, 1983; Nowlin *et al.*, 1977, 1981; Orsi *et al.*, 1993, 1995; Park *et al.*, 1991; Peterson and Stramma, 1991; Peterson and Whitworth, 1989; Piola and Georgi, 1982; Reid, 1989, 1994; Rintoul, 1988, 1991; Saunders and King, 1995; Siedler *et al.*, 1996; Talley, 1996; Whitworth and Nowlin, 1987; Whitworth *et al.*, 1982), so Section 4 will be brief. Again, my main concern is with interbasin exchanges, so that's the category of information presented. In Volume I of this report, I updated (Figure I-12 in Volume I, II-11 here) the northward transport of bottom water into the South Atlantic in a new meridional section for the large-scale thermohaline cell throughout the Atlantic Ocean (discussed a bit more in Section 5 below).

Section 4a contains two figure adaptations from results published by Tsuchiya *et al.* (1994) along 25°W (nominal), as recent additional background relative to how the salinity (and temperature) of UPIW in the SFZ approaching the BCS might be determined. In this context I also introduce some older background for the "Drake" UPIW Dilemma in my brief discussion (Section 4b) of the ACCS [basically, I include two of the sections used by Rintoul (1988, 1991), that is, at Drake Passage and at the Greenwich Meridian (actually at 1°E in the north)]. Stramma and Peterson (1990), in their examination of the transport of the South Atlantic Current, display some very pertinent information that I also use in discussing the UPIW transport and water mass properties at latitudes of approximately 35–40°N along 1°E. Then, in Section 5, I further discuss a "new" idea that could partially resolve the "Drake" UPIW isopycnal modification issue, perhaps even the diapycnal transformation picture as well.

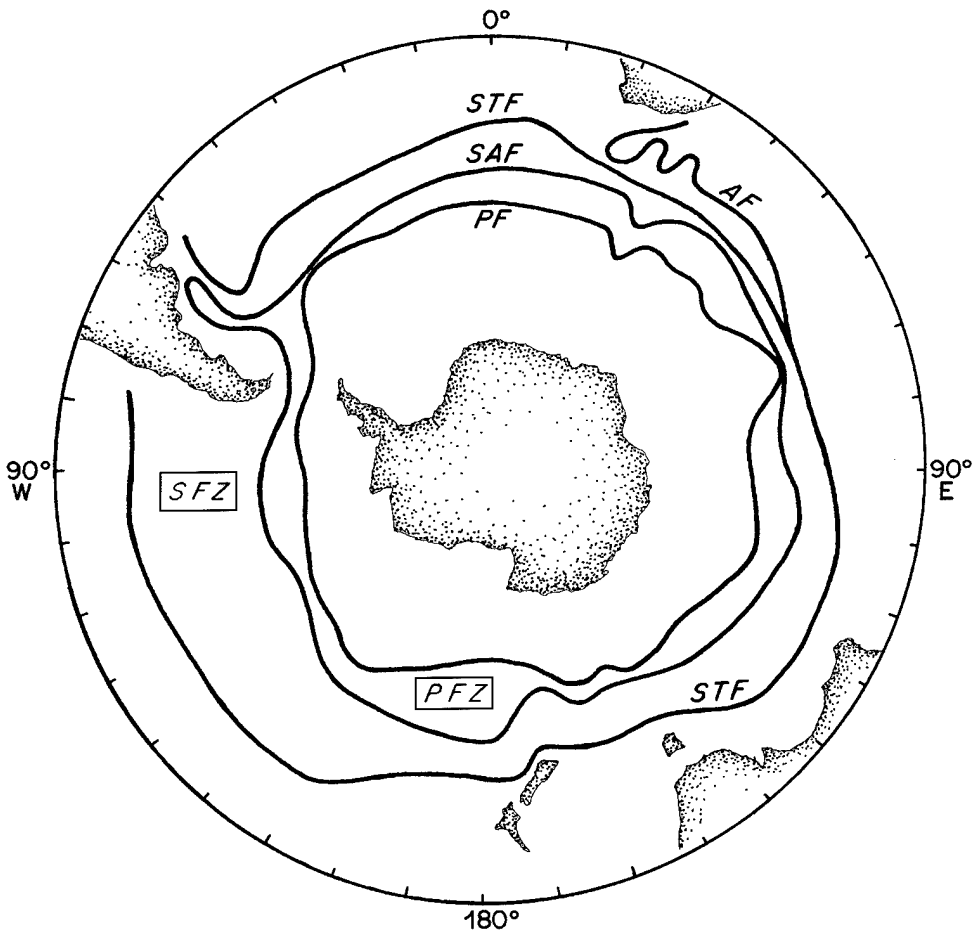

Figure II-140: Location of various frontal features in the Southern Ocean: AF Agulhas Front, STF Subtropical Front, SAF Subantarctic Front, PF Polar Front, SFZ and PFZ Subantarctic and Polar Frontal Zones, respectively; adapted from Belkin and Gordon (1996).

4a. A Few Comments on the South Atlantic Ocean

The large-scale circulation of the Atlanic Ocean in general has been described by Reid (1989, 1994). There is a very nice recent summary of water mass distribution and path in (primarily) the South Atlantic by Siedler *et al.* (1996). A surface current chart for the Atlantic Ocean is presented as Figure II-141 (kindly supplied by Arthur Mariano, personal communication, similar to Figures II-2 through II-7) for orientation purposes. A schematic of the upper level circulation of the South Atlantic according to Peterson and Stramma (1991) is shown in Figure II-142. From the ACCS and South Atlantic interbasin exchange perspective, R8891 is crucial, as are many of Gordon's publications (*i.e.*, Gordon, 1986, 1991; Gordon *et al.*, 1992; Garzoli and Gordon, 1996); please also see Saunders and King (1995), S95, and Volume I of this report.

Selected sections of upper level σ_θ and salinity across the polar and subtropical western Atlantic, adapted from Tsuchiya *et al.* (1994), are contained in Figure II-143 (a, b). These data were taken on Cruise Hydros 3/4, R/V *Melville*, February–April, 1989 (Tsuchiya *et al.*, 1994; their figure 1). Although this section is nominally along 25°W, in the latitudes of prime interest here there is a diagonal change in orientation from north to south, from about 25°W to about 40°W. I will use these data to help resolve the dilemma relative to the large differences in salinity between UPIW at Drake Passage, R8891's entry section, and UPIW at 32°S, R8891's South Atlantic exit section. There are of course, in addition to the differences in *T,S* properties along isopycnal surfaces, diapycnal differences involving UPIW between Drake Passage and 32°S. These are also discussed (in Section 5) along with the isopycnal variations being concentrated on here, but are in some sense more difficult to explain. In Rintoul's (1988, 1991) inverse calculation the average salinity for UPIW at Drake Passage was 34.12, 34.33 at the Greenwich Meridian (actually 1°E near the STC), and at 32°S was 34.49 (Rintoul, 1991; his table 2, Table II-16 here). One can see in Figure II-143 (a, b) salinities of 34.4–34.6 at 42–44°S in the SFZ, just north of the poleward limit of the subtropical gyre, in the UPIW σ_θ range 26.8–27.2. A plot containing this distribution is shown in Section 5, where these data will be used to argue that UPIW (LSAMW; $26.8 \leq \sigma_\theta \leq 27.2$) has salinities $\sim$ 34.5 by the 25°W section (nominal), probably as a result of mixing between the Falkland (or Malvinas) and Brazil Currents. The transport characteristics of the polar branch of the South Atlantic Subtropical Gyre (called the South Atlantic Current by Stramma and Peterson, 1990), along with the Benguela Current Transport

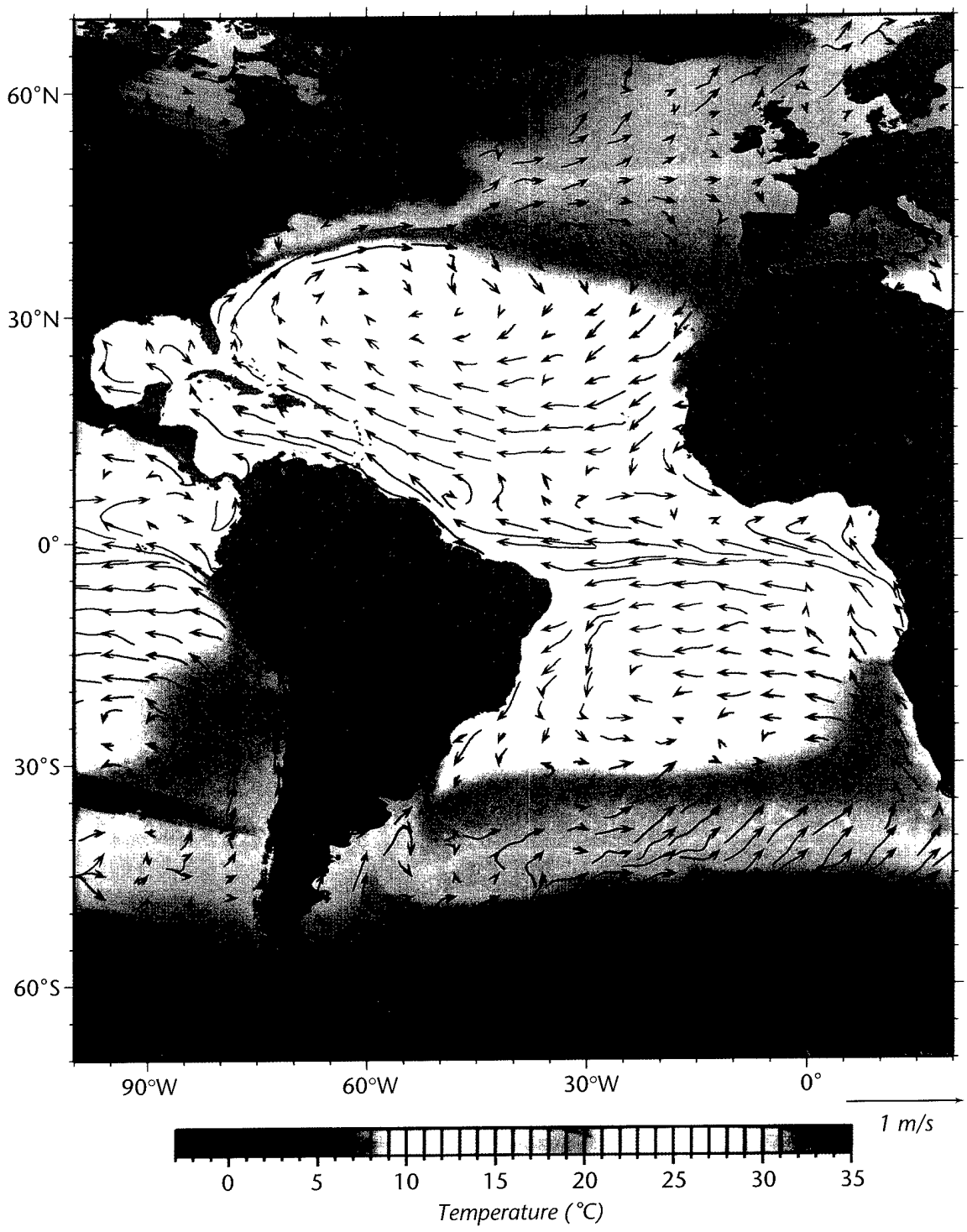

Figure II-141: Yearly-averaged surface current vectors for the Atlantic Ocean based on ship-drift observations, superimposed on SST contours.

(Stramma and Peterson, 1989; Clement and Gordon, 1995; Garzoli and Gordon, 1996), are reasonably well documented. Also, at this time, the "leakage" from the ACS to the BCS is much better determined (Garzoli and Gordon, 1996).

From the interbasin circulation point of view, Rintoul's (1988, 1991) results provide a crucial starting point relative to the South Atlantic Ocean. His layer choices, and the average temperature and salinity for these layers at the essential sections (for my interests) of his inverse model, are contained in Table II-16, adapted from Rintoul (1991, his table 2). A major concern with Rintoul's (1988, 1991) results, and a motivation for looking for a "large" flow around the tip of Africa into the South Atlantic, is to account for the *T/S* (Temperature/Salinity) properties of the intermediate and upper layer water flowing northward in the eastern South Atlantic at 32°S. This water tends

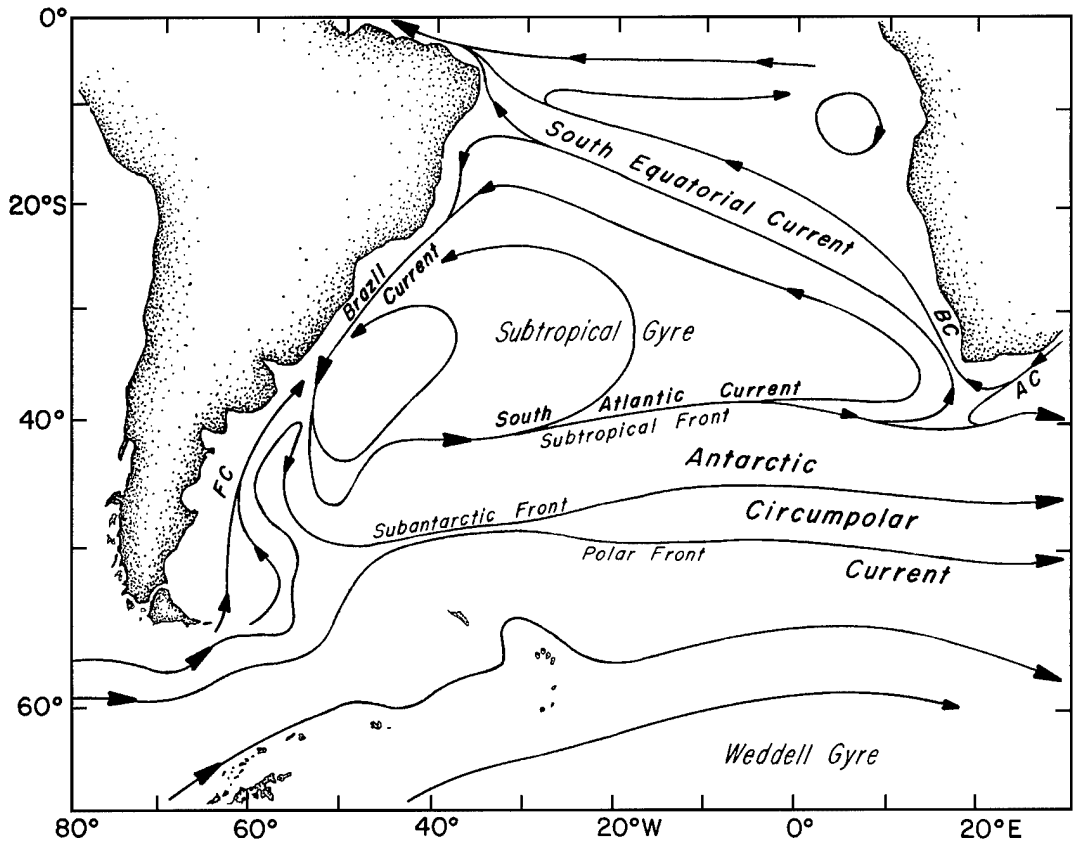

Figure II-142: The upper level circulation of the South Atlantic, adapted from Peterson and Stramma (1991). FC denotes Falkland Currrent, BC denotes Benguela Current, AC Agulhas Current.

to be significantly warmer and saltier than any component of the flow out of Drake Passage, and the explanation for this is still, in my opinion, an open question. There are also diapycnal modifications of UPIW to upper layers prior to (south of) the 32°S section according to Rintoul (1988, 1991). It is more than tempting to rule out Drake Passage as a major source for the BCS and substitute "leakage" around the tip of Africa from the Indian to the Atlantic Ocean. My guess right now is that the upper intermediate water (UPIW, $27.2 \leq \sigma_\theta \leq 26.8$) flowing out of Drake Passage and into the BCS (S95) first interacts (mixes) strongly with the subtropical flows in the western South Atlantic while part of the Malvinas or Falkland Current System, becoming warmer and saltier long before leaving the SFZ for the BCS. Schmitz (1995) previously pointed out that the average salinity of the UPIW on the Greenwich Meridian section, 15 to 20° west of the tip of Africa (Whitworth and Nowlin, 1987), an "exit section" used by R8891, was

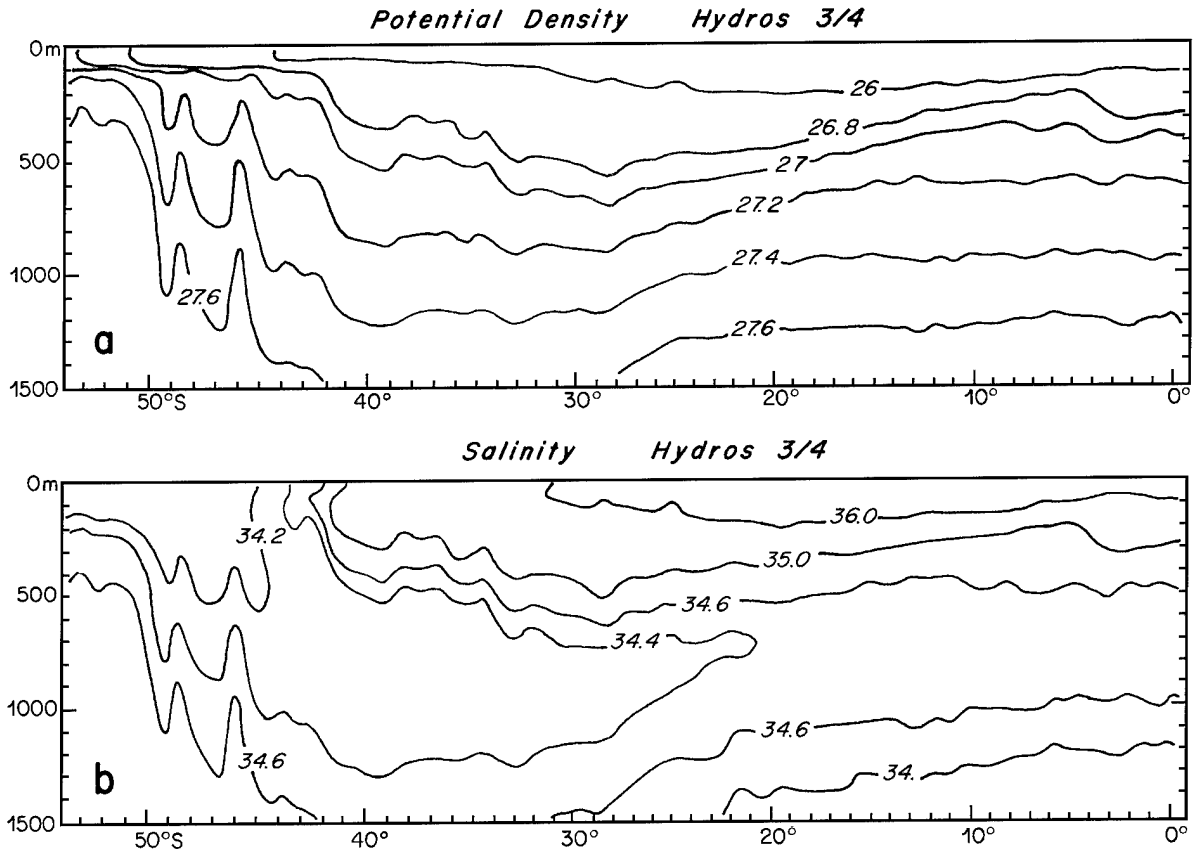

Figure II-143: Upper level section along 25°W for σ_θ (a), and salinity (b); adapted from Tsuchiya *et al.* (1994).

Table II-16: Nominal layer boundaries and layer average potential temperature and salinity at key R8891 sections

Layer	Upper Boundary	Lower Boundary	Drake Passage	1°E	32°S
1	surface	σ_0 = 26.20	*	16.80	18.27
			*	*35.288*	*35.661*
2	σ_0 = 26.20	26.80	6.82	10.21	13.05
			34.070	*34.635*	*35.227*
3	26.80	27.20	4.18	5.85	6.73
			34.137	*34.332*	*34.489*
4	27.20	σ_1 = 32.00	2.72	3.02	3.54
			34.220	*34.245*	*34.321*
5	σ_1 = 32.00	32.16	2.39	2.45	2.91
			34.392	*34.403*	*34.454*
6	32.16	32.36	2.10	2.26	2.76
			34.583	*34.603*	*34.648*
7	32.36	σ_2 = 37.00	1.80	2.21	2.67
			34.698	*34.766*	*34.832*
8	σ_2 = 37.00	σ_3 = 41.50	1.50	1.87	2.32
			34.724	*34.799*	*34.876*
9	σ_3 = 41.50	41.54	1.23	1.49	1.91
			34.726	*34.780*	*34.859*
10	41.54	41.60	0.85	0.92	1.32
			34.719	*34.734*	*34.804*
11	41.60	41.66	0.37	0.40	0.66
			34.705	*34.696*	*34.736*
12	41.66	σ_4 = 46.14	0.06	–0.33	–0.09
			34.687	*34.661*	*34.674*
13	σ_4 = 46.14	bottom	*	–0.73	*
			*	*34.652*	*

Temperatures are in degrees Celsius, salinities (italicized) in psu.
*No water in this layer in this section.

substantially larger (34.33 vs 34.13) than found for UPIW at Drake Passage. Using new data (Tsuchiya *et al.*, 1994) I demonstrate in Section 5 below that the salinity of UPIW is perhaps already near ~ 34.3 → 34.4 as early as 25°W.

The transports found by Rintoul at his three key sections from my point of view are shown in Figure II-144 (a, b, c). Essentially, Rintoul found that the NADW (17 Sv) joining the ACCS between South America and Africa was replaced primarily by the intermediate water entering this region from Drake Passage (11 Sv, modified to 5 Sv intermediate water and 6 Sv "surface" water by 32°S, the latter including Rintoul's layers 1 and 2, all water above $\sigma_\theta = 26.8$), along with 4 Sv of AABW (Table II-17). The "latest word" on the advective leakage around the tip of Africa from the ACS to the BCS is summarized in Figure II-145, taken from Garzoli and Gordon (1996, their figure 7). The most recent estimates of the volume flux exchange between the ACCS and South Atlantic are those of Saunders and King (1995, their table 4); Table II-18 contains their preferred estimates. These results are in line with the estimates by R8891 (Table II-17), although different in detail, that is, by a few Sverdrups here or there.

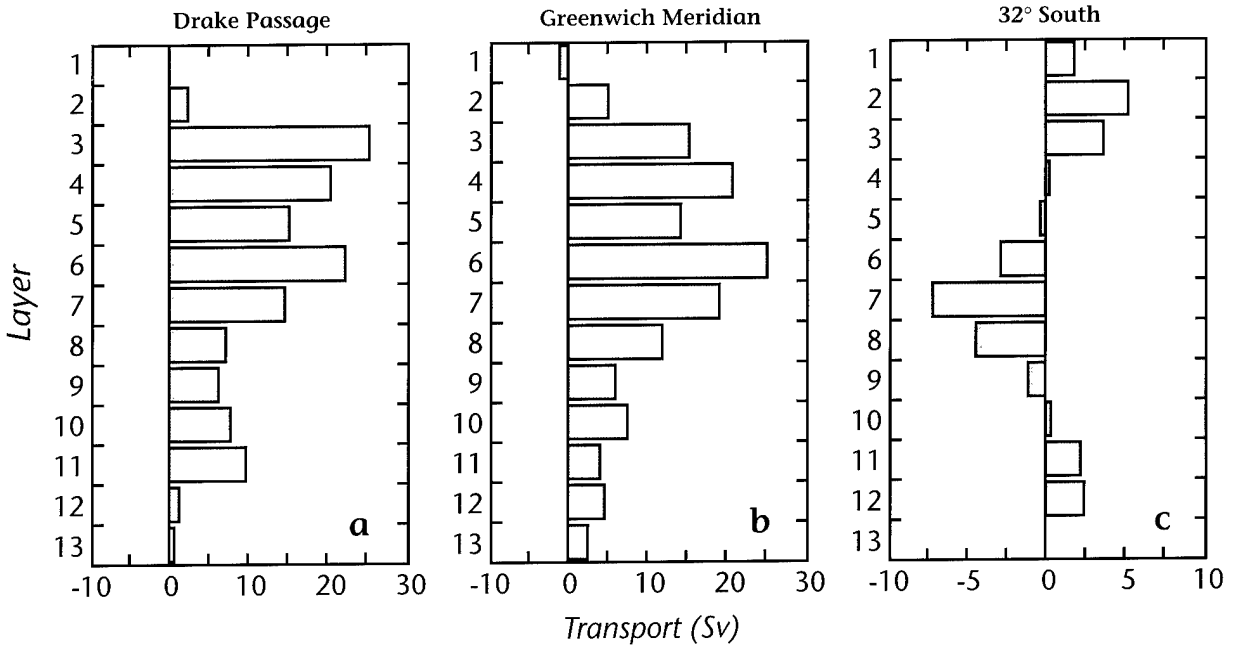

Figure II-144: The vertical structure of the transports at three locations in the southern South Atlantic, taken from Rintoul (1991, parts of his figures 3 and 4): (a) Drake Passage, (b) Greenwich Meridian, and (c) 32°S. Please also refer to the text and Tables II-16 and II-17 for layer structure and background information.

Table II-17: Rintoul's (1988, 1991) Key Transport (Sv) Summary

Water Type	Layers	Drake Passage*	0°*	32°S†
Surface Water	1–2	3	3	8
Intermediate Water	3–6	83	72	5
Deep Water	7–11	43	48	–17
Bottom Water	12–13	0	7	4

Table II-18: Volume Flux estimates across the WOCE A11 Section, adapted from Saunders and King (1995)

Water Type	Layer Definitions	Transport† (Sv)
Surface	$\sigma_0 < 26.8$	11
Intermediate	$26.8\ \sigma_0 \rightarrow 27.6$	4
Deep	$\sigma_4 < 45.95$ or $\sigma_3 < 41.58$	–22
Bottom	below deep	7

*Positive values are eastward (nominal). †Negative values are southward.

These issues are discussed a bit more in Section 5, where my updates of S95 are similar to the estimates by Saunders and King (1995), as was the case in Volume I of this report.

Rintoul (1988, 1991) included three intermediate water layers (his layers 3–6) in the inverse analysis. It was demonstrated from a further breakdown of Rintoul's (1991) results by S95 that the type of intermediate water that both exits Drake Passage eastward and does not continue past the southern tip of Africa was essentially confined to the σ_θ range 26.8–27.2. This is above the salinity minimum normally associated with Antarctic Intermediate Water, the latter typically being in the σ_θ range 27.2–27.5. The σ_θ range of 26.8–27.2 (UPIW) is also in the density parameter range of SAMW ($26.5 \leq \sigma_\theta \leq 27.2$) in the SFZ (McCartney, 1977, 1982). Lower Intermediate Water (LOIW) is

pretty much AAIW regardless of location. I originally locked into the UPIW idea because this dominates the intermediate water making its way out of the northern Straits of Florida and joining the Gulf Stream System, according to Schmitz and Richardson (1991) and Schmitz and McCartney (1993); please also see Volume I of this report.

The geostrophic transports for the upper 500 m of the low-latitude South Atlantic have been mapped by Stramma (1991), and Figure II-146 is an adaptation of his figure 7. The SEC in the South Atlantic splits into two pieces, the Brazil Current and North Brazil Current System (along with a possible variety of recirculations and eddies), as it approaches the coast of South America. The Brazil Current is the southward-flowing western boundary current for the subtropical gyre of the South Atlantic. The North Brazil Current (and Undercurrent; Stramma *et al.*, 1995a) is the low-latitude western boundary current for the tropical Atlantic. These currents have also been described by da Silveira *et al.* (1994), Stramma (1989, 1991), Stramma *et al.* (1990, 1995a), and Zemba (1991). Detailed sections near the branch point along the South American coast have been examined (Figure II-147, Table II-19) by Stramma *et al.* (1990). In Table

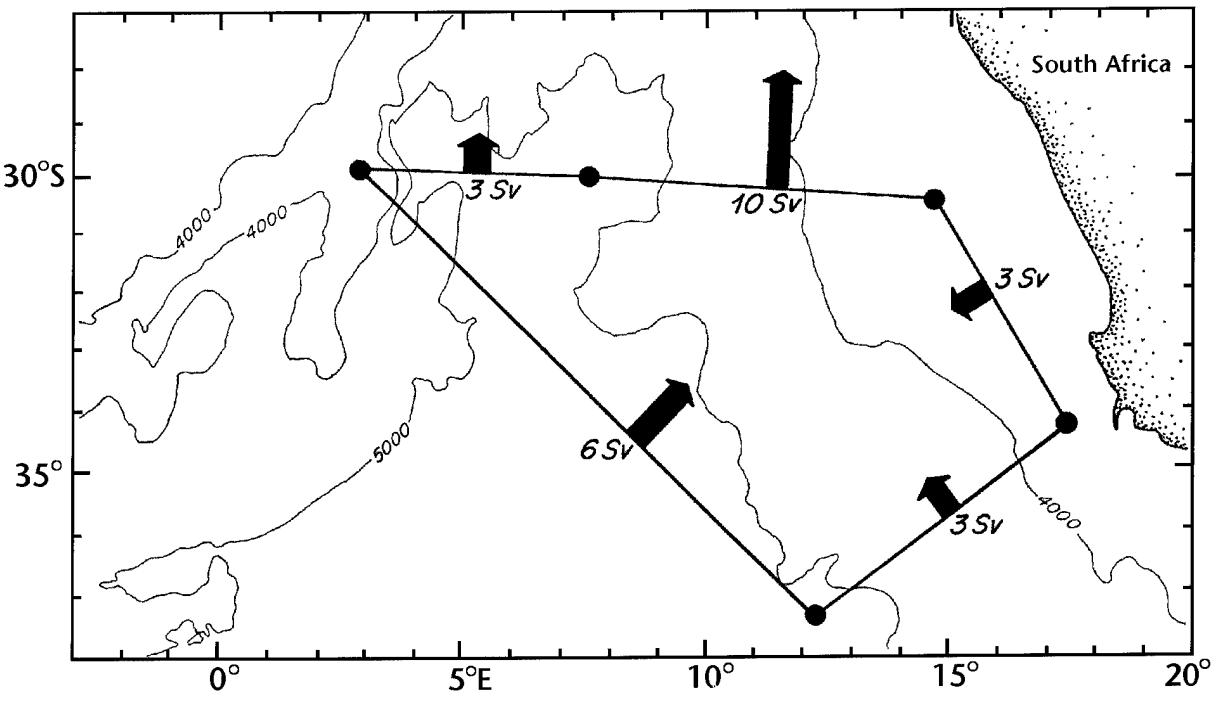

Figure II-145: Transport estimates in the eastern South Atlantic in the vicinity of the Benguela Current System, based on Garzoli and Gordon (1996).

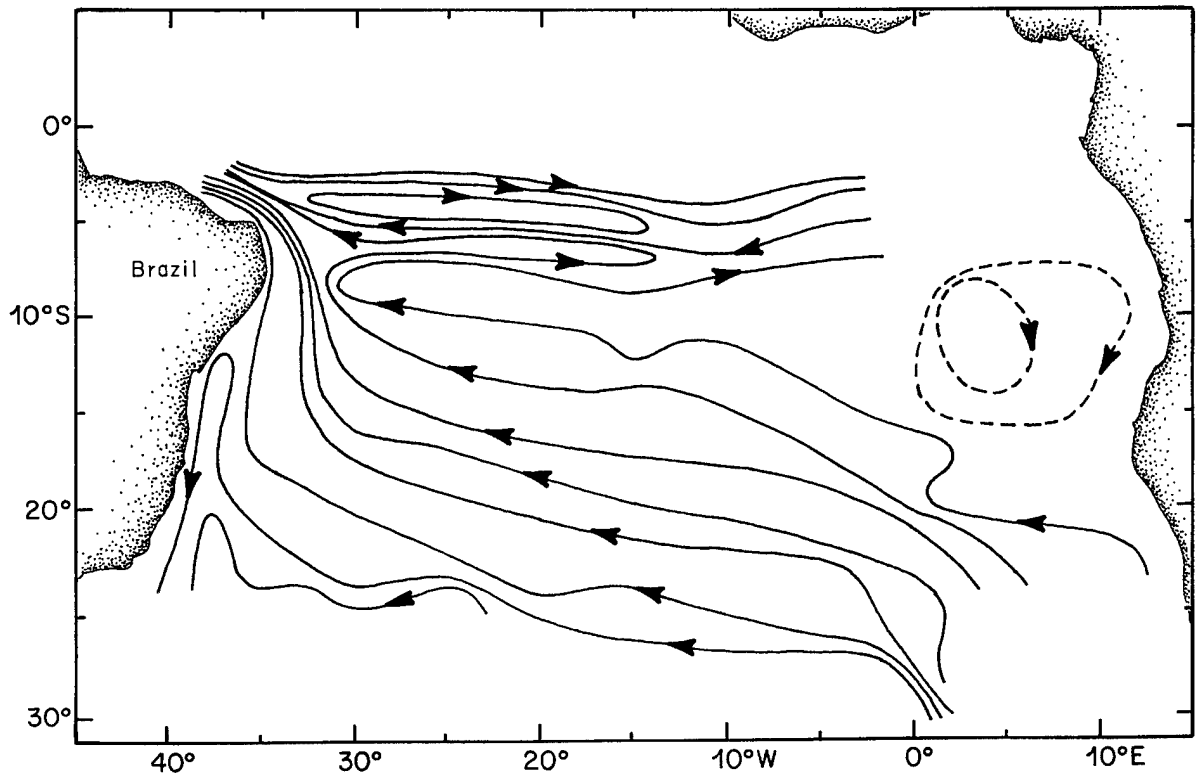

Figure II-146: Schematic representation of the geostrophic flow pattern in the upper 500 m of the low-latitude South Atlantic, based on Stramma (1991, his figure 7). Each solid line represents a transport of 3 Sv, and the dashed lines represent a more hypothetical Angola Gyre (Gordon and Bosley, 1991).

II-19, the North Brazil Current has a transport of about 13 Sv toward the North Atlantic at the South American coast near 8°S, which Stramma *et al.* (1990) note is an important factor contributing to the weakness of the Brazil Current. This 13 Sv [probably fortuitously similar to the 13–14 Sv net cross-equatorial transport that Schmitz and Richardson (1991) found flowing through the northern straits of Florida, please see Volume I of this report] is for a reference level at $\sigma_\theta = 27.05$, and one might anticipate perhaps 20–30 Sv for a reference level $\sigma_\theta \sim 27.5$, at the bottom of intermediate water. I feel that there is a retroflection of at least O(10 Sv) into the EUC. Also, the Ekman transport is important, especially at low latitudes, in describing interbasin exchanges and recirculations (*i.e.*, da Silveira *et al.*, 1994). Recent measurements near 4°N (Johns *et al.*, 1997) support the conclusions by Smith and Richardson (1991).

Table II-19: The hydrographic sections and meridional geostrophic transports (positive southward) for the upper 500 m depth interval using the potential density surface of σ_θ = 27.05 kg m^{-3} as reference.

Ship	Latitude (S)	Time	Section Transport (Sv)
A. Saldanha	7°5'	Oct. 1959	–13.4
Crawford	8°15'	Mar. 1957	–7.3
Crawford	8–9°	Feb. 1963	–9.2
A. Saldanha	10°5'	Feb. 1975	–4.7
Atlantis	12°15'	Mar. 1959	–4.6
Meteor	9–13°	Sep. 1926	–5.7
A. Saldanha	13–14°	Apr. 1957	–1.7
A. Saldanha	15°	Feb. 1975	2.1
Crawford	15°45'	Apr. 1957	–0.5
A. Saldanha	16°6'	Jan. 1975	1.0
Meteor	18–16°	Jun. 1926	–3.1
Prof. Besnard	19°	Sep. 1967	0.8
A. Saldanha	19°25'	Jun. 1970	4.0
A. Saldanha	19°30'	Mar. 1957	2.8
A. Saldanha	20°3'	Jan. 1975	3.9
Atlantis	20°15'	Mar. 1959	4.5

The intermediate water circulation in the South Atlantic has been studied, for example, by Piola and Georgi (1982), Piola and Gordon (1989), Taft (1963), and Talley (1996). Talley (1996) defines AAIW in terms of its classical characteristic, the salinity minimum, and as a layer by $27.0 \leq \sigma_\theta \leq 27.4$ or $31.6 \leq \sigma_1 \leq 32.0$. The primary sources of AAIW according to Talley (1996) are the surface waters in the southeastern Pacific, which produce the South Pacific AAIW, and then the surface waters in the northern Drake Passage and Falkland Current Loop, which produce the South Atlantic AAIW. The South Atlantic AAIW is thought by Talley (1996) to be the source of AAIW for the

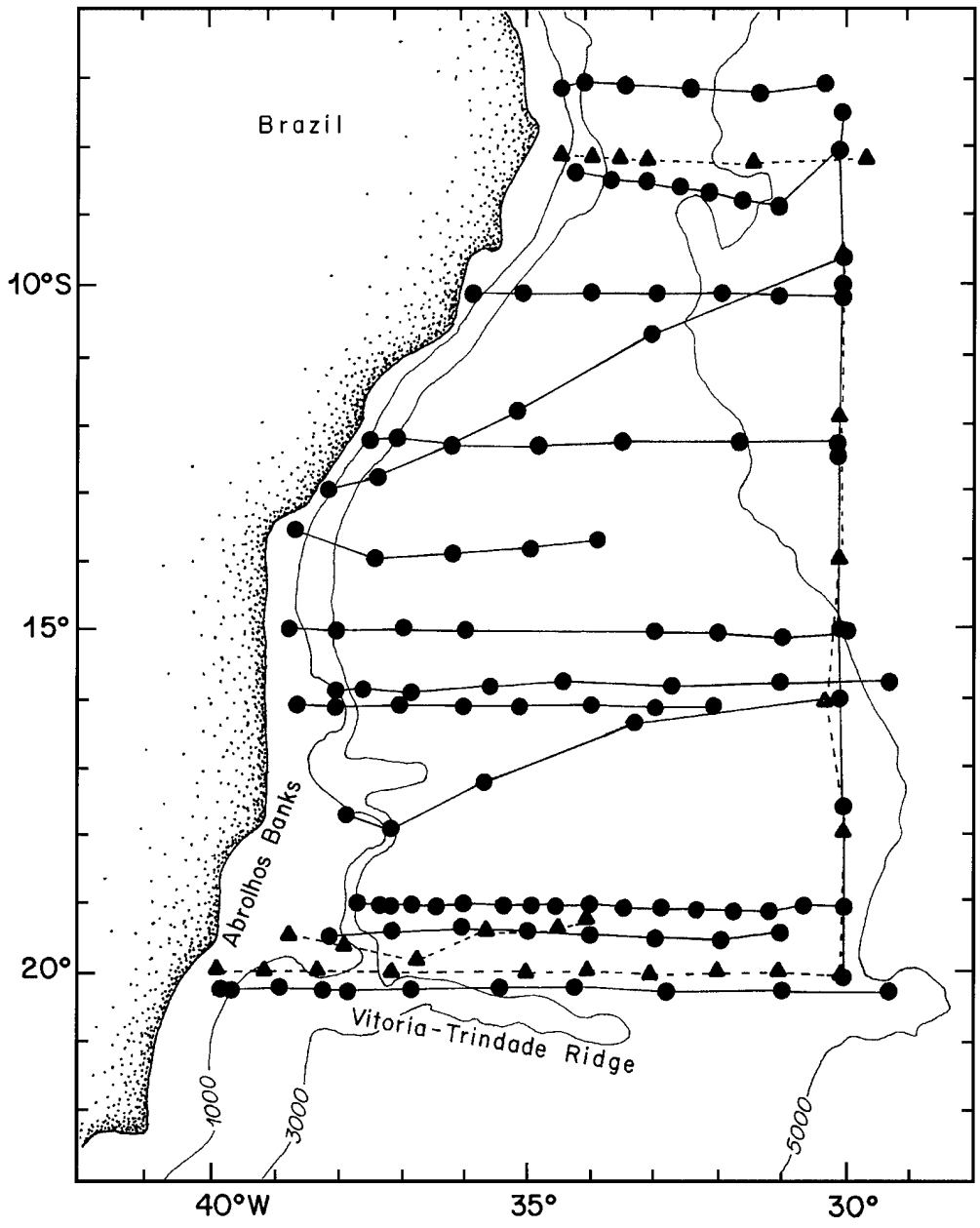

Figure II-147: Locations of the hydrographic stations used by Stramma *et al.* (1990, their figure 1) in constructing Table II-19. Please refer to the quoted publications for the details concerning data location and methods in general.

Indian Ocean as well. The development of our state-of-the-art picture of the deep and abyssal circulation in the South Atlantic is one of the historical success stories in physical oceanography (Peterson and Whitworth, 1989; Reid, 1989, 1994; Reid *et al.*, 1977). And there has been some very recent interesting work there too (De Madron and Weatherly, 1994; Hogg *et al.*, 1996; Siedler *et al.*, 1996).

4b. Brief Remarks on the Antarctic Circumpolar Current System (ACCS)

Most of what little I present in this section is background material relative to Rintoul's (1988, 1991) results. The ACCS is the critical global link connecting all major oceans, as well as an area of strong interest to oceanographers historically for its own sake. Since I've never personally worked there, I will rely heavily on other sources for my treatment of this topic. Also, the concentration here is obviously on interbasin/interocean exchange, not the ACCS itself. I would think that one of the major projects that could be undertaken with the new data now available from recent large field programs would be to repeat some version of Rintoul's (1988, 1991) calculations for all the World's Oceans at their southern end.

Sharp meridional gradients or fronts in a variety of properties typically separate the ACCS from the warmer and saltier subtropical circulations (Figure II-140). Deacon (1933, 1937) called this hydrographic boundary the Subtropical Convergence, a term often replaced by the Subtropical Front (STF) in recent years (Clifford, 1983; Hofmann, 1985; Belkin and Gordon, 1996). The eastward flow of the ACCS is associated with a steep rise of isopycnals toward the south through the water column. Deacon (1937) noted that the poleward rise of isotherms and isohalines was not uniform, but occurred in a series of clear step-like patterns. Bands of large horizontal density gradients characterize the ACCS fronts, here called the Subantarctic Front (SAF) and the Polar Front (PF), to the north of which lie the Subantarctic (SFZ) and Polar (PFZ) Frontal Zones, respectively. Major bottom ridges control the path of the ACCS, with sharp poleward shifts observed through the broad gap in the Southwest Indian Ridge, between 20° and 30°E, and through the narrow fracture zones in the Pacific–Antarctic Ridge, between 145° and 120°W. Downstream of South America there is a sharp northward shift associated with the Scotia Arc (Orsi *et al.*, 1993). Cyclonic cells or gyres of recirculating waters develop south of the Circumpolar Current where it is located sufficiently far from the Antarctic Continent. The Weddell and Ross Gyres are the best known of these subpolar cyclonic circulations (Deacon, 1933; Reid, 1965, 1986). A third smaller cell may also exist east of the Kerguelen Plateau (Deacon, 1937). These gyres are characteristically associated with water mass formation, and along with the PF, PFZ, SAF and SFZ combine to form what I have called the ACCS.

In the past 20 years or so, particularly in the 1970s, considerable effort was focused on Drake Passage (Hofmann and Whitworth, 1985; Nowlin *et al.*, 1977; Sievers and Nowlin, 1984; Whitworth *et al.*, 1982), including the eddy field there (Bryden, 1979; Nowlin *et al.*, 1981). Sections across Drake Passage, as adapted from Nowlin *et al.* (1977, their figure 4) are shown here as Figures II-148, 149, 150 and 151, for density parameter, potential temperature, salinity and oxygen, respectively. Figures II-148

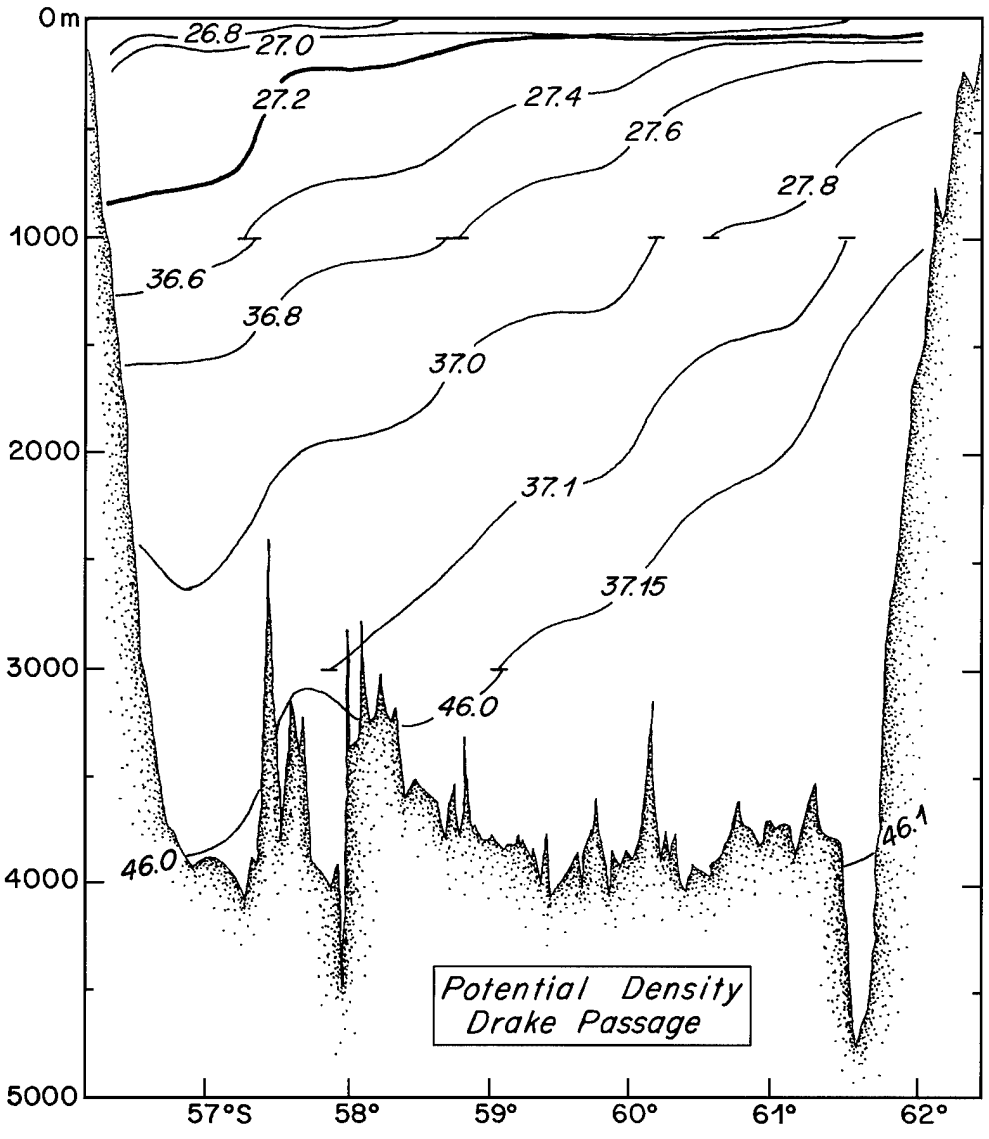

Figure II-148: Potential density parameter section across Drake Passage, FDRAKE 75, *Melville* Section II, a simplified rendition of figure 4d by Nowlin *et al.* (1977).

through II-151 are from *Melville* Section II of FDRAKE 75 (First Dynamic Response and Kinematics Experiment, 1975). Nowlin *et al.* (1977, their figures 5 and 6) also present density parameter sections for FDRAKE 75, *Melville* Section V, and FDRAKE 76, *Thompson* section. All three density parameter sections noted above for Drake Passage are characterized by an area of $26.8 \leq \sigma_\theta \leq 27.2$ in the northernmost corner of the section, with a maximum depth of about 800 m for $\sigma_\theta = 27.2$ at a northern bound-

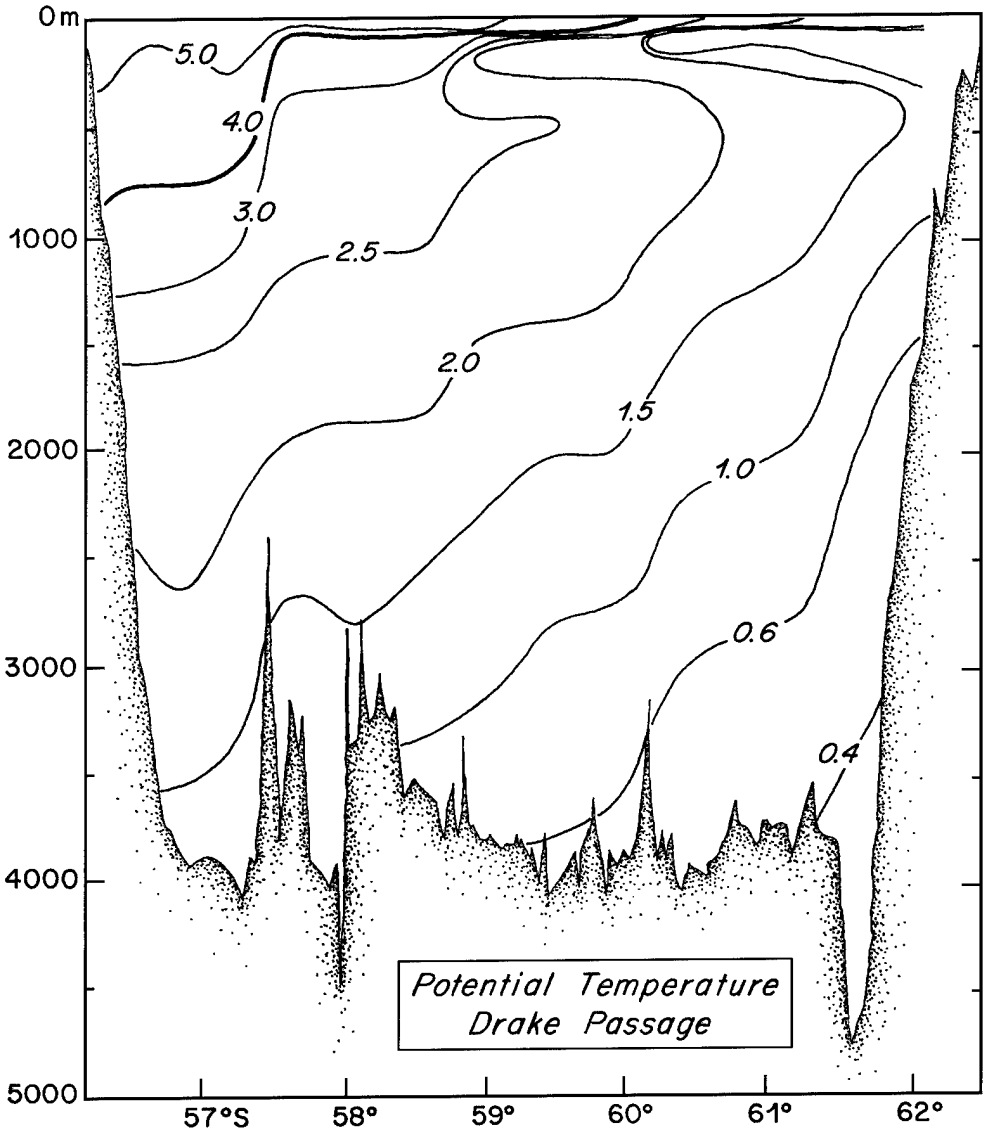

Figure II-149: Potential temperature section across Drake Passage, FDRAKE 75, *Melville* Section II, a simplified rendition of figure 4a by Nowlin *et al.* (1977).

ary in the vicinity of 56–57°S, outcropping near 59–60°S. The average potential temperature for UPIW at Drake Passage was found by Rintoul (1988, 1991) to be 4.18°C, and one can see that the 4°C isotherm in Figure II-149 is roughly at $\sigma_\theta \doteq 27.2$; and potential temperatures of 5°C were contoured at about $\sigma_\theta = 26.8$. Rintoul's (1991, his table 2) average salinity for $26.8 \leq \sigma_\theta \leq 27.2$ was 34.12 (Table II-16), and in Figure II-150 one can see the salinity contour 34.2 in this area, with about 34.0 near the out-

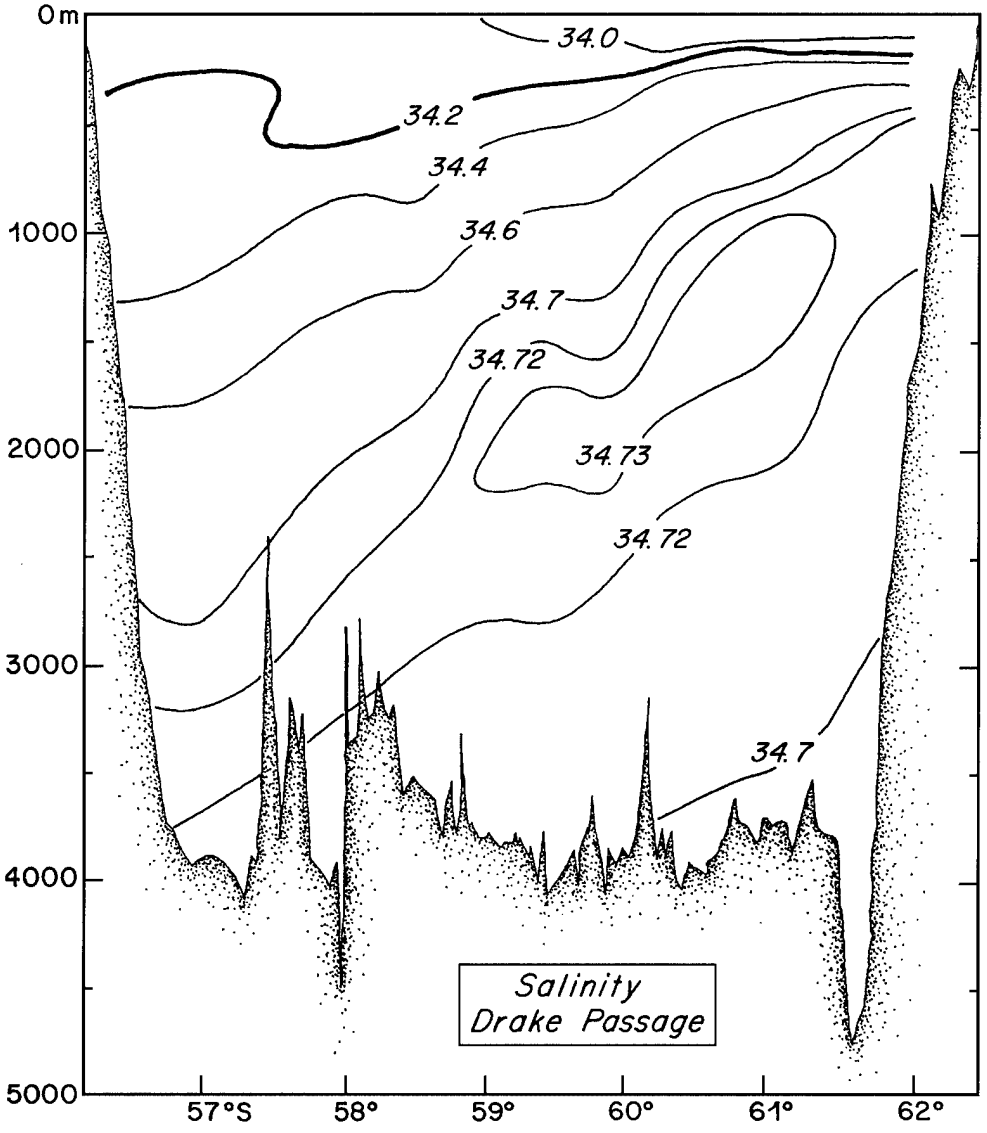

Figure II-150: Salinity section across Drake Passage, FDRAKE 75, *Melville* Section II, a simplified rendition of figure 4b by Nowlin *et al.* (1977).

cropping location for $\sigma_\theta \doteq 27.2$. These points are discussed in more detail in Section 5 below.

The Ajax Expedition results along the Greenwich Meridian have been described and compared to Drake Passage by Whitworth and Nowlin (1987). Sections are shown in Figures II-152–154, for density parameter, salinity, and silica respec-

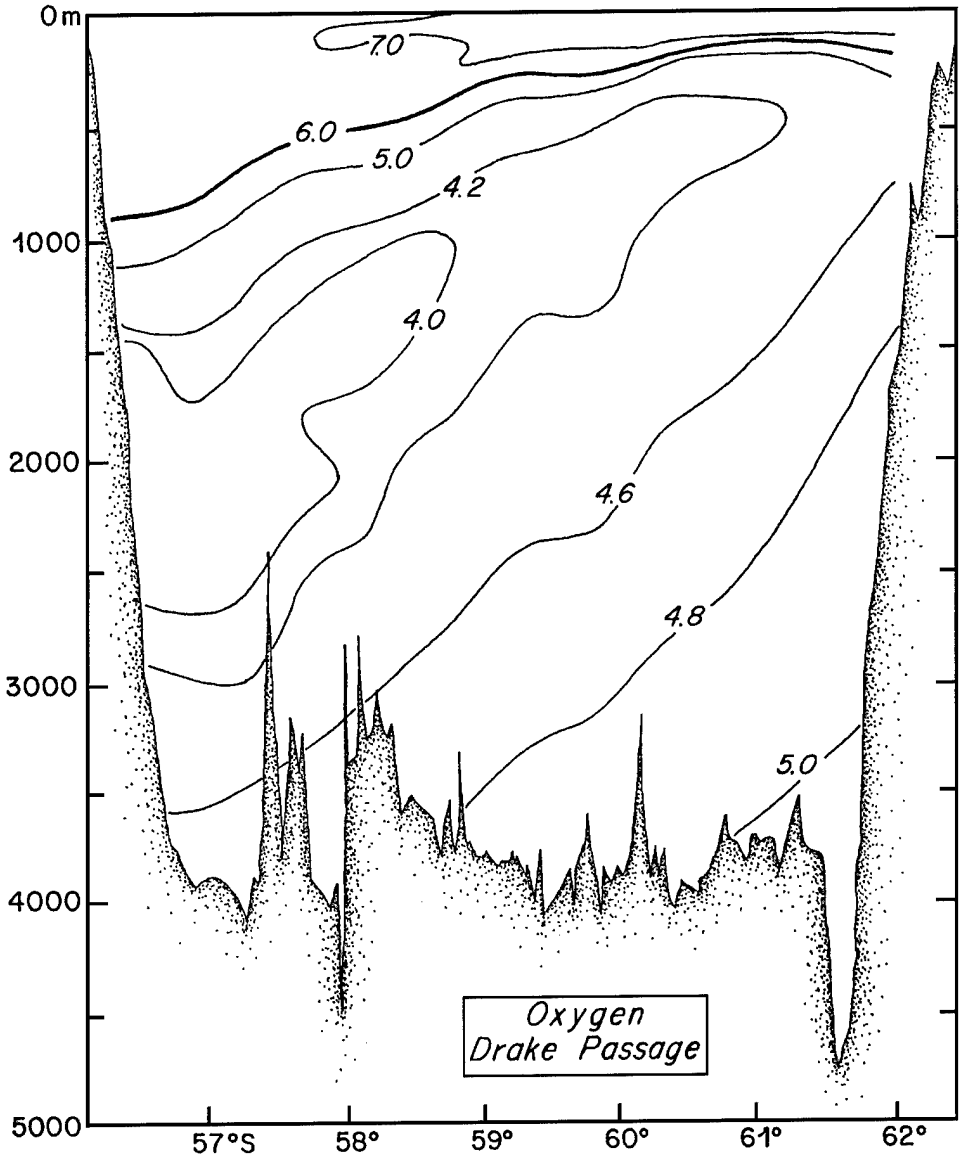

Figure II-151: Oxygen section across Drake Passage, FDRAKE 75, *Melville* Section II, a simplified rendition of figure 4c by Nowlin *et al.* (1977).

tively, adapted from Whitworth and Nowlin (1987, their figure 2). Again the area bounded by $26.8 \leq \sigma_\theta \leq 27.2$ contours is in the northernmost corner of the section. But in this case (in contrast to Drake Passage), salinity contours of 34.6 and 34.4 are part of the bounded area, as well as the 34.2 psu contour. This point was noticed by S95, that is, that UPIW in the SFZ was comparatively salty at 0° (Table II-16), a serious

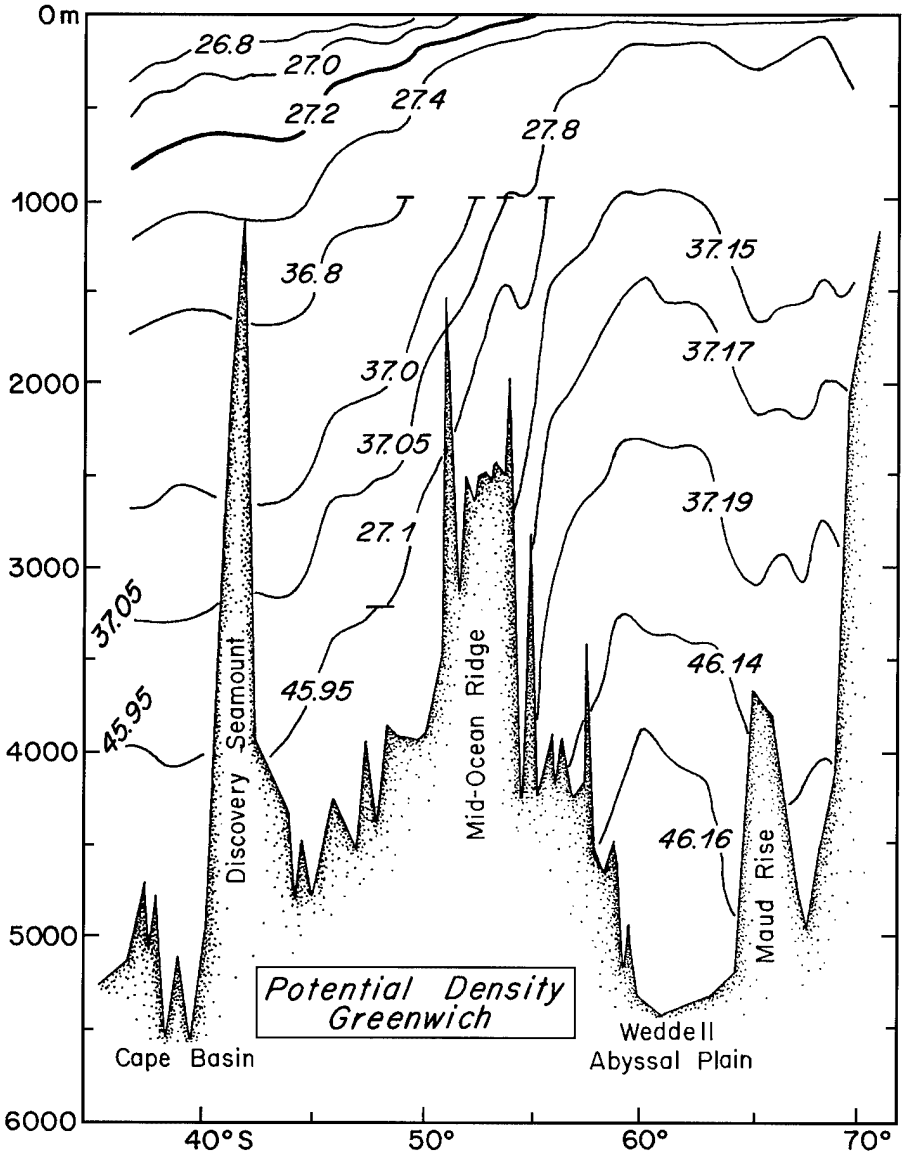

Figure II-152: Potential density parameter section along the Greenwich Meridian (nominal), adapted from Whitworth and Nowlin (1987, their figure 2c).

distance upstream of the tip of Africa. The average salinity of UPIW at 0° was found by Rintoul (1991, his table 2) to be 34.33. Figure II-154 is shown as background data for the large silica values approaching the South Indian Ocean and areas south of there (Mantyla and Reid, 1995), Section 3 above. Various plots from the *Conrad* 30°E section (Jacobs and Georgi, 1977) were presented by Rintoul (1988). This is the easternmost area of investigation associated with Rintoul's (1988, 1991) inverse calculation. The

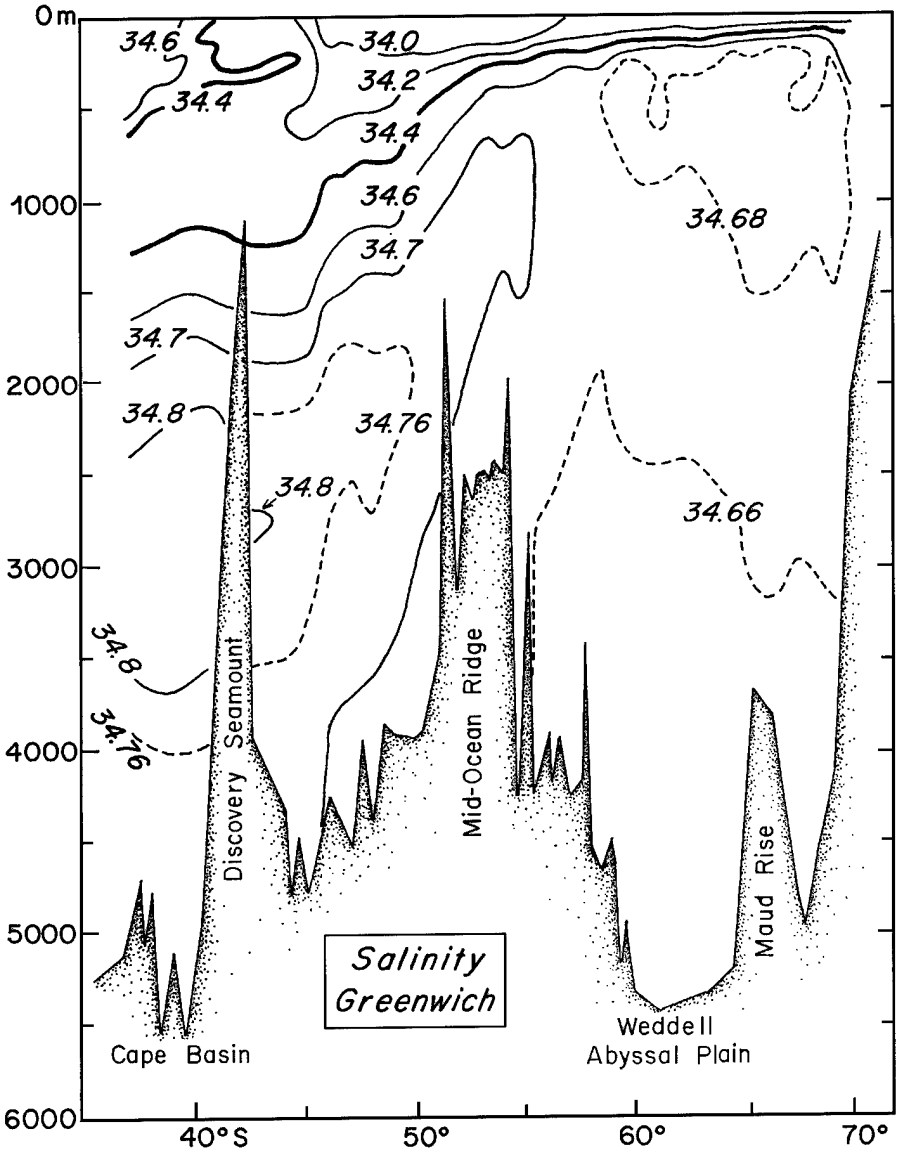

Figure II-153: Salinity section along 1°E, adapted from Whitworth and Nowlin (1987, their figure 2b).

average salinity of UPIW in this section was 34.32 (Rintoul, 1991, his table 2), *fresher* than at 0°. From my point of view, nothing much happened between 1°E and the *Conrad* section insofar as Rintoul's (1988, 1991) transport calculations are concerned (Section 5 below), so these sections will not be discussed here.

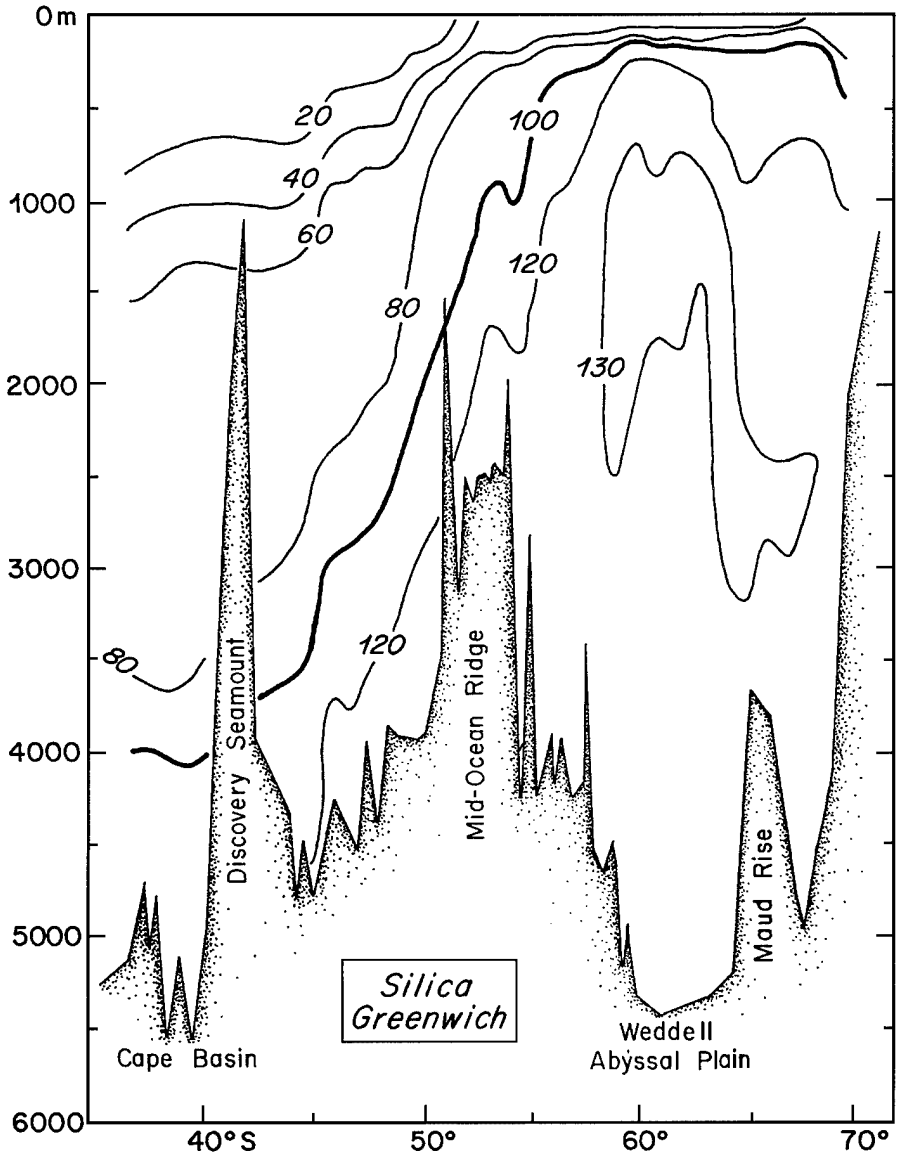

Figure II-154: Silica section down the Greenwich Meridian (nominal), across the ACCS, adapted from Whitworth and Nowlin (1987, their figure 2g).

5. A Summary of the Global Interbasin Exchange Picture

My 1995 article represents the first publication in my career involving a major chunk of time spent on the global interbasin ocean circulation. This effort was motivated to a large extent by how the cross-equatorial transports associated with the replacement flow for NADW formation in the North Atlantic as suggested by Schmitz and Richardson (1991) and Schmitz and McCartney (1993) and based primarily on the transport structure of the Florida Current agreed not only with Hall's and Bryden's (1982) and Roemmich's and Wunsch's (1985) interbasin-scale transports along 24°N, but also with estimates of more globally linked interbasin exchanges along 32°S and across the high-latitude South Atlantic by R8891. As this report volume was being finished, I received a manuscript (Johns *et al.*, 1997) that independently substantiated the general conclusions by Schmitz and Richardson (1991) on the characteristics of the replacement flow for NADW in the tropics. Schmitz's and McCartney's (1993) and S95's results were also in qualitative or semi-quantitative agreement with Hank Stommel's remarkable survey article in 1957, to the extent that 2-layer representations can be. It is of course a much more difficult problem to determine the details of the cross-equatorial flows at low latitudes than it is in the Florida Current, due to the complexities of time-dependence, water mass transformation, and topography, perhaps especially in the latter case for island chains where the flow could be in and out through various passages. Insofar as I can tell, some version of this situation exists in all the oceans, not just the Atlantic. The comparative reproducibility of transport estimates and *T/S* properties for the Florida Current (see Volume I of this report) help a lot in the Atlantic.

My first experience beyond R8891 and the Atlantic Ocean relative to the replacement flow for NADW was in reading Gordon's (1986) work, and the dichotomy between Gordon's and Rintoul's results was a strong driver for a continuing interest. Vitiaz Strait transport estimates (Section 2) have played a key role in my ideas, as did the 32°S sections in both the Pacific and the Indian Oceans, and Fieux *et al.* (1994, 1996a, b) have influenced my thinking a lot, not only about the IT, but also about the general area between Australia and the Indonesian Passages, a location potentially critical to a lot more than just the IT. Volume I of this report contained a partial update of some of the global flow characteristics discussed by S95, mostly changes involving the Atlantic Ocean with a few new ideas and summary graphics. But there are also of course inter-

esting interbasin circulations associated with both Pacific and Indian Oceans, perhaps especially the latter, where RT96 is my baseline.

In Volume I of my report I introduced for the first time a meridional transport cell for the Atlantic with a global linkage (Figures I-12, II-11), which is updated in a small but not trivial way immediately below. The cell structure in Volume I included increasing relative to S95 or R8891 the AABW or LCDW component of influence on NADW from 4 to 7 Sv. There is some introductory review of the global picture in Section 1 of this report volume, and remarks on interbasin exchanges throughout. In this section (5) of Volume II, an effort is made to improve/update further some global summary pictures of interbasin ocean circulations. The major changes of course take place with respect to new pictures of the Pacific and Indian Oceans and how these ideas and data presentations fit into a global scheme, the main topics of this report volume. One of the thoughts I've had in this regard developed too late for me to incorporate it seriously into the graphics associated with this report, so I'm mentioning it in a few places in the text. That is, perhaps IODW and NPDW, products of the deep/bottom water cells in the Indian and Pacific Oceans respectively, could be diapycnally modified upward to LOIW and thence UPIW. These transformations, which I suggest might preferentially take place in the easternmost South Pacific off Chile (45–55°S, say) where the SFZ runs into South America, would couple pretty much all of the interbasin and large-scale thermohaline cells in the World's Oceans.

The first "global" update I have (Figure II-155) is for the meridional cell in the Atlantic Ocean from Volume I of this report (Figure I-12 there, II-11, unmodified, here). Although this is an meridional cell diagram for the Atlantic, it has two global features, one being CDW, and my update (Figure II-155) also has a different and more global view of an Agulhas Leakage, denoted AL on Figure II-155. The various other abbreviations for water masses/layers have been described in the caption to Figure II-11 and throughout Volume I. The essential change that I've made in this diagram, relative to Volume I, is to equipartition the contribution to NADW replacement from the flow through Drake Passage and the exchange with the South Atlantic around the tip of Africa (7 Sv). This is indicated in Figure II-155 by a flow of 7 Sv of intermediate water (red line) toward AL, being converted to ULW (upper layer water, $\sigma_0 > 26.8$, purple line) in transit from the ACCS through the Pacific and Indian Oceans, and perhaps also in the southern segment of the "Benguela Current." There is a tendency

in the literature to use different layer breakdowns for various regions of the ocean, and the reader should be aware that I have not totally homogenized Figure II-155 layer-wise with all of the other diagrams presented in this report volume. In Figure II-155, there is also a new guess concerning the different ways in which NADW (CDW) is converted to intermediate water. Since the reasons for this change are globally linked, they will be discussed below in that context.

The second update I have for Section 5 (Figure II-156) is for the 3-layer global schematic by S95 (figure 9 there). In this figure, red denotes UPOCNW [$\sigma_\theta \leq 27.5(6)$], that is all water masses above deep water, the latter being represented by green lines, with blue for bottom water. In Figure II-156 there are equal contributions to the re-

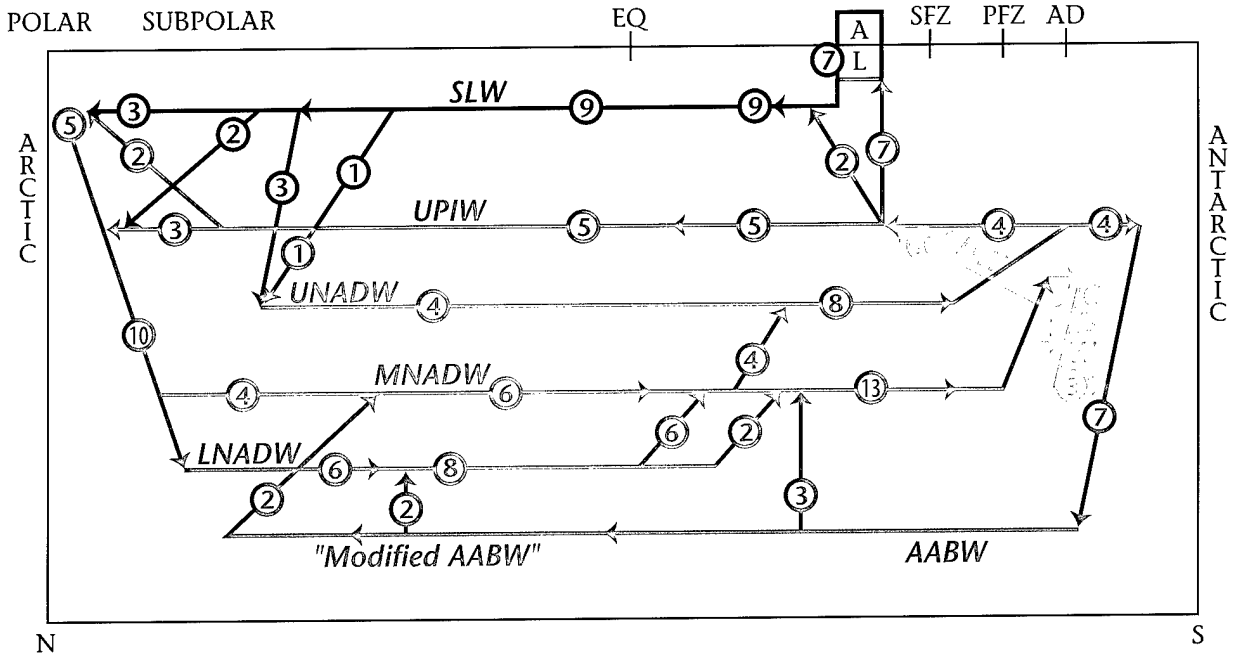

Figure II-155: This diagram is an update for the meridional transport cell depicting the interbasin circulation in the Atlantic Ocean that was introduced in Volume I of my report, Figure I-12 there, and was reproduced without change as Figure II-11 of this report volume. Purple denotes a surface layer, red indicates SAMW and intermediate water (primarily UPIW), green is for deep water, and dark blue represents near-bottom water. Circumpolar Deep Water (CDW) is set off in light blue lines. There are three branches for NADW: Upper, Middle, and Lower North Atlantic Deep Water (UNADW, MNADW, LNADW, respectively). Various geographical and oceanographic features are inserted around the border of the figure. EQ denotes the equator, SFZ is Subpolar Frontal Zone, PFZ is Polar Frontal Zone, AD is Antarctic Divergence, AABW is Antarctic Bottom Water, SLW is Surface Layer Water, AL is the Agulhas Leakage. Transports in Sverdrups in circles.

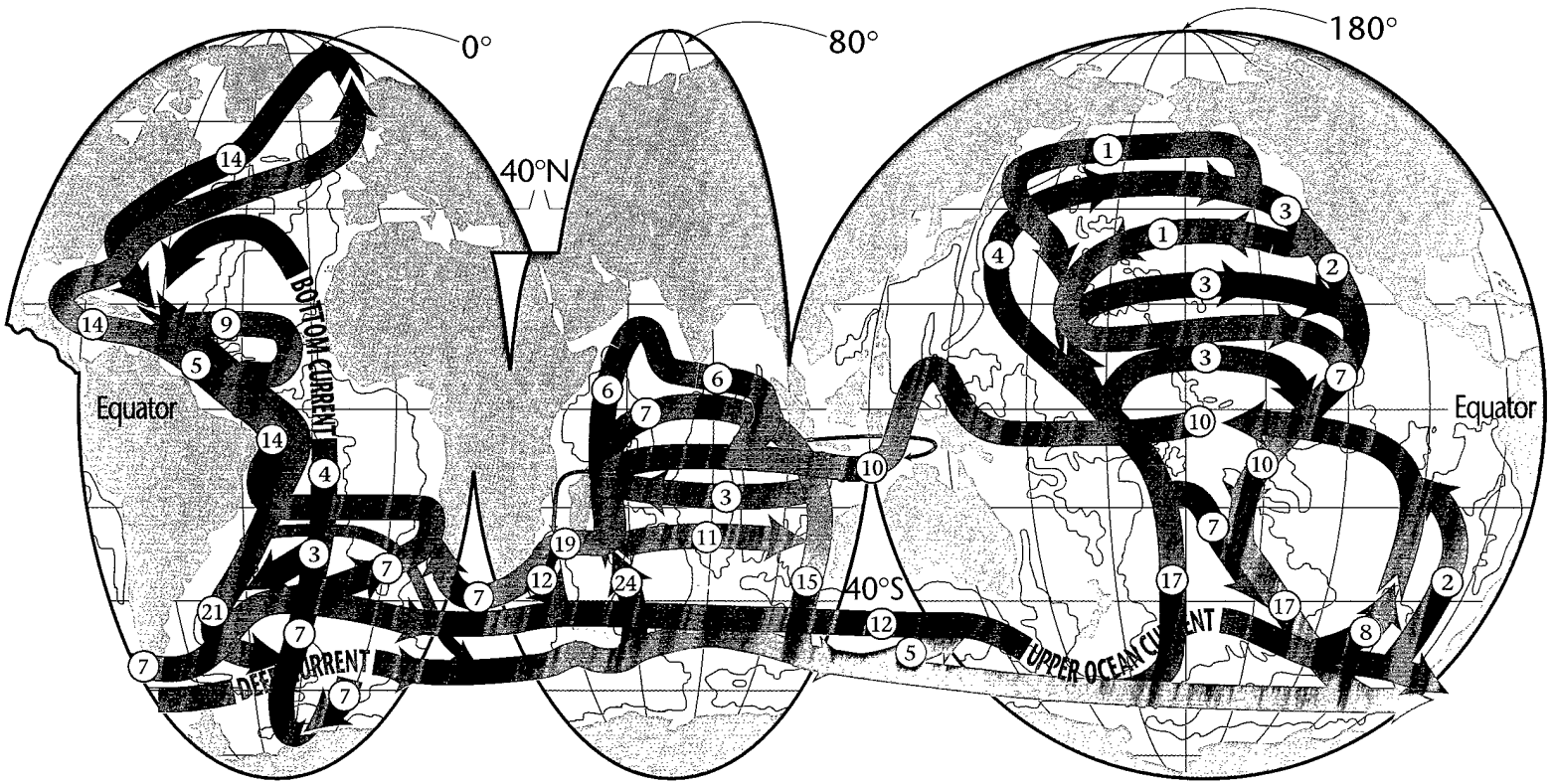

Figure II-156: An update of the 3-layer global interbasin exchange summary by S95, figure 9 there. Blue represents bottom water, green deep, and red the upper ocean. Transports in Sverdrups in circles.

placement of NADW from Drake Passage and the Agulhas Leakage, as in Figure II-155. The Agulhas Leakage is taken to be approximately equipartitioned between a direct advective transfer (Gordon *et al.*, 1992; Garzoli and Gordon, 1996) and the exchange associated with the propagation of cut-off Agulhas Rings into the South Atlantic (Duncombe Rae, 1991; Duncombe Rae *et al.*, 1996). It is also suggested in this report that the influence of Agulhas Rings on the South Atlantic subtropical gyre may lead to a transfer of heat and salt to the upper intermediate water entering the Brazil–Malvinas Confluence from Drake Passage. In Figure II-156, the general picture for the Atlantic Ocean is modified as indicated previously to accommodate 7 instead of 4 Sv of bottom water entering the South Atlantic (this has already been done in Volume I of this report for Figure I-12 there) from the ACCS (Saunders and King, 1995; Speer and Zenk, 1993; Speer *et al.*, 1992). The thick blue arrow indicating the path of AABW into and in the North Atlantic is displaced to the east for clarity in viewing Figure II-156. In general, these thick line presentations involve a good bit of idealization, another particularly notable example being the path(s) of deep and bottom water in the Indian Ocean. A global flow schematic showing interbasin transports in a thin-line, four-layer format was presented by S95 (figure 7 there). The net 14 Sv of UPOCN exchange across the South Atlantic Ocean in Figures II-155 and II-156 (and S95) are close to a comparable volume flux estimate across the South Atlantic Ocean as presented by Saunders and King (1995; please refer to Table II-18). In Figure II-156, the NADW approaching the ACCS in the South Atlantic has both a path along the western boundary and a path shifting from the western boundary to the eastern basin of the South Atlantic per Reid (1989) and Siedler *et al.* (1996). This eastern path is indicated by a line of intermediate width for clarity. The Pacific and Indian Ocean components of Figure II-156 reflect the meridional cells presented in Figures II-68 and II-129, for the Pacific and Indian Oceans respectively, along with some recently identified possibilities with respect to horizontal structure, as discussed earlier in this report.

The major differences between S95 (figure 9 there) and II-156 in the Pacific Ocean include an increased sequence of recirculations for CDW, along with a new (at least for me) flow pattern for NPDW. Significant changes also include a more prominent role for the diapycnal modification of various brands of intermediate water (and maybe even upper deep water) in the eastern South Pacific off the coast of Chile at "high" latitudes (40–50°S), and for SAMW in the Peru Current. The Indian Ocean thermohaline flow

structure is different in a variety of ways relative to S95, but the deep and bottom pathways are similar. The three geographically distinct pathways for the northward flow of bottom water are represented by only one blue line in Figure II-156. A more accurate representation requires a different type of figure; please see S95 (figure 7 there). The new meridional cell structure at 32°S for the Indian Ocean by RT96 is integrated into Figure II-156. Since RT96 convert only 6 Sv of CDW above lower intermediate water to upper intermediate water (4 Sv) and SLW (2 Sv), there remains the global question of converting 8 Sv of NADW (primarily via Circumpolar Deep Water) to LOIW and then above.

Robbins and Toole (1996) also convert 3 Sv of CDW to LOIW in the Indian Ocean that is transformed to UPIW on Figure II-68 in the Chile Current, which, as indicated earlier, is taken to be the flow into the easternmost South Pacific from the ACCS south of the Peru Current, that is, south of 35–40°S. This leaves 5 Sv of CDW (NADW) to be converted to lower intermediate water, perhaps by conventional means in the ACCS (*e.g.*, Sievers and Nowlin, 1984). Insofar as I can tell, this is the mechanism that transforms deep water upward in the circumpolar regime for the model results by Shriver and Hurlburt (1996). In Figure II-156, these ideas are represented by a green arrow transformation to red water south of Australia. The resulting LOIW also has to be converted upward, and this is done for 3 Sv (Figure II-68) in the Chile Current. The other 2 Sv of AAIW entering the eastern South Pacific from the ACCS to "replace" IT in Figure II-156 are converted upward at the equator (1 Sv) or in the North Pacific (1 Sv), as indicated in Figure II-68. Another possibility, that I just thought of, would convert IODW and NPDW to LOIW and then UPIW, presumably in the subantarctic sector of the ACCS.

Some years ago, during the period when I was preparing S95, Lynne Talley told me she wished that I had done more with the deep/bottom cell in the Pacific Ocean. I have tried to respond to this comment in this report, and in Figure II-156. The horizontal structure of the meridional cell in the North Pacific that I have speculatively added in Figure II-156 was strongly affected by Lynne's own work; please see Figures II-64–66 and Talley (1995). I have added three recirculating cells to CDW in the Pacific Ocean, and convert 4 Sv of CDW to NPDW north of the 24°N section. The version of the meridional cell in the Pacific that is shown in Figure II-156 is one where there is no interaction between the deep/bottom cell and IW, and is based on Figures II-68 and

129. Very little is done with the upper ocean in the Pacific in Figure II-156, except to indicate the ultimate "sources" for the IT in the ACCS and Indian Ocean. More detailed description of UPOCNW in the Pacific is contained earlier in this report (please see Figures II-69 and 129) and a global version is mapped later in Section 5.

The most significant differences between S95 and Figure II-156 relative to the Indian Ocean are associated with results presented by RT96, and the structure of the diapycnal conversion to intermediate water that I have discussed in Section 3d. The cell amplitudes in Figure II-156 correspond almost precisely to the results by RT96, which are similar to S95 in general terms but are not identical; specifically they form 3 Sv less intermediate water than S95. Robbins and Toole convert 6 Sv of CDW to UPIW (4) and SLW (2), and 3 Sv to LOIW. This is shown in Figure II-156. These are the only mechanisms published in the literature that convert CDW through UDW to UPIW (6 Sv) and above, and a "new" mechanism for converting CDW (through IODW) to LOIW (3 Sv). In the latter case a small green arrow has been added to Figure II-156 in the Indonesian Passages to indicate some recirculation

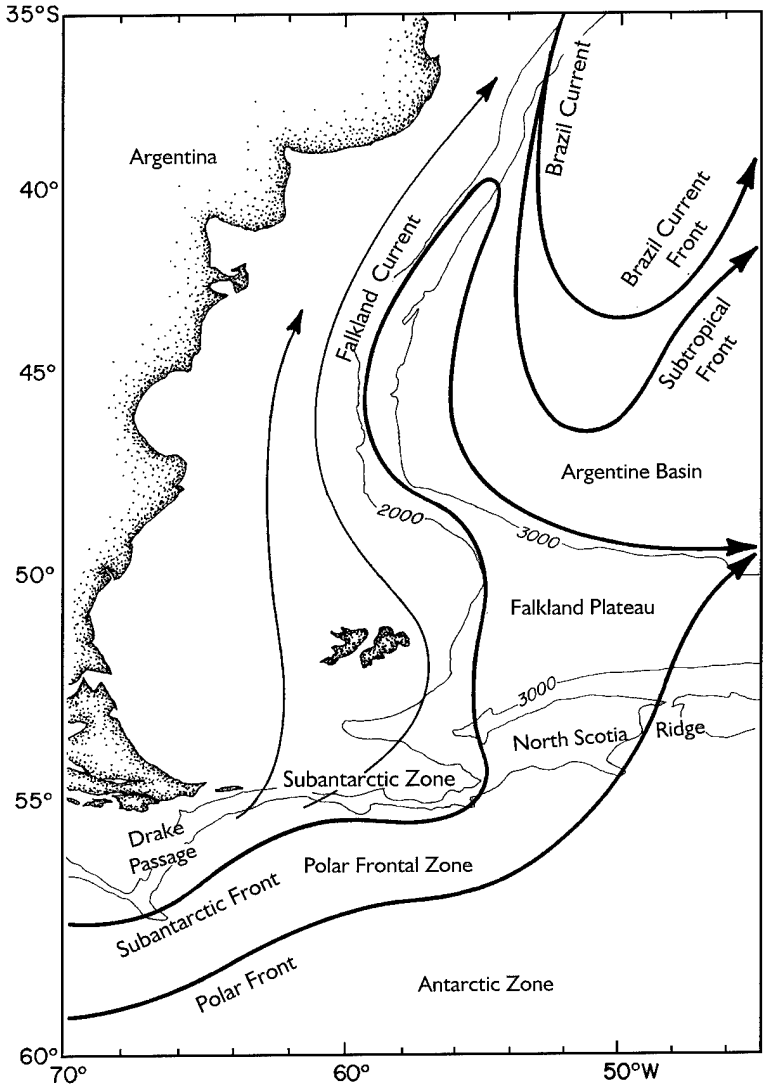

Figure II-157: A diagram showing the location of major fronts and current systems in the southernmost western South Atlantic, adapted from Peterson (1992).

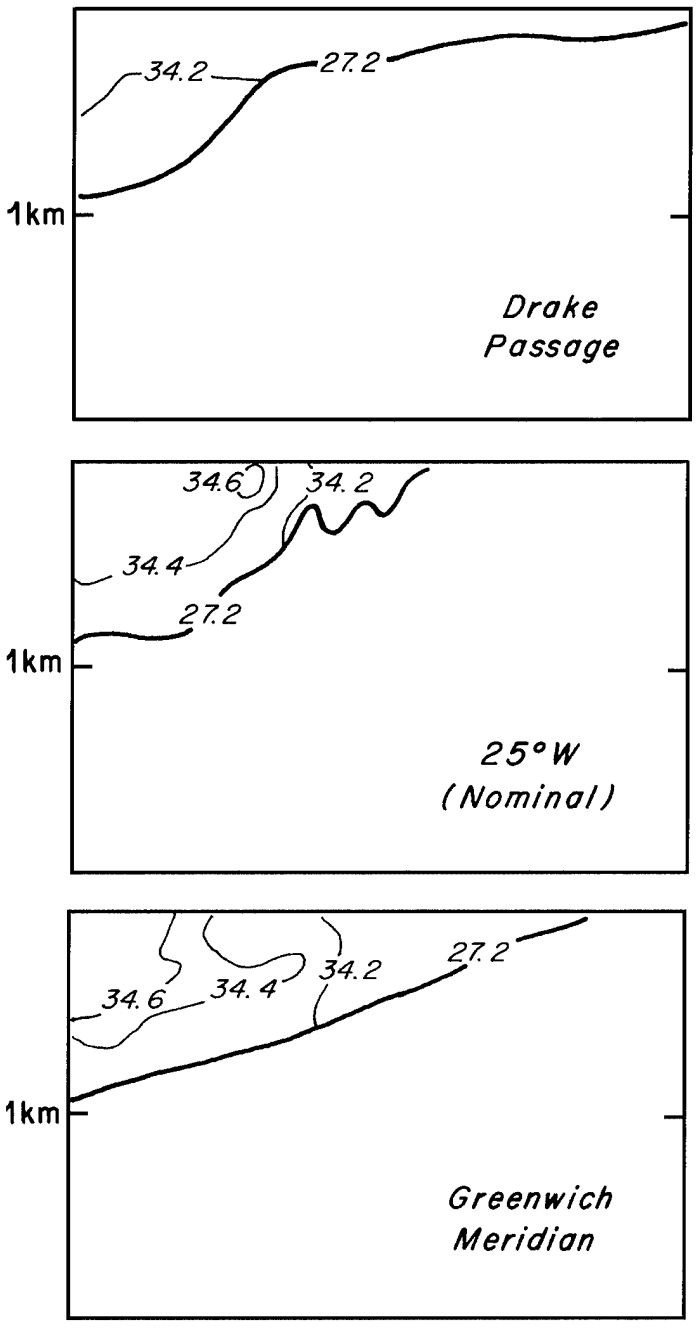

Figure II-158: A superposition of the salinity contours in the area above σ_θ = 27.2, for the SFZ at the indicated sections.

of IODW there in the Banda Sea. Global mass conservation requires formation of 5 Sv LOIW by some mechanism or mechanisms not involved with the Indian Ocean meridional cell according to RT96, taken in Figure II-156 to be a conventional process symbolically. A total conversion of 8 Sv LOIW to LSAMW is also required, which I do by upwelling in the eastern South Pacific via the composite Peru Current System, as discussed previously. It should be understood that in all of my discussions of the intermediate water associated with interbasin circulations, there is no intent to limit or specify the "total" amount of intermediate water formed in any part of the ocean, by whatever mechanisms. Here we are addressing the water mass conversions associated with the global scale interbasin or interocean circulation. In Figure II-156 the red arrows represent a composite upper ocean pathway, which will be mapped into 4 layers later in this section. But first I would like to summarize my current views on the *T/S* characteristics of UPIW entering the southern South Atlantic through Drake Passage.

5. Global Summary

A partial resolution of the dilemma connected with how the very cold and fresh intermediate water in Drake Passage (the UPIW or lower SAMW component, S95) makes its way into the subtropical South Atlantic via the BCS may be associated with the information presented in Figures II-157 and II-158. These figures, in combination with the sections (please see Figures II-149, 150, 152 and 153) used in the inverse calculations by R8891, and a recent section (please see Figure II-143) along 25°W (nominally; Tsuchiya *et al.*, 1994) can be used to examine the evolution of the *T/S* characteristics of UPIW originating in Drake Passage as it transits the southern South Atlantic. First, Figure II-157 (Peterson, 1992) shows how the Falkland or Malvinas Current, which originates in the SFZ in Drake Passage, in its northern end where UPIW is prominent (Figures II-148 and 150), might interact (mix) with the Brazil Current and, in general, the subtropical gyre of the South Atlantic Ocean as it makes its way toward the BCS alongside the STC. The interaction between the Malvinas Current and the Brazil Current Regime, which occurs in the Brazil–Malvinas (Falkland) Confluence, including the characteristics of cut-off eddies there, is well documented (Garzoli and Garraffo, 1989; Gordon, 1989); please also see Section 4. The Brazil–Malvinas (Falkland) Confluence is marked by a complex array of strongly contrasting water types (Gordon, 1989) that could be associated with a diapycnal conversion of UPIW to SAMW as well as with an isopycnal increase in the *T/S* characteristics of the UPIW from Drake Passage. A neat possibility would be if the Brazil Current System and the cut-off eddies there that interact with the UPIW from Drake Passage were provided with the heat and salt to do so by cut-off eddies from the Agulhas Retroflection.

Figure II-158 is a superposition of salinity contours on the area above $\sigma_\theta = 27.2$, for sections across Drake Passage, along 25°W (nominal, please see Section 4), and down the Greenwich Meridian. In each case, the section spans the SFZ, which occupies different latitude ranges at each location. Data from the various sections listed were shown previously as Figures II-143, 148, 150, 152 and 153 and discussed in Section 4 of this report. It is clear in Figure II-158 that there is an increase in the salinity for the UPIW σ_θ range from the Drake Passage section to the 25°W section and then to the Greenwich section. Stramma and Peterson (1990) discuss the northern 10° of the *Knorr* section along 1°E (nominally called Greenwich by Whitworth and Nowlin, 1987; previously shown here in Figures II-152–154) from the point of view of determining the transport of the upper 1000 m near the STC, which they identify as the South Atlantic

Current. From their figure 5, I estimate that about 10 Sv of water in the range $26.8 \leq \sigma_\theta \leq 27.2$ is moving eastward between 35 and 41°S. This water has salinities from 34.2 to 34.8 psu, temperatures from 4 to 9°C, and occupies the depth range from 4–500 m to 8–900 m depending on location. Clement and Gordon (1995) find about 8 Sv moving north with the BCS in the 4–9°C temperature range. So there is no insurmountable problem in getting, say, 7 Sv UPIW from Drake Passage into the BCS, during which transit 3 Sv UPIW (LSAMW) are diapycnally modified to USAMW ($26.5 \leq \sigma_\theta \leq 26.8$). The contribution to the BCS due to "leakage" from the Agulhas Current, which has been taken in Figure II-155 to be equal to the contribution from Drake Passage (both 7 Sv), is presumably concentrated above 9°C, involving perhaps 1 or 2 Sv (UPIW, LSAMW) below this horizon. Rintoul (1988, p. 118) takes the modification of UPIW between Drake Passage and 32°S to be associated with an atmospheric interaction, but I don't see how the atmosphere can lead to a sizable increase in the salinity of IW, or how atmospheric-driven upwelling only can raise the temperature of UPIW to the USAMW ($26.5 \leq \sigma_\theta \leq 26.8$; $\overline{T}$ at 32°S is 13°C) range, from the range $26.8 \leq \sigma_\theta \leq 27.2$, $\overline{T}$ at 32°S is 6.7°C.

Since the circulation of UPOCNW (all water above deep water) is a focal point for a variety of interbasin exchanges and meridional cell return flows, my current guess at a global transport cartoon for UPOCNW in a 4-layer format is shown in Figure II-159. This figure reflects the alternative meridional cells presented in Figures II-69 and II-130, for the Pacific and Indian Oceans respectively. So II-156 is based on the meridional cell #1 guesses (Figures II-68 and 129), and II-159 depicts the more complicated meridional cell #2 guesses. Figure II-159 is not meant to represent the circulation of the upper ocean in general, only that component involved in interbasin exchange. I am somewhat arbitrarily in Figure II-159 making suggestions (decisions) about the relative transports associated with the different formation mechanisms for various brands of intermediate water, by necessity. But I am doing so only in terms of the interbasin flows, and definitely not intending to limit the formation amplitudes or characteristics for the various recirculations of SAMW and AAIW. That is, whereas in Figures 156 and 159 only a few Sverdrups each of LSAMW and AAIW out of a total of 14 Sv involved in NADW replacement are shown being formed, in order to balance the top-to-bottom global thermohaline circulation, it is clear that much more LSAMW and AAIW are formed but recirculate in the various ocean basins.

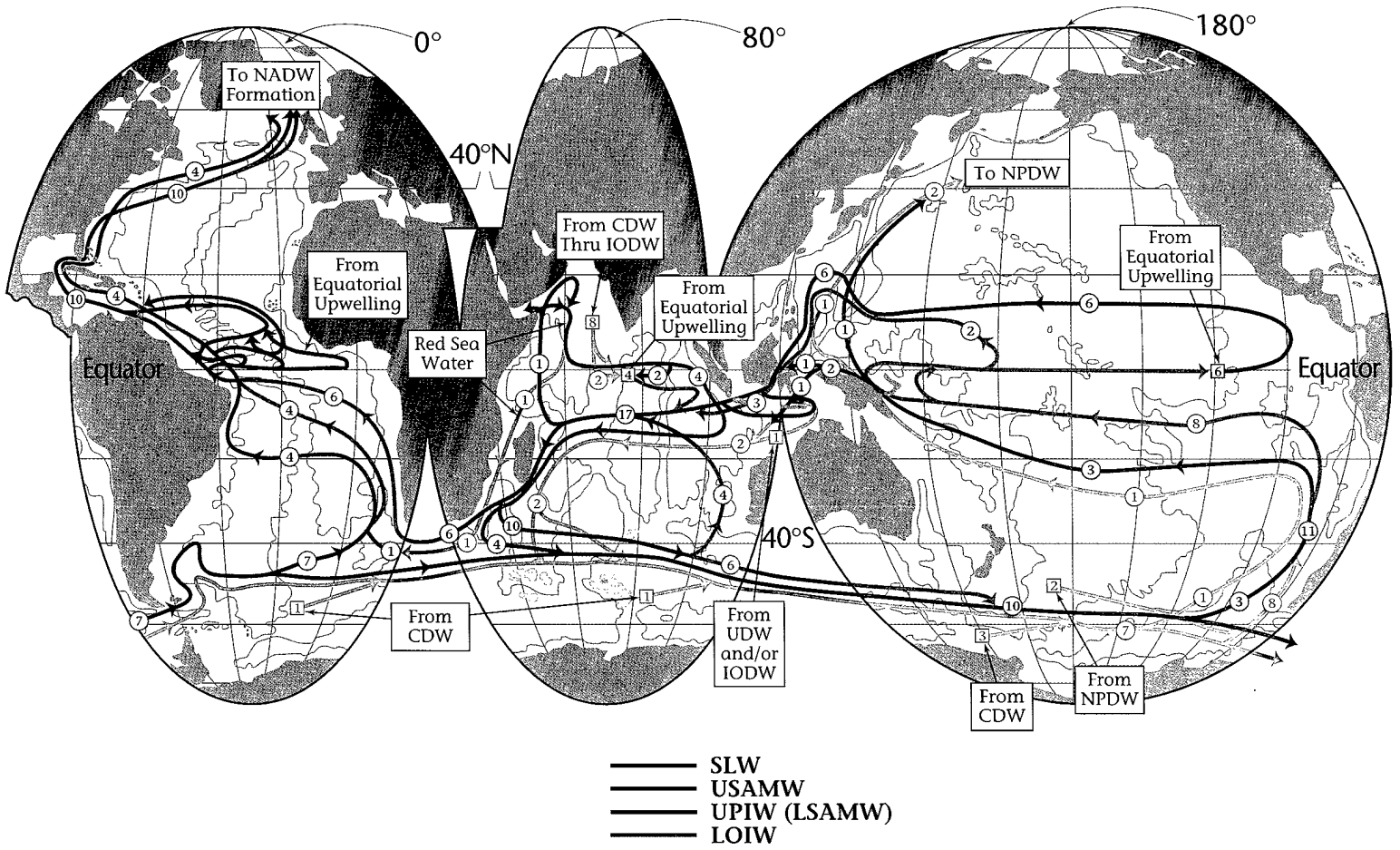

Figure II-159: A global description of the interbasin circulation in the upper ocean in four layers, as described in detail in the text. Transports in circles in Sverdrups.

I also want to reiterate that the results concerning the intermediate water associated with the meridional cell in the Indian Ocean by RT96, along with my attempt to account for the evolution of the characteristics of IW in the South Atlantic and South Pacific, have led me to rethink and change the IW picture presented by S95. All of this couples the Indonesian Throughflow and NADW replacement more strongly than S95. Also in S95, when I suggested an interaction between the deep/bottom cells in oceans other than the Atlantic, I was thinking primarily of the Indian Ocean, along with a general need to convert NADW to CDW. But in this report, I have added the possibility of a stronger coupling for the Pacific, where NPDW may be converted directly to LOIW in the easternmost high-latitude South Pacific, and have noted that this might also happen at the same general location for IODW. That is, the upper deep waters formed from Lower Circumpolar Deep Water in the Indian and Pacific Oceans may be an important link in the water mass conversion processes necessary to convert NADW to its replacement flow. Perhaps it should be restated at this point that I'm also more or less ignoring upper ocean thermohaline processes that are not directly coupled to the deep/bottom cells, *i.e.*, various mode waters other than SAMW. Parts of the large-scale (*i.e.*, top-to-bottom) meridional cells discussed here could "pass through," for example, 18° Water.

For upper intermediate water, I take the primary circumpolar formation mechanism to be convection to LSAMW near the SFZ, an especially strong process in the southernmost and eastern South Pacific (McCartney, 1977, 1982; McCartney and Baringer, 1993), and take NIIW as 4 Sv of upper intermediate water whose source is associated with the meridional cell (RT96) in the Indian Ocean. Northwest Indian Intermediate Water is also possibly modified to LSAMW in the SFZ in the South Pacific. In Figure II-159, 8 Sv SLW from the flow of IT into the Indian Ocean, as well as the 2 Sv of Circumpolar Deep Water converted to SLW by RT96, are converted to a variety of brands of Subantarctic Mode Water, including Lower SAMW, after exiting the Agulhas Front to the SFZ south of the Indian Ocean, and thence south of Australia and across the Pacific Ocean. The 2 Sv SLW and 4 Sv NIIW from the meridional cell in the Indian Ocean are shown being converted upward from IODW through LOIW in Figure II-159 by a 6-Sv green box in the North Indian Ocean. This water is transformed to UPIW (red) and flows across the equator in Figure II-159 off the coast of Sumatra. Some of this water also flows eastward in a boundary current off Java before turning westward

into the SEC. Of this 6 Sv, 2 is converted to SAMW and then SLW in the equatorial regime and 4 Sv flows southward across 32°S as upper intermediate water in the ACS as required by RT96.

In addition to lower intermediate water being an end product of convection in the SAMW regime, I take 5 Sv of transformed NADW within the PFZ to form AAIW. This 5 Sv could be formed "conventionally" by upwelling product(s) of NADW, and is arbitrarily spread out amongst the various ocean basins in Figure II-159. In Figure II-156 this was shown as a single transformation south of Australia for simplicity. Alternatively, the needed 5 Sv of LOIW from below could be formed by transformation upward of IODW and NPDW. Lower intermediate water formed (3 Sv) in the Indian Ocean (possibly some BIW, Section 3d) as part of the meridional cell contributes to the global picture also. In Figure II-159, I form and transport 2 Sv of Banda Intermediate Water in a somewhat different manner (consistent with Figures II-69 and II-130) than I did in Figure II-156, which involved 3 Sv of BIW and was based on Figures II-68, 129 and 155. Other new features in Figure II-159 relative to Figure II-156 involve Red Sea Water (1 Sv) and IW flow (1 Sv) in the Indonesian Throughflow, as discussed below. In Figure II-156, we have 21 Sv of deep water joining the PFZ, basically composed of 7 Sv modified AABW that is converted back to AABW south of the PFZ, and 14 Sv NADW. Some of the latter directly joins the PFZ and some enters the South Indian Ocean and either is converted upward (2 Sv, RT96) or recirculates (~ 5 Sv, RT96) back to the PFZ south of the Indian Ocean to be "homogenized" to Circumpolar Deep Water. In Figure II-159 (and II-69), there are in addition 2 Sv of NPDW shown converted to LOIW in the southern South Pacific and back to NPDW in the North Pacific, a minor coupling of IW with the deep/bottom cell in the Pacific Ocean.

The basic problem in the upper ocean is to determine how the 14 Sv of incoming North Atlantic Deep Water is converted to various layers within UPOCNW, and resupplied to the North Atlantic. In Figure II-159, the upper ocean (UPOCN) is split into the following layers: (1) SLW, $\sigma_\theta \leq 26.5$, purple line; (2) USAMW, $26.8 \geq \sigma_\theta \geq 26.5$, blue line; (3) UPIW or LSAMW, $27.2 \geq \sigma_\theta \geq 26.8$, red line; and (4) LOIW or AAIW, 27.5(or 6) $\geq \sigma_\theta \geq 27.2$, green line. Red Sea Water in the North Indian Ocean, according to Rochford (1964), is on the borderline between UPIW and LOIW, being characterized by a salinity maximum between 27.1 and 27.4. Here I take the upper density range of the water affected by the overflow from the Red Sea to be NIIW and use RSW for the range

$27.2 \leq \sigma_\theta \leq 27.4$ to be the flow from the North Indian Ocean (1 Sv as a guess) that penetrates into the southern Indian Ocean in the west, presumably through Mozambique Channel, at least to some extent (Gründlingh, 1985). Since Figure II-159 represents a detailed and closed volume flux budget for the UPOCNW distribution for the most complicated meridional cells, Figures II-69 and II-130, the reader not interested in a lot of nitty-gritty should stop with Figures II-68, 129, and 156. We now start our wrap-up description of Figure II-159 in the northern Indian Ocean. The meridional cell converts 6 Sv of CDW to lower intermediate water to NIIW in the northern Indian Ocean in Figure II-159, and 2 Sv of this is converted to Upper Subantarctic Mode Water and then SLW near the equator. The remaining 4 Sv of NIIW crosses the equator off Sumatra and eventually flows with the South Equatorial Current into the ACS and Agulhas Front, and thence joins the SFZ in the Crozet Basin. The 2 Sv of SLW so formed near the equator also joins the SEC and ACS and SFZ where it is converted to USAMW and eventually LSAMW (UPIW) in the South Pacific by established means (McCartney, 1977, 1982). This composite 6 Sv, from the upward limb (RT96) of the meridional cell in the Indian Ocean, exits Drake Passage as upper intermediate water and joins the BCS.

According to RT96, 3 Sv of LOIW are formed by the meridional cell in the Indian Ocean and exit southward in the ACS at 32°S. In Figure II-156 these 3 Sv originate in the eastern tropical South Pacific as BIW, possibly involving some recirculation in the Banda Sea. These 3 Sv then exit the ACS southward at 32°S and flow either into the SFZ or into the South Atlantic, because no distinction needs to be made in that figure. This scheme is modified in Figure II-159 in a variety of ways, although 3 Sv of LOIW still exit the ACS southward at 32°S as required by RT96. One Sverdrup of intermediate water joins BIW from the Pacific through the IT in Figure II-159 (please see Figures II-69 and 130). This 1 Sv of UPIW from the Indonesian Throughflow joins 1 Sv of IODW that is diapycnally raised in the North Australian Bight to LOIW in a recirculation and transformation process in the Banda Sea. This 2 Sv then exits the ACS across 32°S into the SFZ toward the South Pacific. One Sverdrup of RSW is formed in the northern Indian Ocean, crosses the equator in the west, and joins the ACS. There it flows around the tip of Africa into the BCS, being converted to UPIW and SAMW on the way. Red Sea Water (1 Sv) is joined by 6 Sv of SLW from the IT around the tip of Africa being converted to USAMW in the BCS.

Since the meridional cell in the Indian Ocean converts (RT96) 9 Sv of CDW to LOIW and above, the other 5 Sv required for NADW replacement is shown in Figure II-156 (and II-159) being converted to LOIW by the "classic wind-driven upwelling and subduction" mechanism. The areas of this conversion in Figure II-159 are somewhat arbitrarily taken to be 1 Sv Atlantic sector, 1 Sv Indian, and 3 Sv Austral–Pacific, due to the immense area and strong winds there. Other mechanisms are of course possible, as indicated throughout this report. This 5 Sv of AAIW (LOIW) is shown upwelling to UPIW (LSAMW) in the Peru Current regime off Chile, along with 2 Sv Banda Intermediate Water and 2 Sv NPDW. The 8 Sv lower intermediate water converted to LSAMW (UPIW) off Chile is transformed to USAMW off Peru and flows in the SEC across the South Pacific and through Vitiaz Strait. Modifications along various paths in the subtropical gyre are also possible mechanisms for diapycnal upward modification of IW and UPIW. Six of the 8 Sv of USAMW flowing through Vitiaz Strait are converted to SLW in the equatorial current regime and supplied to the IT via the Mindanao Current. Two Sverdrups UPIW and 2 Sv USAMW also impinge on the Indonesian basins, and emerge into the Indian Ocean as 3 Sv Upper Subantarctic Mode Water, along with the 1 Sv upper intermediate water that joins 1 Sv Indian Ocean Deep Water to form 2 Sv LOIW (BIW).

6. Discussion, Conclusions and Gazing Ahead

My major interest in the Pacific and Indian Oceans in this report has been in how they fit into the global interbasin circulation picture and in how the mesoscale eddy field is similar or not in different ocean basins. The South Indian Ocean is distinct from the other southern hemisphere oceans in that the South Atlantic and South Pacific subtropical gyres are weakened by their "loss" of transport north across the equator, whereas the South Indian Ocean subtropical gyre is strengthened by the Indonesian Throughflow and by the upward diapycnal limb of a large-scale meridional cell, a total of about 19 Sv, roughly 12 Sv SLW and 7 Sv IW. The North Atlantic subtropical gyre is enhanced by a thermohaline flow in the UPOCN of about 14 Sv, roughly 9 Sv SLW and 5 Sv IW. The South Indian Ocean eddy field is much like that for the North Atlantic in K_E amplitude and vertical structure and frequency spectrum, and the Agulhas Current and the Gulf Stream are similar not only in transport, but also in their structure in density parameter space. The flow from the South to North Pacific is of the same general size as is the case in the Atlantic, about 13 Sv, with about the same vertical partitioning (roughly 10 Sv surface layer water, 3 Sv IW). However, most of this transport is to supply the Indonesian Throughflow, and not to enhance the subtropical gyre circulation or eddy field in the North Pacific anything like the North Atlantic or South Indian Oceans.

Since most of my time and energy in Volume II of this report has been spent on the meridional cells and interbasin circulations for the Pacific and Indian Oceans, I haven't spent enough time or accomplished as much as I had hoped in reviewing the global mesoscale eddy field, especially including numerical model relevance. I'm hoping to spend time on these topics while "retired." My gut feeling is that eddy-resolving numerical models need comparatively a lot of horizontal resolution to get the mix of instability processes "right" in western boundary currents. Unfortunately, they also need a reasonable depiction of the thermohaline interbasin circulations to get relevant eddy field characteristics. The details of the eddy field are necessary to determine the characteristics of the global interbasin circulation in some areas, but not in others. But high resolution may be required for places where the large scale circulation of whatever ilk is dynamically of short scale intrinsically or goes through narrow straits/passages, or in general where topographic variations at short scale are important. Unfortunately, when coupled with the demanding tasks of understanding a variety of scale

transfer mechanisms, all of this makes the realization of relevant numerical experiments a tremendous task.

Some of the hottest topics in physical oceanography today involve the role of the ocean in climate variability. My report has unfortunately directly contributed almost zero to this range of topics, but indirectly the ocean climate may actually represent fluctuations in the large-scale circulation, the main topic of my report. I have been exposed lately to a lot of discussion about decadal scale variability in the northern North Atlantic, primarily in conversations with Mike McCartney. It seems to me that one basic message there is that ocean climate is really to a large extent low-frequency variability in the general circulation of the northern North Atlantic, partly as described in this report, Volume I mostly. So I hope that the material I've presented here could be used in this context as well, perhaps including other areas. There could easily be climatic signals of significance associated with low-frequency temporal variability in a variety of the segments of the interbasin cells I've presented in this report. For example, if there were decadal variability in the Agulhas Leakage due to decadal variability in the Indonesian Throughflow due to El Niño–Southern Oscillation phenomena, how would this variation in the replacement flow for NADW affect the decadal scale variability observed in the northern North Atlantic? Could the ocean be forcing the atmosphere in this regard?

Although this report is written in summary form and will hopefully be a useful reference, it also contains several new and somewhat speculative descriptions of ocean circulation patterns. Nearly all of the comments about the role of IW in the Global Thermohaline and/or Interbasin Circulation that are in S95 or this report are in that category. My reference lists are comparatively very extensive, but I apologize in advance if I've overlooked a personal contribution. Of course I ended up running out of time to complete this report by my retirement date.

Acknowledgements

This report and 35 years of oceanographic research were supported primarily by the Office of Naval Research to whom I am deeply grateful. I know of no finer organization to be associated with. Craig Dorman and Fred Saalfeld and Paul Gaffney have my respect for their leadership ability. It was very helpful talking to Terry Joyce, Paul Robbins, John Toole and Susan Wijffels about the Indian and Pacific Oceans. I have been fortunate to have had a rewarding interaction with Arnold Gordon throughout my excursion into the interbasin circulation world. This journey started during conversations with Lynne Talley and Joe Reid and began to develop while I was a visitor at the Institut für Meereskunde, Kiel. Some of my ideas about the upward limb of the thermohaline cell in the Indian Ocean were moved along while I was visiting the Scripps Institution of Oceanography in early 1995, when Arnold Mantyla and Joe Reid kindly shared their data and ideas with me.

My recognition that Rochford's work on intermediate water in the Indian Ocean probably defines the intermediate water components of the meridional cell there was recent and to some extent accidental, but stimulated by the fact that Mike McCartney suggested some years ago that I take a look at Rochford's publications. I am more than grateful to Mike for countless good interactions over the years, and Paul Robbins and Susan Wijffels significantly helped me with Volume II. I've had very good luck collaborating with Bill Holland, Dana Thompson, Harley Hurlburt, Jay Shriver, Lakshmi Kantha, and Charles Horton in the model–data intercomparison arena. I have also been most fortunate to have the assistance of Barbara Gaffron, Elizabeth Suwijn, Toshiko Turner, Jack Cook and Jeannine Pires in producing this report. The last 10 years or so of my career has been much enhanced by Barbara Gaffron's involvement at many levels.

References

Barton, E. D., and A. E. Hill, Abyssal flow through the Amirante Trench (western Indian Ocean), *Deep-Sea Res.*, *36*, 1121–1126, 1989.

Belkin, I. M., and A. L. Gordon, Southern Ocean fronts from the Greenwich meridian to Tasmania, *J. Geophys. Res.*, *101*, 3675–3696, 1996.

Bernstein, R. L., and W. B. White, Time and length scales of baroclinic eddies in the central North Pacific Ocean, *J. Phys. Oceanogr.*, *4*, 613–624, 1974.

Bernstein, R. L., and W. B. White, Zonal variability in the distribution of eddy energy in the mid-latitude North Pacific Ocean, *J. Phys. Oceanogr.*, *7*, 123–126, 1977.

Bernstein, R. L., and W. B. White, Stationary and traveling mesoscale perturbations in the Kuroshio Extension Current, *J. Phys. Oceanogr.*, *11*, 613–624, 1981.

Bingham, F., and R. Lukas, The southward intrusion of North Pacific Intermediate Water along the Mindanao coast, *J. Phys. Oceanogr.*, *24*, 141–154, 1994.

Bingham, F. M., and L. D. Talley, Estimates of Kuroshio transport using an inverse technique, *Deep-Sea Res.*, *38*, S21–S43, 1991.

Boland, F. M., and J. A. Church, The East Australian Current 1978, *Deep-Sea Res.*, *28*, 937–957, 1981.

Boland, F. M., and B. V. Hamon, The East Australian Current, 1965–1968, *Deep-Sea Res.*, *17*, 777–794, 1970.

Boudra, D. B., and E. P. Chassignet, Dynamics of Agulhas retroflection and ring formation in a numerical model, Part I: The vorticity balance, *J. Phys. Oceanogr.*, *18*, 280–303, 1988.

Bradley, K. F., Technical activities associated with an exploratory array in the western North Pacific, Woods Hole Oceanog. Inst. Tech. Rept., WHOI-82-41, 40 pp., 1982.

Bray, N. A., S. Hautala, J. Chong, and J. Pariwono, Large-scale sea level, thermocline, and wind variations in the Indonesian Throughflow region, *J. Geophys. Res.*, *101*, 12,239–12,254, 1996.

Bruce, J. G., Eddies off the Somali coast during the Southwest Monsoon, *J. Geophys. Res.*, *84*, 7742–7748, 1979.

Bryden, H. L., Poleward heat flux and conversion of available potential energy in Drake Passage, *J. Mar. Res.*, 37, 1–22, 1979.

Bryden, H. L., D. H. Roemmich, and J. A. Church, Ocean heat transport across 24°N in the Pacific, *Deep-Sea Res., 38,* 297–324, 1991.

Burling, R. W., Hydrology of circumpolar waters south of New Zealand, *New Zealand Department of Scientific and Industrial Research Bulletin, 143*, 66 pp., 1961.

Butt, J., and E. Lindstrom, Currents off the east coast of New Ireland, Papua New Guinea, and their relevance to regional undercurrents in the western equatorial Pacific Ocean, *J. Geophys. Res., 99*, 12,503–12,514, 1994.

Cane, M. A., and E. S. Sarachik, Equatorial oceanography, *U.S. National Report to International Union of Geodesy and Geophysics 1979–1982*, Suppl. to *Rev. Geophys., 21*, 1137–1148, 1983.

Chassignet, E. P., and D. B. Boudra, Dynamics of Agulhas retroflection and ring formation in a numerical model, Part II: Energetics and ring formation, J. *Phys. Oceanogr.*, *18*, 304–319, 1988.

Chassignet, E. P., D. B. Olson, and D. B. Boudra, Motion and evolution of oceanic rings in a numerical model and in observations, *J. Geophys. Res., 95*, 22,121–22,140, 1990.

Chen, C., R. C. Beardsley, and R. Limeburner, The structure of the Kuroshio southwest of Kyushu: Velocity, transport and potential vorticity fields, *Deep-Sea Res., 39*, 245–268, 1992.

Church, J. A., G. R. Cresswell, and J. S. Godfrey, The Leeuwin Current, in *Poleward Flows Along Eastern Ocean Boundaries, Coastal and Estuarine Studies,* Vol. *34*, S. J. Neshyba, C. N. K. Mooers, R. L. Smith, and R. T. Barber, editors, pp. 230–254, Springer-Verlag, New York; 1989.

Clement, A. C., and A. L. Gordon, The absolute velocity field of Agulhas eddies and the Benguela Current, *J. Geophys. Res., 100*, 22,591–22,601, 1995.

Clifford, M. A., A descriptive study of the zonation of the Antarctic Circumpolar Current and its relation to wind stress and ice cover, M.S. Thesis, 93 pp., Texas A&M University, College Station, 1983.

References

Clowes, A. J., An introduction to the hydrology of South African waters, *Invest. Rep. Fish. Mar. Biol. Surv., S. Afr., 12*, pp. 1–42, 20 charts, 1950.

Cox, M. D., A baroclinic numerical model of the world ocean, in *Numerical Models of Ocean Circulation*, Proceedings of a Symposium held at Durham, New Hampshire, 17–20 October 1972, pp. 107–120, 1975.

Cresswell, G. R., and T. J. Golding, Observations of a south-flowing current in the southeastern Indian Ocean, *Deep-Sea Res., 27A*, 449–466, 1980.

Cresswell, G. R., T. J. Golding, and F. M. Boland, A buoy and ship examination of the subtropical convergence south of Western Australia, *J. Phys. Oceanogr., 8,* 315–320, 1978.

Cresswell, G., A. Frische, J. Peterson, and D. Quadfasel, Circulation in the Timor Sea, *J. Geophys. Res., 98*, 14,379–14,389, 1993.

da Silveira, I. C. A., L. B. de Miranda, and W. S. Brown, On the origins of the North Brazil Current, *J. Geophys. Res., 99*, 22,501–22,512, 1994.

Deacon, G. E. R., A general account of the hydrology of the South Atlantic Ocean, *Discovery Rep., 7,* 171–238, 1933.

Deacon, G. E. R., The hydrology of the Southern Ocean, *Discovery Rep., 15*, 1–124, 1937.

Deacon, G. E. R., The Southern Ocean, in *The Sea*, Volume *2*, M. N. Hill, editor, John Wiley & Sons, New York, pp. 281–296, 1963.

De Madron, X. D., and G. Weatherly, Circulation, transport and bottom boundary layers of the deep currents in the Brazil Basin, *J. Mar. Res., 52*, 583–638, 1994.

Dickson, R. R., Global summaries and intercomparisons: Flow statistics from long-term current meter moorings, Chapter 15 in *Eddies in Marine Science*, A. R. Robinson, editor, Springer-Verlag, Berlin, pp. 278–353, 1983.

Dickson, R. R., Flow statistics from long-term current-meter moorings, the global data-set in January 1989, World Ocean Circulation Experiment Report No. 46/90, WOCE International Project Office, Wormley, U.K.; World Climate Research Programme WCRP-30 (WMO/TD-No. 337), World Meteorological Organization, Geneva, Switzerland; 413 pp., 1989.

Duncombe Rae, C. M., Agulhas Retroflection rings in the South Atlantic Ocean: An overview, *S. Afr. J. Mar. Sci., 11*, 327–344, 1991.

Duncombe Rae, C. M., F. A. Shillington, J. J. Agenbag, J. Taunton-Clark, and M. L. Gründlingh, An Agulhas ring in the South Atlantic Ocean and its interaction with the Benguela upwelling frontal system, *Deep-Sea Res., 39*, 2009–2027, 1992.

Duncombe Rae, C. M., S. L. Garzoli, and A. L. Gordon, The eddy field of the southeast Atlantic Ocean: A statistical census from the Benguela Sources and Transports project, *J. Geophys. Res., 101*, 11,949–11,964, 1996.

Edmond, J. M., S. S. Jacobs, A. L. Gordon, A. W. Mantyla, and R. F. Weiss, Water column anomalies in dissolved silica over opaline pelagic sediments and the origin of the deep silica maximum, *J. Geophys. Res., 84*, 7809–7826, 1979.

Emery, W. J., On the geographical variability of the upper level mean and eddy fields in the North Atlantic and North Pacific, *J. Phys. Oceanogr., 13*, 269–291, 1983.

Eriksen, C. C., Evidence for a continuous spectrum of equatorial waves in the Indian Ocean, *J. Geophys. Res., 85*, 3285–3303, 1980.

Eriksen, C. C., Geostrophic equatorial deep jets, *J. Mar. Res., 40*, suppl., 143–157, 1982.

Ffield, A., and A. L. Gordon, Vertical mixing in the Indonesian thermocline, *J. Phys. Oceanogr., 22*, 184–195, 1992.

Fieux, M., and C. Levy, Seasonal observations in the western Indian Ocean, in *Hydrodynamics of the Equatorial Ocean*, J. C. J. Nihoul, editor, Elsevier Science Publishers B.V., Amsterdam, pp. 17–29, 1983.

Fieux, M., C. Andrié, P. Delecluse, A. G. Ilahude, A. Kartavtseff, F. Mantisi, R. Molcard, and J. C. Swallow, Measurements within the Pacific–Indian oceans throughflow region, *Deep-Sea Res. I, 41*, 1091–1130, 1994.

Fieux, M., R. Molcard, and A. G. Ilahude, Geostrophic transport of the Pacific–Indian Oceans throughflow, *J. Geophys. Res., 101*, 12,421–12,432, 1996a.

References

Fieux, M., C. Andrié, E. Charriaud, A. G. Ilahude, N. Metzl, R. Molcard, and J. C. Swallow, Hydrological and chlorofluoromethane measurements of the Indonesian throughflow entering the Indian Ocean, *J. Geophys. Res., 101*, 12,433–12,454, 1996b.

Fine, R. A., Direct evidence using tritium data for throughflow from the Pacific into the Indian Ocean, *Nature, 315*, 478–480, 1985.

Fine, R. A., Circulation of Antarctic Intermediate Water in the South Indian Ocean, *Deep-Sea Res. I, 40*, 2021–2042, 1993.

Fine, R. A., R. Lukas, F. M. Bingham, M. J. Warner, and R. H. Gammon, The western equatorial Pacific: A water mass crossroads, *J. Geophys. Res., 99,* 25,063–25,080, 1994.

Firing, E., Deep zonal currents in the central equatorial Pacific, *J. Mar. Res., 45*, 791–812, 1987.

Firing, E., Shallow equatorial jets, *J. Geophys. Res., 93*, 9213–9222, 1988.

Flagg, C. H., R. L. Gordon, and S. McDowell, Hydrographic and current observations on the continental slope and shelf of the western equatorial Atlantic, *J. Phys. Oceanogr., 16*, 1412–1429, 1986.

Fukasawa, M., T. Teramoto, and K. Taira, Abyssal current along the northern periphery of Shikoku Basin, *J. Oceanogr. Soc. Japan, 42,* 459–472, 1987.

Garzoli, S. L., and Z. Garraffo, Transports, frontal motions and eddies at the Brazil–Malvinas Currents Confluence, *Deep-Sea Res., 36,* 681–703, 1989.

Garzoli, S. L., and A. L. Gordon, Origins and variability of the Benguela Current, *J. Geophys. Res., 101*, 897–906, 1996.

Godfrey, J. S., A Sverdrup model of the depth-integrated flow for the world ocean allowing for island circulations, *Geophys. Astrophys. Fluid Dyn., 45*, 89–112, 1989.

Godfrey, J. S., The effect of the Indonesian throughflow on ocean circulation and heat exchange with the atmosphere: A review, *J. Geophys. Res., 101,* 12,217–12,237, 1996.

Godfrey, J. S., and T. J. Golding, The Sverdrup Relation in the Indian Ocean, and the effect of Pacific–Indian Ocean throughflow on Indian Ocean circulation and on the East Australian Current, *J. Phys. Oceanogr., 11,* 771–779, 1981.

Godfrey, J. S., and K. R. Ridgway, The large-scale environment of the poleward-flowing Leeuwin Current, Western Australia: Longshore steric height gradients, wind stresses and geostrophic flow, *J. Phys. Oceanogr., 15,* 481–495, 1985.

Godfrey, J. S., A. C. Hirst, and J. Wilkin, Why does the Indonesian Throughflow appear to originate from the North Pacific?, *J. Phys. Oceanogr., 23*, 1087–1098, 1993.

Gordon, A. L., Oceanography of Antarctic Water, in *Antarctic Oceanography I. Antarctic Research Series*, J. L. Reid, editor, American Geophysical Union, *15*, pp. 169–203, 1971.

Gordon, A. L., An Antarctic oceanographic section along 170°E, *Deep-Sea Res., 22,* 357–377, 1975.

Gordon, A. L., *Southern Ocean Atlas*, 44 pp., 248 plates, 29 microfiche, Columbia Univ. Press, New York; 1982.

Gordon, A. L., Interocean exchange of thermocline water, *J. Geophys. Res., 91,* 5037–5046, 1986.

Gordon, A. L., Brazil–Malvinas Confluence—1984, *Deep-Sea Res., 36*, 359–384, 1989.

Gordon, A., The role of thermohaline circulation in global climate change, in *Lamont-Doherty Geological Observatory 1990 & 1991 Report*, Lamont-Doherty Geological Observatory of Columbia University, Palisades, New York, pp. 44–51, 1991.

Gordon, A. L., When is appearance reality? A comment on why does the Indonesian Throughflow appear to originate from the North Pacific, *J. Phys. Oceanogr., 25,* 1560–1570, 1995.

Gordon, A. L., and K. T. Bosley, Cyclonic gyre in the tropical South Atlantic, *Deep-Sea Res., 38*, Suppl. 1, S323–S343, 1991.

Gordon, A. L., R. F. Weiss, W. M. Smethie, Jr. and M. J. Warner, Thermocline and intermediate water communication between the South Atlantic and Indian Oceans, *J. Geophys. Res., 97*, 7223–7240, 1992.

References

Gründlingh, M. L., Eddies in the southern Indian Ocean and Agulhas Current, Chapter 13 in: *Eddies in Marine Science*, A. R. Robinson, editor, Springer-Verlag, Berlin, pp. 245–264, 1983.

Gründlingh, M. L., Occurrence of Red Sea Water in the southwestern Indian Ocean, 1981, *J. Phys. Oceanogr., 15,* 207–212, 1985.

Halkin, D., and T. Rossby, The structure and transport of the Gulf Stream at 73°W, *J. Phys. Oceanogr., 15*, 1439–1452, 1985.

Hall, M. M., Velocity and transport structure of the Kuroshio Extension at 35°N, 152°E, *J. Geophys. Res., 94*, 14,445–14,459, 1989.

Hall, M. M., and H. L. Bryden, Direct estimates and mechanisms of ocean heat transport, *Deep-Sea Res., 29*, 339–359, 1982.

Hall, M. M., and N. P. Fofonoff, Downstream development of the Gulf Stream from 68° to 55°W, *J. Phys. Oceanogr., 23*, 225–249, 1993.

Hallock, Z. R., and W. J. Teague, Evidence for a North Pacific Deep Western Boundary Current, *J. Geophys. Res., 101*, 6617–6624, 1996.

Hamon, B. V., The East Australian Current, 1960–1964, *Deep-Sea Res., 12*, 899–921, 1965.

Hamon, B. V., Western boundary currents in the South Pacific, in *Scientific Exploration of the South Pacific*, W. S. Wooster, ed., pp. 50–59, Symposium held during Ninth General Meeting of the Scientific Committee on Oceanic Research (SCOR), June 18–20, 1968, at La Jolla, Calif.; National Academy of Sciences, Washington, D.C., 1970.

Harris, T. F. W., Sources of the Agulhas Current in the spring of 1964, *Deep-Sea Res., 19*, 633–650, 1972.

Hastenrath, S., and L. Greischar, The monsoonal current regimes of the tropical Indian Ocean: Observed surface flow fields and their geostrophic and wind-driven components, *J. Geophys. Res., 96*, 12,619–12,633, 1991.

Hautala, S. L., and S. C. Riser, A simple model of abyssal circulation, including effects of wind, buoyancy and topography, *J. Phys. Oceanogr., 19*, 596–611, 1989.

Hautala, S. L., and S. C. Riser, A nonconservative–spiral determination of the deep circulation in the eastern South Pacific, *J. Phys. Oceanogr., 23*, 1975–1999, 1993.

Hautala, S. L., D. H. Roemmich, and W. J. Schmitz, Jr., Is the North Pacific in Sverdrup balance along 24°N? *J. Geophys. Res., 99,* 16,041–16,052, 1994.

Hautala, S. L., J. L. Reid, and N. Bray, The distribution and mixing of Pacific water masses in the Indonesian Seas, *J. Geophys. Res., 101*, 12,375–12,389, 1996.

Hirst, A. C., and J. S. Godfrey, The role of Indonesian Throughflow in a global ocean GCM, *J. Phys. Oceanogr., 23*, 1057–1086, 1993.

Hofmann, E. E., The large-scale horizontal structure of the Antarctic Circumpolar Current from FGGE drifters, *J. Geophys. Res., 90*, 7087–7097, 1985.

Hofmann, E. E., and T. Whitworth, III, A synoptic description of the flow at Drake Passage from year-long measurements, *J. Geophys. Res., 90*, 7177–7187, 1985.

Hogg, N. G., Observations of Gulf Stream meander-induced disturbances, *J. Phys. Oceanogr., 24*, 2534–2545, 1994.

Hogg, N. G., and W. E. Johns, Western boundary currents, *U.S. National Report to International Union of Geodesy and Geophysics 1991–1994*, Suppl. to *Rev. Geophys.*, pp. 1311–1334, 1995.

Hogg, N. G., W. B. Owens, G. Siedler, and W. Zenk, Circulation in the Deep Brazil Basin, in: *The South Atlantic: Present and Past Circulation,* G. Wefer, W. H. Berger, G. Siedler, and D. Webb, editors; Springer-Verlag, Berlin, Heidelberg, in press, 1996.

Holland, W. R., The role of mesoscale eddies in the general circulation of the ocean—Numerical experiments using a wind-driven quasi-geostrophic model, *J. Phys. Oceanogr., 8,* 363–392, 1978.

Holland, W. R., and W. J. Schmitz, Zonal penetration scale of model mid-latitude jets, *J. Phys. Oceanogr., 15*, 1859–1875, 1985.

Holland, W. R., V. Zlotnicki and L.-L. Fu, Modelled time-dependent flow in the Agulhas Retroflection Region as deduced from altimeter data assimilation, *S. Afr. J. Mar. Sci., 10*, 407–427, 1991.

References

Hu, J. H., and P. P. Niiler, NEPAC current meter and XBT data, Scripps Inst. Oceanogr. Ref. No. 87-4, 15 pp., 1987.

Hurlburt, H. E., and J. D. Thompson, A numerical model of the Somali Current, *J. Phys. Oceanogr., 6*, 646–664, 1976.

Hurlburt, H. E., A. J. Wallcraft, W. J. Schmitz, Jr., P. J. Hogan, and E. J. Metzger, Dynamics of the Kuroshio/Oyashio current system using eddy-resolving models of the North Pacific Ocean, *J. Geophys. Res., 101*, 941–976, 1996.

Ichikawa, H., and R. C. Beardsley, Temporal and spatial variability of volume transport of the Kuroshio in the East China Sea, *Deep-Sea Res. I, 40*, 583–605, 1993.

Imawaki, S., and K. Takano, Low-frequency eddy kinetic energy spectrum in the deep western North Pacific, *Science, 216*, 1407–1408, 1982.

Jacobs, S. S., and D. T. Georgi, Observations on the southwest Indian/Antarctic Ocean, in: *A Voyage of Discovery*, George Deacon 70th Anniversary Volume, M. V. Angel, editor, supplement to *Deep-Sea Res.*, pp. 43–84, 1977.

Johns, W. E., T. N. Lee, F. A. Schott, R. J. Zantopp, and R. H. Evans, The North Brazil Current retroflection: Seasonal structure and eddy variability, *J. Geophys. Res., 95*, 22,103–22,120, 1990.

Johns, W. E., T. N. Lee, C-T. Liu, and D. Zhang, PCM-1 array monitors Kuroshio transport, *WOCE Notes*, 7(3), 10–13, U.S. WOCE Office, Department of Oceanography, Texas A&M University, College Station, Texas 77843–3146, 1995.

Johns, W. E., T. N. Lee, R. C. Beardsley, J. Candela, R. Limeburner, and B. Castro, Annual cycle and variability of the North Brazil Current, *J. Phys. Oceanogr.*, accepted, 1997.

Johnson, G. C., Near-equatorial deep circulation in the Indian and Pacific Oceans, Ph.D. Thesis, Massachusetts Institute of Technology and Woods Hole Oceanographic Institution, W.H.O.I. Technical Report WHOI-90-50, 160 pp., 1990.

Johnson, G. C., and J. M. Toole, Flow of deep and bottom waters in the Pacific at 10°N, *Deep-Sea Res. I, 40,* 371–394, 1993.

Johnson, G. C., B. A. Warren, and D. B. Olson, Flow of bottom water in the Somali Basin, *Deep-Sea Res., 38,* 637–652, 1991a.

Johnson, G. C., B. A. Warren, and D. B. Olson, A deep boundary current in the Arabian Basin, *Deep-Sea Res., 38,* 653–661, 1991b.

Johnson, G. C., D. L. Rudnick, and B. A. Taft, Bottom water variability in the Samoa Passage, *J. Mar. Res., 52*, 177–196, 1994.

Joyce, T. M., and W. J. Schmitz, Jr., Zonal velocity structure and transport in the Kuroshio Extension, *J. Phys. Oceanogr., 18*, 1484–1494, 1988.

Kawai, H., Hydrography of the Kuroshio Extension, Chapter 8 in *Kuroshio—Its Physical Aspects*, University of Tokyo Press, pp. 235–352, 1972.

Kelly, K. A., The meandering Gulf Stream as seen by the Geosat altimeter: surface transport, position and velocity variance from 73° to 46°W, *J. Geophys. Res., 96*, 16,721–16,738, 1991.

Kindle, J. C., and J. D. Thompson, The 26- and 50-day oscillations in the western Indian Ocean: Model results, *J. Geophys. Res., 94*, 4721–4736, 1989.

Knauss, J. A., Equatorial current systems, Chapter 10 in *The Sea*, M. N. Hill, ed., Volume *2*, Wiley Interscience, New York, pp. 235–252, 1963.

Knauss, J. A., Further measurements and observations on the Cromwell Current, *J. Mar. Res., 24,* 205–240, 1966.

Knox, R. A., and D. L. T. Anderson, Recent advances in the study of the low-latitude ocean circulation, *Prog. Oceanog., 14*, 259–317, 1985.

Koblinsky, C. J., R. L. Bernstein, W. J. Schmitz, Jr., and P. P. Niiler, Estimates of the geostrophic stream function in the western North Pacific from XBT surveys, *J. Geophys. Res., 89,* 10,451–10,460, 1984.

Leaman, K. D., E. Johns, and T. Rossby, The average distribution of volume transport and potential vorticity with temperature at three sections across the Gulf Stream, *J. Phys. Oceanogr., 19,* 36–51, 1989.

Levitus, Climatological Atlas of the World Ocean, *NOAA Professional Paper 13*, U.S. Government Printing Office, Washington, D.C., 173 pp., 1982.

Levy, E., and S. A. Tarbell, A compilation of moored current meter data from the western North Pacific, Volume XXXI, 1980–1982, Woods Hole Oceanog. Inst. Tech. Rept., WHOI-83-30, 54 + v pp. + 7 microfiche, 1983.

References

Lindstrom, E., R. Lukas, R. Fine, E. Firing, S. Godfrey, G. Meyers, and M. Tsuchiya, The Western Equatorial Pacific Ocean Circulation Study, *Nature, 330*, 533–537, 1987.

Lindstrom, E., J. Butt, R. Lukas, and S. Godfrey, The flow through Vitiaz Strait and St. George's Channel, Papua New Guinea, in *The Physical Oceanography of Sea Straits*, L. J. Pratt, editor, NATO ASI Series C, Vol. 318, Kluwer Academic Publishers, Boston, pp. 171–189, 1990.

Liu, C.-T., S.-G. Liau, S.-C. Pai and K.-K. Liu, Water masses in the western Philippine Sea—Physical aspects, *Acta Oceanographica Taiwanica, No. 17*, 1–17, 1986.

Lukas, R., E. Firing, P. Hacker, P. L. Richardson, C. A. Collins, R. Fine, and R. Gammon, Observations of the Mindanao Current during the Western Equatorial Pacific Ocean Circulation Study, *J. Geophys. Res., 96*, 7089–7104, 1991.

Lukas, R., T. Yamagata, and J. P. McCreary, Pacific low-latitude western boundary currents and the Indonesian throughflow, *J. Geophys. Res., 101*, 12,209–12,216, 1996.

Lutjeharms, J. R. E., Meridional heat transport across the Sub-Tropical Convergence by a warm eddy, *Nature, 331*, 251–254, 1988.

Lutjeharms, J. R. E., and R. C. Van Ballegooyen, The retroflection of the Agulhas Current, *J. Phys. Oceanogr., 18,* 1570–1583, 1988.

Lutjeharms, J. R. E., W. P. M. de Ruijter, and R. G. Peterson, Interbasin exchange and the Agulhas retroflection; the development of some oceanographic concepts, *Deep-Sea Res., 39*, 1791–1807, 1992.

Luyten, J. R., and J. C. Swallow, Equatorial undercurrents, *Deep-Sea Res., 23,* 1005–1007, 1976.

Luyten, J., M. Fieux, and J. Gonella, Equatorial currents in the western Indian Ocean, *Science, 209*, 600–603, 1980.

Lynn, R. J., and J. L. Reid, Characteristics and circulation of deep and abyssal waters, *Deep-Sea Res., 15,* 577–598, 1968.

Macdonald, A. M., Property fluxes at 30°S and their implications for the Pacific–Indian throughflow and the global heat budget, *J. Geophys. Res., 98,* 6851–6868, 1993.

Mantyla, A. W., On the potential temperature in the abyssal Pacific Ocean, *J. Mar. Res., 33,* 341–354, 1975.

Mantyla, A. W., and J. L. Reid, Abyssal characteristics of the World Ocean waters, *Deep-Sea Res., 30,* 805–833, 1983.

Mantyla, A. W., and J. L. Reid, On the origins of deep and bottom waters of the Indian Ocean, *J. Geophys. Res., 100*, 2417–2439, 1995.

McCartney, M. S., Subantarctic Mode Water, in *A Voyage of Discovery*, George Deacon 70th Anniversary Volume, M. V. Angel, editor, supplement to *Deep-Sea Res.*, pp. 103–119, 1977.

McCartney, M. S., The subtropical recirculation of Mode Waters, *J. Mar. Res., 40*, suppl., 427–464, 1982.

McCartney, M. S., and M. O. Baringer, Notes on the S. Pacific hydrographic section near 32°S—WHP P6, *WOCE Notes, 5*(2), 1, 4–11, U.S. WOCE Office, Department of Oceanography, Texas A&M University, College Station, Texas 77843–3146, 1993.

Meyers, G., Do Sverdrup transports account for the Pacific North Equatorial Countercurrent?, *J. Geophys. Res., 85,* 1073–1075, 1980.

Meyers, G., Variation of Indonesian throughflow and the El Niño – Southern Oscillation, *J. Geophys. Res., 101,* 12,255–12,263, 1996.

Meyers, G., R. J. Bailey, and A. P. Worby, Volume transport of Indonesian Throughflow, *Deep-Sea Res., I, 42,* 1163–1174, 1995.

Morales, R. A., E. D. Barton, and K. J. Heywood, Variability of water masses in the western Indian Ocean, *J. Geophys. Res., 101,* 14,027–14,038, 1996.

Murray, S., E. Lindstrom, J. Kindle, and E. Weeks, Transport through the Vitiaz Strait, *WOCE Notes, 7*(1), 21–23, U.S. WOCE Office, Dept. of Oceanography, Texas A&M University, College Station, Texas 77843–3146, 1995.

Niiler, P. P., and M. M. Hall, Low frequency eddy variability at 28°N, 152°W in the eastern North Pacific subtropical gyre, *J. Phys. Oceanogr., 18,* 1670–1685, 1988.

References

Niiler, P. P., W. J. Schmitz, and D.-K. Lee, Geostrophic volume transport in high eddy-energy areas of Kuroshio Extension and Gulf Stream, *J. Phys. Oceanogr., 15,* 825–843, 1985.

Nilsson, C. S., and G. R. Cresswell, The formation and evolution of East Australian Current warm-core eddies, *Prog. Oceanog., 9,* 133–183, 1981.

Nishida, H., and W. B. White, Horizontal eddy fluxes of momentum and kinetic energy in the near-surface of the Kuroshio Extension, *J. Phys. Oceanogr., 12,* 160–170, 1982.

Nitani, H., The beginning of the Kuroshio, in *Kuroshio: Its Physical Aspects*, H. Stommel and K. Yoshida, editors, University of Tokyo Press, pp. 129–163, 1972.

Nowlin, W. D., Jr., T. Whitworth III, and R. D. Pillsbury, Structure and transport of the Antarctic Circumpolar Current at Drake Passage from short-term measurements, *J. Phys. Oceanogr., 7,* 788–802, 1977.

Nowlin, W. D., Jr., R. D. Pillsbury, and J. Bottero, Observations of kinetic energy levels in the Antarctic Circumpolar Current at Drake Passage, *Deep-Sea Res., 28,* 1–17, 1981.

Olson, D. B., Rings in the ocean, *Annu. Rev. Earth Planet. Sci., 19,* 283–311, 1991.

Orsi, A. H., W. D. Nowlin Jr., and T. Whitworth III, On the circulation and stratification of the Weddell Gyre, *Deep-Sea Res. I, 40,* 169–203, 1993.

Orsi, A. H., T. Whitworth III, and W. D. Nowlin Jr., On the meridional extent and fronts of the Antarctic Circumpolar Current, *Deep-Sea Res. I, 42,* 641–673, 1995.

Park, Y.-H., L. Gambéroni, and E. Charriaud, Frontal structure and transport of the Antarctic Circumpolar Current in the south Indian Ocean sector, 40–80°E, *Mar. Chem., 35,* 45–62, 1991.

Park, Y.-H., L. Gamberoni, and E. Charriaud, Frontal structure, water masses and circulation in the Crozet Basin, *J. Geophys. Res., 98,* 12,361–12,385, 1993.

Peterson, R. G., The boundary currents in the western Argentine Basin, *Deep-Sea Res., 39,* 624–644, 1992.

Peterson, R. G., and L. Stramma, Upper-level circulation in the South Atlantic Ocean, *Prog. Oceanog., 26,* 1–73, 1991.

Peterson, R. G., and T. Whitworth III, The subantarctic and polar fronts in relation to deep water masses through the southwestern Atlantic, *J. Geophys. Res., 94,* 10,817–10,838, 1989.

Philander, S. G. H., *El Niño, La Niña, and the Southern Oscillation,* Academic Press, Inc., New York, 293 pp., 1990.

Piola, A. R., and D. T. Georgi, Circumpolar properties of Antarctic Intermediate Water and Subantarctic Mode Water, *Deep-Sea Res., 29,* 687–711, 1982.

Piola, A. R., and A. L. Gordon, Pacific and Indian Ocean upper-layer salinity budget, *J. Phys. Oceanogr., 14,* 747–753, 1984.

Piola, A. R., and A. L. Gordon, Intermediate waters in the southwest South Atlantic, *Deep-Sea Res., 36,* 1–16, 1989.

Ponte, R. M., and J. Luyten, Deep velocity measurements in the western equatorial Indian Ocean, *J. Phys. Oceanogr., 20,* 44–52, 1990.

Qiu, B., Why is the spreading of the North Pacific Intermediate Water confined on density surfaces around $\sigma_\theta = 26.8$?, *J. Phys. Oceanogr., 25,* 168–180, 1995.

Qiu, B., and T. M. Joyce, Interannual variability in the mid- and low-latitude western North Pacific, *J. Phys. Oceanogr., 22,* 1062–1079, 1992.

Qiu, B., and R. Lukas, Seasonal and interannual variability of the North Equatorial Current, the Mindanao Current, and the Kuroshio along the Pacific western boundary, *J. Geophys. Res., 101,* 12,315–12,330, 1996.

Qiu, B., K. A. Kelly, and T. M. Joyce, Mean flow and variability in the Kuroshio Extension from Geosat altimetry data, *J. Geophys. Res., 96,* 18,491–18,507, 1991.

Quadfasel, D., and G. R. Cresswell, A note on the seasonal variability of the South Java Current, *J. Geophys. Res., 97,* 3685–3688, 1992.

Quadfasel, D., and F. Schott, Water-mass distributions at intermediate layers off the Somali coast during the onset of the Southwest Monsoon, 1979, *J. Phys. Oceanogr., 12,* 1358–1372, 1982.

Read, J. F., and R. T. Pollard, Structure and transport of the Antarctic Circumpolar Current and Agulhas Return Current at 40°E, *J. Geophys. Res., 98,* 12,281–12,295, 1993.

References

Reid, J. L., Intermediate waters of the Pacific Ocean, *The Johns Hopkins Oceanographic Studies,* No. *2*, 85 pp., 1965.

Reid, J. L., Transpacific hydrographic sections at Lats. 43°S and 28°S: the SCORPIO Expedition—III, Upper water and a note on southward flow at mid-depth, *Deep-Sea Res., 20,* 39–49, 1973.

Reid, J. L., On the mid-depth circulation of the World Ocean, in *Evolution of Physical Oceanography, Scientific Surveys in Honor of Henry Stommel,* B. A. Warren and C. Wunsch, editors, The MIT Press, Cambridge, Massachusetts; pp. 70–111, 1981.

Reid, J. L., On the total geostrophic circulation of the South Pacific Ocean: Flow patterns, tracers, and transports, *Prog. Oceanog., 16,* 1–61, 1986.

Reid, J. L., On the total geostrophic circulation of the South Atlantic Ocean: Flow patterns, tracers, and transports, *Prog. Oceanog., 23,* 149–244, 1989.

Reid, J. L., On the total geostrophic circulation of the North Atlantic Ocean: Flow patterns, tracers, and transports, *Prog. Oceanog., 33,* 1–92, 1994.

Reid, J. L., and P. F. Lonsdale, On the flow of water through the Samoan Passage, *J. Phys. Oceanogr., 4,* 58–73, 1974.

Reid, J. L., and R. J. Lynn, On the influence of the Norwegian–Greenland and Weddell Seas upon the bottom waters of the Indian and Pacific oceans, *Deep-Sea Res., 18,* 1063–1088, 1971.

Reid, J. L., and A. W. Mantyla, On the mid-depth circulation of the North Pacific Ocean, *J. Phys. Oceanogr., 8,* 946–951, 1978.

Reid, J. L., W. D. Nowlin, Jr., and W. C. Patzert, On the characteristics and circulation of the southwestern Atlantic Ocean, *J. Phys. Oceanogr., 7,* 62–91, 1977.

Ridgway, K. R., and J. S. Godfrey, Mass and heat budgets in the East Australian current: A direct approach, *J. Geophys. Res., 99,* 3231–3248, 1994.

Rintoul, S. R., Mass, heat and nutrient fluxes in the Atlantic Ocean determined by inverse methods, Ph.D. thesis, Massachusetts Institute of Technology and Woods Hole Oceanographic Institution Joint Program, 287 pp., 1988.

Rintoul, S. R., South Atlantic interbasin exchange, *J. Geophys. Res.,* 96, 2675–2692, 1991.

Riser, S. C., Pacific RAFOS floats measure mid-depth flow, *WOCE Notes,* 7(3), 1, 3–6, U.S. WOCE Office, Dept. of Oceanography, Texas A&M University, College Station, Texas 77843–3146, 1995.

Robbins, P. E., and J. M. Toole, The dissolved silica budget as a constraint on the meridional overturning circulation of the Indian Ocean, *Deep-Sea Res.,* in press, 1996.

Rochford, D. J., The intermediate depth waters of the Tasman and Coral Seas, I, The 27.20 σ_t surface, *Aust. J. Mar. Freshw. Res., 11,* 127–147, 1960a.

Rochford, D. J., The intermediate depth waters of the Tasman and Coral Seas, II, The 26.80 σ_t surface, *Aust. J. Mar. Freshw. Res., 11,* 148–165, 1960b.

Rochford, D. J., Hydrology of the Indian Ocean, I, The water masses in intermediate depths of the south-east Indian Ocean, *Aust. J. Mar. Freshw. Res., 12,* 129–149, 1961.

Rochford, D. J., Mixing trajectories of intermediate depth waters of the south-east Indian Ocean as determined by a salinity frequency method, *Aust. J. Mar. Freshw. Res., 14,* 1–23, 1963.

Rochford, D. J., Salinity maxima in the upper 1000 meters of the north Indian Ocean, *Aust. J. Mar. Freshw. Res., 15,* 1–24, 1964.

Rochford, D. J., Distribution of Banda Intermediate Water in the Indian Ocean, *Aust. J. Mar. Freshw. Res., 17,* 61–76, 1966.

Roemmich, D., and T. McCallister, Large scale circulation of the North Pacific Ocean, *Prog. Oceanogr., 22,* 171–204, 1989.

Roemmich, D., and C. Wunsch, Two transatlantic sections: Meridional circulation and heat flux in the subtropical North Atlantic Ocean, *Deep-Sea Res., 32,* 619–664, 1985.

Roemmich, D., T. McCallister, and J. Swift, A transpacific hydrographic section along latitude 24°N: The distribution of properties in the subtropical gyre, *Deep-Sea Res., 38,* Suppl. 1, S1–S20, 1991.

References

Roemmich, D., S. Hautala, and D. Rudnick, Northward abyssal transport through the Samoan Passage and adjacent regions, *J. Geophys. Res., 101,* 14,039–14,055, 1996.

Sætre, R., and A. J. da Silva, The circulation of the Mozambique Channel, *Deep-Sea Res., 31,* 485–508, 1984.

Saunders, P. M., and B. A. King, Oceanic fluxes on the WOCE A11 section, *J. Phys. Oceanogr., 25,* 1942–1958, 1995.

Schmitz, W. J., Jr., A comparison of the mid-latitude eddy fields in the western North Atlantic and North Pacific Oceans, *J. Phys. Oceanogr., 12,* 208–210, 1982.

Schmitz, W. J., Jr., Abyssal eddy kinetic energy levels in the western North Pacific, *J. Phys. Oceanogr., 14,* 198–201, 1984a.

Schmitz, W. J., Jr., Observations of the vertical structure of the eddy field in the Kuroshio Extension, *J. Geophys. Res., 89,* 6355–6364, 1984b.

Schmitz, W. J., Jr., Observations of new, large, and stable abyssal currents at midlatitudes along 165°E, *J. Phys. Oceanogr., 17,* 1309–1315, 1987.

Schmitz, W. J., Jr., Exploration of the eddy field in the midlatitude North Pacific, *J. Phys. Oceanogr., 18,* 459–468, 1988.

Schmitz, W. J., Jr., The MODE Site revisited, *J. Mar. Res., 47,* 131–151, 1989.

Schmitz, W. J., Jr., On the interbasin-scale thermohaline circulation, *Rev. Geophys., 33,* 151–173, 1995.

Schmitz, W. J., Jr., On the eddy field in the Agulhas area, with global implications, *J. Geophys. Res., 101,* 16,259–16,271, 1996.

Schmitz, W. J., Jr., and W. R. Holland, A preliminary comparison of selected numerical eddy-resolving general circulation experiments with observations, *J. Mar. Res., 40,* 75–117, 1982.

Schmitz, W. J., Jr., and W. R. Holland, Observed and modeled mesoscale variability near the Gulf Stream and Kuroshio Extension, *J. Geophys. Res., 91,* 9624–9638, 1986.

Schmitz, W. J., Jr., and J. R. Luyten, Spectral time scales for mid-latitude eddies, *J. Mar. Res., 49,* 75–107, 1991.

Schmitz, W. J., Jr., and M. S. McCartney, On the North Atlantic circulation, *Rev. Geophys., 31,* 29–49, 1993.

Schmitz, W. J., Jr., and P. L. Richardson, On the sources of the Florida Current, *Deep-Sea Res., 38,* Suppl. 1, S389–S409, 1991.

Schmitz, W. J., Jr., and J. D. Thompson, On the effects of horizontal resolution in a limited-area model of the Gulf Stream system, *J. Phys. Oceanogr., 23,* 1001–1007, 1993.

Schmitz, W. J., Jr., P. P. Niiler, R. L. Bernstein, and W. R. Holland, Recent long-term moored instrument observations in the western North Pacific, *J. Geophys. Res., 87,* 9425–9440, 1982.

Schmitz, W. J., Jr., W. R. Holland, and J. F. Price, Mid-latitude mesoscale variability, *Rev. Geophys. Space Phys., 21,* 1109–1119, 1983.

Schmitz, W. J., Jr., P. P. Niiler, and C. J. Koblinsky, Two-year moored instrument results along 152°E, *J. Geophys. Res., 92,* 10,826–10,834, 1987.

Schott, F., Monsoon response of the Somali Current and associated upwelling, *Prog. Oceanog., 12,* 357–381, 1983.

Schott, F., M. Fieux, J. Kindle, J. Swallow, and R. Zantopp, The boundary currents east and north of Madagascar, 2, Direct measurements and model comparisons, *J. Geophys. Res., 93,* 4963–4974, 1988.

Shapiro, G. I., and S. L. Meschanov, Distribution and spreading of Red Sea Water and salt lens formation in the northwest Indian Ocean, *Deep-Sea Res., 38,* 21–34, 1991.

Sharma, G. S., Water characteristics at 200 cl/t in the intertropical Indian Ocean during the southwest monsoon, *J. Mar. Res., 30,* 102–111, 1972.

Sharma, G. S., Transequatorial movement of water masses in the Indian Ocean, *J. Mar. Res., 34,* 143–154, 1976.

References

Shiller, A. M., W. J. Teague, and Z. R. Hallock, Deep water properties near 35°N, 143°E observed during the Kuroshio Extension Regional Experiment, *J. Geophys. Res.*, accepted, 1996.

Shriver, J. F., and H. E. Hurlburt, The contribution of the global thermohaline circulation to the Pacific to Indian Ocean Throughflow via Indonesia, *J. Geophys. Res.*, accepted, 1996.

Siedler, G., T. J. Müller, R. Onken, M. Arhan, H. Mercier, B. A. King, and P. M. Saunders, The zonal WOCE sections in the South Atlantic, in: *The South Atlantic: Present and Past Circulation*, G. Wefer, W. H. Berger, G. Siedler, and D. Webb, editors; Springer-Verlag, Berlin, Heidelberg, pp. 83–104, in press, 1996.

Sievers, H. A., and W. D. Nowlin, Jr., The stratification and water masses at Drake Passage, *J. Geophys. Res., 89,* 10,489–10,514, 1984.

Speer, K. G., and W. Zenk, The flow of Antarctic Bottom Water into the Brazil Basin, *J. Phys. Oceanogr., 23,* 2667–2682, 1993.

Speer, K. G., W. Zenk, G. Siedler, J. Pätzold, and C. Heigland, First resolution of flow through the Hunter Channel in the South Atlantic, *Earth Planet. Sci. Lett., 113,* 287–292, 1992.

Stommel, H., A survey of ocean current theory, *Deep-Sea Res., 4,* 149–184, 1957.

Stramma, L., The Brazil Current transport south of 23°S, *Deep-Sea Res., 36,* 639–646, 1989.

Stramma, L., Geostrophic transport of the South Equatorial Current in the Atlantic, *J. Mar. Res., 49,* 281–294, 1991.

Stramma, L., The South Indian Ocean Current, *J. Phys. Oceanogr., 22,* 421–430, 1992.

Stramma, L., and J. R. E. Lutjeharms, The flow field of the subtropical gyre of the South Indian Ocean, *J. Geophys. Res.*, submitted, 1996.

Stramma, L., and R. G. Peterson, Geostrophic transport in the Benguela Current region, *J. Phys. Oceanogr., 19,* 1440–1448, 1989.

Stramma, L., and R. G. Peterson, The South Atlantic Current, *J. Phys. Oceanogr., 20,* 846–859, 1990.

Stramma, L., Y. Ikeda, and R. G. Peterson, Geostrophic transport in the Brazil Current region north of 20°S, *Deep-Sea Res., 37,* 1875–1886, 1990.

Stramma, L., J. Fischer, and J. Reppin, The North Brazil Undercurrent, *Deep-Sea Res. I, 42,* 773–795, 1995a.

Stramma, L., R. G. Peterson, and M. Tomczak, The South Pacific Current, *J. Phys. Oceanogr., 25,* 77–91, 1995b.

Stramma, L., J. Fischer, and F. Schott, The flow field off southwest India at 8N during the southwest monsoon of August 1993, *J. Mar. Res., 54,* 55–72, 1996.

Sverdrup, H. U., M. W. Johnson, and R. H. Fleming, *The Oceans: Their Physics, Chemistry, and General Biology*, Prentice-Hall, Englewood Cliffs, N.J., 1087 pp., 1942.

Tabata, S., The general circulation of the Pacific Ocean and a brief account of the oceanographic structure of the North Pacific Ocean, Part I—Circulation and volume transports, *Atmosphere, 13,* 133–168, 1975.

Taft, B. A., Distribution of salinity and dissolved oxygen of surfaces of uniform potential specific volume in the South Atlantic, South Pacific, and Indian Ocean, *J. Mar. Res., 21,* 129–146, 1963.

Taft, B. A., Characteristics of the flow of the Kuroshio south of Japan, in *Kuroshio: Its Physical Aspects,* H. Stommel and K. Yoshida, editors, University of Tokyo Press, pp. 165–216, 1972.

Taft, B. A., Structure of the Kuroshio south of Japan, *J. Mar. Res., 36,* 77–117, 1978.

Taft, B. A., A. R. Robinson, and W. J. Schmitz, Jr., Current path and bottom velocity of the Kuroshio, *J. Phys. Oceanogr., 3,* 347–350, 1973.

Taft, B. A., S. R. Ramp, J. G. Dworski, and G. Holloway, Measurements of deep currents in the central North Pacific, *J. Geophys. Res., 86,* 1955–1968, 1981.

Taft, B. A., S. P. Hayes, G. E. Friederich, and L. A. Codispoti, Flow of abyssal water into the Samoa Passage, *Deep-Sea Res., 38,* Suppl. 1, S103–S128, 1991.

Talley, L. D., Ventilation of the subtropical North Pacific: The shallow salinity minimum, *J. Phys. Oceanogr., 15,* 633–649, 1985.

References

Talley, L. D., Distribution and formation of North Pacific Intermediate Water, *J. Phys. Oceanogr., 23,* 517–537, 1993.

Talley, L. D., Some advances in understanding of the general circulation of the Pacific Ocean, with emphasis on recent U.S. contributions, *U.S. National Report to International Union of Geodesy and Geophysics 1991–1994*, Suppl. to *Rev. Geophys.,* pp. 1335–1352, 1995.

Talley, L. D., Antarctic Intermediate Water in the South Atlantic, in *The South Atlantic: Present and Past Circulation,* G. Wefer, W. H. Berger, G. Siedler, and D. Webb, eds., Springer-Verlag, Berlin, in press, 1996.

Talley, L. D., and G. C. Johnson, Deep, zonal subequatorial currents, *Science, 263,* 1125–1128, 1994.

Talley, L. D., and T. M. Joyce, The double silica maximum in the North Pacific, *J. Geophys. Res., 97,* 5465–5480, 1992.

Talley, L. D., and W. B. White, Estimates of time and space scales at 300 meters in the midlatitude North Pacific from the TRANSPAC XBT program, *J. Phys. Oceanogr., 17,* 2168–2188, 1987.

Talley, L. D., T. M. Joyce, and R. A. deSzoeke, Transpacific sections at 47°N and 152°W: Distribution of properties, *Deep-Sea Res., 38,* Suppl. 1, S63–S82, 1991.

Teague, W. J., A. M. Shiller, and Z. R. Hallock, Hydrographic section across the Kuroshio near 35°N, 143°E, *J. Geophys. Res., 99,* 7639–7650, 1994.

Toggweiler, J. R., The ocean's overturning circulation, *Physics Today, 47,* November, 45–50, 1994.

Toggweiler, J. R., and B. Samuels, Is the magnitude of the deep outflow from the Atlantic Ocean actually governed by southern hemisphere winds?, in *The Global Carbon Cycle,* M. Heimann, ed., NATO ASI series, Springer-Verlag, Berlin, pp. 303–331, 1993a.

Toggweiler, J. R., and B. Samuels, New radiocarbon constraints on the upwelling of abyssal water to the ocean's surface, in *The Global Carbon Cycle,* M. Heimann, ed., NATO ASI series, Springer-Verlag, Berlin, pp. 333–366, 1993b.

Toggweiler, J. R., K. Dixon, and W. S. Broecker, The Peru Upwelling and the ventilation of the South Pacific thermocline, *J. Geophys. Res., 96,* 20,467–20,497, 1991.

Toole, J. M., and B. A. Warren, A hydrographic section across the subtropical South Indian Ocean, *Deep-Sea Res., 40,* 1973–2019, 1993.

Toole, J. M., E. Zou, and R. C. Millard, On the circulation of the upper waters in the western equatorial Pacific Ocean, *Deep-Sea Res., 35,* 1451–1482, 1988.

Toole, J. M., R. M. Millard, Z. Wang, and S. Pu, Observations of the Pacific North Equatorial Current bifurcation at the Philippine coast, *J. Phys. Oceanogr., 20,* 307–318, 1990.

Toole, J. M., K. L. Polzin, and R. W. Schmitt, Estimates of diapycnal mixing in the abyssal ocean, *Science, 264,* 1120–1123, 1994a.

Toole, J. M., S. E. Wijffels, M. S. McCartney, B. A. Warren, H. L. Bryden, and J. A. Church, WOCE hydrographic section P6 across the subtropical South Pacific Ocean (poster), in proceedings volume, *The Oceanography Society, Pacific Basin Meeting,* July 19–22, 1994, Honolulu, Hawaii, p. 76 (abstract only), 1994b.

Trenberth, K. E., W. G. Large, and J. G. Olson, The mean annual cycle in global ocean wind stress, *J. Phys. Oceanogr., 20,* 1742–1760, 1990.

Tsuchiya, M., An oceanographic description of the equatorial current system of the western Pacific, *The Oceanographical Magazine, 13,* 1–30, 1961.

Tsuchiya, M., Equatorial circulation of the South Pacific, in *Scientific Exploration of the South Pacific,* W. S. Wooster, ed., pp. 69–74, Symposium held during Ninth General Meeting of the Scientific Committee on Oceanic Research (SCOR), June 18–20, 1968, at La Jolla, Calif.; National Academy of Sciences, Washington, D.C., 1970.

Tsuchiya, M., Subsurface countercurrents in the eastern equatorial Pacific Ocean, *J. Mar. Res., 33,* Suppl., 145–175, 1975.

Tsuchiya, M., The origin of the Pacific equatorial 13°C Water, *J. Phys. Oceanogr., 11,* 794–812, 1981.

Tsuchiya, M., On the Pacific upper-water circulation, *J. Mar. Res., 40,* Suppl., 777–799, 1982.

References

Tsuchiya, M., Flow path of the Antarctic Intermediate Water in the western equatorial South Pacific Ocean, *Deep-Sea Res., 38,* Suppl. 1, S273–S279, 1991.

Tsuchiya, M., and L. D. Talley, Water-property distributions along an eastern Pacific hydrographic section at 135W, *J. Mar. Res., 54,* 541–564, 1996.

Tsuchiya, M., R. Lukas, R. A. Fine, E. Firing, and E. Lindstrom, Source waters of the Pacific Equatorial Undercurrent, *Prog. Oceanogr., 23,* 101–147, 1989.

Tsuchiya, M., L. D. Talley, and M. S. McCartney, Water-mass distributions in the western South Atlantic; A section from South Georgia Island (54S) northward across the equator, *J. Mar. Res., 52,* 55–81, 1994.

Van Ballegooyen, R. C., M. L. Gründlingh, and J. R. E. Lutjeharms, Eddy fluxes of heat and salt from the southwest Indian Ocean into the southeast Atlantic Ocean: A case study, *J. Geophys. Res., 99,* 14,053–14,070, 1994.

Visser, G. A., and M. M. Van Niekerk, Ocean currents and water masses at 1,000, 1,500 and 3,000 metres in the south-west Indian Ocean, *Division of Sea Fisheries Investigational Report No. 52,* Department of Commerce and Industries, Republic of South Africa, 46 pp., 1965.

Warren, B. A., and W. B. Owens, Deep currents in the central subarctic Pacific Ocean, *J. Phys. Oceanogr., 18,* 529–551, 1988.

White, W. B., and R. L. Bernstein, Design of an oceanographic network in the midlatitude North Pacific, *J. Phys. Oceanogr., 9,* 592–606, 1979.

Whitworth, T., III, and W. D. Nowlin, Jr., Water masses and currents of the Southern Ocean at the Greenwich Meridian, *J. Geophys. Res., 92,* 6462–6476, 1987.

Whitworth, T., III, W. D. Nowlin, Jr., and S. J. Worley, The net transport of the Antarctic Circumpolar Current through Drake Passage, *J. Phys. Oceanogr., 12,* 960–971, 1982.

Wijffels, S. E., Exchanges between hemispheres and gyres: A direct approach to the mean circulation of the equatorial Pacific, Ph.D. Dissertation, Massachusetts Institute of Technology and Woods Hole Oceanographic Institution, 267 pp., 1993.

Wijffels, S., E. Firing, and J. Toole, The mean structure and variability of the Mindanao Current at 8°N, *J. Geophys. Res., 100,* 18,421–18,435, 1995.

Wijffels, S. E., J. M. Toole, H. L. Bryden, R. A. Fine, W. J. Jenkins, and J. L. Bullister, The water masses and circulation at 10°N in the Pacific, *Deep-Sea Res.*, in press, 1996.

Wooster, W. S., Eastern boundary currents in the South Pacific, in *Scientific Exploration of the South Pacific*, W. S. Wooster, ed., pp. 60–68, Symposium held during Ninth General Meeting of the Scientific Committee on Oceanic Research (SCOR), June 18–20, 1968, at La Jolla, Calif.; National Academy of Sciences, Washington, D.C., 1970.

Wooster, W. S., and J. L. Reid, Jr., Eastern boundary currents, Chapter 11 in: *The Sea*, Vol. *2*, M. N. Hill, ed., John Wiley, New York, pp. 253–280, 1963.

Wunsch, C., D. Hu, and B. Grant, Mass, heat, salt and nutrient fluxes in the South Pacific Ocean, *J. Phys. Oceanogr., 13,* 725–753, 1983.

Wyrtki, K., The surface circulation in the Coral and Tasman Seas, *Div. Fish. Oceanogr. Tech. Pap. No. 8*, Commonwealth Scientific and Industrial Research Organization, Australia, 44 pp., 1960.

Wyrtki, K., Scientific Results of Marine Investigations of the South China Sea and the Gulf of Thailand, 1959–1961, volume 2, Physical Oceanography of Southeast Asian Waters, *NAGA Rep. 2,* Scripps Inst. of Oceanogr., Univ. of Calif., San Diego, La Jolla, 1961.

Wyrtki, K., The subsurface water masses in the western South Pacific Ocean, *Aust. J. Mar. Freshw. Res., 13,* 18–47, 1962.

Wyrtki, K., The horizontal and vertical field of motion in the Peru Current, *Bull. Scripps Instn. Oceanogr., 8*(4), 313–346, 1963.

Wyrtki, K., Oceanography of the eastern equatorial Pacific Ocean, *Oceanogr. Mar. Biol. Ann. Rev., 4*, 33–68, 1966.

Wyrtki, K., *Oceanographic Atlas of the International Indian Ocean Expedition,* National Science Foundation NSF-IOE-1, 531 pp., 1971.

Wyrtki, K., Physical oceanography of the Indian Ocean, in *The Biology of the Indian Ocean,* B. Zeitzschel and S. A. Gerlach, eds., Chapman and Hall Ltd., London, pp. 18–36, 1973.

References

Wyrtki, K., The dynamic topography of the Pacific Ocean and its fluctuations, *Technical Report HIG-74-5*, Hawaii Institute of Geophysics, University of Hawaii, 19 pp. + 37 figs., 1974.

Wyrtki, K., Indonesian through flow and the associated pressure gradient, *J. Geophys. Res., 92*, 12,941–12,946, 1987.

Wyrtki, K., L. Magaard, and J. Hager, Eddy energy in the oceans, *J. Geophys. Res., 81*, 2641–2646, 1976.

Yasuda, I., K. Okuda, and Y. Shimizu, Distribution and modification of North Pacific Intermediate Water in the Kuroshio–Oyashio interfrontal zone, *J. Phys. Oceanogr., 26,* 447–465, 1996.

Yuan, X., and L. D. Talley, Shallow salinity minima in the North Pacific, *J. Phys. Oceanogr., 22,* 1302–1316, 1992.

Zemba, J. C., The structure and transport of the Brazil Current between 27° and 36° South, Ph.D. Thesis, Woods Hole Oceanographic Institution and Massachusetts Institute of Technology Joint Program in Oceanography and Oceanographic Engineering, Woods Hole Oceanog. Inst. Tech. Rept., WHOI-91-37, 160 pp., 1991.

Curriculum Vitae

William Joseph Schmitz, Jr.
Physical Oceanographer
Senior Scientist
W. Van Alan Clark Chair
Woods Hole Oceanographic Institution

Birth: December 20, 1937

Sc.B., University of Miami, 1961
Ph.D., Physical Oceanography, University of Miami, 1966

Research Aide, 1959–1961; NDEA Fellow, 1961–64; Instructor, 1964–66, Institute of Marine Science, University of Miami

Postdoctoral Fellow, 1966–67, Nova University

Assistant Scientist, 1967–71; Associate Scientist, 1971–79, awarded tenure, 1974; Senior Scientist, 1979–; W. Van Alan Clark Chair for Excellence in Oceanography, 1992–, Woods Hole Oceanographic Institution

Senior Queen's Fellow, Commonwealth of Australia, 1984

Interim Director, Institute for Naval Oceanography, 1986

Fellow, American Geophysical Union, 1987–

Member, Naval Research Advisory Committee, 1990–1996

Meritorious Public Service Award, Department of the Navy, March 1991

Meritorious Public Service Citation, Department of the Navy, July, 1996

Superior Public Service Award, Department of the Navy, September 1996

Visiting Investigator, Institut für Meereskunde, Universität Kiel, September, 1993

Visiting Investigator, Scripps Institution of Oceanography, University of California, San Diego, February–March, 1995

Research Interests: Low frequency, large scale ocean circulation

Author or co-author of 60 refereed scientific publications

Department of the Navy

Certificate of Award

In appreciation of
Meritorious Public Service
to the Department of the Navy

Office of the Chief of Naval Research

takes pleasure in presenting the

MERITORIOUS PUBLIC SERVICE AWARD

to **Dr. William J. Schmitz**

for services set forth in the following

For meritorious public service in the development of the Navy's first operational ocean prediction system, and subsequent use of oceanography in naval operations, from 1986 to the present. As the first Director of the Institute for Naval Oceanography and Chairman of the Commander, Naval Oceanography Command Independent Model Review Panel, Dr. Schmitz provided intellectual leadership to the Navy ocean modeling community that was instrumental in launching the world's first operational ocean prediction system. Dr. Schmitz's vast knowledge of ocean circulation, and his visionary appreciation of the emerging role of ocean modeling in both research and operational prediction, were crucial to that endeavor. His continuing interaction with Navy model developers and senior Navy policymakers will have lasting impact on the use of oceanography in naval operations throughout the next century. His selfless devotion to the Navy and the oceanographic research community reflect great credit upon himself, his country and his profession.

1 March 1991
Date

Department of the Navy

Certificate of Award

In appreciation of
Meritorious Public Service
to the Department of the Navy

The Assistant Secretary of the Navy
(Research, Development and Acquisition)
takes pleasure in presenting the

MERITORIOUS PUBLIC SERVICE CITATION

to **Dr. William J. Schmitz, Jr.**

for services set forth in the following

For exceptionally meritorious service as a member of the Naval Research Advisory Committee from July 1990 through March 1996. Dr. Schmitz's participation during the conduct of four Naval Research Advisory Committee studies was instrumental in providing objective technical analyses and an independent perspective on critical issues in the areas of science, research, and development. His involvement as a panel member ensured accurate, balanced, independent technical studies that helped the Secretary of the Navy, the Chief of Naval Operations, and the Commandant of the Marine Corps to guide the research and development requirements of the Department of the Navy and Nation. As a result of his dedicated efforts, he unequivocally helped the Navy's leadership to formulate strategies leading to significant technological advances for the warfighter. Dr. Schmitz's technical expertise, total objectivity, and unwavering support reflected great credit upon himself and upheld the highest traditions of the United States Naval Service.

2 JULY 1996
Date

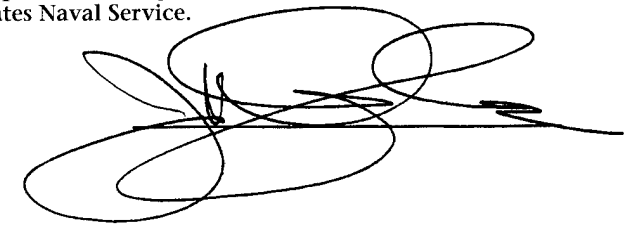

Appendix B

Department of the Navy

Certificate of Award

In appreciation of
Superior Public Service
to the Department of the Navy

The Chief of Naval Research

takes pleasure in presenting the

SUPERIOR PUBLIC SERVICE AWARD

to **Dr. William J. Schmitz, Jr.**

for services set forth in the following

For sustained, superior service as Senior Scientist, Department of Physical Oceanography, Woods Hole Oceanographic Institution throughout his career in physical oceanography research, from June 1961 to September 1996. Dr. Schmitz made extraordinary advances in understanding ocean circulation by conducting a unique program of ocean current measurements. His remarkable, singularly successful measurements of the Gulf Stream's velocity determined, for the first time, the mean value and variability statistics of volume transport of this current. Dr. Schmitz' statistical and geographical structure studies of the low frequency eddy field and currents revolutionized our understanding of both the Gulf Stream and Kuroshio currents. Recognizing the importance of numerical modeling, he collaborated with the Naval Research Laboratory, the Naval Oceanographic Office, and the National Center for Atmospheric Research. These efforts led to significant improvements in complex numerical models that represent today's understanding of ocean circulation. Dr. Schmitz' untiring efforts, professionalism, and total dedication to duty reflect great credit upon himself, the Woods Hole Oceanographic Institution, and the Office of Naval Research and were in keeping with the highest traditions of the United States Naval Service.

10 September 1996
Date

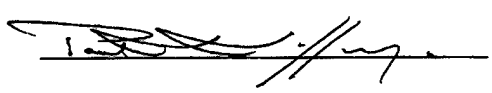

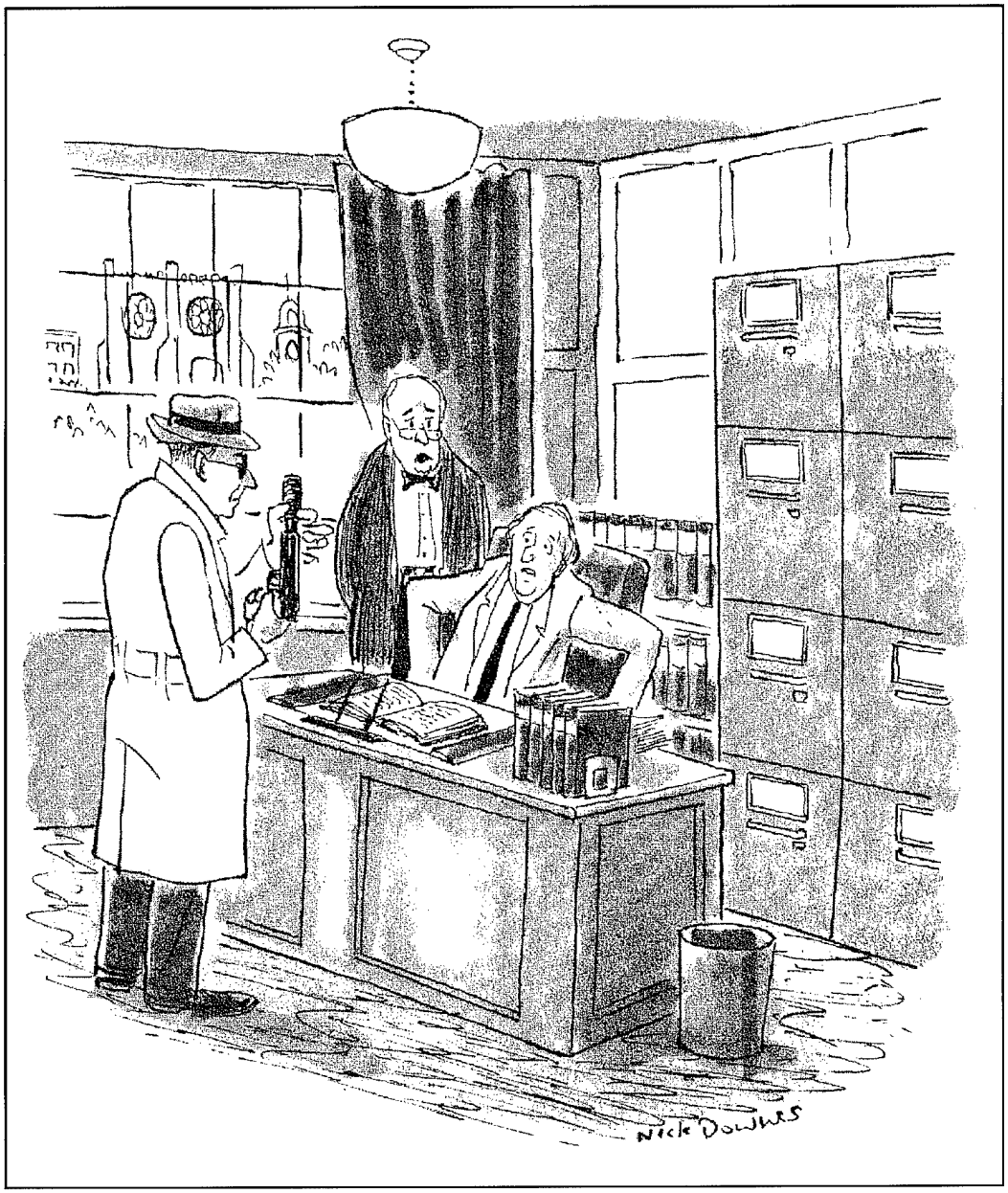

"Surely you were aware when you accepted the position, Professor, that it was publish or perish."

Appendix C

"Apparently big science isn't big enough for both of them."

List of Abbreviations and Symbols

AABW	Antarctic Bottom Water
AAIW	Antarctic Intermediate Water
AASW	Antarctic Surface Water
ACCS	Antarctic Circumpolar Current System
ACS	Agulhas Current System
AF	Agulhas Front
AL	Agulhas Leakage
BCS	Benguela Current System
BIW	Banda Intermediate Water
CDW	Circumpolar Deep Water
CIW	intermediate water of circumpolar origin
CTD	instrument measuring conductivity, temperature and depth
EAC	East Australian Current
EACS	East Australian Current System
ECC	Equatorial Countercurrent
EKE	eddy kinetic energy
EIC	Equatorial Intermediate Current
ENSO	El Niño–Southern Oscillation
EUC	Equatorial Undercurrent
GSS	Gulf Stream System
HE	Halmahera Eddy
IODW	Indian Ocean Deep Water
IT	Indonesian Throughflow
IW	intermediate water
KCC	Kuroshio Counter Current
KCS	Kuroshio Current System

Appendix D

K_E	eddy kinetic energy
LC	Leeuwin Current
LCDW	Lower Circumpolar Deep Water
LLWBCs	Low-Latitude Western Boundary Currents
LOIW	lower intermediate water
LSAMW	Lower Subantarctic Mode Water
MC	Mindanao Current
ME	Mindanao Eddy
MKE	mean kinetic energy
NAB	North Australian Bight
NADW	North Atlantic Deep Water
NBCS	North Brazil Current System
NEC	North Equatorial Current
NECC	North Equatorial Countercurrent
NEPB	Northeast Pacific Basin
NEUC	North Equatorial Undercurrent
NGCU	New Guinea Coastal Undercurrent
NIIW	Northwest Indian Intermediate Water
NPDW	North Pacific Deep Water
NPIW	North Pacific Intermediate Water
NPSTW	North Pacific Subtropical Water
NSSCC	Northern Subsurface Countercurrent
PCS	Peru Current System
PDW	Pacific Deep Water
PF	Polar Front
PFZ	Polar Frontal Zone
R8891	Rintoul, 1988, 1991
RSW	Red Sea Water

RT96	Robbins and Toole, 1996
S	salinity
S95, S96	Schmitz, 1995; Schmitz, 1996
SAF	Subantarctic Front
SAMW	Subantarctic Mode Water
SC	Somali Current
SEC	South Equatorial Current
SECC	South Equatorial Countercurrent
SFZ	Subantarctic Frontal Zone
SLW	surface layer water
SPSTW	South Pacific Subtropical Water
SSSCC	Southern Subsurface Counter Current
SST	sea surface temperature
STC	Subtropical Convergence
STF	Subtropical Front
Sv	Sverdrup, 1 Sv $\equiv 10^6$ m^3 s^{-1}
T	temperature
UCDW	Upper Circumpolar Deep Water
UDW	upper deep water
ULW	upper layer water
UPIW	upper intermediate water
UPOCN	upper ocean
UPOCNW	upper ocean water
USAMW	Upper Subantarctic Mode Water
(u,v)	(eastward, northward) current components
WOC	World Ocean Circulation

DOCUMENT LIBRARY

Distribution List for Technical Report Exchange – February 1996

University of California, San Diego
SIO Library 0175C
9500 Gilman Drive
La Jolla, CA 92093-0175

Hancock Library of Biology & Oceanography
Alan Hancock Laboratory
University of Southern California
University Park
Los Angeles, CA 90089-0371

Gifts & Exchanges
Library
Bedford Institute of Oceanography
P.O. Box 1006
Dartmouth, NS, B2Y 4A2, CANADA

Commander
International Ice Patrol
1082 Shennecossett Road
Groton, CT 06340-6095

NOAA/EDIS Miami Library Center
4301 Rickenbacker Causeway
Miami, FL 33149

Research Library
U.S. Army Corps of Engineers
Waterways Experiment Station
3909 Halls Ferry Road
Vicksburg, MS 39180-6199

Institute of Geophysics
University of Hawaii
Library Room 252
2525 Correa Road
Honolulu, HI 96822

Marine Resources Information Center
Building E38-320
MIT
Cambridge, MA 02139

Library
Lamont-Doherty Earth Observatory
Columbia University
Palisades, NY 10964

Library
Serials Department
Oregon State University
Corvallis, OR 97331

Pell Marine Science Library
University of Rhode Island
Narragansett Bay Campus
Narragansett, RI 02882

Working Collection
Texas A&M University
Dept. of Oceanography
College Station, TX 77843

Fisheries-Oceanography Library
151 Oceanography Teaching Bldg.
University of Washington
Seattle, WA 98195

Library
R.S.M.A.S.
University of Miami
4600 Rickenbacker Causeway
Miami, FL 33149

Maury Oceanographic Library
Naval Oceanographic Office
Building 1003 South
1002 Balch Blvd.
Stennis Space Center, MS, 39522-5001

Library
Institute of Ocean Sciences
P.O. Box 6000
Sidney, B.C. V8L 4B2 CANADA

National Oceanographic Library
Southampton Oceanography Centre
European Way
Southampton SO14 3ZH UNITED KINGDOM

The Librarian
CSIRO Marine Laboratories
G.P.O. Box 1538
Hobart, Tasmania AUSTRALIA 7001

Library
Proudman Oceanographic Laboratory
Bidston Observatory
Birkenhead
Merseyside L43 7 RA UNITED KINGDOM

IFREMER
Centre de Brest
Service Documentation - Publications
BP 70 29280 Plouzane FRANCE

50272-101

REPORT DOCUMENTATION PAGE	1. REPORT NO. WHOI-96-08	2.	3. Recipient's Accession No.

4. Title and Subtitle
On the World Ocean Circulation: Volume II, The Pacific and Indian Oceans / A Global Update

5. Report Date
December 1996

6.

7. Author(s)
William J. Schmitz, Jr.

8. Performing Organization Rept. No.
WHOI-96-08

9. Performing Organization Name and Address
Woods Hole Oceanographic Institution
Woods Hole, Massachusetts 02543

10. Project/Task/Work Unit No.

11. Contract(C) or Grant(G) No.
(C)
(G) N00014-89-J-1039
N00014-95-1-0356

12. Sponsoring Organization Name and Address
Office of Naval Research and the Clark Foundation

13. Type of Report & Period Covered
Technical Report

14.

15. Supplementary Notes
This report should be cited as: Woods Hole Oceanog. Inst. Tech. Rept., WHOI-96-08.

16. Abstract (Limit: 200 words)

This is the second and final volume of a report that describes some of my investigations over the last 35 years or so into low-frequency ocean current structures, a topic which I will call the World Ocean Circulation (WOC). The material presented constitutes my final report to the Office of Naval Research, and their support over the years is deeply appreciated. I was also fortunate to have been partially supported by the National Science Foundation during my career and, for some of the preparation of this report, by the Clark Foundation. Volume I was focused on the North Atlantic Ocean, after a global scale summary. This volume (II) will consider first the Pacific and Indian Oceans, concentrating on interbasin circulations, meridional cells, and mesoscale eddy fields. Then, there is an exceptionally brief discussion of the Southern Ocean(s) for background only, followed by a global summary. Lately, I have worked intensely on intergyre and interbasin exchanges, including an inter- comparison of some of the properties of the eddy field in the World's Oceans (Schmitz, W.J., Jr., *Rev. Geophys., 33*, 151–173, 1995; *J. Geophys. Res., 101*, 16,259–16,271, 1996). Volume II contains not only an update of the global picture, but also new representations of the transport structure of various components of the meridional overturning cells for each ocean. In summary, several similarities as well as dissimilarities between different oceans relative to both their general circulation and their mesoscale eddy field are shown to be associated with interbasin exchanges.

This report is meant to be an informal, occasionally anecdotal, state-of-the-art summary account of the World Ocean Circulation. Seemingly simple questions about how ocean currents behave, such as where various brands of sea water are coming from and going to, have been exciting research topics for many years. This report is not remotely about "all" of the WOC, it is simply a set of comments about what I have looked into during the preparation of this document. I do believe that the results in this report, although presented in a personal way, are consistent with community wisdom. The document is intended to be readable by non-specialists who have a basic scientific/technical background, especially in other oceanographic areas or meteorology or the geophysical disciplines, not only by specialists in physical oceanography.

17. Document Analysis a. Descriptors

global ocean circulation
Pacific and Indian Oceans
ocean currents

b. Identifiers/Open-Ended Terms

c. COSATI Field/Group

18. Availability Statement	19. Security Class (This Report)	21. No. of Pages
Approved for public release; distribution unlimited.	UNCLASSIFIED	241
	20. Security Class (This Page)	22. Price

(See ANSI-Z39.18) *See Instructions on Reverse* OPTIONAL FORM 272 (4-77)
(Formerly NTIS-35)
Department of Commerce

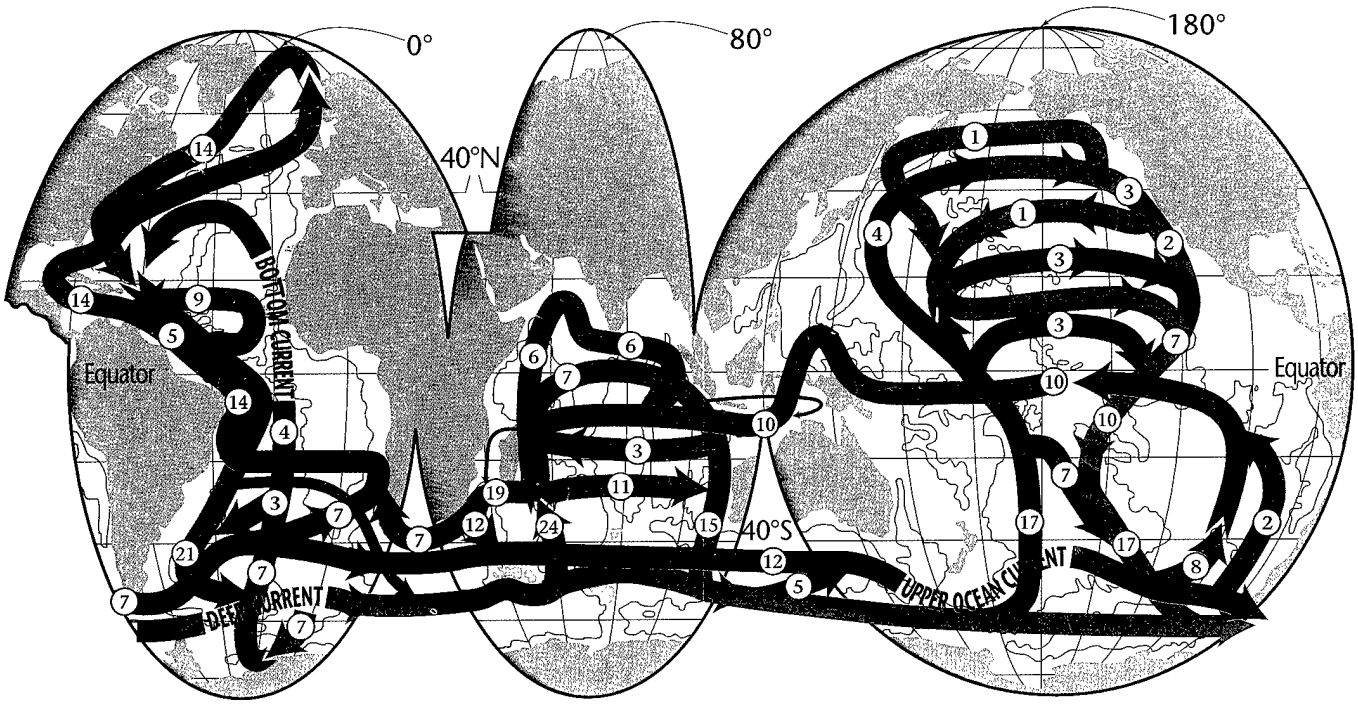

An updated three-layer global interbasin circulation summary. Blue represents bottom water, green deep, and red the upper ocean. Transports in Sverdrups in circles. See page 189 for a larger view.